



HAL
open science

Structural and functional study of the interaction between CXCL12 chemokine and its receptors: CXCR4 and ACKR3/CXCR7

Pasquale Cutolo

► **To cite this version:**

Pasquale Cutolo. Structural and functional study of the interaction between CXCL12 chemokine and its receptors: CXCR4 and ACKR3/CXCR7. Immunotherapy. Université Paris Saclay (COMUE), 2016. English. NNT: 2016SACLS550 . tel-01674198v2

HAL Id: tel-01674198

<https://theses.hal.science/tel-01674198v2>

Submitted on 2 Jan 2018

HAL is a multi-disciplinary open access archive for the deposit and dissemination of scientific research documents, whether they are published or not. The documents may come from teaching and research institutions in France or abroad, or from public or private research centers.

L'archive ouverte pluridisciplinaire **HAL**, est destinée au dépôt et à la diffusion de documents scientifiques de niveau recherche, publiés ou non, émanant des établissements d'enseignement et de recherche français ou étrangers, des laboratoires publics ou privés.

NNT 2016SACLS550

université
PARIS-SACLAY

ÉCOLE DOCTORALE

Innovation thérapeutique :
du fondamental à l'appliqué

Instituts
thématiques

Inserm

Institut national
de la santé et de la recherche médicale

Thèse de doctorat
De
L'Université Paris-Saclay

Ecole Doctorale n° 569

INNOVATION THÉRAPEUTIQUE : DU FONDAMENTAL À L'APPLIQUÉ

Spécialité de doctorat :

IMMUNOLOGIE ET BIOTHÉRAPIES

Présentée par

Pasquale CUTOLO

Etude de l'interaction structurelle et fonctionnelle entre la chimiokine
CXCL12 et ses récepteurs : CXCR4 et ACKR3/CXCR7

Thèse présentée et soutenue à Châtenay-Malabry, le 16 septembre 2016

Composition du Jury :

Françoise BACHELERIE
Esther KELLENBERGER
Eric REITER
Philippe DETERRE
Thierry DURROUX
Sandrine ONGERI

DR, Inserm UMR-S 996, Clamart
Prof., Faculté de Pharmacie de Strasbourg
DR, INRA, Tour
DR, Inserm UMR-S 945, Paris
DR, CNRS – IGF, Montpellier
Prof. de l'Université Paris-Saclay

Directrice de thèse
Rapporteuse
Rapporteur
Examineur
Examineur
Examinatrice

INDEX

Abbreviations	4
Introduction	7
Chapter I - <i>Chemokines structure and interactions</i>	7
<i>Preamble on Chemokines</i>	7
<i>I.1 Primary structure and classification of Chemokines (CKs)</i>	9
<i>I.2 Topology and Folding of CKs</i>	12
<i>I.3 Oligomerization of CKs</i>	14
<i>I.4 Interaction with Glycosaminoglycans (GAGs)</i>	18
<i>I.5 Interaction of CKs with receptors</i>	24
Chapter II - <i>G-protein Coupled Receptors (GPCRs) structural basis</i>	38
<i>Preamble on GPCRs</i>	38
<i>II.1 Current Chemokine Receptors (CKRs) Crystal Structures</i>	40
<i>II.2 Oligomerization of GPCRs</i>	41
<i>II.3 Atypical Chemokine Receptors (ACKRs)</i>	47
<i>II.4 CXCR4 receptor-dependent signaling pathways</i>	53
Chapter III - <i>Nanobodies (NBs) as new innovative tools</i>	59
<i>Preamble on NBs: the smallest natural antigen-binding fragment</i>	59
<i>III.1 Antibodies for biomedical applications</i>	63
<i>III.2 NBs in structural biology</i>	64
<i>III.3 CXCR4- and CXCR7/ACKR3- targeting NBs</i>	67
Objectives	68
Results	69
Paper n°1	72
Paper n°2	118
Paper n°3	158

Discussion and perspectives	196
I - Mechanism of the interaction and stoichiometry of CXCL12 with CXCR4 and CXCR7/ACKR3 receptors.....	197
<i>I.1 Modeling the three-dimensional structure of GPCRs</i>	197
<i>I.2 Modeling the binding of ligands to GPCRs</i>	199
<i>I.3 Conclusions</i>	201
II – Nanobodies	203
<i>II.1 Characterization of NBs against CXCR4</i>	203
<i>II.2 NBs applications</i>	203
<i>II.3 Conclusions</i>	204
References	207
Annexes	238
Curriculum Vitae	243
Acknowledgement.....	238

“Eppur si muove”

"And yet it moves" or "Albeit it does move", one of the most famous Galileo Galilei's citation for Earth movement, is the good sentence to introduce my thesis.

The Italian scientist spoke about the movement of our planet and its “migration” around the Sun, people are moving around the world during their life, but deeply inside this movement is also the base of our biology, from the embryogenesis to the adult life.

How can our cells “migrate” and decide where and when “be or not to be”?

The answer is in small molecules called chemokines and their fascinating and highly intricate networks with chemokine receptors.

Abbreviations

7-TM	Seven transmembrane
TM	Transmembrane
BRET	Bioluminescent resonance energy transfer
C-terminus	Carboxyl-terminal extremity
CDRs	Complementary determining regions
CFP	Cyan fluorescent protein
CKs	Chemokines
CKRs	Chemokines Receptors
CRS1	Chemokine recognition site 1
CRS2	Chemokine recognition site 2
CS	Chondroitin sulfate
CX3R,	CX3C chemokine receptors
CXCR	CXC chemokine receptor
Cyt	Cytoplasmic region
DS	Dermatan sulfate
ECL	Extracellular loop
ECM	Extracellular matrix
ELR	Glu-Leu-Arg sequences
Fig	Figure
FRET	Förster Resonance Energy Transfer
GAGs	Glycosaminoglycans
GPCRs	G-protein coupled receptors
HA	Hyaluronic acid
HCAbs	Heavy-chain antibodies
HIV	Human Immunodeficiency Virus
HS	Heparan sulfate
HTRF	Homogeneous time-resolved FRET
ICL	Intracellular loop
KS	Keratin sulfate
mAbs	Monoclonal antibodies
MOR	mu opioid receptor
N-terminus	Amino-terminal extremity
NB	Nanobody

NMR	Nuclear magnetic resonance
PDB	Protein DATA Bank
sTyr	Sulfotyrosine
Tab	Table
TM	Transmembrane region
TNF	Tumor necrosis factor
VHH	Camelid heavy-chain antibody
YFP	Yellow fluorescent protein

- Table of Amino Acid abbreviations:

Name	3-Letters	1-Letter
Alanine	Ala	A
Arginine	Arg	R
Asparagine	Asn	N
Aspartic acid	Asp	D
Cysteine	Cys	C
Glutamic acid	Glu	E
Glutamine	Gln	Q
Glycine	Gly	G
Histidine	His	H
Isoleucine	Ile	I
Leucine	Leu	L
Lysine	Lys	K
Methionine	Met	M
Phenylalanine	Phe	F
Proline	Pro	P
Serine	Ser	S
Threonine	Thr	T
Tryptophan	Trp	W
Tyrosine	Tyr	Y
Valine	Val	V

Introduction

❖ *Chapter I: Chemokines structure and interactions*

❖ *Chapter II: G-Protein Coupled Receptors structural basis*

❖ *Chapter III: Nanobodies as new innovative tools*

Introduction

Chapter I

Preamble on Chemokines

Proteins called “chemokines” are cytokines, usually of a molecular weight between 8 and 14 kDa with a high structural homology, and the peculiar chemo-attractive function (CHEMOtactic cytoKINES).

We can define the chemotaxis as the oriented cell migration through the concentration gradient of a chemical signal (called chemotactic or chemo-attractive signal, (Mc 1946, Harris 1953, Harris 1953).

These proteins have historically been known under several other names including the SIS family of cytokines, SIG family of cytokines, SCY family of cytokines, Platelet factor-4 superfamily or intercrines. In 1977 the first one was described as a molecule capable to activate platelets during platelet aggregation and to promote blood coagulation (platelet factor 4, PF4 or now according to the new nomenclature CXCL4) and today 44 chemokines (CKs) are known in all vertebrates and are conserved for their different functions notably on immune responses (naïve and adaptive), inflammation, hematopoiesis and angiogenesis. They exert these functions by interacting with chemokine receptors (CKRs) that are 7-transmembrane (7-TM) -domains G-protein coupled receptors (GPCRs). To date 19 receptors have been identified, forming a highly intricate and precisely regulated network (Bonecchi, Galliera et al. 2009, Bachelierie, Ben-Baruch et al. 2014).

Expression of the CKs can be induced by cytokines (for example interferons (IFNs), tumor necrosis factor (TNF)- α , in inflammatory conditions) in a variety of immune and non-immune cells. These various cell types non-exhaustively include fibroblasts, epithelial, endothelial and smooth muscle cells, as well as mononuclear leukocytes and granulocytes. (Brown, Gerritsen et al. 1994)

On the basis of their expression and thereafter their function, CKs were initially classified in two main categories. Some are considered as homeostatic being produced constitutively (ex. CCL19, CXCL13), and generally involved in lymphocyte trafficking, immune surveillance and localization of immune cells in the lymphatic system (Fernandez and Lolis 2002), but

also for the central nervous system cells disposition and angiogenesis (Strieter, Polverini et al. 1995, de Haas, van Weering et al. 2007).

Other CKs were considered as being only produced during infection or following a pro-inflammatory stimulus and involved in immune cells recruitment to damaged tissues (ex. CXCL8, CXCL10). For instance, in case of skin wound, such inflammatory CKs can also activate cells to raise an immune response and start the wound healing process (Rollins 1997). This functional classification was based on the idea that cells are producing CKs either constitutively or under different pathogenic conditions and in a soluble secreted form. However, the knowledge built up over years indicates that CKs instead of being secreted as soluble proteins are rather interacting with extracellular matrix (ECM) glycosaminoglycans (GAGs) and the concept that adhesion events between cells not only provide a method of cellular interaction, but also may aid in the activation of the cells and induce the production of CKs in non-inflammatory conditions (Rot 1993).

Moreover, CKs are also involved in other functions than chemoattraction. A good example is CXCL12, a chemokine also involved in angiogenesis and considered as a growth factor. Moreover, this CK has been shown to be able to act as a chemo-repulsive agent. For instance, high concentrations of CXCL12 have been shown i) to repulse human thymocytes in vitro, a “run away” process that could be abolished using a neutralizing CXCL12 antibody (Poznansky, Olszak et al. 2000) and ii) to permit the firm adhesion of CD4 and CD8 T cells to microvascular endothelium from pancreatic islet thus resulting in a decrease of T-cell integrin activation in a CXCR4-independent manner (Sharp, Huang et al. 2008).

Such a process might account for the decreased chemotaxis observed at high concentration of a CK evidenced by the typically bell shaped response upon CK concentration. However the exact molecular mechanisms of CK-induced chemorepulsion are still undefined. Zlatopolskiy and Laurence (Zlatopolskiy and Laurence 2001) postulated that CK-mediated repulsion would be triggered by an excess of free ligand in the vicinity of the cell that would lead to a dimerization of the receptor, followed by an internalization of the ligand/receptor complexes. Internalization, degradation of the ligand, and recycling of the receptors would be realized under the same way than during the chemoattraction process. The difference between these two processes would take place through the localization of the recycled receptors. Appearance of the internalized receptors may occur not on the apical side of the cell but on the basal side resulting in a reverse movement. Summarizing, the direction of a CK-triggered movement is gradient dependent and concentration dependent.

I.1 Primary structure and classification of CKs

As mentioned above, expression of CKs being both constitutive and inducible (ex. CXCL12, CCL20) rendered obsolete the use of a “functional nomenclature”. Based on their structural features, namely the position of two cysteines located at the N-terminal part of the peptide chain, it is possible to distinguish four different families. CKs primary structure is composed of a single polypeptide chain of 70-100 aminoacid residues in length, with high variable sequence identity to each other (20-95%), including the conserved cysteine residues that have also been the basis for subfamily nomenclature.

Four subfamilies of CKs can be distinguished by the pattern of these four near-identical cysteine residues position. Two principals cysteines are located at the N-terminal part and are involved in the formation of two important disulfide bonds with two (or one) distal cysteines for the protein folding (Fig 1).

Based on this structural characteristic we can divide CKs in:

- ❖ CXC or alpha family, grouping CKs with one amino acid between the two first cysteines
- ❖ CC or beta family, for CKs with none residues between the two cysteines
- ❖ XC or gamma family, for CKs with only one cysteine and one disulfide bond
- ❖ CX3C or delta family, which has only one known member (CX3CL1 or “fractalkine” or “neurotactin”), with three amino acids between the two cysteines.

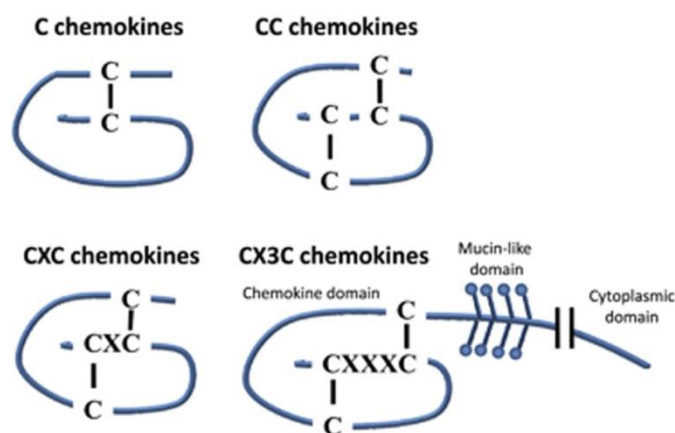


Fig 1. Schematic view of CKs subfamilies based on primary structure

CK genes are clustered on specific chromosomal regions and there are two major gene clusters comprising exclusively either CXC or CC genes on chromosome 4q13.3-q21.1 and 17q12, respectively (Tab 1). These major clusters can be subdivided into two regions. For the CXC gene cluster, the regions are named GRO and IP10 while the regions of the CC gene cluster are called MCP and MIP (Nomiyama, Osada et al. 2010). The GRO region contains the CXCL1–CXCL8 genes and the IP10 region the CXCL9–CXCL13 genes, respectively (with the exception of CXCL12 that is located on chromosome 10).

In the CC major cluster, the MCP and MIP regions comprise 6 and 12 genes, respectively (CCL2, CCL7, CCL11, CCL8, CCL13, CCL1 versus CCL5, CCL16, CCL14, CCL15, CCL23, CCL18, CCL3, CCL4, CCL3L3, CCL4L1, CCL3L1, CCL4L2). In addition to the two major clusters, a CC “mini”-cluster is found on chromosome 7 (comprising the CCL26 and CCL24 genes), on chromosome 9 (CCL27, CCL19, CCL21), and on chromosome 16 (CCL22, CX3CL1, and CCL17), respectively. Both XCL1 and XCL2 are also found in a “mini”-cluster on chromosome 1 (Maho, Carter et al. 1999, Nomiyama, Fukuda et al. 1999, O'Donovan, Galvin et al. 1999).

The CX3C CK is unusual because it is part of a cell surface receptor: the CK comprises a CK module (related in structure to the other families), as well as a stalk, a transmembrane region (TM), and a short cytoplasmic region (Cyt).

The relative proportions of these components are not drawn to scale in Fig 1, as the stalk comprises approximately 75% of the CX3C CK.

Name	Official symbol	Conventional name	Chromosome	Gene size (kb)	Number of exons	Number of amino acids (mature form)	Cluster name	Receptor ¹
CCL								
CCL1	CCL1	TCA3; I-309	17q11.2	2.85	3	73	MCP	CCR8
CCL2	CCL2	MCP-1; MCAF; JE	17q11.2-q21.1	1.93	3	76	MCP	CCR2, CCR3, DARC, CCBP2
CCL3	CCL3	MIP-1 α ; LD78 α	17q12	1.90	3	69	MIP	CCR1, CCR5, CCBP2
CCL3L1	CCL3L1	LD78 β	17q12	1.89	3	70	MIP	CCR1, CCR5
CCL3P1	CCL3L2	–	17q21.1	–	–	–	MIP	–
CCL3L3	CCL3L3	LD78 β	17q12	1.88	3	70	MIP	CCR1, CCR5
CCL4	CCL4	MIP-1 β	17q21-q23	1.79	3	69	MIP	CCR5, CCBP2
CCL4L1	CCL4L1	LAG-1	17q12	1.80	3	69	MIP	CCR5, CCBP2
CCL4L2	CCL4L2	LAG-1	17q12	1.80	3	68	MIP	CCR5, CCBP2
CCL5	CCL5	RANTES	17q11.2-q12	8.88	3	68	MIP	CCR1, CCR3, CCR5, DARC, CCBP2, CCRL2
CCL7	CCL7	MCP-3; MARC	17q11.2-q12	2.01	3	76	MCP	CCR1, CCR2, CCR3, CCR5, DARC, CCBP2
CCL8	CCL8	MCP-2	17q11.2	2.35	3	76	MCP	CCR2, CCR3
CCL11	CCL11	Eotaxin ₁	17q21.1-q21.2	2.51	3	74	MCP	CCR3, CCR5, DARC, D6
CCL13	CCL13	MCP-4	17q11.2	2.21	3	82	MCP	CCR2, CCR3, CCR5, DARC, CCBP2
CCL14	CCL14	HCC-1	17q11.2	3.07	4	74	MIP	CCR1
CCL15	CCL15	HCC-2	17q11.2	4.46	4	92	MIP	CCR1, CCR3, DARC
CCL16	CCL16	HCC-4; LEC	17q11.2	4.98	3	97	MIP	CCR1
CCL17	CCL17	TARC; ABCD-2	16q13	11.29	3	71	"Mini"-CC 16	CCR4, DARC, CCBP2
CCL18	CCL18	DC-CK1; PARC; AMAC-1	17q11.2	7.2	3	69	MIP	DARC
CCL19	CCL19	MIP-3 β ; ELC; Exodus-3	9p13	1.71	4	77	"Mini"-CC 9	CCR7, CCRL1, CCRL2
CCL20	CCL20	MIP-3 α ; LARC; Exodus-1	2q33-q37	3.72	4	70, 69	–	CCR6
CCL21	CCL21	6CKine; SLC; Exodus-2	9p13	1.14	4	111	"Mini"-CC 9	CCR7, CCRL1
CCL22	CCL22	MDC; STCP-1; AMCD-1	16q13	7.41	3	69	"Mini"-CC 16	CCR4, DARC, CCBP2
CCL23	CCL23	CK β 8; MPIF-1	17q11.2	4.91	4	99, 116	MIP	CCR1, FPR2
CCL24	CCL24	Eotaxin-2; MPIF-2	7q11.23	1.92	3	93	"Mini"-CC 7	CCR3
CCL25	CCL25	TECK	19p13.2	34.81	5	127, 61	–	CCR9, CCRL1
CCL26	CCL26	Eotaxin-3; MIP-4 α ; IMAC	7q11.2	20.22	3	71	"Mini"-CC 7	CCR3
CCL27	CCL27	CTACK; ILC; ESKINE	9p13	0.80	3	88	"Mini"-CC 9	CCR10
CCL28	CCL28	MEC	5p12	30.88	3	108	–	CCR3, CCR10
CXC								
CXCL1	CXCL1	GRO- α ; MGSA- α ; MIP-2; KC	4q13.3	1.85	4	73	GRO	CXCR2, DARC
p-CXCL1	CXCL1P	–	4q13.3	–	4	–	GRO	–
CXCL2	CXCL2	GRO- β ; MGSA- β ; MIP-2 α	4q13.3	2.24	4	73	GRO	CXCR2, DARC
CXCL3	CXCL3	GRO- γ ; MGSA- γ ; MIP-2 β	4q13.3	2.18	3	73	GRO	CXCR2, DARC
CXCL4	PF4	PF4	4q13.3	0.92	3	70	GRO	CXCR3
CXCL4L1	PF4V1	PF4-ALT; CXCL4V1	4q13.3	1.18	4	70	GRO	–
CXCL5	CXCL5	ENA-78	4q13.3	3.05	4	78	GRO	CXCR2, DARC
CXCL6	CXCL6	GCP-2	4q13.3	2.20	3	77	GRO	CXCR1, CXCR2, DARC
CXCL7	PPBP	NAP-2; beta-TG; CTAP-III	4q13.3	1.75	3	81, 85, 94	GRO	CXCR2, DARC
p-CXCL7	PPBPL1	–	4q13.3	–	–	–	GRO	–
CXCL8	IL8	IL8	4q13.3	3.21	4	79, 82	GRO	CXCR1, CXCR2, DARC
CXCL9	CXCL9	MIG	4q21.1	6.02	4	103	IP10	CXCR3
CXCL10	CXCL10	IP10; CRG-2	4q21.1	2.42	4	77	IP10	CXCR3
CXCL11	CXCL11	I-TAC	4q21.1	2.51	4	73	IP10	CXCR3, CXCR7, DARC
CXCL12	CXCL12	SDF-1 α	10q11.1	14.94	4	68	–	CXCR4, CXCR7
CXCL12	CXCL12	SDF-1 β	–	–	–	72	–	–
CXCL12	CXCL12	SDF-1 γ	–	–	–	98	–	–
CXCL13	CXCL13	BCA-1; BLC	4q21.1	100	4	87	IP10	CXCR5
CXCL14	CXCL14	BRAK	5q31	8.60	4	77	–	?
CXCL16	CXCL16	SR-PSOX	17p13.2	6.39	5	225 ²	–	CXCR6
CXCL17	CXCL17	DMC	19q13.2	14.44	4	98	–	?
XC								
XCL1	XCL1	Lymphotactin; SCM-1 α ; ATAC	1q23	5.60	3	93	"Mini"-CC 1	XCR1
XCL2	XCL2	SCM-1 β	1q24.2	3.23	3	93	"Mini"-CC 1	XCR1
CX3C								
CX3CL1	CX3CL1	Fractalkine; Neurotactin; ABCD-3	16q13	12.54	3	355 ²	"Mini"-CC 16	CX3CR1
NOT ASSIGNED								
MIF	MIF	Macrophage migration inhibitory factor, glycosylation-inhibiting factor	22q11.23	0.84	3	114	–	CXCR2, CXCR4; CXCR7, CD74

Tab 1. Liste of human CK and relative gene position (Blanchet, Langer et al. 2012).

1.2 Topology and Folding of CKs

As mentioned above the primary sequence homology between CKs is highly variable, ranging from less than 20% to over 90%, but all share very similar structures. These proteins are produced in both membrane-bound and soluble forms and can act not only as chemo-attractants, but also as adhesion molecules, at least in the case of CX3CL1.

The first CK structure to be determined was that of CXCL8 in 1990 (Cloure, Appella et al. 1990). Subsequent to the structures of CXCL8 and other CXC CKs, the structure of the CC CK, CCL4, was solved (Lodi, Garrett et al. 1994), followed by CCL5 (Skelton, Aspiras et al. 1995) and CCL2 (Lubkowski, Bujacz et al. 1997) shortly thereafter. Today in the Protein Data Bank (PDB) we can find multiple structures of 24 CKs that have been solved by solution NMR (60 different structures) or X-ray crystallography (86 different structures, 7 with less than 1.5 Å of resolution) and have revealed that despite low sequence homology, CKs adopt a remarkably conserved folding (Fig 2).

The CK topology consists of an elongated N-terminus that precedes the first cysteine, with no particular structural features and in most cases was unobservable by high-resolution structural studies.

A loop of approximately ten residues follows the first two cysteines, known as the N loop, which plays functional roles and is succeeded by one strand of a 3_{10} helix (Crump, Rajarathnam et al. 1998, Nomiyama, Mera et al. 2001). Three β -strands single-turn succeed the 3_{10} helix and the C-terminus part forms an α -helix structure. Each secondary structural unit is connected by turns known as the 30s, 40s, and 50s loops (Eigenbrot, Lowman et al. 1997, Rajarathnam, Crump et al. 1999), which reflects the numbering of residues in the mature protein. In addition of having important roles in connecting secondary structures, the 30s and 50s loops possess the latter two of the four cysteines characteristic of the family. The first two cysteines following the N-terminal region limit the flexibility of the N-terminus, owing to the disulfides bonds with the third cysteine on the 30s loop and the fourth cysteine in the 50s loop, respectively.

Despite the presence of the two cysteines following the N-terminus, NMR dynamics studies indicate that the flexibility of the N loop is greater than the flexibility of other regions of the protein (excluding the N- and C- termini). This flexibility may play a role in the mechanism of binding to and/or activation of CKRs (Keizer, Crump et al. 2000).

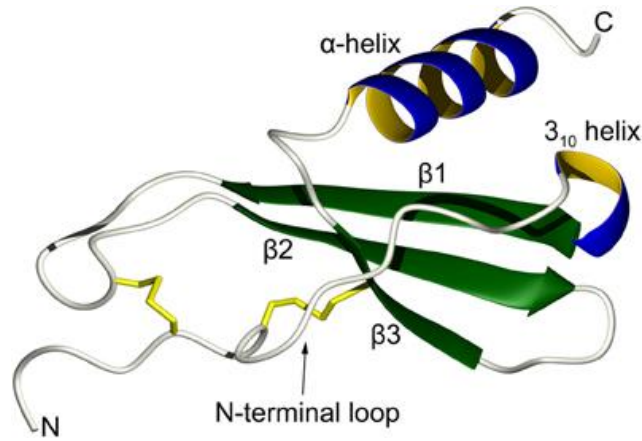


Fig 2. The CK fold consists of a flexible N-terminus, an N-loop, occasionally a 3_{10} helix, an antiparallel three-stranded β -sheet, and a C-terminus α -helix. Within the antiparallel three-stranded β -sheet, the $\beta 1$ -strand is connected to $\beta 2$ -strand by the 3_{10} loop and $\beta 2$ -strand is linked to $\beta 3$ -strand by the 4_{0s} loop.

I.3 Oligomerization of CKs

One peculiarity of many CKs is their reported capacity to form dimers or higher-order oligomers in solution or upon binding to proteins and other components of the ECM, as GAGs (Johnson, Handel et al 2005, Handel et al 2004). CKs can interact with themselves (homo-oligomerization) or between them (hetero-oligomerization).

I.3a Homo-Oligomerization

These interactions are proposed to be different into the two main subfamilies of CKs (CC and CXC).

CC CKs (Fig 3) associate in an elongated structure with a considerable flexibility between the two subunits. The interaction is established through the formation of an antiparallel β -sheet structure involving residues near the N-terminus, including the first two cysteines (for example, residues 9–12 in CCL2). Although the structure of CCL2 was initially solved as a dimer (in solution by NMR), subsequent crystallographic studies revealed the potential formation of both dimers and tetramers from two different crystal forms (Lubkowski, Bujacz et al. 1997, Sticht, Escher et al. 1999, Blaszczyk, Coillie et al. 2000).

Other CKs such as CCL5, CCL3, and CCL4 can aggregate into even higher-order oligomers. Tetramers are likely to be the next level of organization, as point mutants of both CCL5 and CCL3 have been identified that form predominantly CC dimers or tetramers of as yet unknown structures. Thus, the higher-order structures are likely organized assemblies rather than random precipitates (Shaw, Johnson et al. 2004, Dias, Losberger et al. 2009).

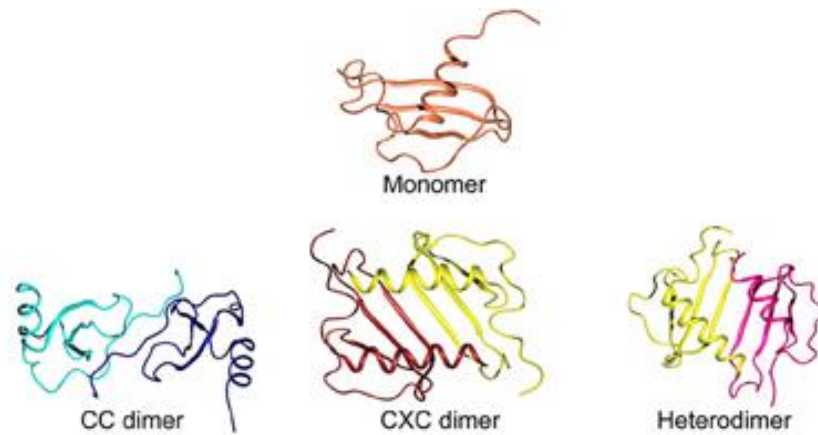


Fig 3. A typical CK monomeric unit is shown at the top (CCL20; PDB ID 2JYO). The CC-type dimer is formed from contacts between the N-terminal fragments of each subunit to create an elongated shape (CCL2 homodimer; PDB ID 1DOM). The CXC-type dimer is created by the continuation of the β -sheets via their first strands and a small reorientation of the α -helices, running anti-parallel to each other (CXCL8; PDB ID 1IL8). Heterodimerization is also possible, modeled here from two subunits of CXCL8 and CXCL4 (PDB ID 1IL8 and 1RHP, respectively) (adapted from Nguyen et al 2012).

Regarding the propensity of CXC CKs to oligomerize, it was reported that residues in the first strand of the β -sheet form hydrogen bonds with the same strand from a second subunit, forming one extended six-stranded sheet (Fig 3)(Wang, Sharp et al. 2013). To stabilize these conformations, interactions between the ends of the C-terminus α -helices with the β -sheet of the opposing subunit are formed. When compare with CC dimers, the shapes of the CXC ones are much more globular and the overall topology is effectively a β -sheet platform topped by two α -helices with a slight cavity between the helices. As for CC CKs, studies of CXC structures (i.e. CXCL4 and CXCL10) suggest that the “tetrameric architecture” is the dominant form of the proteins in solution. In the case of CXCL10, two different tetramers were reported by crystallography, one similar to the CCL2 and CXCL4 tetramers and the other consisting of a novel 12-stranded β -sheet structure (Swaminathan GJ, 2003) (Kuo, Chen et al. 2013).

Despite the propensity of CKs to oligomerize, the prevalent concept is that CKs interact with receptors as monomers, at least in the context of their directed-migration function. This finding was highly suggested by structure-based design of mutants that are obligate monomers.

Clark-Lewis’group made a synthetic variant of CXCL8 containing a methyl group on the amide of Leu25 in the central β -strands of opposing subunits in the dimer which is normally involved in H bonding across the dimer interface (Crump, Rajarathnam et al. 1998, Rajarathnam, Crump et al. 1999). The mutant with Leu25 methylated does not dimerize, but its binding affinity and ability to induce cell migration and elastase release in vitro were found to be equivalent to those of the wild-type CK thus strongly suggesting that a monomeric form of CXCL8 is sufficient for receptor binding and full in vitro biological activity.

Subsequently, a similar chemical modification of Thr8 in the N-terminus of CCL5 produced a monomeric variant with in vitro activity equivalent to the wild-type protein (Proudfoot, Handel et al. 2003). A different strategy was used with CCL2 and CCL4. In the recombinant forms of these CKs, mutation of Pro8 (N-terminus), an amino acid that flanks the dimer interface and is present in many CC CKs, results in variants that do not dimerize (Paavola, Hemmerich et al. 1998, Laurence, Blanpain et al. 2000). Like for CXCL8 and CCL5, these mutants also displayed in vitro binding and chemotaxis equivalent to their wild-type counterparts. With data from these four CKs, it is tempting to generalize the monomer-binds-receptor hypothesis to most if not all CKs, at least with respect to the induction of cell

migration. However oligomerization seems to be required for the chemotactic function of some CKs and was correlated with the ability of the CKs to bind GAGs.

Thus, the propensity of CKs to oligomerize can be beneficial for some CKs depending the cells, the tissues and the physiological contexts and can also add some diversity with regard to receptors activation and signaling, most notably in the case of CKs hetero-oligomerization.

1.3b Hetero-Oligomerization

The finding that CKs can form hetero-oligomers is not entirely surprising since all CKs have a similar folding and use a limited set of dimer interface motifs. Additionally, because structural studies have revealed tetrameric complexes in which both CC and CXC dimer-like interfaces and alternative interfaces occur (Swaminathan et al. 2003(Lau, Paavola et al. 2004), formation of CC/CXC hetero-oligomers is not out of the question (Fig 3). Indeed, heterodimerization has been proposed for CCL3/CCL4, CXCL4/CXCL8, CCL21/CXCL13, CXCL4/CCL5, and CCR2 ligands, particularly CCL2 and CCL8 (Nesmelova IV, (Paoletti, Petkovic et al. 2005).

The formation of hetero-oligomers may be a common property of CKs and possibly important modulate their functions.

Indeed, hetero-oligomers binding to receptors might have cooperative or, conversely, inhibitory consequences on receptors functions, or induce the emergence of new signaling pathways downstream activated receptors and potentially new physiological responses of CK-stimulated cells.

We also have to consider that the effects of hetero-oligomerization can be indirect (Paoletti, Petkovic et al. 2005, Allen, Crown et al. 2007, Koenen, von Hundelshausen et al. 2009). For example, heterodimers may regulate the pre-binding quantities and availability of the CKs, as well as changes in the affinity and/or selectivity of CKs for GAGs relative to homodimers. CKs hetero-dimerization may also negatively regulate receptor activation by sequestering CKs into non-functional heterodimers, somewhat akin to the role of scavenger receptors in dampening the immune response. In the context of receptor signaling, two CKs may act independently at the cell surface, although their signals integrate downstream to modulate the response of the cell. On the other hand, in contrast to the monomer-binds-receptor paradigm, it remains entirely possible that some hetero-oligomers of CKs could bind directly to

receptors via a different interaction surface than do the CKs monomers, or they may act through alternate receptors (than their cognate ones) to produce novel responses. For both homo- and hetero- oligomerization, much work needs to be done to determine the diversity of their functional effects, the supra structures involved (in relationship with their receptors) and most important, their *in vivo* existence.

I.4 Interaction with glycosaminoglycans (GAGs)

I.4a Early evidence

The importance of CKs binding to endothelium was suggested soon after the family was identified by the demonstration that neutrophils migrated toward immobilized CXCL8 by a mechanism called haptotaxis (Rot 1993). Interestingly, this concept was strengthened with the identification of CXCL4 upon heparin-sepharose affinity chromatography (Deuel, Keim et al. 1977). While from this earlier works, it was well accepted that CKs are immobilized on the endothelial surface through their interaction with GAGs in order to provide a directional signal, direct evidence of this binding process and its functional consequences were more recently provided by the use of CK mutants with abrogated GAGs-binding capacity and that consequently have lost their ability to recruit cells *in vivo* (Proudfoot, Handel et al. 2003). Formation of CK gradients on cell surfaces is considered to be critical for haptotactic cell migration (Middleton, Neil et al. 1997, Patel and Haynes 2001) and the absence of such gradients leads to impaired migration either because of the lack of directional signals (Weber, Hauschild et al. 2013) or due to bulk receptor desensitization (Ali, O'Boyle et al. 2007).

I.4b GAGs structure

GAGs or mucopolysaccharides are long unbranched chains composed of repeating disaccharide units. These carbohydrate structures found on the surfaces of virtually all cells, are classified into several families on the basis of the identity of their repeating disaccharide units and the variability in their lengths (Fig 4). GAGs have high degrees of heterogeneity with regards to molecular mass, disaccharide construction, and sulfation due to the fact that their synthesis, unlike that of proteins or nucleic acids, is not template driven, and dynamically modulated by processing enzymes. CKs binding to GAGs can be determined by

several methods. These include affinity chromatography to heparin sepharose, binding assays, isothermal fluorescence titration, and surface plasmon resonance to name a few, which were described in detail elsewhere (Hamel, Sielaff et al. 2009). It should be noted that the majority of these assays use heparin as a GAGs prototypic model since it is readily available commercially and is less expensive than the other classes of GAGs. There are six major classes of GAGs, which include heparin, heparan sulfate (HS), chondroitin sulfate (CS), dermatan sulfate (DS), keratin sulfate (KS), and hyaluronic acid (HA). Heparin and HA are soluble GAGs, whereas HS, DS, KS, and CS are usually covalently attached to a protein core, referred to as proteoglycans. It should be noted that heparin is more highly sulfated than HS, the most abundant GAGs, which is found on almost every cell in the body. CKs therefore exist both in the fluid phase in the circulation and as a bound form immobilized on proteoglycans-expressing GAGs. In some cases, the CKs/GAGs interaction may not just provide a mechanism for localization, but could also induce modification in the receptor activation that may differentially contribute to some steps of cell migration in vivo, such as leukocyte arrest that cannot be easily modeled in vitro.

1.4c Functions of GAGs

Recent methodological improvements including studies of transendothelial migration under shear flow (Cinamon, Shinder et al. 2001) have notably improved our understanding of the critical role for GAGs in the presentation and functions of CKs for lymphocyte interactions with vasculature. It was shown that blood vessels create steep gradients of HS between their luminal and basolateral surfaces and that further inflammation significantly increases HS deposition in the ECM, thereby providing a mechanism for patterning CKs gradients (Stoler-Barak, Moussion et al. 2014). Moreover, several studies have shown that the ability of some CKs to bind GAGs is important for their function using in vivo models of inflammation (Proudfoot, Handel et al. 2003, Ali, Robertson et al. 2005) where CKs–GAGs interactions are involved in the transport of CKs across endothelial cells from their site of production at inflammatory foci (Wang, Fuster et al. 2005). CKs–GAGs interactions were also involved in the storage and release of CKs from T cells (Wagner, Kurtin et al. 1998) and in the secretion of CKs from tumor cells (Soria, Lebel-Haziv et al. 2012).

1.4d Affinity and structural determinants for GAGs binding

While the importance of these interactions has motivated numerous studies to determine binding affinities of CKs with GAGs, there are few quantitative comparisons of the affinities of CKs for GAGs apart from some early studies (Hoogewerf, Kuschert et al. 1997, Kuschert, Coulin et al. 1999). Compiling comparisons based on studies of individual CKs is, however, challenging due to the use of a wide range of techniques, solution conditions and types/sources of GAGs in these studies (Hamel, Sielaff et al. 2009). Nevertheless, such comparisons are important as they may reveal differences in the specificity of CKs for GAGs and/or be relevant to the role of such interactions in CK function. The molecular details of how CKs bind to GAGs are also poorly understood and the characterization of GAGs binding sites remains a complex issue.

Among studies based on heparin binding protein sequence comparison, an early work led to the identification of two binding consensus sequences, XBBXB or XBBBXXB clusters, where B stands for a basic residue and X for any others (Cardin and Weintraub 1989). However, recent analyses have challenged the universality of this paradigm. Site directed mutagenesis, structural characterization of protein/heparin complexes and the development of a new approach, which relies on the proteolytic digestion of protein/heparin complexes and the subsequent identification of the heparin bound peptides by N-terminus sequencing (Vives, Crublet et al. 2004), clearly indicate that binding sites are not exclusively composed of linear sequences, but can also include conformational epitopes comprising distant amino acids organized in a precise spatial orientation through the folding of the protein.

For CKs, amino acids involved in GAGs recognition are more or less scattered along the polypeptide chain, however, they systematically form well-defined clusters at the surface of the folded protein (Lortat-Jacob, Grosdidier et al. 2002). Four of these clusters have been characterized, one for each of the CC and CX3C type of CKs and two within the CXC family (Fig 5). Cluster 1, characteristic of CXCL8 and most CXC CKs is created by the residues of the C-terminal α -helix together with the loop connecting the extended N-terminal strand region with the first β -strand. Cluster 2, which has only been observed in CXCL12, forms a crevasse at the interface between the β -strands, where three basic amino acids in both b(1) and b(2) characterize the binding site. Cluster 3 is observed in most CC CKs and mainly consists of the loop between b(2) and b(3) strands with a typical BBXB conserved motif. Basic amino acids located at the beginning and the end of the loop connecting b(N) and b(1) also

participate in the establishment of such a cluster. Finally, cluster 4 (CX3C CK) comprises a flat area made up of loops between b(1) and b(2) and loop connecting b(3) and a(c). Except for a single Lys, shared by cluster 2 and cluster 3, these GAGs binding sites are not overlapping and thus represent specific binding signature of each group of CKs.

Focusing on CXCL12, we observed that data on this CK have been obtained from two isoforms (CXCL12 α and β), arising from the alternative splicing of a single gene. CXCL12 α binding to HS critically involves amino acids K24 and K27, which together with R41 form the essential part of the HS-binding site and are distinct from those required for binding to CXCR4 (Fig. 6) (Sadir, Baleux et al. 2001). A novel isoform, CXCL12 γ , has been identified more recently (Laguri, Arenzana-Seisdedos et al. 2008) and is characterized by a distinctive 30 amino acids long C-terminus peptide. This peptide contains as much as 18 basic residues, nine of which are clustered into three putative ‘BBXB’ HS-binding domains. As shown by NMR spectroscopy, this C-terminal peptide (residues 69–98) is characterized by an important flexibility, and was highly disordered in solution, while the first 68 residues of CXCL12 γ have a structure very similar to that of CXCL12 α with a typical CK fold (Laguri, Arenzana-Seisdedos et al. 2008). Binding assays in which reducing end biotinylated HP, HS or DS were captured on top of a streptavidin coated sensor chip, showed that CXCL12 γ interacts not only with HP and HS (as the α and β isoforms) but also with DS.

On the CXCL12 γ core region, the most perturbed residues form a continuous surface, from R20 to R41. On the C-terminal extension, most of the residues were perturbed by the interaction in particular residues 83–97, demonstrating that the C-terminal extension was strongly involved in GAGs recognition, and specific mutations within these domains were found to decrease the binding reaction. Specific mutations within both the core domain and the C-terminal sequence were found to inhibit the binding (Laguri, Arenzana-Seisdedos et al. 2008).

The biochemical characterization of the CXCL12-HS complex showed that, in that particular system, the GAGs binding domain and the receptor binding site are spatially distant, and any mutations that prevent binding to either one did not affect the recognition of the other. In addition, the observation that CXCL12 α and γ mostly differ by their ability to bind GAGs provides a useful system of investigation. The comparison of the activity of these two naturally occurring variants, without the need of using mutant forms of the CK should give

rise to a better understanding of the importance of GAGs in mediating CK localization in vivo (Rueda, Richart et al. 2012).

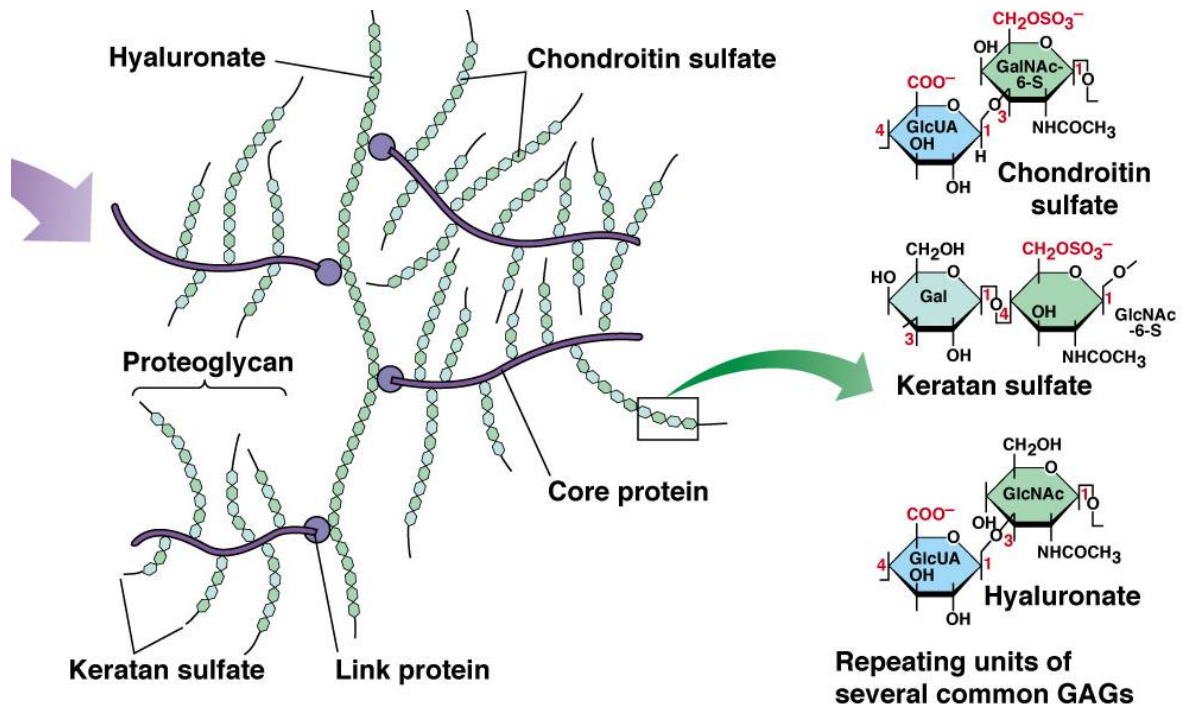


Fig 4. Example of chemical differences between GAGs (Bertoni, 2015).

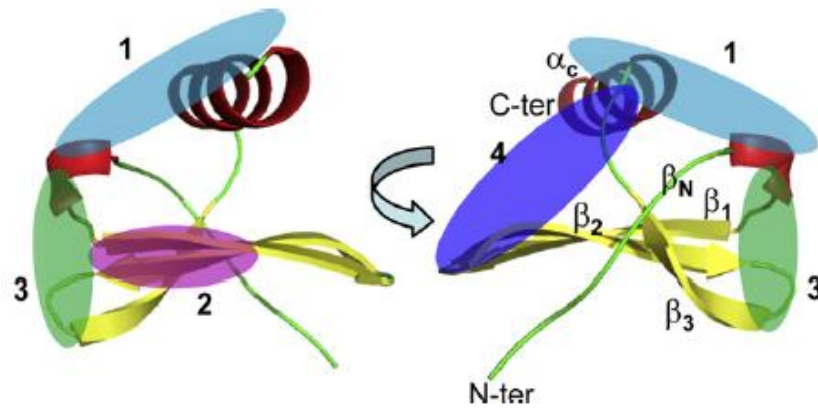


Fig 5. Binding epitopes on GAGs. The figure shows surface topology and ribbon diagrams for CKs that were biochemically characterized to identify the domain important for GAGs binding. Those residues are labeled and highlighted in cyan, magenta, green and blue.

I.5 Interaction of CKs with receptors

CKs act by binding specialized receptors on the target cell surface, named CKRs (ChemoKines Receptors). These receptors are also grouped into four families, CXCR, CCR, XCR, and CX3R, based on the CK family they bind (Bachelierie, Ben-Baruch et al. 2014).

Similar to the challenges associated with structurally characterizing CKs-GAGs interactions, determining structures of CKs in complexes with CKRs is also challenging, in this case because the receptors are conformationally flexible 7-TM proteins (see below in II.4b). Thus mutagenesis coupled with binding and functional assays have dominated efforts to determine molecular details of binding and activation. Moreover this question is further confounded by the established promiscuity found in the ligand-receptor interactions that may occur between the multiple members of the CK family. As shown in Table 2, CKs may bind to various receptors, but it may not be too surprising that sharing the same structural basis may give rise to some degree of CKR promiscuity (Kunkel 1999).

Early work on CXCL8 by Clark-Lewis revealed the critical role of the CK N-terminus in receptor activation and that receptor binding and activation could be uncoupled (Clark-Lewis, Schumacher et al. 1991). Specifically, N-terminal modifications (deletions or mutations) were identified that converted CXCL8 from an agonist into an antagonist (Moser, Dewald et al. 1993). Subsequent studies of many other CKs also supported the generality of this phenomenon (Clark-Lewis, Kim et al. 1995). Moreover, naturally occurring proteolytic modification of CKs N-termini was discovered as a natural mechanism for regulating CKs functions (Moelants, Mortier et al. 2013). On the receptor side, mutagenesis studies revealed the general trend that the N-termini of GPCRs are also important for binding to the structured CK “core domain” (Monteclaro and Charo 1997, Pease, Wang et al. 1998). Together, these findings gave rise to a paradigm referred to as the two-site model of receptor binding/activation, in which the receptor N-terminus interacts with the CK core domain (CK recognition site 1, CRS1), while the N-terminus of the CK interacts with the receptor ligand-binding pocket (CK recognition site 2, CRS2) (Fig 6). This paradigm has guided the field for many years, even in the absence of high-resolution structural information. Consistent with this model, an NMR study of CXCL12 in the presence of detergent solubilized-CXCR4 demonstrated the ability of the small molecule antagonist compound, AMD3100, to specifically dislodge the CXCL12 N-terminus from its binding site on CXCR4 without

displacing the bound CK core domain (Kofuku, Yoshiura et al. 2009). Since AMD3100 binds to the TM binding pocket (Gerlach, Skerlj et al. 2001), the logical conclusion was that the CXCL12 N-terminus binds in the pocket as well, and that the CRS1 core domain and CRS2 N-terminal interactions can be at least partially decoupled.

1.5a Structural determinants of CK-CKR interaction

Since the earliest studies of CXCL8 by Clark-Lewis' group (Clark-Lewis, Schumacher et al. 1991) and then on CXCL12 (Crump, Gong et al. 1997), the general concept has emerged that the N-termini of CKs are key signaling domains. It was also proposed that the N-termini sequences can mark the CKs function with Glu-Leu-Arg (ELR) sequences for CXC angiogenic CKs (e.g. CXCL1–8) whereas most non-ELR CXC CKs are angiostatic (e.g., CXCL9–11, CXCL4, CXCL13) with the notable exception of CXCL12 which contradicts this assumption (Strieter, Polverini et al. 1995).

Nevertheless, studies of CCL2, CCL5, CCL9, CCL19, CXCL10 and CXCL12 CK variants have confirmed the importance of the N-terminus of these CKs for inducing signaling but not binding to their respective receptors some signaling-death CK mutants retaining high-affinity interactions with their receptors.

For example, deletion of seven residues from the N-terminus of CCL2 results in a CCR2 antagonist (Hemmerich, Paavola et al. 1999). The N-terminus of all CKs studied to date is believed to activate the receptor subsequent to the recognition and binding steps. Although cleavage of the N-terminal first lysine of CXCL12 results as expected in a loss of function that does not induce Ca²⁺ mobilization, β -arrestin recruitment and arrestin-dependent MAP kinase phosphorylation, surprisingly, the mutant CK maintains the potency to induce CXCR4-dependent G α -i protein activation thus acting as a partial agonist (Levoye et al. *unpublished*).

In CCL5, if the N-terminal serine is preceded by a methionine the resulting molecule is a potent antagonist (Proudfoot, Power et al. 1996). Likewise, for the CCR2-binding CCL2₇ the whole 10-residues in the N-terminus preceding the first cysteine are involved in receptor binding and activation. Deletion of the N-terminal glutamate results in a marked reduction in activity and that of the first two residues results in the conversion from an agonist to an antagonist. Interestingly, deletion of the first N-terminal residue leads to a mutant CCL2 protein that acquires a novel activity toward eosinophils, which become responsive to the

mutant CK but presumably through binding to CCR3 (i.e. Ca²⁺ mobilization and actin polymerization) (Zhang, Rutledge et al. 1994).

Certain motifs in the N-terminus of CKs were found to correlate with specific function: CXC CKs containing N-terminal ELR sequences are angiogenic (e.g., CXCL1–8), whereas most non-ELR CXC CKs are angiostatic (e.g., CXCL9–11, CXCL4, CXCL13), with one notable exception: CXCL12.

In the CK, the N-loop region that follows the first two cysteines and connects the N-terminus to the β -sheet region through the single turn of a 310 helix (Fig 2) is the major receptor-binding site, and the sequence therein confers receptor specificity. In CXCL8 residues YSKPF (13-17) confer slightly greater specificity toward CXCR1 over CXCR2 (Schraufstatter, Barritt et al. 1993, Williams, Borkakoti et al. 1996). In CXCL1, the residues LQGI (15-18) confer specificity only to CXCR2. Switching these regions in CXCL8 and CXCL1 results in a reversal of receptor binding and activation by the chimeric proteins (Lowman, Slagle et al. 1996). In CXCL12, the sequence RFFESH (12-17) confers specificity to CXCR4. A chimeric molecule generated by replacing the N-terminus and N-loop region of CXCL1 with that of CXCL12 results in a CXCR4 agonist with only sevenfold less potency than wild-type CXCL12 (Crump, Gong et al. 1997).

The type I or type III turn connecting the first and second β -strands have also been implicated in receptor binding (Beall, Mahajan et al. 1996, Hemmerich, Paavola et al. 1999). Following the 30s loop is the second β -strand, which has a significant number of cationic residues. In most CXC and CC CKs, the C-terminus of the second β -strand has a lysine or arginine. This region of the CKs is speculated to be the GAGs binding site (as mentioned in I.4) (Sadir, Baleux et al. 2001).

Little is known about the involvement of the third β -strand in CK activity. Finally, the C-terminal α -helix of CKs has been shown to modulate the activity of at least three CKs, CCL2 (Zhang, Rutledge et al. 1994), CXCL1 (Roby and Page 1995) and CXCL12 (Luo, Luo et al. 1999), but in general it is not believed to be involved in receptor activation.

An alternative approach toward defining receptor-binding epitopes includes the characterization of the electrostatic surface potential of the CK, an approach that has been used to probe the growth hormone agonist-receptor system (Clackson and Wells 1995).

Changes in the surface area of this region brought about by mutating residues that contribute to the bulge, result in lowered binding affinities of the CK agonist for its receptor, particularly for CCL5 and CXCL12 (Clark-Lewis, Kim et al. 1995, Pakianathan, Kuta et al. 1997).

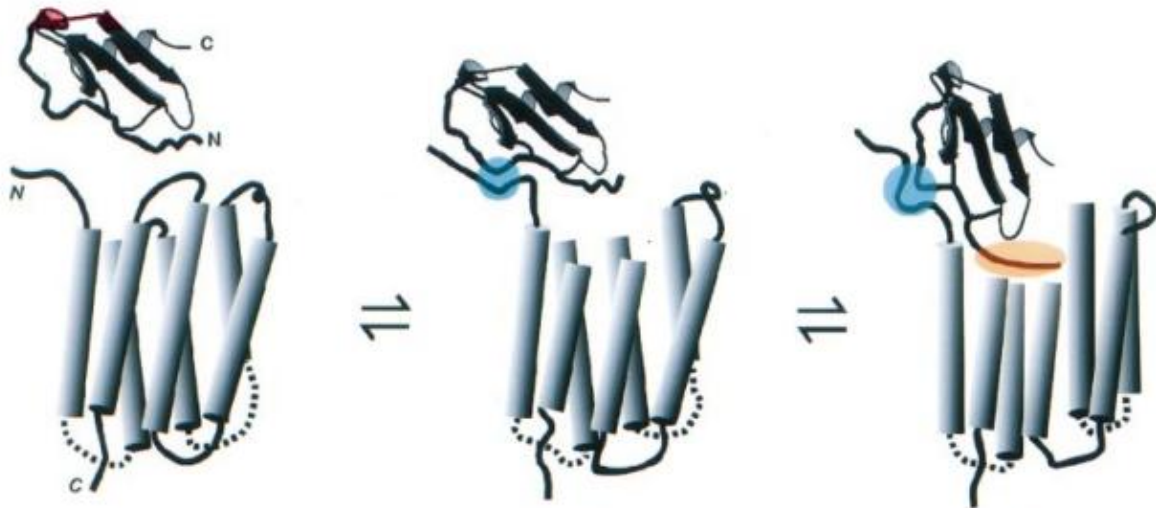


Fig 6. Two-steps mechanism for CK-CKR interaction (Crump, Gong et al. 1997).

1.5b CK recognition site CRS1 and CRS2 interactions with the receptor

As described above, the first interaction thought to occur between CK and receptor is binding of the receptor N-terminus to the CK core domain (CRS1). CRS1 docking of the CK is then thought to orient the CK N-terminal signaling domain in a manner that enables it to bind to the CRS2 TM pocket (Fig 6). Ideally, one would have structures of CKs in complex with intact receptors to understand this recognition process. However, the challenge of working with membrane receptors, has historically led to a divide and conquer approach, with focus on the more tractable CRS1 interactions that can be recapitulated as soluble complexes. These studies have provided important insights into the structural role of tyrosine sulfation (sTyr), a frequent post-translational modification observed in the N-termini of many CKRs. Specifically many groups have utilized NMR methods to investigate CRS1 interactions of CKs with peptides corresponding to CKR N-termini (Skelton, Quan et al. 1999, Veldkamp, Seibert et al. 2008, Millard, Ludeman et al. 2014).

In all studies, the CKR peptides bind on the same face of the CK, and show interactions with the N-loop as expected from mutagenesis studies. Skelton and coworkers were able to determine a structure of CXCL8 in complex with a peptide from the N-terminus of CXCR1, which was modified with hexanoic acid to increase its affinity (Skelton, Quan et al. 1999). Two subsequent studies utilized sulfated receptor peptides; sulfation generally increases the affinity of CKs for their receptors and thereby permitted structure determination (Veldkamp, Seibert et al. 2008, Millard, Ludeman et al. 2014). Veldkamp and coworkers reported the structure of an N-terminal sulfopeptide derived from CXCR4 bound to a “disulfide-locked” dimer of CXCL12 in a 2:2 complex, while Millard and coworkers revealed the structure of a peptide from CCR3 bound to a CK monomer, CCL11, in a 1:1 complex.

In all three complexes, some common interactions were observed; specifically, the receptor peptides were found at a CK interface formed by the N-loop and $\beta 2$ - $\beta 3$ strands and where present, the sTyr_s formed salt bridge interactions with homologous basic residues in the $\beta 2$ - $\beta 3$ hairpin of the CK (e.g. R47/K47). However the receptor peptides differ quite dramatically in their orientation on the CK surface (Stephens and Handel 2013). The CXCR1: CXCL8 structure is closest to what one might expect in order to accommodate CRS2 interactions in intact CKR:CK complexes since the receptor C-terminus points in the direction of the CK N-terminus. CXCR1: CXCL8 is also most similar to the orientation of the CXCR4 N-terminus on the surface of CK vMIP-II in the structure of an intact CXCR4: vMIP-II complex (described in the I.5c section) (Qin, Kufareva et al. 2015). Quite the opposite, the CXCR4: CXCL12 complex cannot be reconciled with the expected CRS2 interaction as it suggests that the CK N-terminal signaling domain points away from the receptor binding pocket (Kufareva, Stephens et al. 2014). One possible explanation for these differences is that structural rearrangements occur after binding CRS1 in order to engage CRS2, and that these rearrangements differ from complex to complex. Another possibility for the incompatible orientation of the receptor peptide in the CXCR4: CXCL12 structure is that it is derived from a disulfide-locked dimer structure. As dimers of CXC CKs have been shown to bind their respective receptors with high affinity and to function as partial agonists (Veldkamp, Peterson et al. 2005, Nasser, Raghuwanshi et al. 2009), the CXCR4: CXCL12 structure may therefore better reflect the CK dimer complex. In support of an alternative structure for the monomer bound form of CXCL12, a separate study using disulfide crosslinking to determine distance restraints between N-terminal residues in intact CXCR4 with monomeric CXCL12 led to a model in which the receptor peptide is oriented in the opposite direction from the dimeric

CXCR4: CXCL12 NMR structure, and more compatible with the expected interaction of the CK N-terminus with the TM CRS2 domain of the intact receptor (Kufareva, Stephens et al. 2014).

High-resolution structures of complexes with intact receptors will obviously be needed to understand how CK monomers and dimers bind their receptors. Nevertheless, the described NMR studies provide insight into the structural role of sTyr. Furthermore, the disulfide-locked dimer of CXCL12 is under investigation as an antimetastatic biotherapeutic, due to its oligomerization-enhanced serum stability over wild-type CXCL12 (Takekoshi, Ziarek et al. 2012). Finally, the CXCR4: CXCL12 complex motivated investigations of the druggability of the CRS1 interaction, however it remains to be seen whether CRS1-targeted compounds can be identified that have sufficient potency for overcoming the CRS2 interaction and sufficient specificity, given the sequence and structural homology of CKs.

1.5c Receptors structural determinant

The importance in the CKRs of conserved extracellular disulfide bridges and aromatic residues in their extracellular loop 2 (ECL2) for ligand binding and activation was also shown. For example in CCR8 receptor mutagenesis showed that the 7-TM receptor conserved disulfide bridge (7TM bridge) linking TM helix III and ECL2 is crucial for CK and small molecule action, whereas the conserved disulfide bridge between the N-terminus and TM-VII is needed only for CKs action. Furthermore, two distinct aromatic residues in ECL2, Y184 (Cys+1) and Y187 (Cys+4), are crucial for the binding of the CC CK CCL1 (agonist) and MC148 (antagonist), but not for that of the small molecule (Barrington, Rummel et al. 2016). This aromatic cluster appears to be present in a large number of CC CKRs and thereby could play a more general role to be exploited in future drug development targeting these receptors. The same critical involvement of the second ECL and N-terminal domain for CK binding was showed for CCR5, whereas the TM helix bundle is involved in receptor activation. CK domains and residues important for CCR5 binding and/or activation have also been identified, but the precise way by which CKs interact with and activate CCR5 is presently unknown. The binding and functional properties of CK variants onto wild-type CCR5 and CCR5 point mutants on the extracellular domains (E172A, R168A, K191A, and D276A) strongly affected the binding of CCL3 but had little effect on CCL5 binding. However, a CCL3/CCL5 chimera, containing the CCL3 N-terminus and the CCL5 core, bound to these mutants with an affinity similar to that of CCL5 (Blanpain, Doranz et al. 2003). Several CCR5 mutants affecting TM

helices 2 and 3 (L104F, L104F/F109H/F112Y, F85L/L104F) reduced the potency of CCL3 by 10–100 fold with little effect on its activation by CCL5. However, the CCL3/CCL5 chimera, containing the CCL3 N-terminus and the CCL5 core, which retains the CCL5 affinity (Blanpain, Doranz et al. 2003), activated these CKRs mutants with a potency similar to that of CCL3. These results suggest that the core domains of CCL3 and CCL5 bind distinct residues in CCR5 extracellular domains, whereas the N-terminus of CKs mediates receptor activation by interacting with the TM helix bundle (CRS2) (Blanpain, Doranz et al. 2003).

1.5d CXCL12 - CXCR4 interactions

Binding of CXCL12 to CXCR4 triggers typical activation of G-proteins and β -arrestins dependent pathways of a GPCR (see below in Ch. II), that cannot solely account for the wide spectrum of physiological activities of this axis (Busillo and Benovic 2007). It is rather hypothesized that such functional complexity originates from various determinants, including the cell context, the available receptor interactome (receptorosome), together with the reported ability of both CXCL12 and CXCR4 to oligomerize (Bachelierie, Ben-Baruch et al. 2014). This is also consistent with observations made in live cells, from the use of biophysical techniques, including bioluminescence and fluorescence resonance energy transfer, which indicate that monomers, dimers and higher-order oligomers of CXCR4 might coexist (Ferre, Casado et al. 2014). Such as emerged for other GPCRs, CXCR4 dimers might display unique ligand-binding properties and functional selectivity.

Theoretically, CXCR4 in dimer is able to accommodate one ligand or a dimer of ligands, forming a 2:1 or a 2:2 CXCR4-CXCL12 complex, respectively. However, a forced-dimeric CXCL12 was shown to behave as a partial agonist capable of inducing intracellular calcium mobilization but not chemotaxis (Veldkamp, Peterson et al. 2005). Thus, when considering the full agonist signaling process, the question of whether the CXCR4-CXCL12 complex has a 1:1 or 2:1 preferential stoichiometry with regard to the stability of their respective tridimensional structures and signaling properties remains an open question (Kufareva, Stephens et al. 2014) (Fig 7).

The interaction of CXCR4 with its agonist CXCL12 implicates residues in the N-terminus and ECL2 of the receptor. The three N-terminal residues Glu-14, Glu-15, and Tyr-21 of CXCR4 are of particular importance for the binding to CXCL12 (Doranz, Orsini et al. 1999, Brelot, Heveker et al. 2000). Residues in ECL2, especially the acidic sequence of Glu-179,

Ala-180, Asp-181, and Asp-182, are critical for activation of CXCR4 (Doranz, Orsini et al. 1999). CXCL12 has a high positive charges potential, and a significant amount of this positive charges, so it is possible that the interactions of the positive charges on CXCL12 with the negatively charged regions on CXCR4 contribute to the association of these two proteins. Negatively charged residues of CXCR4 also appear to be involved in the interactions with the basic V3 loop of gp120, the envelope glycoprotein of X4 HIV-1 strains (Kajumo, Thompson et al. 2000). Mutagenesis of specific residues on the CXCR4 N-terminus, ECL1, and ECL2 identified glutamate and aspartate residues, specifically Glu-15, Glu-32, Asp-97, Asp187, and Asp-193, as being important for interactions with X4 HIV-1 gp120 (Chabot, Zhang et al. 1999, Kajumo, Thompson et al. 2000). Other residues such as Asn-11, Arg-30, and Arg-188 have also been identified as binding determinants for HIV-1 gp120. Based on chimeric mutants that involved replacing ECL2 of CXCR2 with the corresponding loop from CXCR4, the observation was made that the CXCR4 ECL2 was able to confer the chimeric CXCR2 with HIV-1 coreceptor function (Lu, Berson et al. 1997). Since both CXCL12 and the V3 loop domain of X4 HIV-1 gp120 that interact with CXCR4 have a high positive potential, and since the interacting domains of CXCR4 are mostly negatively charged, it is likely that the interactions between CXCR4 and these molecules are highly driven by charges complementarity.

In the TM cavity of the receptor, several negative residues were found by site-directed mutagenesis studies to be important for CXCR4 signaling, including the region from Glu179 to Asp182 in ECL2, the residues Asp97 in TM helix 2 (TMH2), Asp187 in ECL2, Glu288 in TMH7, Tyr190 in ECL2 and Glu268 in ECL3 (Doranz, Orsini et al. 1999, BreLOT, Heveker et al. 2000, Zhou, Luo et al. 2001, Tian, Choi et al. 2005).

It should be emphasized that the three residues Asp97, Asp187 and Glu288 of CXCR4 are also critical for the CK interaction with the CRS2 region (BreLOT, Heveker et al. 2000). More specifically, they probably make contacts with the CXCL12 first two residues Lys1 and Pro2 (Heveker, Montes et al. 1998), from the disordered N-terminus (residues 1–8) critical for CXCR4 activation, as suggested by the recent crystal structure of CXCR4 with the viral CK vMIP-II (Qin, Kufareva et al. 2015).

These evidences are consistent with a two-site, two-step proposed model for the CXCR4-CXCL12 interactions, where the CXCL12 motif RFFESH first binds the receptor N-terminus, and then the CK N-terminus KPVLSYR enters the buried cavity within the CXCR4 TM

helices, triggering receptor activation, probably mediated by a change in the conformation of the receptor TM helices (Crump, Gong et al. 1997, Kofuku, Yoshiura et al. 2009). Nevertheless, despite the important recent structural data, there is not yet a comprehensive characterization of the quaternary structures and dynamics of the CXCR4-CXCL12 associations, as the receptor like other GPCRs is difficult to express in sufficient quantities and to purify, because of its instability and ability to aggregate in detergent, and displays a reduce polar surface area for crystallization. With few exceptions, ligand-receptor structures require appropriate ligands that provide sufficient stability for purification and stabilization into well-defined crystallizable constructs, making the best targets those identified in drug discovery with high affinity.

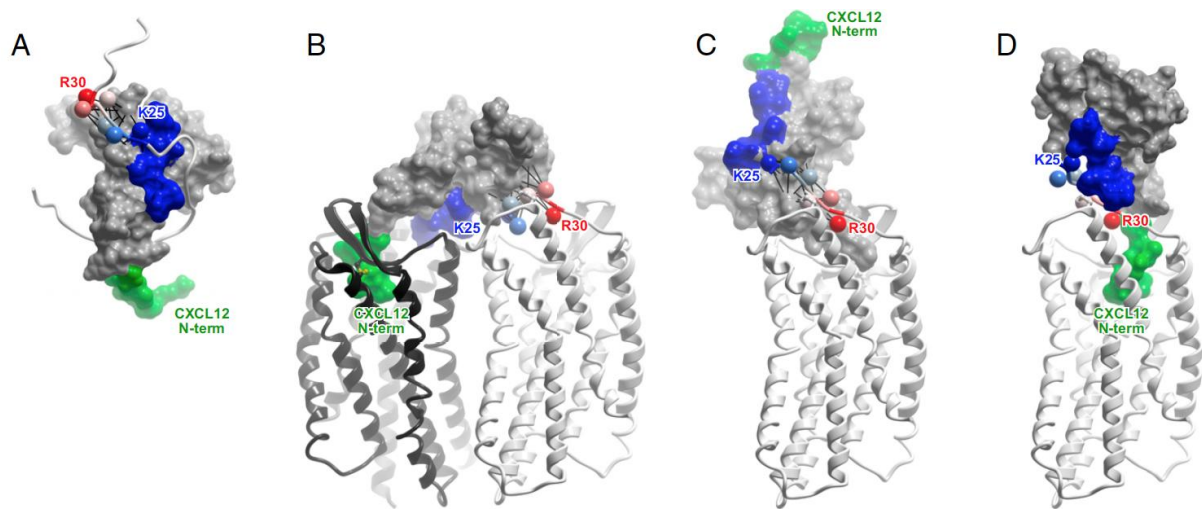


Fig 7. Molecular models and experimental designs of CXCR4: CXCL12 interaction. (A) NMR structure of CXCL12 (skin mesh) in complex with the N terminus of CXCR4 (residues M1–K38, ribbon). CK N-terminus (green) and N-loop (blue) correspond to the expected interactions with the receptor in CRS2 and CRS1, respectively. Receptor residues K25–R30 are shown as spheres, labeled, and colored in order from blue to red. (B) A 2:1 model of the receptor:CK interaction accommodates both NMR proximity restraints (black lines) and the mutagenesis data. (C) A hybrid 1:1 model that accommodates NMR proximity restraints (black lines) is inconsistent with mutagenesis and with the two-site interaction hypothesis, because the N terminus of the CK invariably points away from the receptor CRS2. (D) A 1:1 model consistent with the two-site interaction hypothesis contradicts NMR proximity restraints, as receptor residues K25–R30 are directed along the CK N-loop toward its N-terminus. (Kufareva, Stephens et al. 2014)

Given the clear role of CXCR4 in pathogenesis (exp. HIV and cancer metastasis), much efforts have been deployed successfully permitting the first structure determination of a CKR in 2010. CXCR4 was crystallized with two different synthetic ligands, a small molecule antagonist, IT1t, and a 16-residue cyclic peptide antagonist, CVX15 (Wu, Chien et al. 2010). While the overall geometry of the receptor resembled structures of other GPCRs with the typical seven-helix topology, CXCR4 revealed for the first time the large acidic binding pocket of the receptor relative to other solved GPCR structures, which is consistent with the fact that the natural ligands are basic proteins. IT1t occupies a small part of the cavity (430 Å³) in the minor sub-pocket defined by TM helices I, II, III and VII and is stabilized by contacts with a number of polar side chains implicated in binding CXCL12. CVX15 fills a much larger fraction of the binding pocket (2200 Å³), particularly the major sub-pocket (TM helices III–VII). It is stabilized by interactions with some similar but also many different receptor side chains as IT1t, including residues identified as important for binding CXCL12. Along with pharmacological data, these structures suggest that IT1t and CVX15 act as orthosteric antagonists by interfering with the CXCR4-CXCL12 CRS2-driven interaction, while occupying very different parts and fractional volumes of the binding pocket. As described below, the CXCR4:CVX15 complex provided insight for the modeling of the interactions of CXCR4 with HIV-1 gp120 (Wu, Chien et al. 2010).

In total, five structures of IT1t and CVX15 complexes were solved, and all demonstrated that CXCR4 forms dimers with a roughly consistent dimer interface involving TM helices V and VI. These finding corroborated a wealth of cell-based studies suggesting that CXCR4 forms homo- and heterodimers (Stephens and Handel 2013) as proposed for other class A GPCRs, although mostly by the way of overexpression systems (Stephens and Handel 2013).

They also raised the question of whether the stoichiometry of CKR-CK complexes is 1:1 as historically envisioned, or 2:1, which also seemed feasible and consistent with the two-site model, but contradict by a study which favored the 1:1 CKR-CK stoichiometry and by extension the binding of two CKs on one CXCR4 dimer (Kufareva, Stephens et al. 2014). Thus the structure of CXCR4 and more generally CKRs dimers and their contribution to the receptors functions remain an open question awaiting proofs for their existence in physiological settings.

1.5e Structure of CXCR4 bound to the viral CK antagonist, vMIP-II

In 2015, the first structure of a CKR, CXCR4, in complex with a CK (vMIP-II) was solved, and provided detailed insight into the recognition of CKRs by their natural ligands (Qin, Kufareva et al. 2015). vMIP-II is a virally encoded high affinity antagonist for CXCR4 and was chosen over the main CK ligand, CXCL12, because the CK requires G-protein coupling for high affinity binding (Nijmeijer, Leurs et al. 2010), but antagonists generally do not. Additionally, vMIP-II binds promiscuously to both CC and CXC receptors, and is a CC like-CK; thus along with the solved structure of CCR5, the CXCR4vMIP-II structure was expected to provide insight into the specificity of CKs for CC and CXC CKRs.

In the vMIP-II-bound state, CXCR4 formed dimers that were spatially similar to those in the IT1t- and CVX15-bound structures; however, the structure of the complex confirmed the 1:1 stoichiometry anticipated from prior studies (Kufareva, Stephens et al. 2014), with ligand occupancy of both receptor subunits (Qin, Kufareva et al. 2015). The structure generally conforms to the concept of the two-site model in that the CK core domain interacts with the receptor N-terminus (CRS1) while the CK N-terminus binds in the CRS2 TM binding pocket of the receptor. Surprisingly, however, in contrast to the two-site model, where the expectation was that these two sites would be decoupled, the interaction between CXCR4 and vMIP-II involves an extensive contiguous interface, necessitating the introduction of an intermediate region termed CRS1.5 (Fig 8). In fact, every residue of the CK N terminal domain and N-loop (residue 1–16) as well as residues in the third β -strand, interact with the receptor (Qin, Kufareva et al. 2015).

Part of the CXCR4 N-terminus (residues 1–22 involving the key sulfated tyrosine, sTyr21), is missing from the electron density. Nevertheless, the visible CRS1 region (CXCR4 residues 23–27) showed interactions with the CK N-loop, as expected from numerous mutagenesis studies, and with the β 3-strand in the CK core domain. Moreover, as the electron density stops just before sTyr21, it was fairly straightforward to generate a model containing sTyr21, which suggested a compelling interaction with nearby R46 of the CK, similar to the basic residue interactions reported for sTyr in (CXCR4: CXCL12)₂ and CCR3: CCL11 complexes. In CRS1.5, CXCR4 forms an anti-parallel β -sheet with the di-cysteine motif of vMIP-II. Finally, in CRS2 the CK makes numerous interactions within the binding pocket including many residues known as determinants of vMIP-II binding or CXCR4: CXCL12 binding and activation. The N-terminus of vMIP-II overlaps with the binding site of IT1t in the

CXCR4:IT1t complex, while it only partially overlaps with CVX15, reflecting the structural plasticity of CXCR4 and its ability to accommodate diverse ligands via overlapping but distinct interfaces (macrophage migration inhibitory factor (MIF), extracellular ubiquitin (eUb), antimicrobial protein human β 3-defensin (HBD-3), HIV (Human Immunodeficiency Virus) protein gp120 (Pawig et al. 2015)).

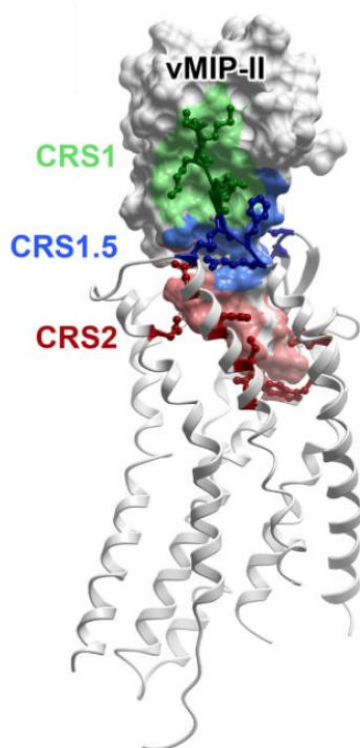


Fig 8. Interaction between CXCR4 and vMIP-II. The interaction is mediated by a contiguous interface containing CRS1 (green), CRS2 (red) and CRS1.5 (blue). The receptor is shown as a ribbon, receptor residues making substantial contacts with CK are shown as sticks, and vMIP-II is shown as a surface mesh (Qin, Kufareva et al. 2015).

vMIP-II is also a high affinity antagonist of CCR5, and the availability of the CCR5:Maraviroc (Lagane, Garcia-Perez et al. 2013) structure along with CXCR4:vMIP-II facilitated modeling of the complex (Qin, Kufareva et al. 2015). An important sequence difference relates to the presence of two adjacent sTyrs (sTyr14 and sTyr15) (Farzan, Mirzabekov et al. 1999) proximal to the conserved N-terminal Cys residue in the two receptors. These CCR5 sTyrs along with E18 are predicted to interact with the basic residues in the vMIP-II N-loop (K17 and R18) and β 2- β 3 loop (R46 and R48). By comparison, CXCR4 has only the single proximal sTyr21, but in concert with two acidic groups (D22 and E26), makes similar interactions with the basic residues on the vMIP-II surface. These CRS1 models thus provide a plausible explanation for the unusual ability of vMIP-II to interact with both a CC and CXC CKR. By contrast, the CRS1 interaction between CXCR4 and the CXCL12 monomer is predicted to be quite different due to absence of basic residues in the CXCL12 N- and β 2- β 3 loops. Instead, the backbone of CXCR4 N-terminal residues S23 and M24 lie in a groove formed by the N- and β 2- β 3- loops, and position sTyr21 at the top of the core domain where it interacts with backbone amides of the CXCL12 residues R20 and A21. Notably, these interactions mimic the placement of a small molecule CXCR4: CXCL12 inhibitor (Smith, Ogert et al. 2014) as well as sulfate groups and ions observed in several CXCL12 X-ray structures (Murphy, Yuan et al. 2010), which adds support for the CRS1 predictions.

However, additional structures will be required to confirm the above-mentioned models and also to better understand the structural basis for the generally strict recognition of CC CKs for CC receptors and CXC CKs for CXC receptors.

Chapter II

Preamble on GPCRs

All CKRs are G-protein-coupled receptors (GPCRs) (Fig 9), a superfamily of 7-TM helix proteins, which encompasses approximately 791 genes encoding for the six different receptor subtypes. Currently, all 19 known CKRs belong to the class A (rhodopsin-like) family of GPCRs and are classified into four main subfamilies based upon which CKs they bind: CC, CXC, XC, and CX3C receptors. Many of the CKRs are promiscuous and bind to several CKs within their family and allow for tailored CK response and redundancy (Bachelierie, Ben-Baruch et al. 2014).

In this section it will be discussed the structure and oligomerization of GPCRs, focusing on CXCR4 and CXCR7/ACKR3 receptors of the CXCL12 CK and the drug design on these receptors using structural information. To simplify we will talk about the hypothesis of dimer forms, but higher form of oligomers organization can be formed.

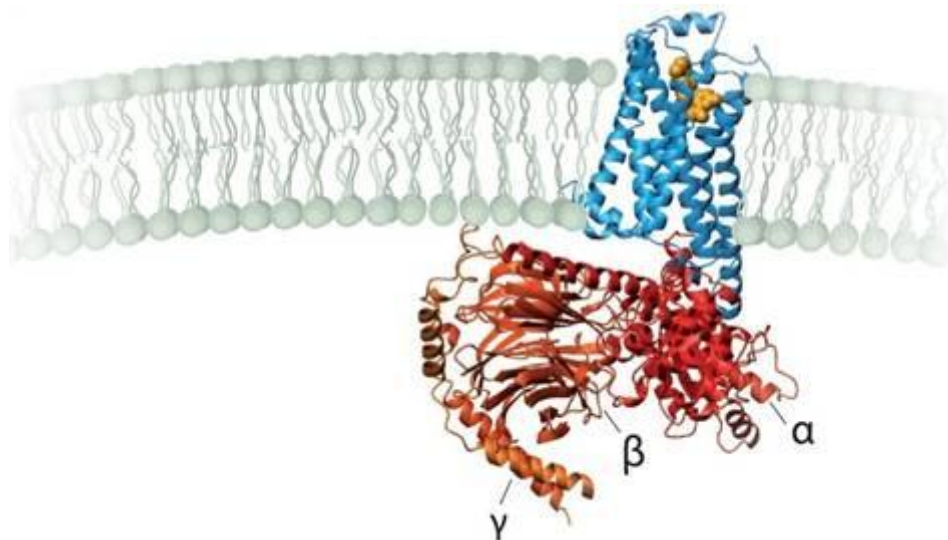


Fig 9. The GPCRs 7-TM helix class A subfamily illustrated by the β -adrenergic receptor structure coupled to heterotrimeric G-proteins (Rasmussen, Choi et al. 2007).

Name	Conventional name	Chromosome	Gene size (kb)	Number of exons	Number of amino acids	Ligands
CXCR						
CXCR1	IL8R1; IL8RA; CMKAR1	2q35	4.15	2	350	CXCL6, CXCL8,
CXCR2	IL8R2; IL8RB; CMKAR2	2q35	11.96	4	360	CXCL1, CXCL2, CXCL3, CXCL5, CXCL6, CXCL7, CXCL8, MIF
CXCR2P1	CXCR2P; IL8RBP	–	–	1	–	–
CXCR3A	IP10-R; MigR; CMKAR3;	Xq13.1	2.60	2	368	CXCL4, CXCL4L1, CXCL9, CXCL10, CXCL11,
CXCR3B	IP10-R; MigR; CMKAR3;	–	–	2	415	–
CXCR3-alt	–	–	–	2	267	–
CXCR4	LAP3; LCR1	2q21	2.60	2	352, 356	CXCL12, MIF
CXCR5	BLR1; MDR15	11q23.3	12.43	2	372, 327	CXCL13
CXCR6	BONZO; CD186	3p21.26	4.87	2	342	CXCL16
CCR						
CCR1	CKR1; CMKBR1; MIP1aR	3p21	6.63	2	355	CCL3, CCL3L1, CCL3L3, CCL5, CCL7, CCL14, CCL15, CCL16; CCL23,
CCR2A	CMKAR2; CD182; CKR2B	3p21.31	7.18	2	374	CCL2, CCL7, CCL8, CCL13,
CCR2B	CKR2B	–	–	3	360	–
CCR3	CKR3; CMKBR3	3p21.3	24.32	3	355	CCL2, CCL5, CCL7, CCL8, CCL11, CCL13, CCL15, CCL24, CCL26, CCL28,
CCR4	CKR4; CMKBR4; ChemR13	3p24	3.33	2	360	CCL17; CCL22
CCR5	CMKBR5; CKR5	3p21.23	6.06	3	352	CCL3, CCL3L1, CCL3L1, CCL4, CCL4L1, CCL4L2, CCL5, CCL7, CCL11, CCL13
CCR6	BN-1; DCR2; CKR-L3	6q27	27.33	3	374	CCL20
CCR7	BLR2; CMKBR7; EB11	17q12-q21.2	11.71	3	378	CCL19, CCL21
CCR8	CKRL1; CMKBR8; CMKBTER1	3p22	3.97	2	355	CCL1
CCR9A	GPR-9-6; GPR28	3p21.3	16.67	4	359	CCL25
CCR9B	GPR-9-6; GPR28	–	–	–	357	CCL25
CCR10	GPR2	17q21.1-q21.3	2.42	2	362	CCL27, CCL28
XCR						
XCR1	CCXCR1; GPR5	3p21.3	7.68	2	333	XCL1, XCL2
CX3CR						
CX3CR1	CMKDR1; GPR13; CCRL1	3p21.3	18.24	4	355, 387, 362	CX3CL1
DECOYRECEPTORS						
CXCR7	RDC1; GPR159	2q37.3	12.61	2	362	CXCL11, CXCL12, MIF
CCRL1	CCR11; CCBP2; VSHK1; CCX-CKR; PPR1	3q22	5.29	2	350	CCL19, CCL21, CCL25
CCRL1P1	dJ509I19.4	6q23.3	–	1	–	–
CCRL2	CKRX; CRAM-A; CRAM-B; HCR	3p21	2.29	3	344, 256	CCL5, CCL19
CCBP2	D6	3p21.3	57.81	3	384	CCL2, CCL3, CCL4, CCL4L1, CCL4L2, CCL5, CCL7, CCL11, CCL13; CCL17, CCL22,
DARC	Duffy; FY	1q21-q22	2.48	2	336, 338	CCL2, CCL5, CCL7, CCL11, CCL13, CCL15, CCL17, CCL18, CCL22, CXCL1, CXCL2, CXCL3, CXCL5, CXCL6, CXCL7, CXCL8, CXCL11
FORMYL PEPTIDE RECEPTOR						
FPR2	FPRL1; LXA4R; FMLP-R-II; FMLPX; FPR2A; FPRH1	19q13.3-q13.4	9.33	3	351	CCL23, Lipoxin A4, serum amyloid A, β amyloid peptide A β 42, SAA, MMK, Hp-(2-20)

Tab 2 CKRs and their corresponding CKs (Blanchet, Langer et al. 2012).

II.1 Current CK Receptors Crystal Structures

In 2010, the first CKRs (CXCR4) was crystallized at the Scripps Research Institute (Wu, Chien et al. 2010). The CXCR4 crystal structure was the first peptide GPCR to be solved and represented a major breakthrough in this field. It is important to note that several structural changes were used in order to stabilize the receptor for crystallography (Rasmussen, Choi et al. 2007, Jaakola, Griffith et al. 2008, Warne, Serrano-Vega et al. 2008, Wu, Chien et al. 2010). Using the T4 Lysozyme (T4L) strategy, intracellular loop 3 (ICL3) of CXCR4 was replaced with T4L along with truncating its C-terminus and using point mutations for stabilizing the receptor structure (Wu, Chien et al. 2010). While these techniques have been used successfully to crystallize GPCRs, they may introduce or induce unnatural receptor conformations (Fanelli and De Benedetti 2011, Arnatt and Zhang 2013). However, GPCR crystal structures have provided a wealth of knowledge concerning ligand binding that have confirmed or disproved modeling and mutagenesis data. More importantly, CXCR4 was crystallized in two dimeric forms with resolutions of 2.5 and 3.2 Å and these two dimers had either a TM5 and TM6 interface or a TM3 and TM4 interface respectively (Wu, Chien et al. 2010).

The antagonist ligands used in the CXCR4 crystallization process were the small molecule antagonist IT1t and a cyclic peptide antagonist CVX15. In the presence of either ligand the binding pocket was shown to be much larger than expected and comparable to that of class A aminergic receptors, which accommodates large endogenous peptide agonists. The increase in the size of the binding pocket presumably led to both antagonists binding shallowly near ECL2, which is important in ligand recognition and receptor activation (Clark-Lewis, Kim et al. 1995). While the large binding pocket may make computational modeling and docking difficult, the CXCR4 crystal structure has permitted subsequently numerous studies using structural-based drug design in order to make new CXCR4 ligands (Xu, Zhao et al. 2015).

In 2013 the CKR CCR5 (CCR5) was crystallized by Tan et al. and revealed both similarities and differences within the CKRs family (Tan, Zhu et al. 2013). Like for CXCR4, the binding pocket of CCR5 was large due to its endogenous peptide agonists, but the co-crystallized antagonist, maraviroc, occupied a deeper domain into the pocket as compared to CXCR4 in complex with IT1t or CVX15. Due to the depth of the maraviroc binding-pocket, ECL2 did not play a role in binding, which contrasts with the CXCR4 structure (Tan, Zhu et al. 2013). Such variation could reflect differences in the mechanisms of binding of the used antagonists

or general structural differences between the receptors. Nevertheless, both CKRs crystal structures constitute strong bases for the rational design of new ligands, for modeling ligand binding and for the homology modeling of other CKRs.

In addition the CXCR4 crystal structure allows for a unique approach to model CKRs dimers. Previously, the only methods to model GPCRs dimers were either sequence-based or docking-based, which are largely pragmatic and easily biased (Fanelli and De Benedetti 2011). However, crystallized GPCRs homodimers offer a new method for modeling other GPCRs dimers. For example, using the crystal structure of the bovine rhodopsin homodimer, Gorinski et al. were able to model the serotonin receptor 1A homodimer by superimposing monomer units over the dimer, based upon sequence similarities (Gorinski, Kowalsman et al. 2012). When combined with site directed mutagenesis, the work supported a TM4/TM5 interface for serotonin receptor 1A homodimers (Gorinski, Kowalsman et al. 2012).

Presumably different receptor types may lead to different dimer interfaces; therefore, it is critical to choose a dimer template that is similar to the target dimer being modeled. The CXCR4 homodimer crystal structure thus allows for other CKRs dimers to be more confidently modeled. For example, the CCR5- μ opioid receptor (MOR) heterodimer was recently modeled utilizing the CXCR4 homodimer crystal structure as a template (El-Hage, Dever et al. 2013). The heterodimer was based on the TM5-TM6 dimer interface that was seen in the IT1t-bound CXCR4 crystal structure (Wu, Chien et al. 2010). Using this method the heterodimer of CCR5 with the MOR model showed favorable electrostatic and hydrophobic interactions between receptors and could represent a possible conformation of the heterodimer. Furthermore, such models can be used to map the interactions between ligands and their respective receptors dimers (Lagane, Garcia-Perez et al. 2013).

II.2 Oligomerization of GPCRs

Originally, it was postulated that GPCRs function in a monomeric fashion and that there was a general stoichiometry of 1:1 for the receptor ligand interaction. However, increasing evidence has begun to support the possibility that GPCRs may act in dimeric, or even oligomeric assemblies (George, O'Dowd et al. 2002).

One of the first observations of dimerization in rhodopsin-like GPCRs was reported for β -adrenergic receptors; it was seen that binding of one ligand decreased the binding of a second one (Hebert, Moffett et al. 1996). This type of “cross-talk,” or better known as negative

cooperativity, occurs when a dimer bound ligand either inhibits the binding or signaling of a second ligand to the dimer pair.

One of the earliest methods for investigating potential dimers were co-immunoprecipitation (co-IP) techniques, subsequently used as preliminary techniques to study the potential homo- and hetero-dimerization of numerous GPCRs (Bai 2004).

Another important technique for studying the likelihood of GPCRs dimerization/oligomerization is Förster Resonance Energy Transfer (FRET) based on bioluminescence or fluorescence (BRET and FRET respectively) detection.

For FRET detection, the two receptors suspected of dimerizing are tagged with two different fluorescent proteins: i.e., a cyan and a yellow fluorescent protein (CFP and YFP, respectively). It is essential for the FRET that the excited state of one fluorescent protein (donor chromophore) can transfer energy at a very specific distance to an acceptor chromophore thus permitting it to emit its unique excitation wavelength. In order for FRET to take place, the two chromophores (and associated proteins) must be in close proximity ($< 100 \text{ \AA}$) (Pfleger and Eidne 2005).

This technique can also be coupled with bioluminescence emitted from the reaction of the luciferase enzyme and its substrate, such as firefly luciferase and luciferin through BRET (Angers, Salahpour et al. 2000). The combination of co-immuno-precipitation and FRET/BRET methods has led to a network of potential GPCRs homodimers and heterodimers being discovered (Bai 2004). Recent improved variant of this technique is the Homogeneous Time-Resolved FRET (HTRF or TR-FRET) allowing analyzing oligomers in native conditions (Albizu, Cottet et al. 2010, Cottet, Faklaris et al. 2012, Faklaris, Cottet et al. 2015) for vasopressin, oxytocin and dopamine receptors (Cottet, Albizu et al. 2010, Hounsou, Margathe et al. 2015) (Fig 10).

HTRF methods are currently used to study GPCRs oligomerization. This method is based on receptors labeled with rare elements, called lanthanides and more specifically with terbium and europium. Lanthanides exhibit long-lasting light emission and although this photoluminescence is, strictly speaking, neither fluorescence nor phosphorescence, HTRF has been assimilated to FRET. Lanthanides are inserted in a cage, which plays the role of lanthanide carrier in order to increase brightness of fluorophores and protects lanthanides from quenching by water molecules (Selvin 2002). HTRF improves the FRET technology according to three principal parameters:

- ❖ The temporal selectivity: upon excitation, lanthanide fluorescence half time is in the range of 1 ms while it is in the range of few nanoseconds for classic fluorophores. The introduction of a time delay (typically around 50 μ s) between the excitation and the fluorescence signal detection allows discriminating between short-lived and longer-lasting fluorescence. Therefore all shortlived fluorescence provided by the medium the biological preparation or the direct excitation of the acceptor will be eliminated by the time delay. Only the long-lived fluorescence resulting from the donor or the acceptor engaged in a FRET process will be measured after the time delay.
- ❖ The spectral compatibility: both europium and terbium cryptates are excited at 300–350 nm. They both exhibit an important Stoke shift and complex emission spectra with multiple fluorescent peaks. This makes europium and terbium cryptates compatible with deep red Cy5- or dy647-like fluorophores to perform FRET. Moreover because of the emission peak around 490nm, terbium-cryptate is also compatible with fluorescein-like fluorophore as acceptor.
- ❖ The orientation independence: by contrast to BRET or FRET performed with classic fluorophores the dependence of HTRF to the relative orientation of the fluorophore is very weak because the lanthanide emission is not polarized. The relative orientation of the acceptor cannot impact the R0 more than 12% due to the random orientation of the lanthanide cryptate donor (Selvin 2002).

Various approaches have been developed using cryptates of lanthanides for receptor labeling. First experiments were performed with antibodies against small tags fused to the N-terminus of the receptor and randomly labelled with lanthanides cryptates or compatible acceptors. Because of the reversibility of the GPCRs labeling and the steric hindrance generated by fluorescent antibodies, alternative approaches based on fusion of self-labeling proteins (also called suicide enzyme) have been developed. Their size (23 kDa for the Snap-tag; 33 kDa for the Halotag for example), the covalent labeling of GPCRs and the efficiency of the labeling makes this strategy interesting to label receptors. Expression of two receptors fused to different self-labeling proteins allows orthogonal labeling of receptors to study GPCR heterodimerization.

In addition to these biochemical techniques, evidence for the existence of GPCRs dimers has been obtained using both GPCRs crystallization and atomic-force microscopy techniques (Fotiadis, Liang et al. 2003, Wu, Chien et al. 2010, Manglik, Kruse et al. 2012). Using atomic-force microscopy, oligomer formations of rhodopsin were observed, providing the first visualization of GPCRs oligomerization (Fotiadis, Liang et al. 2003). Additionally, both CXCR4 and MOR were observed to form dimers within their crystals. While these observed dimers might partially be due to an artifact of the crystallization process, it did lend credence to GPCR dimerization (Wu, Chien et al. 2010, Manglik, Kruse et al. 2012).

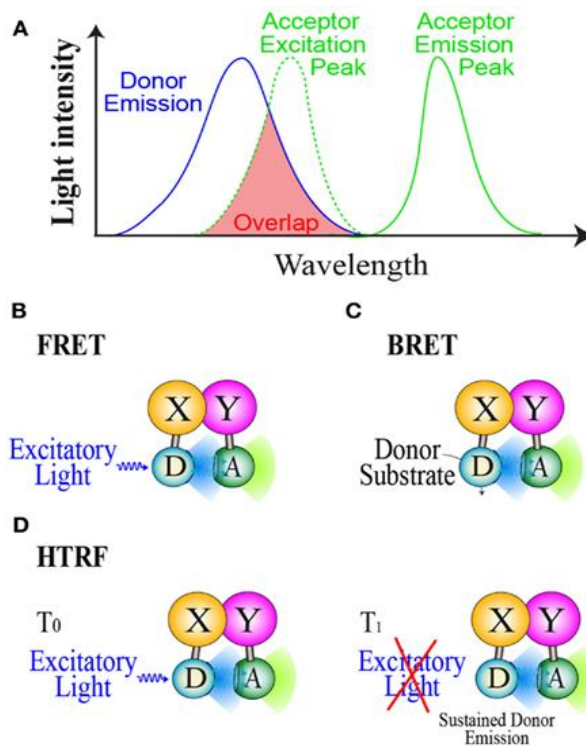


Fig 10. Resonance energy transfer methods. (A) Basic properties of donor/acceptor compatible couple in order to gain resonance energy transfer. Principles of (B): the FRET, (C): The BRET, and (D): the HTRF methods (Couturier and Deprez 2012).

Several types of interactions between dimerized GPCRs have been proposed, and two main dimerization models have subsequently been described: a contact dimer model, and a domain-swapped dimer, which proposes that TM6 and TM7 are exchanged between monomers to form a dimer (Gouldson, Higgs et al. 2000). The contact dimer model proposes that dimerization occurs through direct contact between the different interfaces of GPCRs helices: TM5/TM6, TM3/TM4, and TM1/TM2 interfaces have been observed (Wu, Chien et al. 2010, Manglik, Kruse et al. 2012). Both dimerization models have been supported by mutation and computational studies, but given the observations of GPCRs crystal structures, the contact dimer may represent a more realistic model.

An important potential consequence of GPCRs dimerization is its effect on receptors signaling and function with notably the possible outcome of positive and negative cooperativity (Fig 11). Positive cooperativity occurs when binding of a ligand to one receptor leads to partial, full, or enhanced activation of the second receptor. It may also occur when two ligands bind both receptors promoting an enhanced activity. Negative cooperativity can occur when one bound ligand leads to either inhibition of the binding of a second ligand to the dimer, or inhibition of signaling from a second bound ligand (Bai 2004).

Functionally, heterodimers may increase the diversity of signaling pathways downstream GPCRs. For example, it was proposed that within the CCR2-CCR5 heterodimer, the receptors are able to couple with $G\alpha_q/11$, which is not the case for the individual receptors (Mellado, Vila-Coro et al. 2001). A similar effect was reported for the MOR-delta opioid receptor heterodimer; the signaling of which is not sensitive to pertussis toxin whereas the receptors are sensitive, thus coupled $G\alpha_i$ proteins, when expressed alone (George, Fan et al. 2000). These results suggested that the heterodimer could couple to different G-proteins than the original monomers. Dimerization of GPCRs may also affect receptor desensitization and internalization. Similarly, CKRs dimers led to unique pharmacological profiles, which can add upon the already intricate receptor-ligand interactions. Targeting these CK dimer interactions may lead to unique therapies with marked potential. Nevertheless, only class C-GPCRs are in obligatory dimer forms and all findings on the potential of class A receptors to form dimers need to be demonstrated in native conditions.

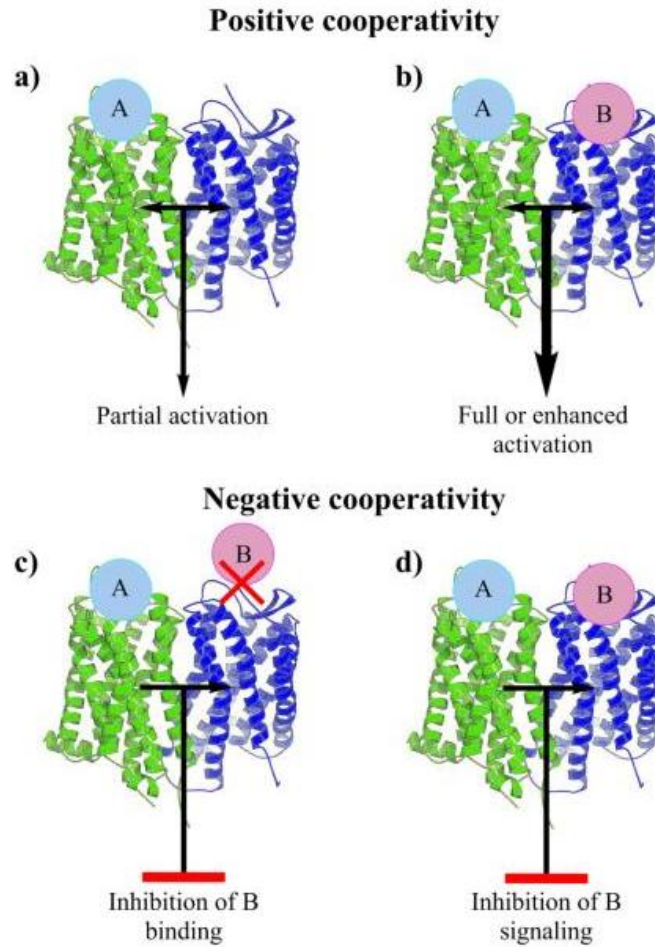


Fig 11. Positive and negative cooperativity in GPCRs dimerization. a) Agonist A binding to one GPCR (in green) results in partial activation of another GPCR (in blue). b) When two agonists, A and B, bind to the GPCRs there will be enhanced activation, synergism. c) In negative cooperativity binding of A to one GPCR (in green) leads to inhibition of the binding of B to another GPCR (in blue) and thus ligand B-related signaling. d) Binding of A leads to inhibition of signaling from the GPCR (in blue) even with B bound to it (Zhang et al, 2014).

II.3 Atypical Chemokine Receptors

Historically, some receptors defined as non-signaling receptors were named decoy based on their capacity to act as molecular trap for cytokines or CKs thus regulating their availability for signaling receptors (Mantovani, Locati et al. 2001). Decoy receptors have been described as a general strategy conserved in evolution from *Drosophila* to man to tune inflammation by regulating cytokine, CKs and growth factor availability (Mantovani, Locati et al. 2001, Klein and Mlodzik 2004).

Structural, functional, and genetic evidence supported the idea that a group of “silent” CKRs act as decoy and scavenger receptors for CKs, and this new class of receptors is emerging as a mechanism to control CKs both in homeostasis and in pathology. Four CKRs structurally related to signaling receptors but unable to activate G-proteins have been identified so far, each of them interacts with a specific set of CKs: Duffy Antigen Receptor for CKs (DARC) (Lee, Koszinowski et al. 2003), D6 (Fra, Locati et al. 2003, Comerford and Nibbs 2005), CXCR7 (Balabanian, Lagane et al. 2005), and CCX-CKR (Gosling, Dairaghi et al. 2000), recently renamed as Atypical Chemokine Receptors (ACKRs) ACKR1, ACKR2, ACKR3 and ACKR4 respectively (Tab 3)(Bachelierie, Ben-Baruch et al. 2014). Detailed structure-function analysis of these so-called ‘silent’ receptors is not available yet, but it is interesting to note that structural determinants required for receptor signaling, including key residues in the second ICL involved in the activation of G-proteins, are not conserved in these receptors.

Name	Aliases	UniProt accession code	Ligands
ACKR1	DARC, Duffy antigen, Fy antigen, CD234	Hs: Q16570 Mm: Q9QU16	CCL2, CCL7, CCL8, CCL13, CCL14, CCL16, CCL17, CCL22, CXCL1, CXCL5, CXCL6, CXCL7, CXCL8, CXCL9, CXCL11, CXCL13
ACKR2	D6, CCR9, CCR10, CCBP2, CMKBR9	Hs: 000590 Mm: Y12879	CCL2, CCL3, CCL3L1, CCL4, CCL5, CCL7, CCL8, CCL11, CCL13, CCL14, CCL17, CCL22
ACKR3	CXCR7, RDC1, CMKOR1	Hs: P25106 Mm: P56485	CXCL11, CXCL12
ACKR4	CCRL1, CCX-CKR, CCR11	Hs: Q9NPB9 Mm: Q92413	CCL19, CCL21, CCL25, CXCL13

Tab 3. The new nomenclature for ACKRs (Bachelierie, Ben-Baruch et al. 2014).

II.3a Atypical ChemoKine Receptor 3: CXCR7

CXCR7, recently renamed ACKR3 (Bachelierie, Ben-Baruch et al. 2014), is the most recently identified CKR, binding with high affinity to both CXCL11 and CXCL12 CKs. CXCR7/ACKR3 was originally identified from a dog thyroid cDNA (Libert, Parmentier et al. 1989) and known for many years as an orphan GPCRs named RDC1. I will keep the CXCR7 nomenclature in this introduction.

CXCR7 was suggested to be a CKR based on sequence homology and its genomic localization (Heesen, Berman et al. 1998) and de-orphanized 10 years ago as a receptor for CXCL12 and CXCL11 (Balabanian, Lagane et al. 2005, Burns, Summers et al. 2006). The discovery of CXCR7 as a second receptor for CXCL12 refuted previous conclusions that CXCL12 and CXCR4 constitute a unique ligand-receptor pair while CXCR3 was known to bind CXCL9 and CXCL10 in addition to CXCL11 (Ma, Norsworthy et al. 2009).

Despite its original inclusion in the systematic CKRs nomenclature, CXCR7 is not coupled to G-protein activation and was shown to function more as an ACKR than a GPCR. Indeed, the initial findings showing CXCR7 signaling and involvement in mediating cell migration (Balabanian, Lagane et al. 2005) have not been consistently reported across the different cell types and model systems (Burns, Summers et al. 2006, Sierro, Biben et al. 2007, Boldajipour, Mahabaleshwar et al. 2008, Levoye, Balabanian et al. 2009). CXCR7-mediated downstream cellular responses and its role in cell survival and adhesion (Miao, Luker et al. 2007, Wang, Shiozawa et al. 2008) were linked to its ability to recruit β -arrestin resulting in MAP-kinase activation (Luker, Gupta et al. 2009, Rajagopal, Kim et al. 2010).

CXCR7 seems to have critical functions in normal development, as evidenced by embryonic lethality of mice lacking this gene, and the receptor is also upregulated in disease processes including cancer and stroke (Sierro, Biben et al. 2007, Schonemeier, Schulz et al. 2008). The main function of CXCR7 is likely to be, in line with its ACKR nature, the sequestration of CXCL12 and possibly CXCL11. This function of CXCR7 is essential in controlling the formation of CXCL12 gradients required for instance for the optimal migration of primordial germ cells in the zebrafish development (Dambly-Chaudiere, Cubedo et al. 2007, Valentin, Haas et al. 2007, Boldajipour, Mahabaleshwar et al. 2008). Internalization, sequestration and scavenging of CXCL12 and CXCL11 by CXCR7 was later shown in mammalian models such as mouse heart valves and human umbilical vein endothelial cells (Naumann, Cameroni et al.

2010). The latter may explain a feature observed in CXCR7 deficient mice involving heart valve malformation, which causes perinatal or early postnatal lethality (Sierro, Biben et al. 2007, Gerrits, van Ingen Schenau et al. 2008). Scavenging function of CXCR7 was also reported in breast cancer cells (Luker, Steele et al. 2010). It is not clear how this activity in cancer cells translates into tumor growth and metastasis-promoting effects exerted via CXCR7 in several experimental tumors, including breast and lung cancers. In addition to tumor parenchyma, CXCR7 is also overexpressed in the tumor vasculature (Miao, Luker et al. 2007). CXCR7 expression in vascular endothelium may have a function distinct from CK scavenging. It is possible that CXCR7, by analogy to DARC, may also be involved in CKs transcytosis. CXCR7 promotes growth and metastasis of breast and lung cancer cells in animal models, and similar results have been obtained in a mouse model of prostate cancer (Miao, Luker et al. 2007, Wang, Shiozawa et al. 2008). Expression of CXCR7 in tumor cells may contribute to excessive signaling through CXCR4, a landmark of the pathophysiology of WHIM syndrome, the CXCR4-gain of function of which is also associated with tumor development (Balabanian, Lagane et al. 2005). Whereas these studies strongly link CXCR7 to cancer biology, functions of CXCR7 and its transduction pathways and activities promoted in cells after ligand binding remain poorly defined and still controversial.

II.3b Signaling of CXCR7

Some studies suggest that CXCR7 functions as a signaling receptor, promoting cell adhesion, chemotaxis, and activation of downstream signaling molecules such as AKT (i.e. a serine/threonine-specific protein kinase also known as Protein kinase B) (Balabanian, Lagane et al. 2005, Burns, Summers et al. 2006, Valentin, Haas et al. 2007, Chow, Brotin et al. 2010). However, these effects of CXCR7 have not been identified consistently in different model systems (Infantino, Moepps et al. 2006). CXCR7 shares high structural homology with related CXCRs such as CXCR4 (Fredriksson, Lagerstrom et al. 2003), but lacks the conserved DRYLAIV-motif in ICL2 that is critical for G-proteins binding and has a DRYLSIT motif instead. While CXCR7 has been shown to interact constitutively with G-proteins, the receptor does not initiate calcium fluxes characteristic of most CKRs signaling (Levoye, Balabanian et al. 2009, Decailot, Kazmi et al. 2011).

It is able however to promote intracellular signaling through recruitment of β -arrestin in a ligand-dependent manner (Balabanian, Lagane et al. 2005, Rajagopal, Kim et al. 2010),

eliciting both ERK (i.e. extracellular signal–regulated kinases ERK1/2 or MAP kinases) and AKT activation (Kumar, Tripathi et al. 2012).

Sierro et al. showed that ERK phosphorylation is triggered by CXCR4/CXCR7 heterodimers, whereas other studies have shown that homomeric CXCR7 complexes induce ERK activation (Decaillot, Kazmi et al. 2011). One study showed that CXCL12 signals through CXCR7 to promote T-cell migration, an effect that was reduced by a CXCR7-blocking antibody (Balabanian, Lagane et al. 2005), whereas in another study, blockade of CXCR7 with a neutralizing antibody or the small-molecule compound CCX733 showed no impact on CXCL12-promoted T-cell chemotaxis (Hartmann, Grabovsky et al. 2008). In B-lymphocytes, Humpert et al. showed that blocking CXCR7 in in vitro-differentiated cells enhances CXCR4-dependent migration of B cells toward CXCL12, implicating CXCR7 in the migration of B cells during maturation (Humpert, Tzouros et al. 2012). Both CXCR4 and -7 were found to form homo- and hetero-dimers (Sierro, Biben et al. 2007, Lagane, Chow et al. 2008, Luker, Gupta et al. 2009) in which, depending the context, CXCR7 has been reported to enhance CXCR4-mediated chemotaxis in response to CXCL12 (Decaillot, Kazmi et al. 2011) or to inhibit it (Levoye, Balabanian et al. 2009). See below.

II.3c The C-terminus domain of CXCR7

CXCR7 constitutively internalizes and recycles from the cell membrane, a property that relates to the function of CXCR7 in scavenging CXCL12 and CXCL11. Deletion of the intracellular tail of CXCR7 dramatically changes localization of the receptor. Though the receptor predominantly localizes into intracellular compartments, including early and late endosomes, lysosomes, and potentially the endoplasmic reticulum (Shimizu, Soda et al. 2000, Boldajipour, Mahabaleshwar et al. 2008, Luker, Steele et al. 2010), progressive truncation of the C-terminus of CXCR7 (up to 16 amino acids, CXCR7-346) redistributed mutant receptors from endosomes to the cell membrane. This shift in the localization of CXCR7 most likely increases the numbers of receptors available at the cell surface to bind CXCL12 (truncated mutants are not affected in their affinity for CXCL12), as shown by flow cytometry, Gaussia luciferase complementation assay, and binding of radiolabeled CXCL12 (Zabel, Wang et al. 2009, Ray, Mihalko et al. 2012).

Changes in subcellular localization and internalization of CXCR7 are due to disrupting interactions with β -arrestin-2, which is interacting with CXCR7 constitutively and in a ligand-

dependent manner, and is known to promote receptor internalization and intracellular accumulation of CK ligands (Kalatskaya, Berchiche et al. 2009, Luker, Gupta et al. 2009). Loss of functional β -arrestin-2 reduced CXCR7-dependent uptake of CXCL12 from the extracellular space, establishing that β -arrestin 2 is necessary for the decoy function of the receptor. Beside, β -arrestin-2 interactions with CXCR7 are required for CXCL12-induced CXCR7-dependent activation of ERK1/2. Of note, the kinetics of this signaling are consistent with prior reports for β -arrestin-2-dependent signalling by other 7-TM receptors (Drake, Violin et al. 2008). Using the Protein fragment Complementation Assay (PCA), Luker et al. have show that the receptor preferentially interacts with β -arrestin-2 relative to β -arrestin-1 (Luker, Gupta et al. 2009). Unlike its brief interaction with CXCR4, CXCL12-induced β -arrestin-2 association with CXCR7 increased over time. Thus CXCR7 C-terminus interaction with β -arrestin-2 may be a critical determinant of CXCR7 signaling and decoy functions.

II.3d Interaction between CXCR7 and its ligands

It is currently accepted that CXCR7 has two CK ligands, CXCL12 and CXCL11, which may also bind to CXCR4 and CXCR3, respectively. CXCL12 binds to CXCR7 with greater affinity than to CXCR4 ($K_d = 0.4$ nM versus 3.6 nM (Crump, Gong et al. 1997, Balabanian, Lagane et al. 2005)), and CXCR7 binds CXCL12 with 10- to 20-fold greater affinity than CXCL11 (Burns, Summers et al. 2006). Of note, the binding affinity of CXCL12 for CXCR7 was suggested to be reduced by the expression of CXCR4 at the membrane implicating that within CXCR4/CXCR7 heterodimers the affinity of CXCR7 for CXCL12 could be reduced thus favoring the binding of CXCL12 to CXCR4 (Burns et al. 2006).

Previous studies have defined the N-terminus of CXCL12 as critical for binding and signaling through CXCR4 as truncation of the N-terminus by 2–6 amino acids abrogates receptor signaling and switches CXCL12 from an agonist to an antagonist (Loetscher, Gong et al. 1998). Amino acids 1–17 of CXCL12 are sufficient to activate CXCR4 signaling but with greatly reduced potency as compared to wild-type CK (Heveker, Montes et al. 1998, Loetscher, Gong et al. 1998). Conversion of the three arginine residues in the first 20 amino acids of CXCL12 to citrulline, which reduces total positive charges of the CK, eliminates binding to CXCR7 (Struyf, Noppen et al. 2009). However, the role of specific N-terminal amino acids of CXCL12 on CXCR7 binding and activation remain to be defined.

Combined CXCR7 receptor mutagenesis and use of TC14012 (a known antagonist of CXCR4) derivatives such as CVX15, have shown i) that TC14012 is an agonist of CXCR7 that can activate the β -arrestin pathway downstream CXCR7 and ii) similarities between the mode of binding of TC14012 to CXCR7 and that of CXCR4 to CVX15. In both cases, receptors Asp residues on ECL2 and TM6 play key roles to form salt bridges with the Arg residue of the compound (TC14012 or CVX15). In addition, Hbond (hydrogen bond electrostatic interactions) between TC14012 and CXCR7 ECL2 (instead of salt bridges in CVX15/CXCR4 interactions) are observed, so that, like in CXCR4, TC14012 roughly covers the major binding pocket (Wu, Chien et al. 2010). Of note, the identified key residues for TC14012/CXCR4 interactions are similar to those reported for other CXCR4 antagonists; namely D171 and D187 for AMD3100 with CXCR4 ECL2 (Gerlach, Skerlj et al. 2001). The role played by CXCR7 ECL2 in binding was difficult to assess. Indeed, CXCR7 ECL2 is very different from CXCR4 ECL2 in both amino acid sequence and length. Nevertheless, Hbond networks resembling those seen between CVX15 and CXCR4 were observed and it became clear that residues in CXCR7 ECL2 (R197 and S198, respectively) are important for TC14012 binding. While substitution of R197D in CXCR7 stabilized the orientation of TC14012 by creating a salt bridge with Arg1, removal of the charge with the R197A substitution failed to do so but nevertheless resulted in a much higher potency of activation by TC14012, which equaled that of CXCL12. This suggests that the repulsive force of CXCR7 R197 is the major reason for the relatively weak potency of the compound on CXCR7.

Additionally, Yoshikawa et al. have also developed an interaction model between CXCR7 and TC14012 that this time highlights positions D179 (ECL2) and D275 (TM6) as other key residues of the receptor pharmacophore (Yoshikawa, Oishi et al. 2013). Moreover modeling the interactions with T140, a TC14012 derivative, which is almost devoid of CXCR7 agonist activity identified that T140 binding to CXCR7 implicates only alternate but not simultaneous engagement of CXCR7 D179 and D275 residues. This shortcoming was adjusted by the introduction into the receptor of the above-mentioned R197D mutation in CXCR7, which led to the interaction of T140 Arg1 with D197, analogous to what was observed in the CVX15–CXCR4 crystal. These data point toward a necessity for CXCR7 agonists to concurrently interact with the upper parts of TM4 and TM6 to draw them together or, alternatively push them apart, possibly involving TM3. In CXCR4, T140 and AMD3100 are believed to exert their antagonistic effect by denying access of the N-terminus of CXCL12 to the interaction with the CRS2, thought to lie deeper in the binding crevice. CXCR7 apparently does not

require this second step to recruit arrestin because ligand/receptor interactions closest to the receptor surface seem to be sufficient to trigger CXCR7 activation, without the need for interactions deeper into the binding pocket. Indeed, these are only speculations and comparisons of the ligand binding pockets for CXCR7 and CXCR4 are still needed.

II.4 CXCR4 receptor signaling pathways

CXCR4 is a 352 amino acids rhodopsin-like GPCR that is expressed constitutively in a wide variety of tissues, including lymphatic tissues, thymus, brain, spleen, stomach, and small intestine (Nagasawa, Kikutani et al. 1994).

Binding of CXCL12 to CXCR4 activates a variety of intracellular signal transduction pathways and effector molecules that notably regulate cell survival, proliferation, chemotaxis, migration and adhesion (Fig 12).

As CXCR4 couples to the Gi family of proteins, G α i pathway is able to inhibit adenylyl cyclase as well as to activate the Src family of tyrosine kinases while liberated-G $\beta\gamma$ activate phospholipase C- β (PLC- β) and phosphoinositide-3 kinase (PI3K) ultimately leading to the regulation of processes such as gene transcription, cell migration, and cell adhesion.

After exposure to CXCL12, G-protein coupled receptors kinases (GRKs) phosphorylate the C-terminus of the receptor allowing the recruitment of β -arrestin-2 that promotes internalization of the receptor into endosomes. This process of internalization of CXCR4 is part of a process known as desensitization and attenuates activation of G-proteins. Unlike the negative effects of β -arrestins on activation of G-proteins by CXCR4, Cheng et al. showed that β -arrestin-2 significantly enhanced signaling through p42/44 MAP kinases (greater activation of β -arrestin-2 compared to the β -arrestin-1). β -arrestin-2 also control chemotaxis of cells in response to CXCL12, likely through activation of p38 MAPK. These two effects of β -arrestin-2 appear to be mediated through distinct interactions with the ICL3 and C-terminus of CXCR4, respectively (Lagane et al 2008).

The mitogen-activated protein kinase pathway (MAP kinase pathway) is another signal transduction pathway regulated by CXCR4. In response to CXCL12, CXCR4 activates the kinase MEK, the upstream activator of the p42/44 MAP kinases (an acronym for MAPK/ERK Kinase). Because p42/44 activate the same downstream signal transduction pathway, these two related kinases generally are referred to as a single effector. Activated p42/44 MAP kinases phosphorylate transcription factors including Elk-1 to increase

expression of genes that promote proliferation and survival of cancer cells.

CXCL12 and CXCR4 stimulate the PI3K pathway that subsequently activates the protein kinase AKT. Activated AKT phosphorylates a wide variety of intracellular targets, that can inhibit apoptosis and prolong survival of many different types of cancer cells. Beyond functions in promoting cell survival, AKT has also been implicated in the activity of CXCR4 on cells proliferation and migration toward a chemotactic gradient of CXCL12.

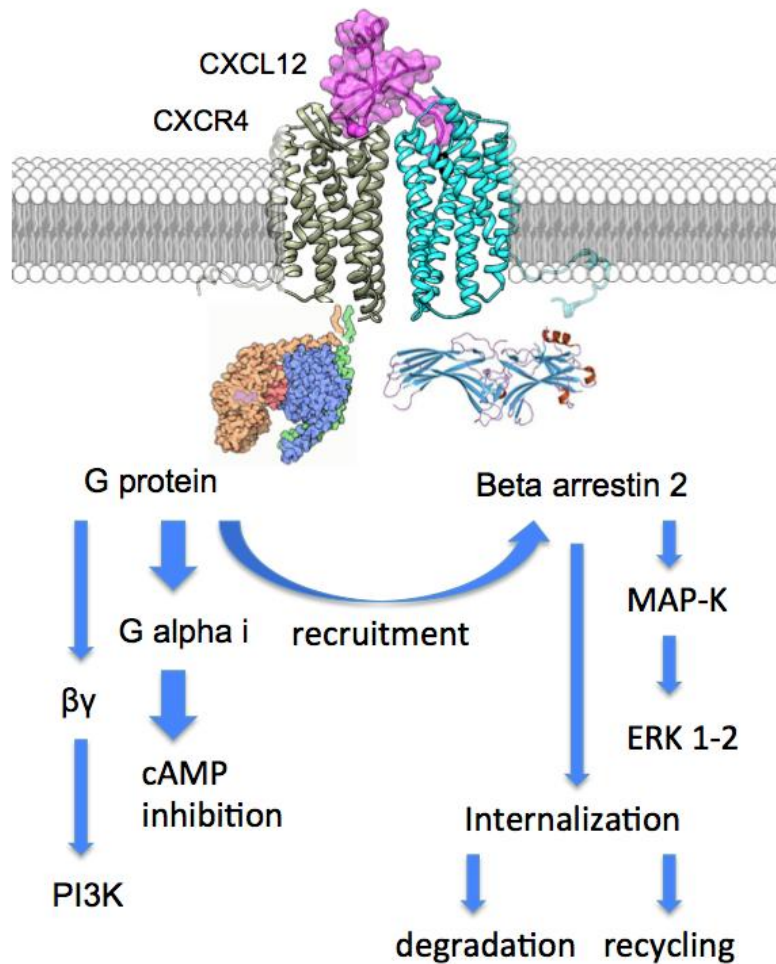


Fig 12. CXCR4 downstream signaling pathways via G-proteins and β -arrestin activation.

II.4a CXCR4/CXCR7 Hetero-oligomerization

CXCR7 functions seem to be directly or indirectly associated with CXCR4 activation (Sanchez-Alcaniz, Haege et al. 2011), and hetero-dimerization between CXCR4 and CXCR7, which has been reported in transfected cells, has been shown to modulate signaling pathways initiated through CXCL12-CXCR4 both positively or negatively (Fig 13)(Sierro, Biben et al. 2007, Levoye, Balabanian et al. 2009, Decaillot, Kazmi et al. 2011, Hartmann, Grabovsky et al. 2008). CXCR4/CXCR7 heterodimers apparently form as efficiently as the receptors homodimers (Levoye, Balabanian et al. 2009) suggesting that changes in CXCL12/CXCR4 responses during organogenesis, B cell lymphopoiesis or tumorigenesis that has been correlated to the regulation of CXCR7 expression might also arise from heterodimer formations. Such a cross-talk between CXCR7 and CXCR4 that can take place into heterodimers, and apart the decoy function of CXCR7, was also involved in the migration of primordial germ cells (Boldajipour, Mahabaleshwar et al. 2008) and lateral-line primordial cells (Dambly-Chaudiere, Cubedo et al. 2007).

Thus, although the precise mechanisms involved in such regulation remain poorly defined, the co-expression of an atypical and classical receptors as reported for other CKRs, may allow fine-tuning of cellular responses downstream of classical CKRs (Graham, Locati et al. 2012). Of note, CXCR4 has also been shown to form constitutive homodimers, but also heterodimers with distant CKRs such as CCR5 or CCR2 in heterologous systems (Issafras, Angers et al. 2002, Isik, Hereld et al. 2008). Thus although numerous evidence point to the importance of CKRs oligomerization in the fine-adjustment of various biologic responses such a process is awaiting its demonstration in native systems as for class A GPCRs.

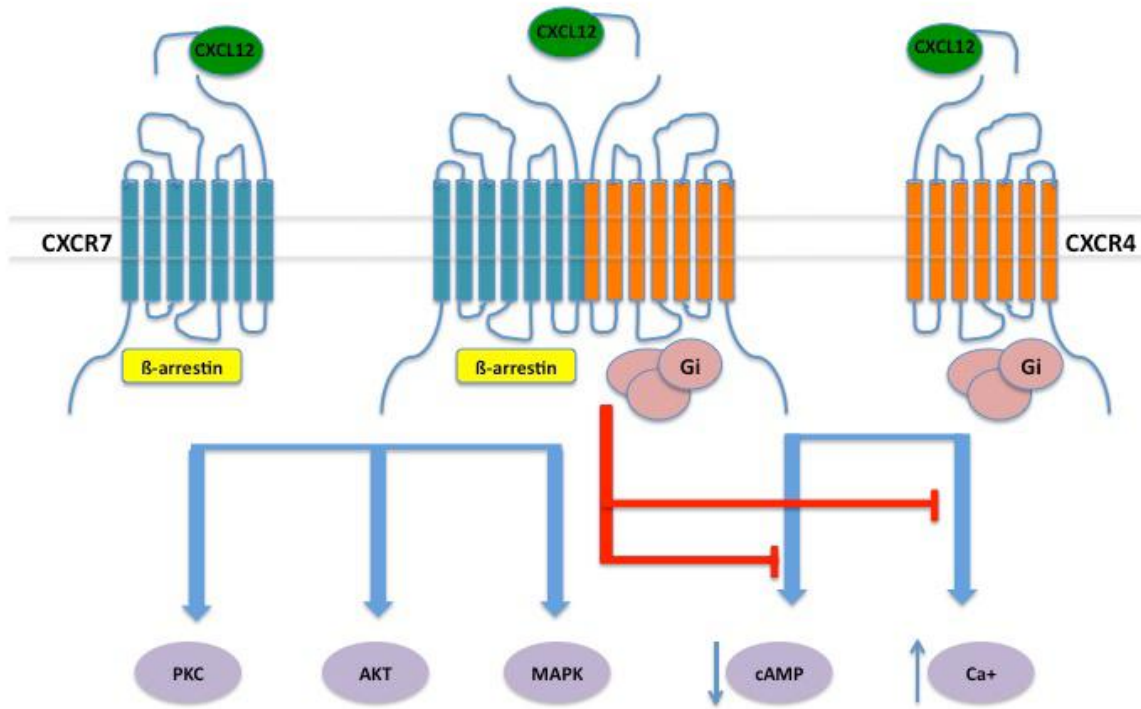


Fig 13. Heterodimerization of CXCR7 and CXCR4 can impact on CXCR4-signaling upon interaction with CXCL12. Signaling pathways described (blue lines) are shown for CXCR7. This receptor signals through β-arrestin and modulate CXCL12/CXCR4 G-protein-mediated signaling (red lines).

II.4b CXCR4 conformational heterogeneity

GPCRs, such as CXCR4, can exhibit conformational heterogeneity. The pharmacology of these receptors has long been based on two-states receptor models. In these models, ligands modulate the equilibrium between two distinct conformations (active and inactive) of the receptor. However, evidence from both cell-based and biophysical studies suggests that structurally different agonists (and partial agonists) of a given GPCR can induce distinct conformational states, rather than simply altering the equilibrium between two states (inactive and active). Furthermore, many GPCRs show a considerable amount of basal, agonist independent activity (agonist-independent conversion from an inactive (R) state to an active (R*) state); in other words, GPCRs can activate its G-proteins in the absence of an agonist (Kobilka 2007).

Accordingly, the conformational heterogeneity of CXCR4 might explain the cell-type-dependent ability of CXCR4-directed antibodies to block chemotaxis in response to CXCL12. Thus, the monoclonal antibody (mAb) most commonly used to study CXCR4 expression, the 12G5, appear to recognize only a subpopulation of CXCR4 molecules among analyzed primary cell types (Baribaud et al 2001). As a result, CXCR4 expression levels on these important cell types have been approximate to date. The factors responsible for altering CXCR4 conformation are not fully known (to cite few examples: other membrane proteins, lipid raft domains, intracellular interactions with effector molecules or post-translational modifications). For instance, CXCR4 can be post-translationally modified by sulfation of its aminoterminal tyrosines, and by a chondroitin sulfate chain at serine 18. This phenomenon may explain in part the difference in conformation, antibody specificity and function of CXCR4 (Farzan, Babcock et al. 2002).

II.4c Development of CXCR4-directed therapeutics

CXCR4 antagonists were initially developed as new potential drugs for treatment of HIV-induced disease, considering the role of CXCR4 as a co-receptor for HIV entry. Four major classes of CXCR4 antagonists can be distinguished:

- ❖ small modified peptide;
- ❖ small-molecule, such as the bicyclam AMD3100;

- ❖ antibodies directed to CXCR4;
- ❖ modified agonists and antagonists targeting CXCL12, such as Chalcone (Ziarek et al 2012).

ALX40-4C, a polypeptide of nine Arg residues, is the first CXCR4 antagonist clinically used in Phase I and Phase I/II trials in HIV-infected patients (Doranz, Filion et al. 2001). This peptide is no longer under development, because of no oral availability and lack of efficacy.

The second CXCR4 antagonist that entered clinical trial for HIV-infected patients was AMD3100, which is no longer in clinical development for this use because of no oral availability and some severe side effects. However, taking advantage of the mobilization of hematopoietic cells from the bone marrow to the blood upon blockade of the CXCL12/CXCR4 axis by AMD3100, this small molecule was recently approved by the FDA (Food and Drug Administration) for its acute administration together with granulocyte-colony-stimulating factor (G-CSF) for the mobilization of stem cells for autologous transplant in non-Hodgkin's lymphoma and multiple myeloma (Stiff et al 2009).

Development of therapeutic mAb(mAb) to CXCR4 is challenging due to the fact that CXCR4 can exhibit conformational heterogeneity. However, two different antibodies, MDX-1338/BMS93656 (<http://clinicaltrials.gov>) and ALX-0651 (<http://clinicaltrials.gov>), a llama-derived immunoglobulin single variable domain nanobody, are in Phase I/II and Phase I respectively.

The majority of CXCR4 antagonists in development induce the mobilization of hematopoietic cells, such as neutrophils, monocytes, T cells and NK cells from the bone marrow into the circulation; although this property is actually used for autologous transplantation, this may also be a severe safety issue when trying to treat chronic diseases associated to CXCR4 such as HIV infection, or immune diseases such as the WHIM syndrome due to CXCR4-gain of function mutation. The development of CXCR4 antagonists that will not induce a significant mobilization of hematopoietic cells is one potential path to overcome this difficulty.

Promisingly, novel CXCR4 antibodies (i-body) were found to inhibit CXCL12/CXCR4-dependent T cell migration and recruitment but not mobilization of hematopoietic stem cells (Katherine Griffithsa et al., 2106) and others (nanobodies) were found to behave as neutral antagonists and inverse agonists in monovalent and bivalent states, respectively (Sven Jähnichena 2010). Thus a better understanding of CXCR4 pharmacology is welcome for the development of biased antagonists with extended pharmacokinetics and pharmacodynamics.

Chapter III

Preamble on Nanobodies: the smallest natural antigen-binding fragment

Nanobodies (NBs) correspond to the variable domains of camelid heavy-chain antibodies (HCAs). HCAs were discovered in 1989 by the group of Hamers (Hamers-Casterman, Atarhouch et al. 1993), as immunoglobulin G (IgG) antibodies lacking the light chains and the first constant domain of the heavy chains (i.e., the CH1 domains) present in their conventional counterparts.

HCAs are composed therefore of only two heavy chains (Fig 14). They are synthesized by Camelidae (including camels, llamas and dromedaries) in addition to conventional antibodies and their proportion depends on the species: HCAs represent 50% of the IgG in dromedaries and camels and 25 to 45% in llamas (van der Linden, de Geus et al. 2000). The antigen-binding domain of HCAs is naturally reduced to a single domain of ~130 amino acids (~14 kDa) and therefore corresponds to the smallest available natural antigen-binding fragment: a NB, VHH or single-domain antibody. In spite of their small size, NBs bind to their antigens with high affinity (i.e. in the nanomolar range) and specificity (Dumoulin, Conrath et al. 2002).

The tridimensional structure of VHHs corresponds to a typical immunoglobulin fold (Fig. 15). It is composed of nine β -strands organized into two β -sheets, stabilized by a conserved disulphide bridge between Cys23 and Cys94 (IMGT numbering (Conrath, Wernery et al. 2003)). The amino acid sequence of VHHs presents a high degree of identity (~80%) with the human VH3 (variable domain of the heavy chain of conventional antibodies) gene family (Conrath, Wernery et al. 2003), it has however evolved to compensate for the absence of the VL domain as follows:

- ❖ Four hydrophobic amino acids conserved among all VHS are substituted by more hydrophilic residues in the VHH sequences (V42F or V42Y, G49E, L50R and W52G, IMGT numbering)(Vu, Ghahroudi et al. 1997). These amino acids are located in the framework 2, corresponding to the region of the VH domain that interacts with the variable domain of the light chain in conventional antibodies.

- ❖ The complementarity determining regions (CDRs, i.e. regions of the antibody that interact with the antigen) of VHHs are longer than those of VHS, and particularly the CDR1 and CDR3 (Fig 15). The average length of the CDR3 from human VHS is 12 residues while that from dromedary VHHs contains most frequently ~16 to 18 amino acids. Several VHHs with CDR3 longer than 25 residues have been reported (Desmyter, Transue et al. 1996). The larger size of the CDRs is believed to compensate for the absence of the three CDRs from the VLs (the antigen is recognized by only three CDRs instead of six in conventional antibodies) and therefore provide a sufficiently large antigen interacting surfaces. Moreover, the long CDR3 can form a protruding loop, allowing VHHs to bind unique conformational epitopes, such as cryptic epitopes, clefts or cavities that are generally inaccessible to conventional VH and VL pairs (Marquardt, Muyldermans et al. 2006).
- ❖ An additional disulphide bond is present in many VHH sequences, especially those originating from dromedaries; it is generally located between CDR1 and CDR3 (64%) but can also be located between CDR3 and FR2 (Conrath, Wernery et al. 2003). This disulphide bond probably restricts the flexibility of long CDRs, which is expected to be entropically counterproductive for binding, and therefore allows a strong interaction (Govaert, Pellis et al. 2012).

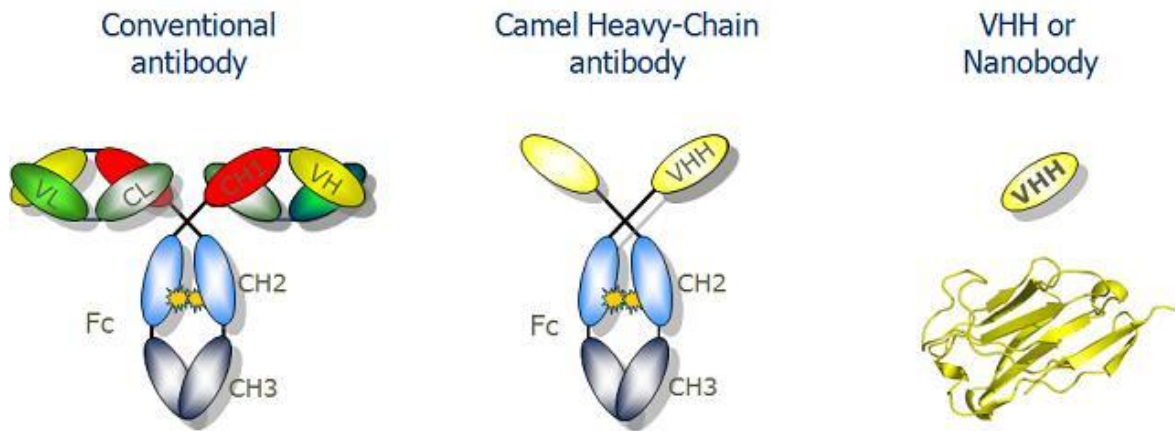


Fig 14. Representation of conventional antibody and comparison with HCAb and VHH REF?

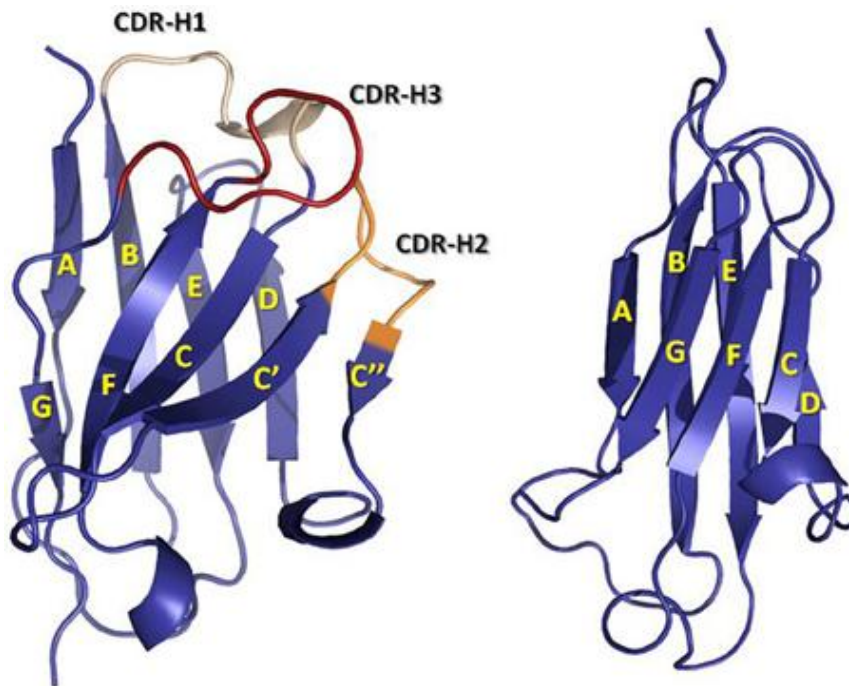


Fig 15. Structural model of the VHH conformation (Almagro et al 2012).

NBs can be obtained from immune, naive or synthetic libraries. In the first case, an animal is immunized with the antigen of interest and, after 5 or 6 weekly injection, lymphocytes are isolated from the peripheral blood. cDNAs are prepared from total extracted RNA, and those encoding VHH genes are selected by PCR (Muyldermans 2001). Since the entire antigen-binding fragment of HCAb consists of one domain, encoded by a gene fragment of only ~360 bp that is easily amplified by PCR, small libraries are already representative of the immune repertoire. Naive libraries are generated in the same manner from the blood of a non-immunized animal, while synthetic libraries are created, for example, by randomly mutating the amino acids belonging to CDR3 of a VHH exhibiting a robust scaffold (Nguyen, Hamers et al. 2000). Antigen-specific NBs are retrieved from these libraries by phage display or other selection protocols such as bacterial display, yeast display or ribosome display. Due to its robustness, the phage display method is the most often used one. The VHH genes, amplified by PCR, are generally cloned into an appropriate vector (phagemid) at the 3'-end of a gene coding for a coat protein of a filamentous phage (generally M13) (Muyldermans 2001). VHHs are then expressed at the tip surface of the phages and the most specific binders are panned on antigens, which are most of the time immobilized in wells of a microtiter plate by passive adsorption or biotinylated on streptavidin-coated solid supports.

NBs repertoires present a great advantage over those of conventional antibodies: they do not need the random combination of VH and VL chains which lead to the generation of many nonproductive combinations due to the loss of the original pairing. Moreover, the whole procedure is also much less time and money consuming.

Finally, the selected NBs can be expressed as recombinant protein with a high yield in bacteria (~40 to 70 mg per liter of culture) (Rahbarizadeh, Rasaee et al. 2006), in yeast (>100 mg per liter of culture) (Frenken, van der Linden et al. 2000) or in plants (up to 30% total leaf proteins) (De Buck, Viridi et al. 2012). Their purification is usually achieved by immobilized metal ion affinity chromatography (IMAC) via an engineered C-terminus His6 tag, or by other affinity chromatography as NB gene is easily cloned in another vector to change the tag.

III.1 Antibodies for biomedical applications

Monoclonal antibodies are indispensable molecules for therapeutic, diagnostic as well as for biotechnological applications (Aggarwal 2012). Their remarkable clinical efficacy in conjunction with several dozen marketed antibodies and hundreds of mAbs in clinical development is corroborating their great therapeutic potential (Dubel 2007). However, for specific applications, such as in vivo imaging, the efficacy of classical antibody molecules might be impaired by reason of their large hetero-tetrameric structure and slow blood clearance, as well as their restricted tumor penetration together with non-specific uptake by healthy tissues might pose problems for distinct applications (Mordenti, Cuthbertson et al. 1999, Huang, Ginkam et al. 2008, Vaneycken, D'Huyvetter et al. 2011).

To address these issues, next generation antibodies, such as antibody-drug conjugates (Casi and Neri 2012, Bouchard, Viskov et al. 2014), immunocytokines (Pasche and Neri 2012), antibody fragments (Huehls, Coupet et al. 2015), scaffold proteins (Kolmar 2011) and VHH camelids antibody-derivatives (Hamers-Casterman, Atarhouch et al. 1993, Greenberg, Avila et al. 1995) were engineered. Recombinant production of VHHs emerged as a seemingly inexpensive alternative to the production of mAbs (see above, (Zarschler, Wittey et al. 2013) (Arbabi Ghahroudi, Desmyter et al. 1997)).

With respect to the biomedical use of VHHs, a low immunogenicity can be expected due to the high sequence similarity to the human heavy chain variable domain, which differs of about 10 amino acids. Further attempts to reduce the risk of immunogenicity led to a general humanization strategy. Therefore, a stable humanized VHH scaffold was generated that allows grafting of antigen binding loops from other VHHs while retaining antigen affinities and specificities (Vincke, Loris et al. 2009). A variety of potential biomedical applications for VHHs are described in the literature, although no therapeutics based on VHHs have found their way to the market yet, six have entered clinical trials phase I or II. The popular term “NB” serves as trade name for VHHs belonging to the commercial biopharmaceutical company Ablynx (www.ablynx.com), which was originally the main driver of development of VHHs for biomedical applications.

In addition, VHHs are attractive for addressing difficult targets, for instance GPCRs. In this respect, the cryptic epitopes of GPCRs are located within TM regions and are poorly accessible with mAbs and therefore small molecules are mostly used for GPCRs targeting (Overington, Al-Lazikani et al. 2006). Studies highlighting this targeting approach using NBs

were recently described for CXCR4 (Jahnichen, Blanchetot et al. 2010) and CXCR7 (Maussang, Mujic-Delic et al. 2013).

Beside their use as potential therapeutics, VHHs are also promising tools for probing in diagnostic applications. For the diagnosis of HIV-infection, a VHH directed against human glycophorin A (a protein on red blood cells) was developed as a fusion protein with p24 (the HIV capsid protein). When the fusion protein is added to the serum of HIV-positive donors, rapid agglutination is induced due to cross-linkage of red blood cells in the presence of anti-p24 antibodies (Habib, Smolarek et al. 2013). Furthermore, radiolabeled VHHs have been used for tumors imaging. In a preclinical validation, labeled NBs directed against the macrophage mannose receptor, which is consistently upregulated in tumor associated macrophages (TAM), led to an efficient *in vivo* targeting and imaging, and could be a novel approach for the diagnosis of cancer (Movahedi, Schoonooghe et al. 2012).

NBs can also be linked to any module of interest for biotechnological, pharmaceutical or structural purposes. For example in traditional indirect immunofluorescence, epitopes are initially decorated with a primary antibody and detected with a fluorophore-labeled secondary one, each around 12–15 nm in size (Harris, Skaletsky et al. 1998). The effective displacement between label and epitope can reach up to 24–30 nm and thus significantly deteriorate the achievable precision and accuracy of protein localization by super-resolution fluorescence microscopy (Huang, Gaiakam et al. 2008). NBs (diameter: 4nm) are an ideal solution to this problem (Ries, Kaplan et al. 2012, Szymborska, de Marco et al. 2013). This, however, requires a direct NB labeling. Ideally, labeling should be site-specific, so that the remaining small displacement between epitope and fluorescent dye can be predicted and corrected for in the measurements.

III.2 NBs in structural biology

NBs exhibit interesting properties that may help difficult proteins to crystallize, they can:

- ❖ Prevent domain mobility and hide mobile protein-bound polysaccharides;
- ❖ Insert in clefts or between interfaces, thus stabilizing loops or large complexes;
- ❖ Assist in the solubilization of proteins with low solubility or provide useful crystal contacts for membrane proteins.

Moreover, due to the protruding nature of NBs and their binding to crevices, they are excellent inhibitors or modulators of enzymes, receptors or virus; these features are also

favorable for crystallization. Many examples of the usefulness of NBs in coupled functional and structural studies have been reported in the literature in the past two years (Acharya, Luongo et al. 2013, Desmyter, Farenc et al. 2013, Kruse, Ring et al. 2013, Ring, Manglik et al. 2013, Schmitz, Bagchi et al. 2013, Ward, Szewczyk et al. 2013, Abskharon, Giachin et al. 2014, Hassaine, Deluz et al. 2014, Pathare, Nagy et al. 2014).

III.2a NBs as mobility blockers or inserting modules

NBs have been revealed to be very useful in crystallizing conformationally mobile proteins because they can freeze a unique conformation (Ward, Szewczyk et al. 2013). The crystal structure of human IL23 in its glycosylated form was made possible when complexed simultaneously with three NBs (PDB: 4GRW). The property of NBs to bind concave epitopes has also proven to be very useful. Two NBs were shown to inhibit the epidermal growth factor receptor (EGFR) by blocking a new epitope not reached by classical Ig. They could bind an epitope close to the EGFR domain II/III junction, thus hindering the mandatory conformational changes of the receptor, preventing high-affinity ligand binding and dimerization. This epitope is accessible to the protruding NB paratope but inaccessible to the flat monoclonal antibody binding surface (Schmitz, Bagchi et al. 2013).

III.2b NBs and membrane proteins

The most striking example of NBs utilization in the field of membrane protein structure is the complex of the beta2 adrenoreceptor (b2Ar), GPCR, with a NB (nb80) (Rasmussen, Choi et al. 2011, Steyaert and Kobilka 2011). The most important effect was the stabilization of the agonist-bound form of the β -arrestine 2 (β 2Ar), because the active-state GPCR structure has been difficult to stabilize in the absence of G-proteins.

Nb80 inserts its CDR3 into the core of the receptor between TM helices 3, 5 and 6. As a result, these helices move by several Å, reaching an agonist bound-like conformation, the same as the one observed in the presence of the G-proteins (Rasmussen, Choi et al. 2011).

This new stabilizing NB variant made it possible to obtain structures of β 2Ar/NB in complex with new agonists with a wide range of affinities (Ring, Manglik et al. 2013). The same strategy of employing a stabilizing NB was used with another GPCR, the human M2 muscarinic acetylcholine receptor (4MQS) (Kruse, Ring et al. 2013). Here again, the NB

CDR inserts within TM helices 3, 5 and 6, inducing them to adopt the agonist-bound conformation and making it possible to bind agonist molecules with sufficient affinity and stability.

Another important asset of GPCR-targeting NBs in GPCRs research is their use as conformation-specific biosensors. Fluorescently tagged NBs provide a means of tracking proteins in live cells with unprecedented resolution (Ries, Kaplan et al. 2012).

Recent efforts to study the spatial localization of β 2AR signaling using NBs that recognized activated β 2AR (Rasmussen, Choi et al. 2011) and nucleotide-free (active) Gas (Westfield, Rasmussen et al. 2011), respectively. By genetically fusing these NBs to green fluorescence protein (GFP) and expressing them in β 2AR-expressing cells, followed by microscopic examination of GFP localization following β 2AR activation, direct evidence for G-proteins activation from internalized GPCRs was provided (Irannejad, Tomshine et al. 2013), a phenomenon that has been suggested to occur for multiple GPCRs but was never directly ascertained (Calebiro, Nikolaev et al. 2010).

In addition, these intracellularly expressed NBs, also termed intrabodies, can also be utilized to modulate receptor-dependent signaling. A recent study showed that conformation-specific β 2AR intrabodies inhibit downstream signal transduction (Staus, Wingler et al. 2014), illustrating the potential of NBs as research tools to study receptor-specific GPCRs signaling.

III.2c NBs and viruses

NBs have been reported to bind viruses and phages (or parts of them) with the potential capacity to neutralize them. A very interesting study made use of a chimeric construct between a NB and a viral protein: a complex formed between the HIV Nef protein and a stabilizing SH3 domain bound to a NB (SdAb19) was crystallized exhibiting 1:1 stoichiometry (Lulf, Matz et al. 2014). Interestingly, the NB-SH3 entity, termed Neffin, binds the Nef protein with increased affinity compared to each partner alone and inhibits all functions of Nef as well as HIV infectivity and replication. The NB was found to inhibit Nef by directly interacting with the C-terminal Lys192 and Phe195 residues of the Nef protein involved in the targeting of the Pak2 serine/threonine kinase (Lulf, Matz et al. 2014).

III.3 CXCR4 and CXCR7 targeting NBs

Using a time-efficient whole cell immunization of llamas with CXCR4-expressing HEK293T cells, followed by phage display and counter selection, NBs against CXCR4 were identified and characterized as neutral antagonists in their monovalent forms (Jahnichen, Blanchetot et al. 2010). The reported CXCR4–NBs bind with high affinity and specificity to the ECL2 and potently inhibit CXCL12-induced signaling and chemotaxis. They are highly selective for human CXCR4 and do not recognize the murine receptor, indicating that minor changes (five additional amino acids in the mouse receptor) in ECL2 are sufficient to affect Nb affinity for CXCR4. This underlines the exquisite selectivity that can be achieved by NBs.

Specific NBs binding to CXCR7 were also recently developed and characterized (Maussang, Mujic-Delic et al. 2013). They display high affinity and antagonistic properties, as they are able to inhibit CXCL12-induced recruitment of β -arrestin2 to CXCR7. Moreover, CXCR7–NBs were shown to inhibit head and neck cancer tumor growth in a mouse xenograft model.

Finally, generation of NBs targeting CKs have also been recently reported (Blanchetot, Verzijl et al. 2013). Inflammatory CKs CCL2 (binding to CCR2), CCL5 (binding to CCR1, CCR3, and CCR5), and CXCL11 (binding to CXCR3 and CXCR7), as well as CXCL12, were successfully targeted by CK-specific NBs. All these NBs inhibit CK binding to their cognate CKR. Furthermore, the CXCL11- and CXCL12-specific NBs inhibit G_i signaling and chemotaxis through CXCR3 and CXCR4, respectively (Blanchetot et al 2013). Collectively, NBs against CXCR4 and CXCR7, as well as against a panel of CKs, show great promise as therapeutics and research tools to further characterize the CKR system.

Objectives

Objectives

The CXCR4 crystal structure solved in 2010 was a tremendous breakthrough for the CKR field although it has left many questions unanswered such as the determinants, the stoichiometry and the mechanisms of the interaction between the receptor and its chemokine ligand CXCL12.

Moreover, despite the large interest on CXCR4 three-dimensional structure, very few structural information are known on CXCR7, the recently discovered second receptor of CXCL12. This receptor is another key player in the CXCL12/CXCR4-dependent signaling and contributes to the formation of a functional gradient of CXCL12 through its scavenging activity. Though, in agreement with this function, CXCR7 behaves as an atypical CKR that fails to activate G proteins upon agonist (CXCL11 or CXCL12) binding, it does activate MAPK through the recruitment of β -arrestins and can thus *per se* contribute to CXCL12-dependant functions.

Apart from shaping CXCL12 gradients, CXCR7 has also the propensity to modify CXCR4-dependent signaling (G-proteins and β -arrestins) by the way of heterodimers with CXCR4, the formation of which in endogenous setting remains nevertheless open. The role of CXCR7 in CXCL12-dependent functions and, behind, its importance in physiological and pathological processes, have boosted research devoted to this atypical receptor. However, the knowledge stays limited notably with regard to molecular aspects related to CXCL12 binding and signaling.

The first objective of my project was to model the stoichiometry of CXCR4/CXCL12 interaction starting from the crystal structure, in monomeric and dimeric forms, to generate a complete model of CXCR4 structure and then to simulate the interaction with the chemokine CXCL12 using molecular modeling tools: peptide-peptide docking and molecular dynamics. Our purpose was to investigate differences in stability, interactions and conformations comparing the model structure of 1:1 stoichiometry versus the 2:1 one. Therefore, we focused our attention on CXCR4 residues shown to be important for binding and G proteins activation, analyzing the distances and positions between the N-terminus of the chemokine and receptor key residues.

The second objective of my thesis work was to characterize new tools to investigate CXCR4 biology on native systems and tissues. We choose to study three different clones of nanobodies (NBs) targeting the extracellular domains of CXCR4, since they are new useful and innovative molecules. We performed in vitro and in silico experiments in order to describe their pharmacological activity on the CXCR4 activation pathways and their mechanism of interaction with the receptor.

The third part of my project was focused in the structure modeling and analysis of CXCR7 and the comparative study with CXCR4-CXCL12 interaction. First we proposed a model of the three-dimensional structure of CXCR7 using homology modeling and then analyzed the possible interaction mechanisms with CXCL12, by peptide-peptide docking and molecular dynamics simulations, to investigate the molecular determinants of this interaction. We were able to identify two possible CXCR7 residues involved in the interaction with CXCL12 and conversely the residues in the N-terminus of CXCL12 important for binding to and activating CXCR7. With this knowledge together with that of CXCR4 residues important for CXCL12-induced G proteins activation, we performed mutagenesis studies on the hypothetical CXCR7 CRS1 and CRS2 domains to compare the interaction and the signaling properties of CXCL12 engagement to its two receptors.

Results

❖ Paper n°1:

Interaction of chemokine receptor CXCR4 in monomeric and dimeric state with its endogenous ligand CXCL12:
Coarse-grained simulations identify differences

❖ Paper n°2:

Conformationally selective Nanobodies for regulation of CXCR4 functions

❖ Paper n°3

Differential activities of CXCL12 analogs at the CXCR4 and CXCR7/ACKR3 receptors:
Study of interaction determinants

Paper n°1

Interaction of chemokine receptor CXCR4 in monomeric and dimeric state with its endogenous ligand CXCL12:
Coarse-grained simulations identify differences

Journal of Biomolecular Structure and Dynamics

ISSN: 0739-1102 (Print) 1538-0254 (Online) Journal homepage: <http://www.tandfonline.com/loi/tbsd20>

Interaction of chemokine receptor CXCR4 in monomeric and
dimeric state with its endogenous ligand CXCL12:
Coarse-grained simulations identify differences

Pasquale Cutolo¹, Nathalie Basdevant², Guillaume Bernadat³
Françoise Bachelerie¹, and Tâp Ha-Duong³

¹ UMR-996, Université Paris-Sud, INSERM, Université Paris-Saclay, Clamart, France

² LAMBE, CNRS, Université d'Evry-Val-d'Essonne, Evry, France

³ BioCIS, Université Paris-Sud, CNRS, Université Paris-Saclay, Châtenay-Malabry, France

Corresponding author: tap.ha-duong@u-psud.fr

Publisher: Taylor & Francis

Journal: Journal of Biomolecular Structure and Dynamics

DOI: <http://dx.doi.org/10.1080/07391102.2016.1145142>

Abstract

Despite the recent resolutions of the crystal structure of the chemokine receptor CXCR4 in complex with small antagonists or viral chemokine, a description at the molecular level of the interactions between the full-length CXCR4 and its endogenous ligand, the chemokine CXCL12, in relationship with the receptor recognition and activation, is not yet completely elucidated. Moreover, since CXCR4 is able to form dimers, the question of whether the CXCR4-CXCL12 complex has a 1:1 or 2:1 preferential stoichiometry is still an open question. We present here results of coarse-grained protein-protein docking and molecular dynamics simulations of CXCL12 in association with CXCR4 in monomeric and dimeric states. Our proposed models for the 1:1 and 2:1 CXCR4-CXCL12 quaternary structures are consistent with recognition and activation motifs of both partners provided by the available site-directed mutagenesis data. Notably, we observed that in the 2:1 complex, the chemokine N-terminus makes more steady contacts with the receptor residues critical for binding and activation than in the 1:1 structure, suggesting that the 2:1 stoichiometry would favor the receptor signaling activity with respect to the 1:1 association.

Introduction

The chemokine receptor CXCR4, which was originally described as a coreceptor for human immunodeficiency virus (Feng et al., 1996), is a class A G-protein-coupled receptor (GPCR) with a unique chemokine ligand, CXCL12, previously called stromal cell-derived factor 1 (SDF-1) (Bleul et al., 1996; Oberlin et al., 1996). Both CXCR4 and CXCL12 are expressed by a vast array of cell types in many tissues. Targeted disruptions of either genes are embryo lethal in mice, promoting defects in cardiac, hematopoietic and cerebellar development, evidencing a broad spectrum of activities (Nagasawa et al., 1996; Ma et al., 1998). The CXCR4-CXCL12 pair, which is essential for the proper migration of leukocytes, hematopoietic stem cells and progenitors, also controls many physiological functions, such as survival, repair, growth, and neovascularization (Puchert and Engele, 2014). Besides, this axis is endowed with pathogenic roles notably in immune diseases and in the progression of various cancers (Kryczek et al., 2006; Sun et al., 2010), including virus-related ones (Freitas et al., 2014). It is therefore considered as a very attractive therapeutic target (Peled et al., 2012).

Binding of CXCL12 to CXCR4 triggers typical activation of G-protein and arrestin dependent pathways of a GPCR that cannot solely account for the wide spectrum of physiological activities of this axis (Busillo and Benovic, 2007). It is rather hypothesized that such functional complexity originates from various determinants, including the cell context, the available receptor interactome (receptorosome), together with the reported ability of both CXCL12 and CXCR4 to oligomerize (Bachelierie et al., 2013).

This is also consistent with observations made in live cells, from the use of biophysical techniques, including bioluminescence and fluorescence resonance energy transfer, which indicate that monomers, dimers and higher-order oligomers of CXCR4 might coexist (Hamatake et al., 2009; Ferr et al., 2014). Such as emerged for other GPCR, CXCR4 dimers might display unique ligand-binding properties and functional selectivity. In line with this, dimerization is the most likely mechanism to explain the functional dominance of a gain of function of the CXCR4 mutant over its wild type congener (Lagane et al., 2008; Balabanian et al., 2012) in the context of the rare WHIM disorder associated with heterozygous CXCR4 mutations (Hernandez et al., 2003).

The possibility that CXCR4 forms dimers is also supported by the recent crystal structures of CXCR4 in complex with small antagonists (Wu et al., 2010) or with the viral chemokine

encoded by Kaposi's sarcoma-associated herpesvirus (vMIP-II) (Qin et al., 2015). These CXCR4 structures (PDB codes 3ODU, 3OE0 and 4RWS) revealed a dimeric arrangement of the receptor which is able to accommodate one ligand or a dimer of ligands, forming a 2:1 or a 2:2 CXCR4-CXCL12 complex, respectively. Indeed, chemokines are proposed to exist in an equilibrium of monomeric and dimeric species (Veldkamp et al., 2005), with the dimeric CXCL12 being a partial agonist capable of inducing intracellular calcium mobilization but not chemotaxis (Veldkamp et al., 2008; Drury et al., 2011).

Thus, when considering the full agonist signaling process, the question of whether the CXCR4-CXCL12 complex has a 1:1 or 2:1 preferential stoichiometry with regard to the stability of their respective tridimensional structures remains to be investigated.

The GPCR typical seven transmembrane helices are well observed in the 3ODU, 3OE0 and 4RWS crystal structures of CXCR4. However, the receptor N-terminus (up to residue Asp22) is not visible in the electron density maps, witnessing its flexible and disordered character, even in the presence of the viral chemokine vMIP-II (Wu et al., 2010; Qin et al., 2015). In the transmembrane cavity of the receptor, several residues were found by site-directed mutagenesis studies to be important for CXCR4 signaling, including the region from Glu179 to Asp182 in extracellular loop 2 (ECL2) (Doranz et al., 1999), the residues Asp97 in transmembrane helix 2 (TMH2), Asp187 in ECL2, Glu288 in TMH7 (Brelot et al., 2000; Tian et al., 2005), Tyr190 in ECL2 and Glu268 in ECL3 (Zhou, 2001). On the other hand, NMR experiments revealed that CXCL12 has a disordered N-terminus (residues 1-8), which includes residues critical for CXCR4 activation, notably Lys1 and Pro2 (Crump et al., 1997; Heveker et al., 1998; Veldkamp et al., 2008; Kofuku et al., 2009). Besides, it should be emphasized that the three receptor residues Asp97, Asp187 and Glu288 are also critical for the chemokine binding (Brelot et al., 2000). More specifically, they probably make contacts with the CXCL12 first two residues Lys1 and Pro2, as suggested by the crystal structure of CXCR4 with the viral chemokine vMIP-II (Qin et al., 2015).

Based on these evidences, a two-site, two-step model for the CXCR4-CXCL12 interactions was proposed, where the CXCL12 motif ${}_{12}\text{RFFESH}_{17}$ first binds the receptor N-terminus, and then the chemokine N-terminus ${}_{1}\text{KPVLSYR}_8$ enters the buried cavity within the CXCR4 transmembrane helices (Crump et al., 1997; Doranz et al., 1999; Veldkamp et al., 2008; Kofuku et al., 2009), triggering receptor activation, probably mediated by a change in the conformation of its transmembrane helices. Nevertheless, despite the important recent structural data, there is not yet a comprehensive characterization of the quaternary structures

and dynamics of the CXCR4-CXCL12 associations, which could confirm this model and provide information on the stoichiometry of the functional receptor-ligand complexes.

We investigated this issue using coarse-grained molecular modeling tools, by following a two-step strategy similar to the one employed by Xu et al. and by Tamamis and Floudas in their recent theoretical studies (Xu et al., 2013; Tamamis and Floudas, 2014), and extending it to investigate the CXCR4-CXCL12 1:1 or 2:1 stoichiometry.

The first step consists in generating plausible initial conformations of the complex by coarse-grained rigid-body docking the chemokine onto the receptor. Then, from docked conformations having the chemokine N-terminus located in the receptor transmembrane cavity, we explored the conformational ensemble of the complexes, using coarse-grained MD simulations, to search for the most populated structures. This approach enabled us to identify models of the CXCR4-CXCL12 association in which the chemokine residues Lys1 and Pro2 are in close contact with the three receptor residues Asp97, Asp187 and Glu288, known to be critical for both binding and activation (Brelot et al., 2000). In the modeled 1:1 stoichiometry, we noticed that the chemokine core domain would be more stable when positioned above the transmembrane helices of a putative other protomer if CXCR4 was considered as a dimer. We thus hypothesized that such position of CXCL12 could better fit to a dimeric receptor. Using the same procedure consisting in docking CXCL12 on the dimeric receptor and relaxing the complex with MD simulations, we propose here a model of CXCR4-CXCL12 association that better accommodates to the 2:1 combination.

Results and Discussion

Structure of wild type 1:1 CXCR4-CXCL12 complexes

Each docking of the twenty CXCL12 NMR structures on the monomeric CXCR4 generated approximately 28 000 complexes. For each of the twenty docking calculations, we visually inspected the five lowest energy structures, and found all together seventeen CXCR4-CXCL12 complexes for which the chemokine N-terminus is located within the receptor transmembrane pocket. In these latter, the chemokine core domain is rather positioned outside the receptor transmembrane helix bundle, as shown in Fig. 1. In all other low energy conformations of the complex, the CXCL12 core domain is positioned and centered above the CXCR4 helix bundle, but its N-terminus points towards the solvent (data not shown). It could be noted that the protein-protein rigid-body docking was able to identify several complexes with the CXCL12 N-terminus in the CXCR4 activation site probably because the receptor conformation used for these calculations comes from a co-crystal structure of CXCR4 in complex with a ligand in its transmembrane pocket (PDB ID: 3ODU). This "bound" structure would allow the receptor to accommodate the chemokine N-terminus without large conformational change of its activation site. The seventeen complexes, that were found with the CXCL12 N-terminus inside the CXCR4 transmembrane cavity, were clustered by visual inspection of the chemokine core domain position with respect to the receptor helix bundle (Fig. 1). We identified four clusters, two of which having only one representative conformation (clusters 3 and 4). We observed that the vector joining the CXCL12 pivotal residue Ser6 to the antipodal Asn45 points towards the receptor transmembrane helices II and III in the first cluster (7 structures), towards helices III and IV in cluster 2 (8 structures), towards helix V in cluster 3 (1 structure) and towards helix VI in cluster 4 (1 structure).

Then, using coarse-grained MD simulations, we considered exploring the conformational dynamics of the two most populated complexes having the chemokine N-terminus within the receptor transmembrane cavity (clusters 1 and 2, with simulations 11-WTA and 11-WTB, respectively). Nevertheless, the question of whether the complex CXCR4-CXCL12 has a 1:1 or a 2:1 stoichiometry prompted us to also consider the cluster 3 structure (simulation 11-WTC), since it interestingly has the CXCL12 core domain located above an other putative protomer if CXCR4 was dimeric (Fig. 1). In contrast, we did not performed MD simulation of cluster 4, since this single conformation has a chemokine core domain position that would not

be influenced by a putative other protomer. RMSD relative to the initial conformation of the receptor and the chemokine as well as position of the CXCL12 core domain are shown as a function of time in Fig. 2.

Due to the elastic network model used here, both receptor and chemokine of the simulated complexes rapidly reached equilibrated tertiary structures which did not much during the 5 μ s trajectories. In contrast, it can be observed that CXCL12 has larger amplitude global motion relative to CXCR4, especially in the case of complex 11-WTC whose chemokine exhibited broad translational and rotational movements. It could be noted that a conformational change of the receptor occurred around 1 μ s of the 11-WTC simulation. It is analyzed as a local transition from a compact to an extended form of its C-terminus region 302-328 (data not shown). However, since the CXCR4 helix bundle is maintained by an elastic network, which biases its conformational changes, the receptor C-terminus structural transition, located in the intracellular side, can hardly be related to the dynamics of the chemokine / receptor interface, which occurs in the extracellular side.

Among the previous 1:1 complexes, the most plausible quaternary structure was identified by examining contacts between the CXCR4 and CXCL12 residues involved in the receptor activation as previously identified by site-directed mutagenesis studies (Crump et al., 1997; Heveker et al., 1998; Doranz et al., 1999; Brelot et al., 2000; Zhou, 2001; Tian et al., 2005; Murphy et al., 2007; Veldkamp et al., 2008; Kofuku et al., 2009; Qin et al., 2015). Fig. 3 indicates the percentages of simulation time for which the chemokine first eight residues are in contact with the receptor key residues. Among the latter, Glu179, Asp187, Tyr190 and Asp193 are located on the ECL2, and Glu268 on the ECL3. According to the subdivision of the receptor transmembrane cavity into a major sub-pocket surrounded by helices III to VII and a minor one by helices I to III and VII (Roumen et al., 2012), the receptor residues Asp171, Tyr255 and Asp262 belong to the major sub-pocket, the residues Trp94 and Asp97 to the minor one, and residues Tyr116 and Glu288 are at the edge of the two sub-pockets. Fig. 3 shows that the chemokine N-terminus mainly lies in the major sub-pocket in the complex 11-WTA, its residue Lys1 predominantly contacting the receptor residue Asp262. In the complex 11-WTB, the chemokine N-terminus is partially buried in the transmembrane cavity, with its residue Lys1 pointing towards the ECL2 β -turn, but establishing no steady contact with any of the minor sub-pocket residues. In contrast, the complex 11-WTC exhibits a chemokine N-terminus that partially occupies the CXCR4 major sub-pocket but interacts mostly with the minor one (Fig. 4). Indeed, the CXCL12 first two residues Lys1 and Pro2

make durable contacts with residues Trp94 and Asp97, as well as with residues Tyr116 and Glu288 at the edge of the two sub-pockets, and to a lesser extent with residues Asp171 and Tyr255 in the major one (Fig. 3). Noticeably, not only CXCL12 residue Lys1 makes steady contacts with the receptor residues critical for binding and activation (i.e. Asp97, Asp187 and Glu288), but the remaining seven N-terminal residues also interact with the CXCR4 important residues Glu179, Asp187 and Tyr190. These interactions were not recovered in the two conformations 11-WTA and 11-WTB, highly suggesting that 11-WTC would be the most representative structure of a functional 1:1 receptor-ligand complex.

In the latter model, the position and orientation of the chemokine N-terminus within the CXCR4 minor sub-pocket are very similar to those observed in the crystallographic structure of CXCR4 in complex with the viral chemokine vMIP-II, as well as in the CXCR4-CXCL12 model built using the CXCR4-vMIP-II structure as a template (Qin et al., 2015). However, in our model, the global position of the chemokine core domain is located outside the receptor transmembrane helix bundle, whereas it is more centered above it in the crystallographic structure. This apparent discrepancy could be explained by the packing of the proteins in the crystal unit cell of the CXCR4-vMIP-II complex. Indeed, analysis of the latter reveals close contacts between two vMIP-II of two adjacent head to tail subunits, as well as between the T4 lysozyme and the chemokine of two neighboring complexes (Fig. S3). These steric interactions could constrain the ligand vMIP-II to adopt a different position and orientation from those in our liquid phase model. Another explanation could be the disulfide bond between the receptor residue D187C and the chemokine W5C that was introduced to trap the complex in a crystallizing conformation and which could artificially constrain packing of the ligand N-terminal region from residue 5, leading to a different position and orientation of its core domain.

Structure of 1:1 CXCR4-CXCL12 complexes with mutated chemokine

The position of the CXCL12 N-terminal residues among those of the CXCR4 transmembrane cavity and their contacts observed in the 11-WTC complex were further assessed using simulations of CXCR4 in complex with the K1R and P2G chemokine mutants. Starting from the final conformation of the 11-WTC simulation, the time evolution of the receptor and the mutated chemokine RMSD as well as the position of CXCL12 core domain are displayed in Fig. S4. It is observed that, with respect to the wild type CXCL12, the P2G mutation induces

a global rotation of the chemokine core domain towards the receptor helices III and IV. In contrast, the K1R mutation does not much affect the global position of the chemokine relative to the receptor. However, we found that the K1R mutation influences the accommodation of the CXCL12 N-terminus in the receptor minor sub-pocket (Fig. 4) and the contacts with the residues critical for CXCR4 activation (Fig. S5). For instance, the contacts of the chemokine's first four residues with the CXCR4 residue Asp187 are partially disrupted by the K1R substitution. We also observed a loss of contacts of the chemokine second residue (Gly2 when mutated or Pro2 in the context of the K1R mutant) with the CXCR4 residues Tyr255 and Glu288 (Fig. S5 compared to Fig. 3). In the context of the K1R mutant, these observations are probably due to a weakening of the hydrophobic cluster, involving, in the wild type complex, the aliphatic moiety of the Lys1 side chain and the side chains of residues Trp94 and Tyr116. Consequently, the mutated chemokine residue Arg1 is hardly held in place, resulting in turn in the destabilization of the hydrophobic interaction between Pro2 and Tyr255.

In both mutated K1R or P2G complexes, the chemokine's first residue (Lys1 or Arg1) is flipped over with respect to its orientation in wild type, so that its side chain amine group makes a salt-bridge with the receptor residues Glu288, instead of Asp97 as observed in 11-WTC (Fig. 4). These structural effects of the chemokine mutations are reflected in the interaction energies of the chemokine first eight residues with the receptor. These non-bonded energies (Lennard-Jones + Coulomb), calculated with the MARTINI force field and averaged over each MD trajectory, are equal to -748.4 ± 65.0 , -669.8 ± 48.2 and -690.0 ± 39.1 kJ/mol for the 1:1 CXCR4-CXCL12 chemokine wild type (11-WTC), K1R and P2G mutants, respectively. Although these energy estimations are rather crude due to the simplified protein model used here, they tend to confirm that the chemokine mutations K1R and P2G induce a destabilization of the chemokine N-terminus interaction with the receptor transmembrane cavity when compared with the wild type.

From a dynamics point of view, the first residue K1R substitution also influences the duration of the chemokine N-terminus contacts with the three residues critical for the receptor activation. Indeed, as shown in Fig. 5, the period during which the chemokine first residue is simultaneously in contact with the receptor residues Asp97, Asp187 and Glu288 is significantly shorter in the 11-K1R mutant than in the wild type complex (these periods represent 48.8 % and 17.3 % of the 11-WTC and 11-K1R simulation times, respectively). These differences in the packing and dynamics of the chemokine N-terminus within the receptor cavity could account for the antagonist behavior of the K1R and P2G CXCL12

mutants on calcium mobilization used as a readout for CXCR4 activation (Crump et al., 1997). All together, our results indicate that the 11-WTC quaternary structure is the most probable conformation of the 1:1 CXCR4-CXCL12 functional complex. Consistently with most of the site-directed mutagenesis studies of CXCR4, our model exhibits a chemokine N-terminus lying at the bottom of the receptor minor sub-pocket and making persistent contacts with receptor residues critical for activation, including Asp97, Asp187 and Glu288.

Structure of 2:1 CXCR4-CXCL12 complexes

Since, in the 11-WTC model, the chemokine core domain is located beyond the receptor helix V, it could interact with a putative adjacent protomer if CXCR4 was a dimer. Indeed, when docking the twenty NMR structures of CXCL12 on the crystallographic receptor dimer, we found among the 20 x 5 lowest energy conformations three 2:1 CXCR4-CXCL12 complexes, in which the chemokine N-terminus is located within the transmembrane pocket of one CXCR4 protomer whereas its core domain is partially covering the cavity of the other protomer (Fig. S6). Again, we explored the conformational ensemble of one of these 2:1 complexes by coarse-grained MD simulation (hereafter referred to as 21-WT). This revealed that the chemokine global movements relative to the receptor dimer are more restrained than in the case of the 1:1 association (Fig. 6 compared to Fig. 2). Moreover, during the 5 μ s simulation, the two N-terminal residues Lys1 and Pro2 of the chemokine mostly occupy the receptor minor sub-pocket and make very steady contacts with the CXCR4 critical residues Asp97, Asp187 and Glu288 (Fig. 7 and 8), demonstrating that the 21-WT complex enables the chemokine N-terminus to trigger the receptor signaling activity, by contacting the key transmembrane pocket residues.

These contacts, which were established for significantly longer duration than those in the 1:1 complex (Fig. 5), suggest that the 2:1 stoichiometry would favor the receptor activation as compared to the 1:1 association. Interestingly, the K1R mutation of the chemokine N-terminus had not the same impact on the 2:1 CXCR4-CXCL12 complex as compared to the 1:1 association. Indeed, in the simulation time course of the chemokine mutant K1R of the 2:1 complex (simulation 21-K1R), the chemokine N-terminus maintained the contacts with the receptor residues critical for activation established by the wild type CXCL12 (Fig. 7), whereas the same mutation partially disrupted the interactions of the CXCL12 residues Lys1 and Pro2 with the CXCR4 important residues Asp187, Tyr255 and Glu288 in the 11-K1R

simulation (Fig. S5). In contrast, the chemokine mutant P2G in complex with the CXCR4 dimer did not maintain its global position and orientation relative to the receptor (Fig. 6). The consequence is dramatic for the residue Lys1, which cannot make any contacts with the CXCR4 residues critical for activation (Fig. 7). More broadly, the first residues of the chemokine N-terminus left the receptor minor sub-pocket to the benefit of the major one, close to the residue Asp262, and even can transiently exit the transmembrane cavity, supporting the observation that the P2G mutant does not promote CXCR4 activation. As for the 1:1 CXCR4-CXCL12 complexes, we calculated, using the MARTINI force field, the averaged non-bonded energy between the chemokine first eight residues and the receptor in the 2:1 associations. These interaction energies are equal to -742.9 ± 36.5 , -782.7 ± 37.9 and -403.0 ± 60.2 kJ/mol for the chemokine wild type, K1R and P2G mutants of the 2:1 complex, respectively. In contrast to the 1:1 stoichiometry, and unlike the P2G mutant, the K1R mutation of the 2:1 CXCR4-CXCL12 complex does not destabilize the interaction between the chemokine N-terminal residues and the receptor transmembrane cavity when compared to the wild type. These energy data corroborate the observed lifetimes of the contacts between the chemokine N-terminus and the CXCR4 key residues for binding and activation (Fig. 7). Overall, these results suggest that the K1R chemokine mutant would maintain the capacity of CXCL12 to activate CXCR4 when engaged into a 2:1 CXCR4-CXCL12 association, but not in the 1:1 complex. These observations are in good agreement with comparative analysis of CXCR4-dependant G-protein activation promoted by the wild type and derived-chemokine mutants, which suggest a partial agonism of some latter ones (Levoye et al., unpublished results).

Structure of 1:1 and 2:1 CXCR4-CXCL12 complexes with mutated receptor

In the 11-WTC structure, the chemokine N-terminus makes contacts with the receptor residues Asp97, Asp187 and Glu288 critical for its activation. Nevertheless, it is curiously observed in this model that the receptor residue Asp193 makes a steady salt-bridge with the chemokine residue Arg8, whereas it was shown that mutations D193K and D193A have little effect upon CXCR4 activation (Doranz et al., 1999; Brelot et al., 2000).

This apparent contradiction was investigated using a coarse-grained MD simulation of CXCL12 bound to the monomeric mutated D193K receptor (simulation 11-D193K). As shown in Fig S7, the mutation does not affect the global position and orientation of the

chemokine with respect to the receptor. Moreover, most of the contacts between the CXCL12 residues Lys1 and Pro2 with the important residues of the receptor transmembrane pocket are conserved (Fig. S8). In detail, the Lys193 ammonium group makes a salt-bridge with the Glu268 side chain, but the Lys193 backbone group still remains in contact with the chemokine Arg8 backbone, while its side chain tends to come closer to the residue Asp262. Notwithstanding these slight adaptations at the chemokine interface with the receptor ECL2, the CXCL12 N-terminus still occupies the D193K receptor minor sub-pocket, supporting the fact that the D193K mutation has little effect on the CXCR4 activation. This result is also consistent with the experimental observation that the CXCL12 residue Arg8 is not absolutely required for triggering the receptor signaling, as shown by studies on the chemokine R8K mutant activities (Crump et al., 1997; Murphy et al., 2007).

Another intriguing result in our study concerns the receptor residue Glu268 which was never observed being in contact with the chemokine N-terminus (Fig. 3 and 7), whereas the receptor E268A mutant was reported to be impaired in its capacity to bind and to be activated by CXCL12 (Zhou, 2001). In the 11-WTC complex, the distance from the receptor residue Glu268 to every chemokine residues was measured (data not shown) and a minimum distance of 8.9 Å was found, indicating that Glu268 was not involved in the receptor-ligand interactions. However, in the 21-WT complex, Glu268 was observed close to the CXCL12 residue Arg41, at a distance of 4.5 Å, meaning that it participates in the 2:1 CXCR4-CXCL12 interface. To further investigate the role of CXCR4 residue Glu268, we performed an additional MD simulation of the E268A mutant of the CXCR4 dimer in complex with CXCL12 (simulation 21-E268A). The simulation analysis shows that the chemokine core domain keeps its position above one of the two protomers, whereas its orientation, which was stabilized by a salt-bridge between the receptor Glu268 and the chemokine Arg41 in the wild type 2:1 complex, is no more maintained in the E268A mutant (Fig. 8). Accordingly, the E268A mutation influences the accommodation of the chemokine N-terminus within the receptor cavity, which is characterized by the Lys1 side chain amine group in contact with residues Glu288 and Asp187, similarly to what is observed for the mutants 11-K1R and 11-P2G complexes (Fig. 8 compared to Fig. 4).

This difference in the packing of the chemokine N-terminus within the receptor minor sub-pocket could again account for the experimentally observed loss of signaling activity of the E268A mutant (Zhou, 2001). Interestingly, this mutation influences the 2:1 CXCR4-CXCL12 complex, but has probably no impact on the 1:1 association, in which the receptor residue

Glu268 does not interact with any of the chemokine residues, providing further support for the existence of the 2:1 stoichiometry.

These results do not accord with the conclusions made by Kufareva et al., who proposed that CXCR4 interacts with CXCL12 in a 1:1 stoichiometry, despite its dimeric nature and subsequently to the exclusion of the 2:1 hypothesis on the basis of functional complementation and dilution assays (Kufareva et al., 2014). Nevertheless, the functional rescue that can be observed upon co-expression of complementary mutants of CXCR4 (between 60 and 100 % as seen in Fig. 4 of Ref. (Kufareva et al., 2014)), while supporting the existence of receptor dimers, does not exclude the 2:1 stoichiometry hypothesis. We herein propose a dynamic model which could fit with the coexistence of both 1:1 and 2:1 complexes. We hypothesize that during the second step of the two-site two-step mechanism of the CXCR4-CXCL12 recognition (Crump et al., 1997; Kofuku et al., 2009), the chemokine N-terminal tail ¹KPVSLSYR⁸ enters the CXCR4 transmembrane cavity, while the receptor N-terminus partially detaches from the chemokine core domain recognition site ¹²RFFESH¹⁷. Indeed, intrinsically disordered regions such as the CXCR4 N-terminus are known to bind their protein partners with high specificity but low affinity (Huang and Liu, 2009; Uversky and Dunker, 2010). For the CXCR4-CXCL12 complex, it was reported that the receptor N-terminal peptide 1-38 binds to the chemokine core domain with a dissociation constant of 4.5 μM (Veldkamp et al., 2006).

This micromolar low affinity, compared to the affinity of the chemokine for the whole receptor (K_d = 3:6 nM (Crump et al., 1997)), suggests that the CXCR4 N-terminus could easily unbind from its chemokine recognition site after or during the correct positioning of the CXCL12 N-terminus into the receptor transmembrane cavity. In our study, the MD simulations 11-WTC and 21-WT show that the CXCR4 N-terminus, which was initially in contact with the chemokine recognition site ¹²RFFESHV⁸, partially unbinds from this region (Fig. S9). This unbinding process would comply with the engagement of one CXCR4 protomer with both chemokine recognition site and N-terminus, in the 1:1 or 2:1 complex, consistently with both NMR data and mutagenesis experiments.

Conclusion

The main advantage of coarse-grained models over all-atom descriptions is that they smooth the energy landscapes of the studied protein complexes, allowing a more efficient exploration of their conformational ensemble. In particular, coarse-grained MD simulations enable studied complexes to visit structures far from the initial guess and to reach more rapidly the most stable conformations. This advantage was used here to model the most probable conformations of the 1:1 and 2:1 CXCR4-CXCL12 complexes, with regard to the receptor activation, taking into consideration evidences from NMR, X-ray and mutagenesis studies. In this way, the quasi-exhaustive coarse-grained docking calculations of monomeric CXCL12 on either a monomeric or a dimeric receptor generated several complexes in which the chemokine N-terminus lies in the CXCR4 transmembrane cavity, satisfying the overall geometrical criteria required to trigger its activation, as envisioned by Crump et al. and later on confirmed by Kokufu et al. (Crump et al., 1997; Kofuku et al., 2009).

The coarse-grained MD simulation of one of the 1:1 complexes (11-WTC) converged towards a conformation in which the chemokine N-terminus mainly occupies the transmembrane minor sub-pocket of the receptor, with chemokine residues Lys1 and Pro2 making steady contacts with CXCR4 key residues Asp97, Asp187 and Glu288. The packing of the chemokine N-terminus within the receptor cavity are stabilized by hydrophobic interactions between the apolar groups of the Lys1 and Pro2 side chains with the CXCR4 residues Trp94, Tyr116 and Tyr255, which are disrupted upon K1R or P2G mutations. These findings are consistent with most of the site-directed mutagenesis studies of CXCR4, as well as with the crystallographic structure of CXCR4 in complex with the viral chemokine vMIP-II, with the notable difference that in our model, the CXCL12 core domain is located outside the receptor transmembrane helix bundle and above a putative adjacent protomer if the receptor was in a dimeric form.

By means of a second coarse-grained study, motivated by the hypothesis raised by the 11-WTC model, we subsequently generated a very stable 2:1 CXCR4-CXCL12 complex (21-WT), in which the chemokine core domain partially covers the cavity of one of the two CXCR4 protomers. In this model, the chemokine N-terminus is found to be located within the transmembrane minor sub-pocket of the other protomer, with very steady contacts between the receptor key residues Asp97, Asp187 and Glu288 and the CXCL12 first residues Lys1 and Pro2. More broadly, our results demonstrated that both monomeric and dimeric CXCR4

can bind a monomeric chemokine CXCL12 in a way (i.e. with its N-terminus buried in the transmembrane cavity) that would be functional regarding the triggering of CXCR4 signaling activities.

Acknowledgments

P.C., G.B., F.B. and T.H. are members of the Laboratory of Excellence in Research on Medication and Innovative Therapeutics supported by the french Agence Nationale de la Recherche (Investissements d'Avenir ANR-10-LABX-0033-LERMIT).

The authors declare no financial conflict of interest regarding the publication of this manuscript.

Experimental procedures

Building CXCR4-CXCL12 complexes using docking calculations

Quaternary structures of the CXCR4-CXCL12 complex were first generated by rigid body protein-protein docking, using the molecular modeling toolbox PTools which manipulates biomolecules at a coarse-grained level (Saladin et al., 2009). We used, for these calculations, the SCORPION coarse-grained force field which was shown to correctly predict several protein-protein interfaces (Basdevant et al., 2007, 2013). PTools performs systematic docking as follows: First, the ligand is placed at regular positions around the receptor surface, at a distance slightly larger than its largest dimension. Depending on the receptor size, the number of initial positions typically varies from about 100 to 300. For each position, about 250 regular orientations of the ligand were generated by systematically changing its three Euler angles. Then, each of these several tens of thousands of initial conformations was submitted to six consecutive minimizations (with decreasing cutoff distances) of the protein-protein interaction energy, using the ligand six transitional and rotational degrees of freedom. The minimized complex conformations were finally clustered by similarity and ranked according to their interaction energy.

The receptor conformation was extracted from the crystal structure 3ODU (Wu et al., 2010) taken from the PDB, by excising the lysozyme fragment (residues 1002-1161) and all the co-crystallized ligands. It should be noted that the N-terminal first 26 residues of the receptor are missing in the crystal structure. We did not include these missing residues in the docking calculations, since this first step mostly aims to generate plausible initial conformations of the CXCR4-CXCL12 complex, prior to molecular dynamics simulations. These residues will be added to the selected protein-protein models before running the simulations (see below). The dynamics behavior of the CXCR4 N-terminus is briefly discussed at the end of the Results and Discussion section. The chemokine structures were taken from the PDB file 2K04 (Veldkamp et al., 2008), which contains twenty NMR-resolved conformations of a dimeric form of CXCL12 complexed with the first 38 residues of the CXCR4 N-terminus. It is noted that the N-terminal segment 1-21 of the human CXCL12 sequence (UniProt entry P48061) is annotated as a signal peptide. These residues are therefore removed in the mature protein and do not appear in the chemokine NMR structure. The twenty chains A were isolated and docked into the CXCR4 receptor, starting from positions exclusively located in the

extracellular side of the receptor. Each docking calculation yielded about 28 000 quaternary structures of the CXCR4-CXCL12 complex, which were subsequently clustered by similarity. The five lowest energy clusters generated by each of the twenty docking were then visually analyzed to identify those having the chemokine N-terminus inside the receptor trans-membrane cavity.

Molecular dynamics simulations of CXCR4-CXCL12 complexes

In a second step, representative conformations of the CXCR4-CXCL12 complex were submitted to extensive molecular dynamics (MD) simulations in order to explore its conformational space and to examine its most populated structures. Before that, the missing N-terminal region 1-26 in the CXCR4 crystal structure was reconstructed on the basis of the complex conformations generated by docking: the NMR structure of CXCL12 complexed with the N-terminal residues 1-38 of CXCR4 (PDB file 2K04) were first superimposed onto the chemokine structure obtained by docking. Then, the segment 27-38 of CXCR4 in the NMR structure was deleted, and the receptor residue 26 of the NMR complex was linked to the residue 27 of the receptor crystal structure (PDB file 3ODU). Finally, the reconstructed structure was minimized in order to optimize the length of the newly created peptidic bond. In this procedure, it could be noted that we had the choice to remove the redundant segment 27-38 of the receptor either from the NMR file or from the crystal structure. We chose to delete the NMR segment 27-38 in order to preserve the disulfide bridge present in the receptor crystal structure between Cys28 and Cys274.

MD simulations were performed with the GROMACS software package (Hess et al., 2008), using the MARTINI coarse-grained models of proteins and lipids (Marrink et al., 2007; Monticelli et al., 2008). This change in coarse-grained model is explained by the fact that the SCORPION force field was designed for protein-protein docking calculations and is not suitable for membrane protein MD simulations. Conversely, the MARTINI model was not optimized for protein-protein docking, but was extensively tested on membrane proteins and is now very reliable for simulating these systems. It could be noted that a similar strategy, using one force field for docking calculations and another one for MD simulations, was used by Xu et al. and by Tamamis and Floudas, but at the atomic level, to predict the CXCR4-CXCL12 quaternary structure. Specifically, they used the ZDOCK force field to perform the docking of the chemokine on the receptor and then the AMBER or CHARMM models for the

complex MD simulations (Xu et al., 2013; Tamamis and Floudas, 2014). We adopted the same approach but at the coarse-grained level which allows to explore the membrane protein conformational space more widely than with all-atom simulations.

We employed the improved version of MARTINI for proteins (de Jong et al., 2013) in combination with the elastic network model ELNEDIN (Periole et al., 2009) to maintain the overall shape of proteins. In this approach, all pairs of backbone grains, separated by at least three covalent bonds and distant by less than the cutoff distance $R_c = 0.9$ nm, are linked by a spring with the force constant $F_c = 500$ kJ/mol/nm². These parameter values allow to accurately reproduce the structural deformations and dynamics fluctuations of protein backbone (Periole et al., 2009). It should be remarked that, although the elastic network maintains the secondary structures and their close interactions, it does not restrain much the solvated disordered regions, especially the N-terminal and C-terminus tails, which keep most of their intrinsic flexibility (Fig. S1 of the Supplementary Information). Most importantly, elastic networks are defined for each protein (no intermolecular springs) and the six global degrees of freedom between two proteins are completely unrestrained. In the coarse-grained simulations, the chemokine core domain and N-terminus are thus still able to explore various positions and orientations relative to the receptor activation site.

Each CXCR4-CXCL12 complex previously identified was embedded in a rectangular box containing about 300 molecules of 1-palmitoyl-2-oleoyl-sn-glycero-3-phosphatidylcholine (POPC) with initial random position and orientation, along with between 8500 and 12500 coarse-grained non-polarizable water particles and the appropriate number of counterions required to neutralize the system (Marrink et al., 2007). A relative dielectric constant $\epsilon_r = 15$ was used to screen coulombic interactions as recommended by Marrink et al. in their original paper (Marrink et al., 2007). This solvent model was used although the more recent polarizable coarse-grained water model describes more accurately the solvent dielectric property, but at a greater computational cost (Yesylevskyy et al., 2010). Nevertheless, the non-polarizable solvent model was extensively tested and successfully used in many membrane protein simulations, as recently reviewed in (Marrink and Tieleman, 2013). This incited us to adopt this solvent model with confidence. Keeping the proteins rigid, the coarse-grained POPC and water molecules were first submitted to a 200 ns MD run, using a 20 fs timestep, in order to build the lipid bilayer around the CXCR4 receptor. Removing the proteins position restraints, an additional 200 ns MD simulation was then performed to equilibrate the system around the temperature $T = 310$ K and the pressure $P = 1$ bar. The

system was finally allowed to evolve without any constraint for a 5000 ns production run in the NPT ensemble, using a Nose- Hoover coupling method to keep the temperature constant and a Parrinello-Rahman algorithm for the semi-isotropic pressure. The trajectory coordinates were saved every 500 ps for structural analysis, using GROMACS tools. For characterization of the chemokine position with respect to the receptor, we chose the angle made between the vector joining the CXCL12 pivotal residue Ser6 to the antipodal Asn45 and the vector joining the CXCR4 residues Tyr45 to Gln200 (Fig. S2).

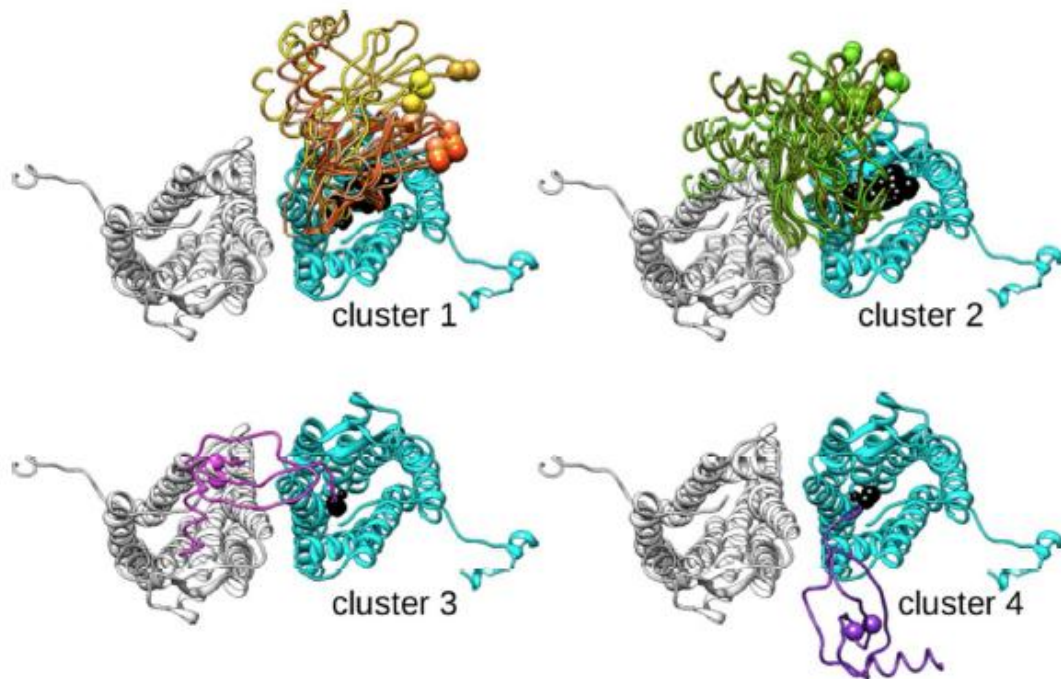


Fig 1. Top view of the CXCL12 poses on the extracellular side of the CXCR4 monomeric receptor (cyan ribbon). The chemokine is displayed with graduated orange (cluster 1), green (cluster 2), magenta (cluster 3) and purple (cluster 4). The second protomer in the dimeric crystal structure is represented as a white ribbon to provide a visual reference for the chemokine positions. The CXCL12 residue Lys1 is indicated by black spheres and its residue Asn45 by colored ones.

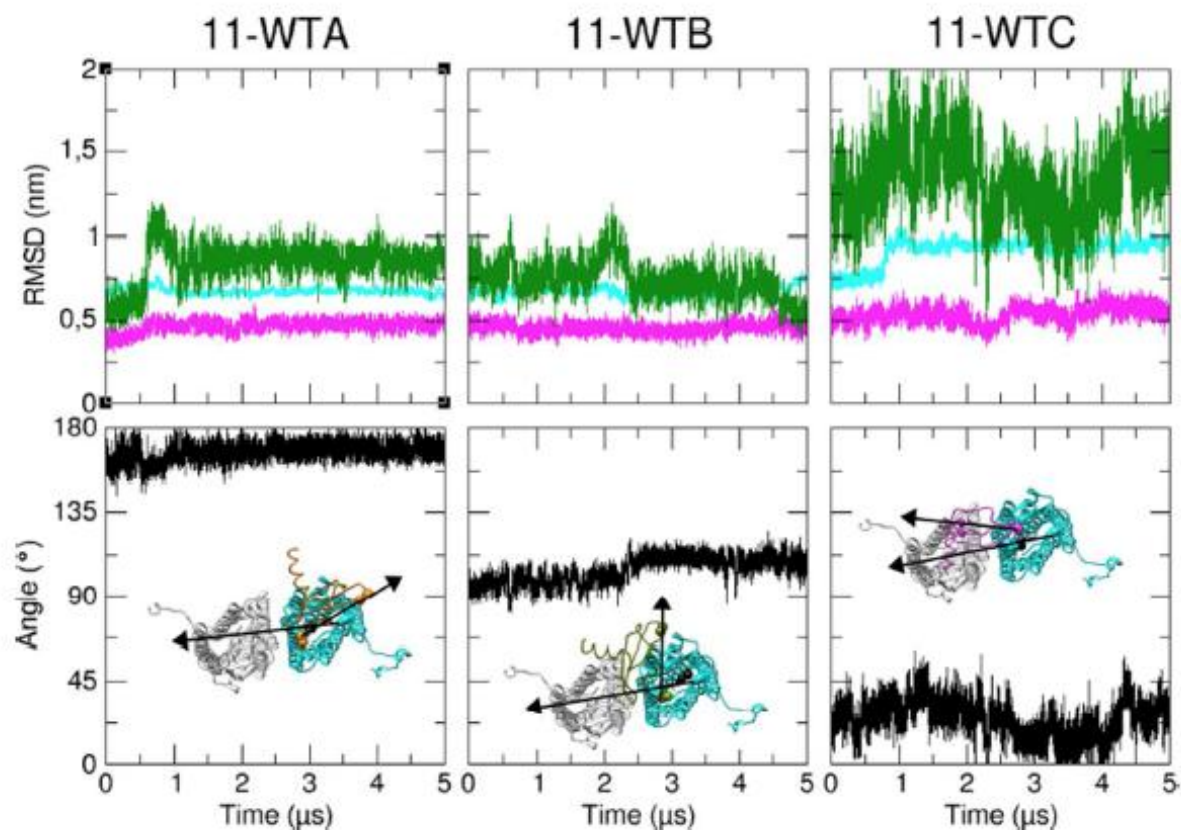


Fig 2. Time evolution of the RMSD (top row) of the receptor (cyan line), the chemokine (magenta line), the chemokine with respect to the receptor (green line), and the chemokine position relative to the receptor (bottom row), for the three wild type complexes 11-WTA, 11-WTB and 11-WTC. The position of the chemokine with respect to the receptor is indicated by the angle between the vector joining the CXCL12 pivotal residue Ser6 to the antipodal Asn45 and the vector joining the CXCR4 residues Tyr45 to Gln200. In the inset pictures, the second protomer of the dimeric CXCR4 is represented in white ribbon as a visual reference for the chemokine positions. The CXCL12 residue Lys1 is indicated by black spheres and its residues Ser6 and Asn45 by colored ones.

Fig 3 (top)

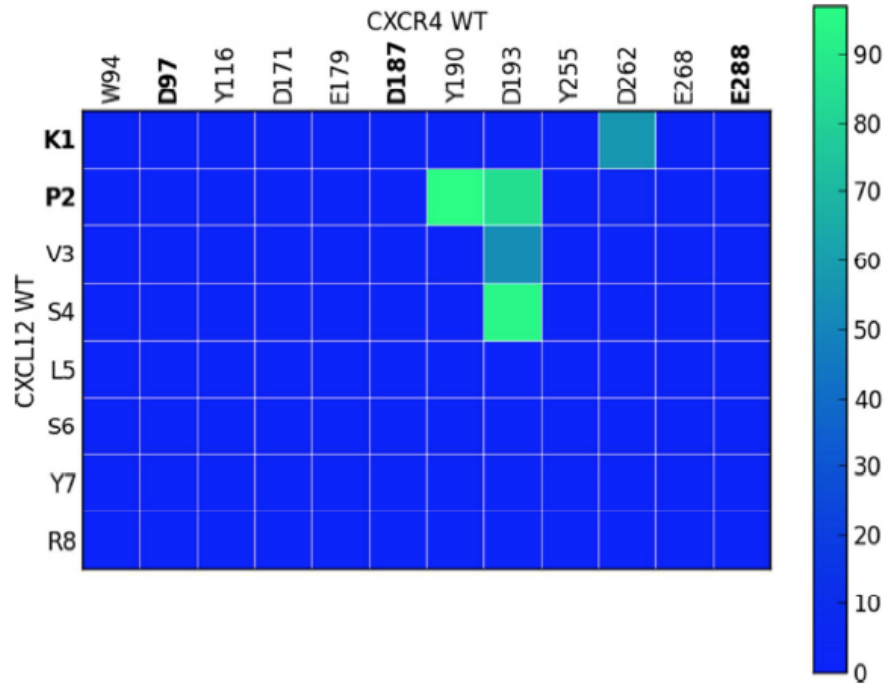
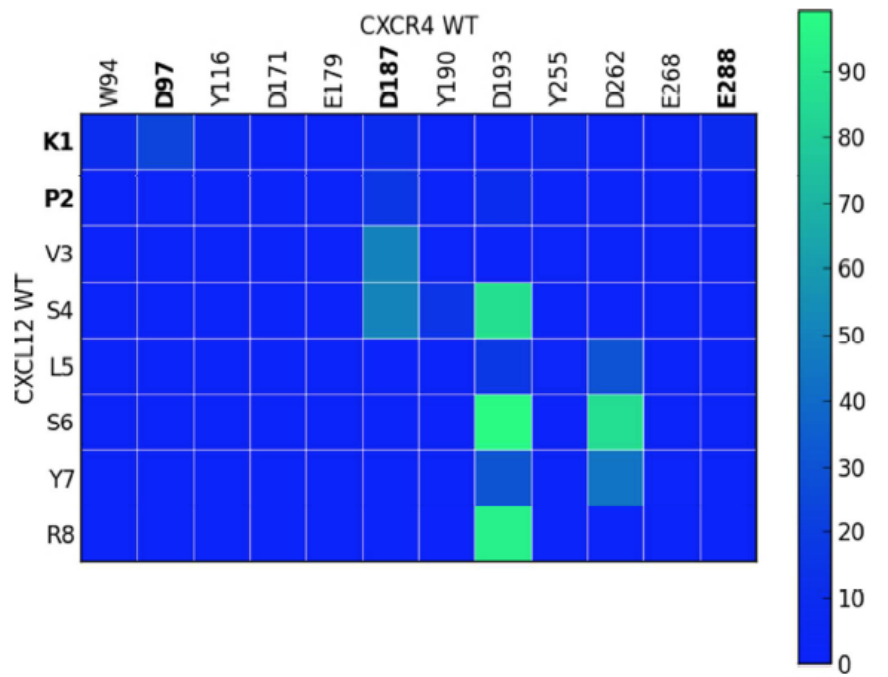


Fig 3 (middle)



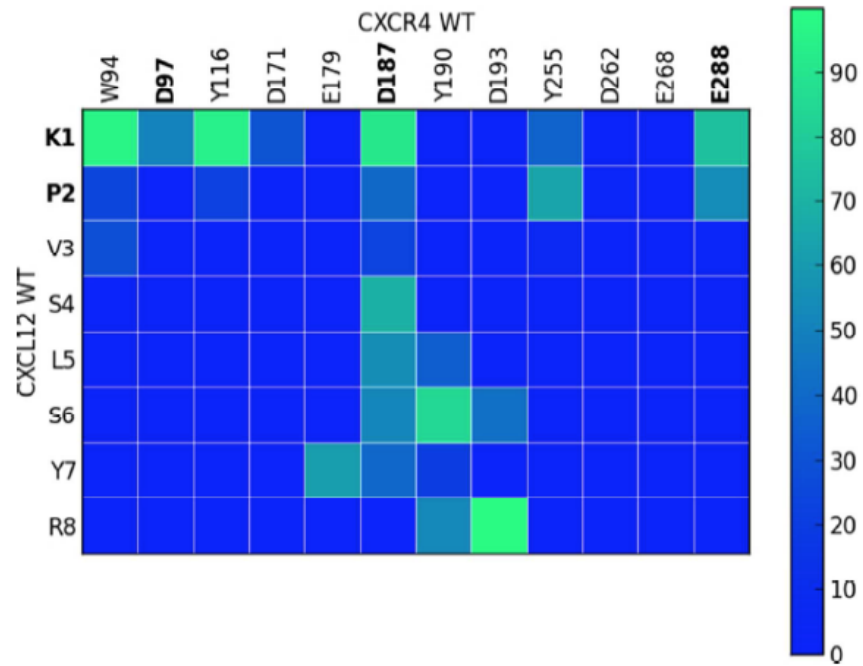


Fig 3 (bottom).

Percentages (right bicolor scale) of the complexes 11-WTA (top), 11-WTB (middle) and 11-WTC (bottom) simulation time for which the chemokine N-terminal first eight residues are distant by less than 6 Å to the receptor residues important for activation. Critical residues for CXCR4 activation are emphasized in bold print.

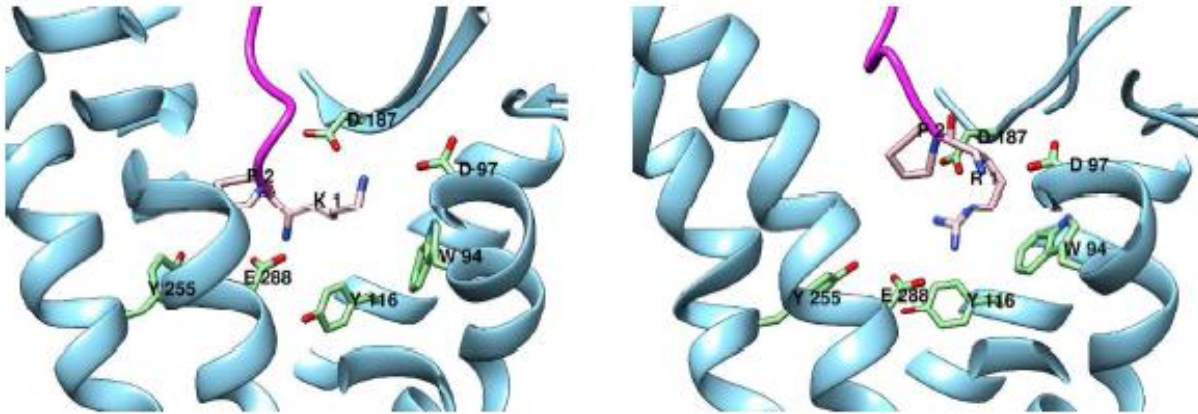


Fig 4. Position and orientation of the wild type (left) and K1R mutant (right) CXCL12 N-terminus within the monomeric CXCR4 transmembrane cavity. The chemokine is displayed with magenta ribbon and pink sticks; the receptor with blue ribbon and green sticks.

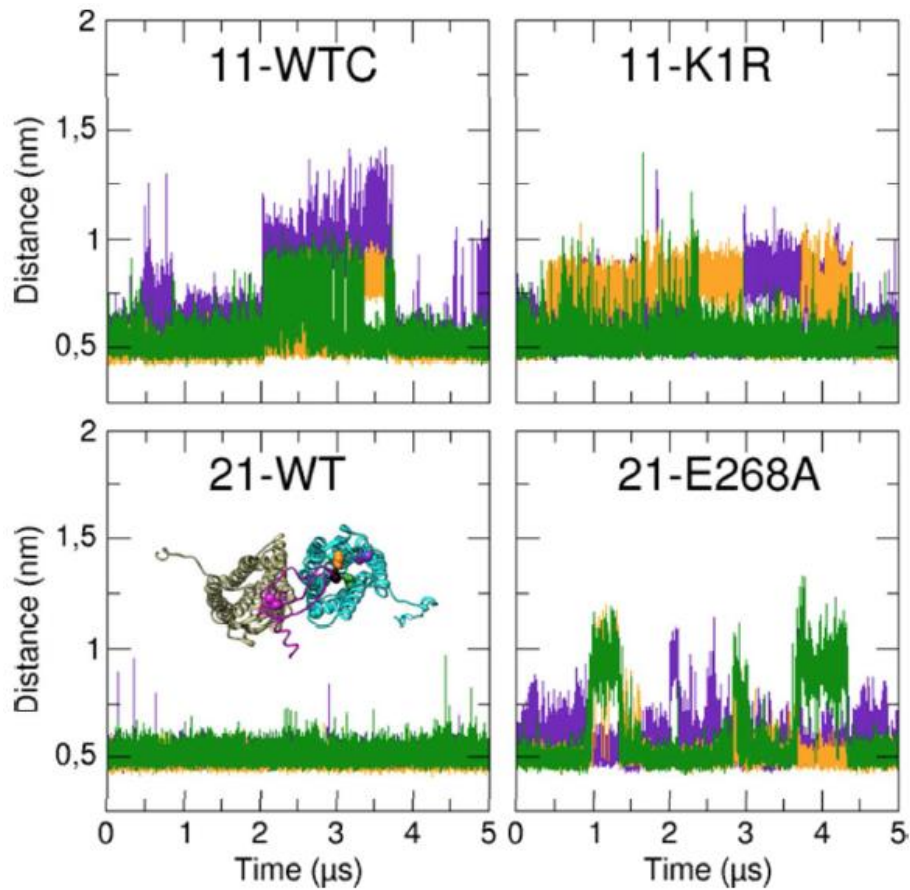


Fig 5. Time evolution of the distance between the chemokine first residue and the receptor Asp97 (purple line), Asp187 (orange line) and Glu288 (green line), for the 11-WTC, 11-K1R, 21-WT and 21-E268 simulations. The inset picture displays in colored spheres the chemokine residues Lys1 (black) and Asn45 (magenta), as well as the receptor key residues Asp97 (purple), Asp187 (orange) and Glu288 (green).

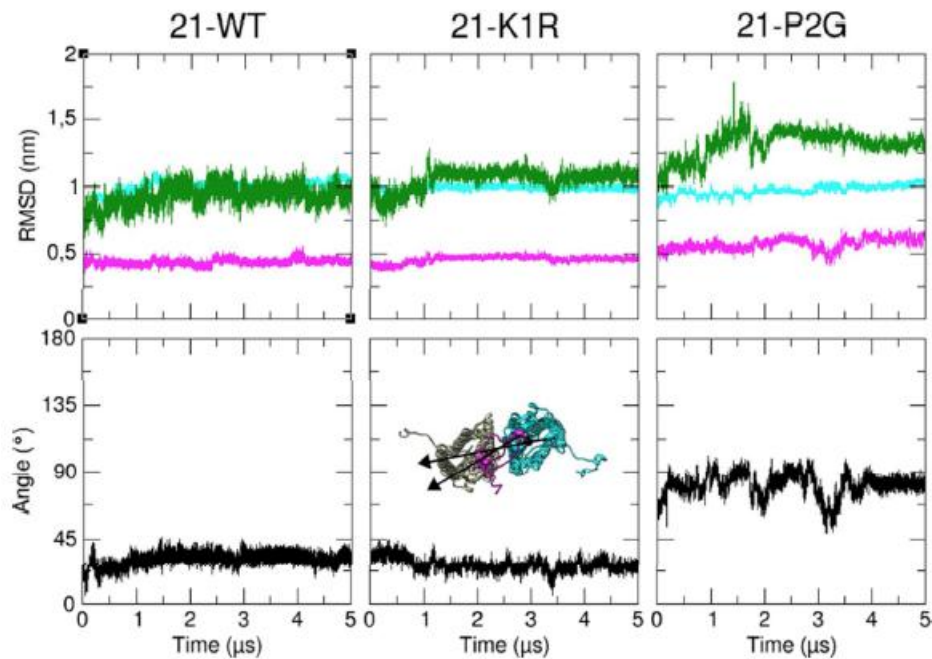


Fig 6. Same as Fig. 2 but for the wild type 2:1 CXCR4-CXCL12 complex (left) and the K1R (middle) and P2G (right) chemokine mutants. The inset picture displays the two protomers of the dimeric CXCR4 with cyan and tan ribbons. The CXCL12 residue Lys1 is indicated by black spheres and its residues Ser6 and Asn45 by magenta ones.

Fig 7 (top)

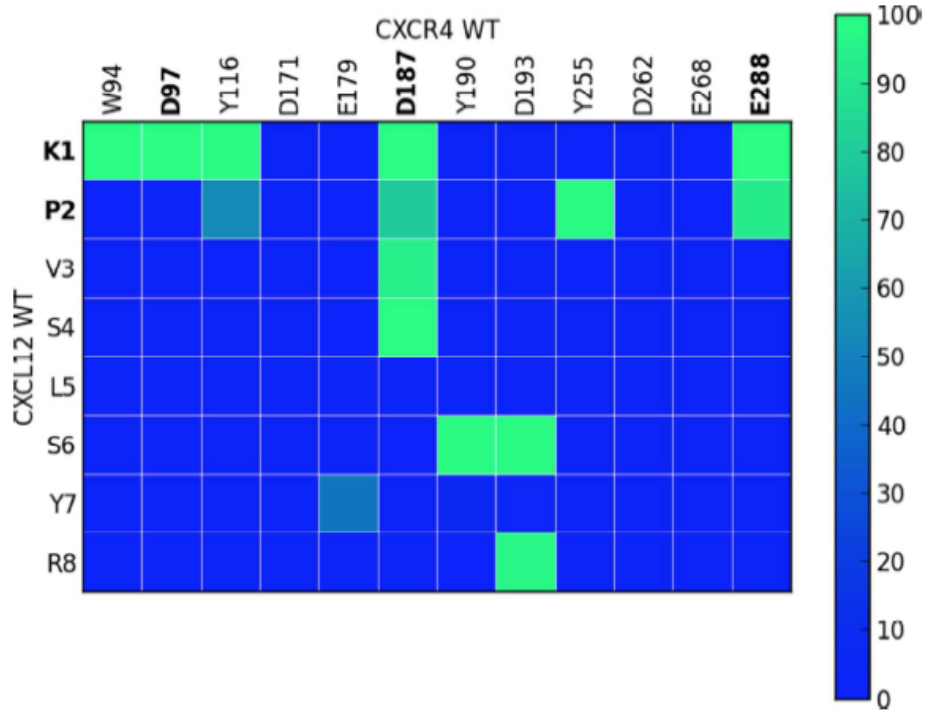
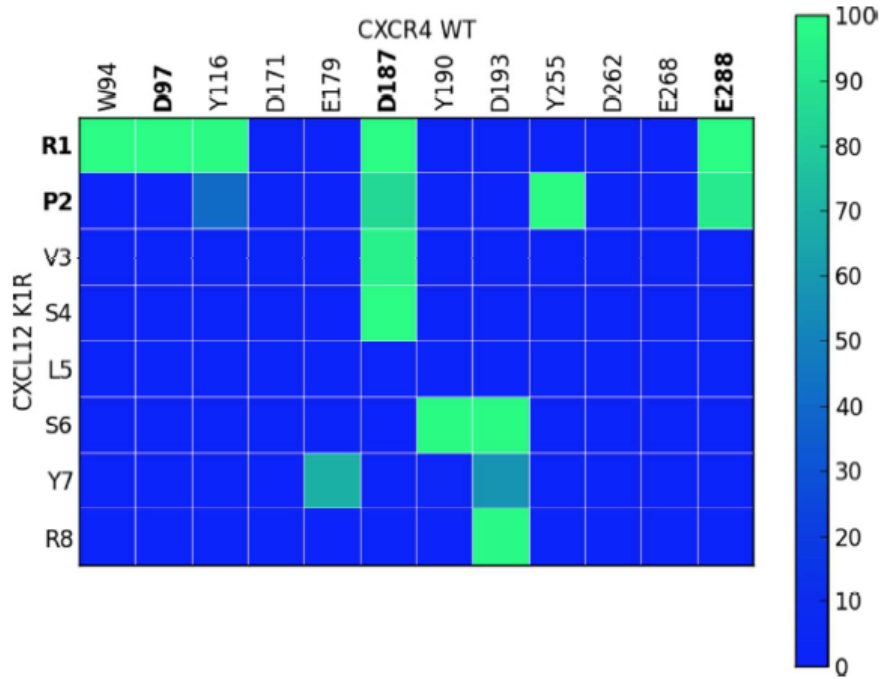


Fig 7 (middle)



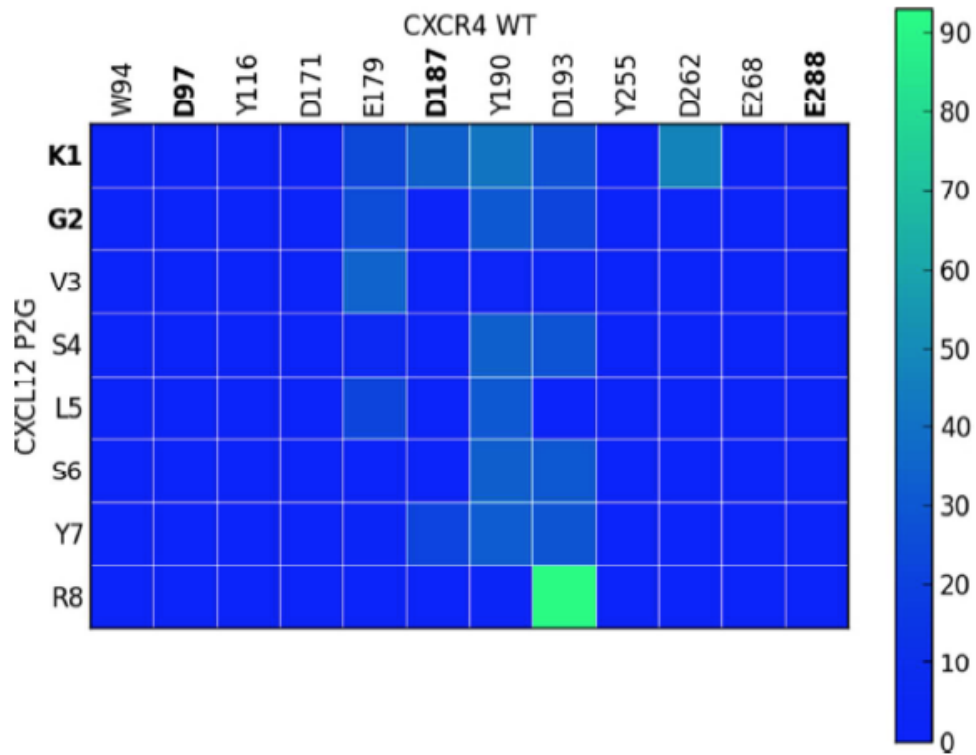


Fig 7 (bottom).

Same as Fig. 3 but for the wild type 2:1 CXCR4-CXCL12 complex (top) and its K1R (middle) and P2G (bottom) chemokine mutants.

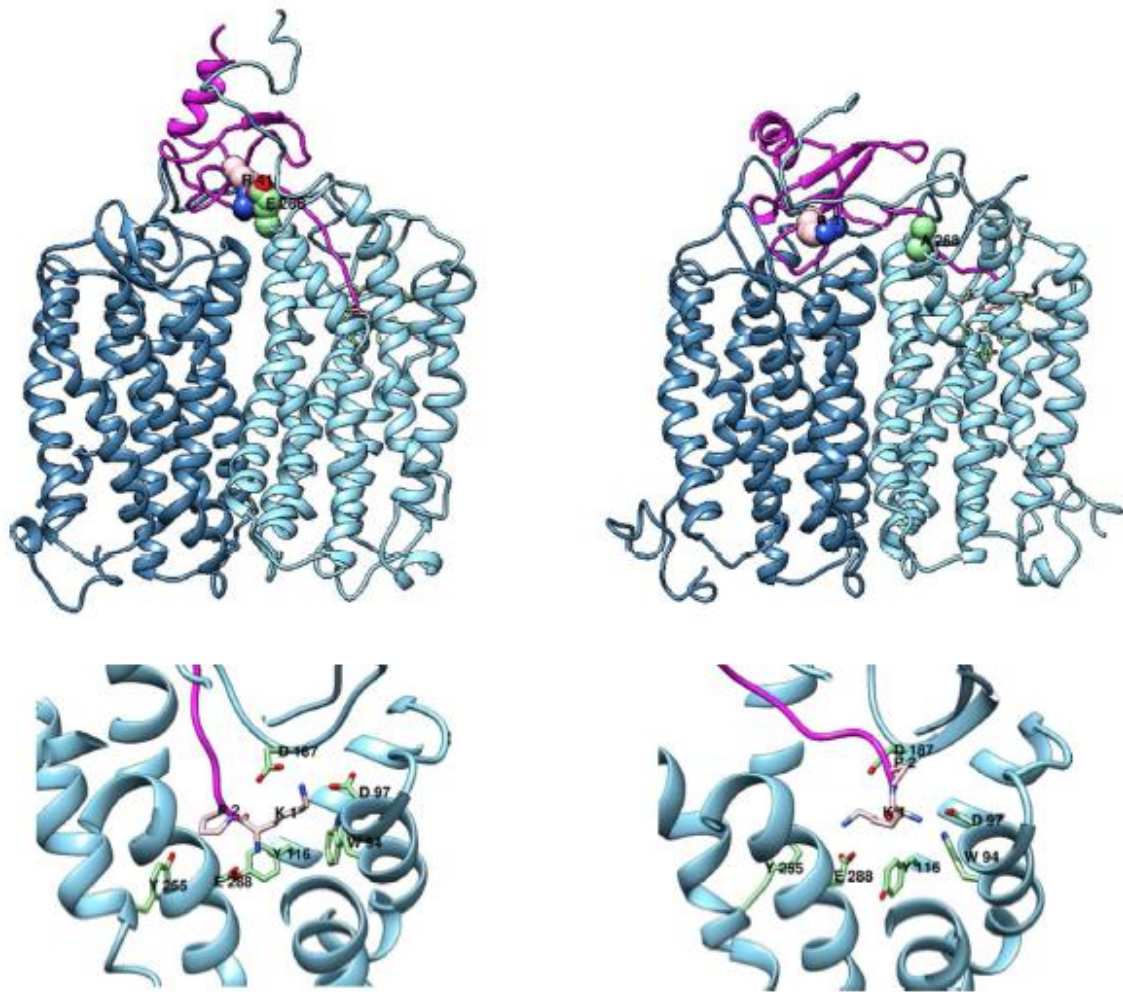


Fig 8. Top: Quaternary structures of the wild type (left) and E268A mutant (right) of the dimeric receptor in complex with CXCL12. Bottom: Position and orientation of the chemokine N-terminus within the wild type (left) and E268A (right) dimeric receptor transmembrane cavity. The chemokine is colored in magenta and the receptor protomers in cyan and tan.

SUPPLEMENTAL MATERIAL FOR

Interaction of chemokine receptor CXCR4 in monomeric and dimeric state with its endogenous ligand CXCL12: Coarse-grained simulations identify differences

Pasquale Cutolo¹, Nathalie Basdevant², Guillaume Bernadat³
Françoise Bachelerie¹, and Tâp Ha-Duong³

¹ UMR-996, Université Paris-Sud, INSERM, Université Paris-Saclay, Clamart, France

² LAMBE, CNRS, Université d'Evry-Val-d'Essonne, Evry, France

³ BioCIS, Université Paris-Sud, CNRS, Université Paris-Saclay, Châtenay-Malabry, France

Corresponding author: tap.ha-duong@u-psud.fr

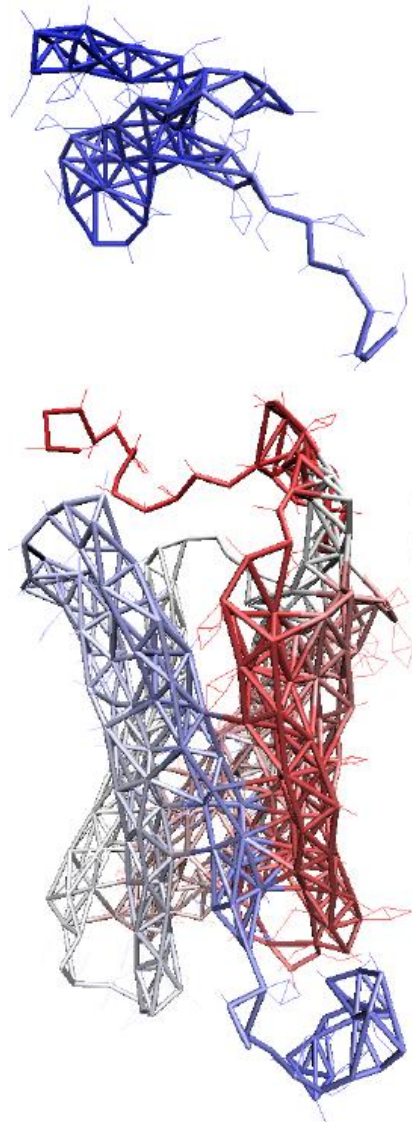


Fig S1. Elastic network models of the CXCL12 (top) and CXCR4 (bottom) proteins. The secondary structures are maintained through dense networks of springs, whereas the unstructured terminal tails keep their intrinsic

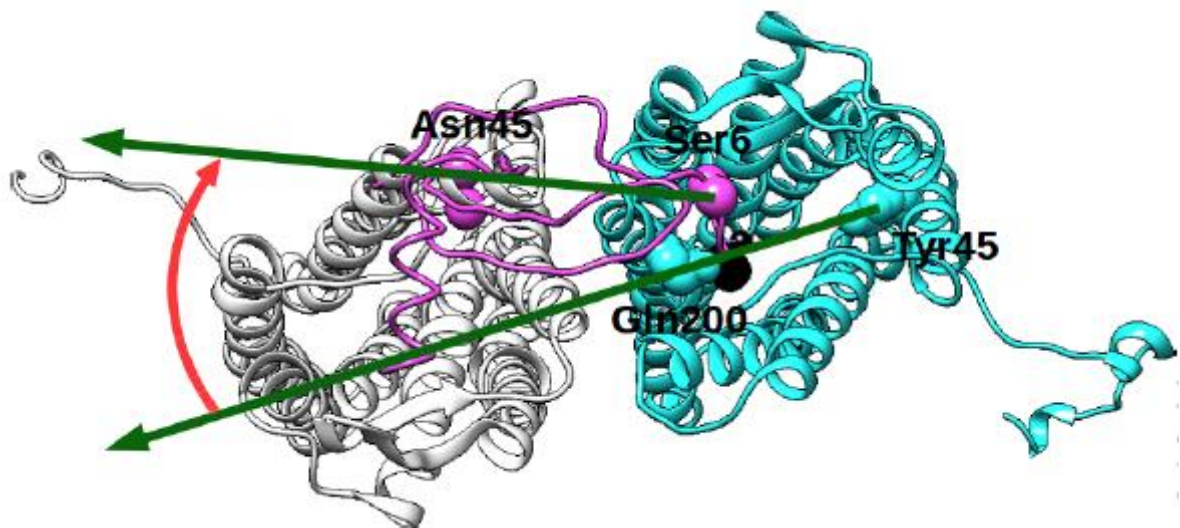


Fig S2. Definition of the angle that characterizes the position of the chemokine core domain with respect to the receptor helix bundle. The angle is defined between the vector joining the CXCR4 residues Tyr45 to Gln200 (cyan spheres) and the vector joining the CXCL12 pivotal residue Ser6 to the antipodal Asn45 (magenta spheres).

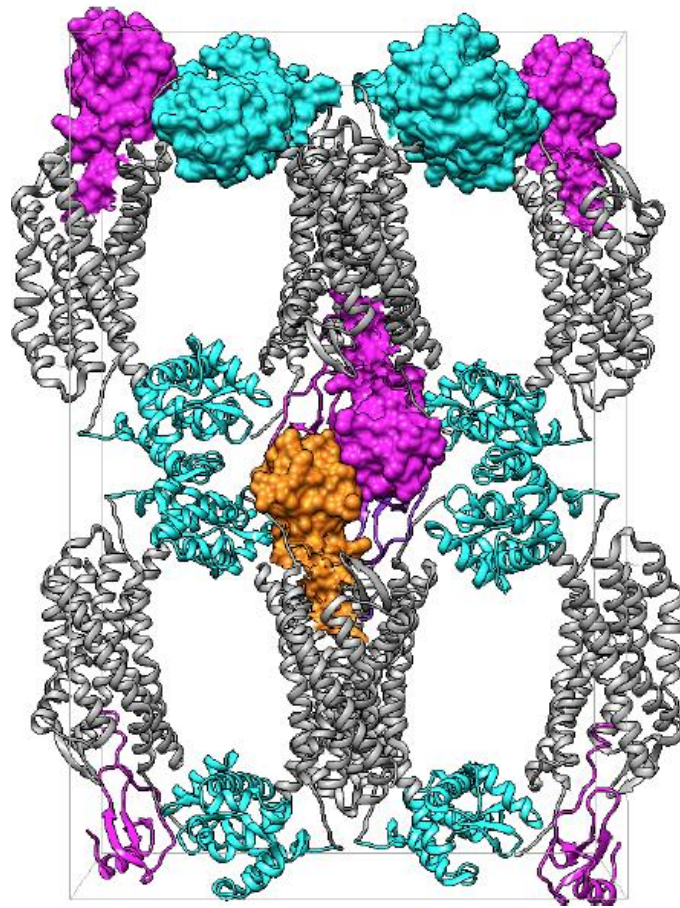


Fig S3. Unit cell of the crystal CXCR4-vMIP-II structure (PDB code 4RWS). CXCR4, vMIP-II and T4 lysozyme are respectively colored in grey, magenta/orange and cyan.

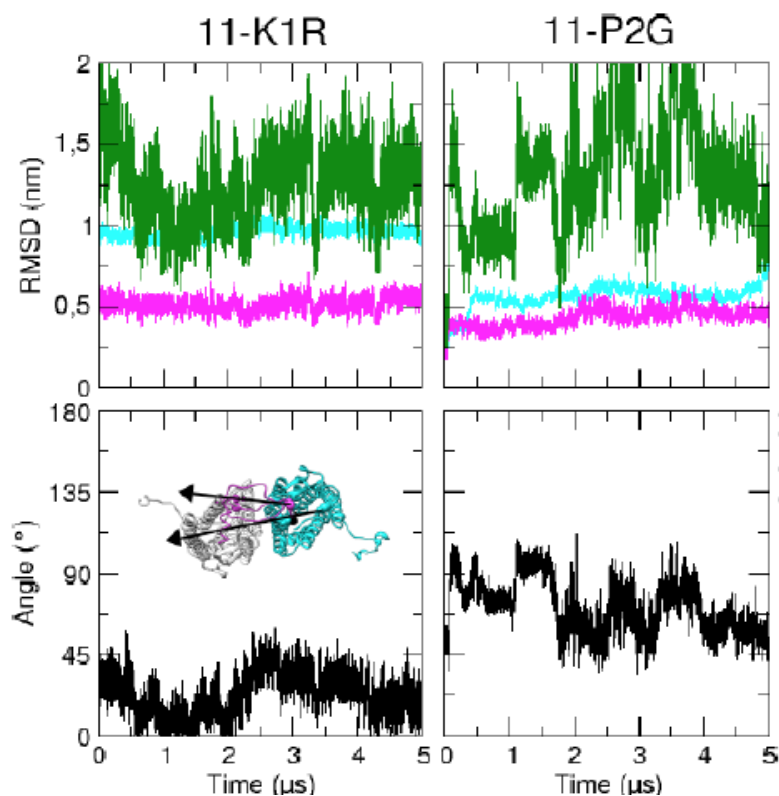


Fig S4. Time evolution of the RMSD (top row) of the receptor (cyan line), the chemokine (magenta line), the chemokine with respect to the receptor (green line), and the chemokine position relative to the receptor (bottom row), for the two chemokine mutant complexes 11-K1R and 11-P2G. The position of the chemokine with respect to the receptor is indicated by the angle between the vector joining the CXCL12 pivotal residue Ser6 to the antipodal Asn45 and the vector joining the CXCR4 residues Tyr45 to Gln200. In the inset picture, the second protomer of the dimeric CXCR4 is represented in white ribbon as a visual reference for the chemokine position. The CXCL12 residue Lys1 is indicated by black spheres and its residues Ser6 and Asn45 by magenta ones.

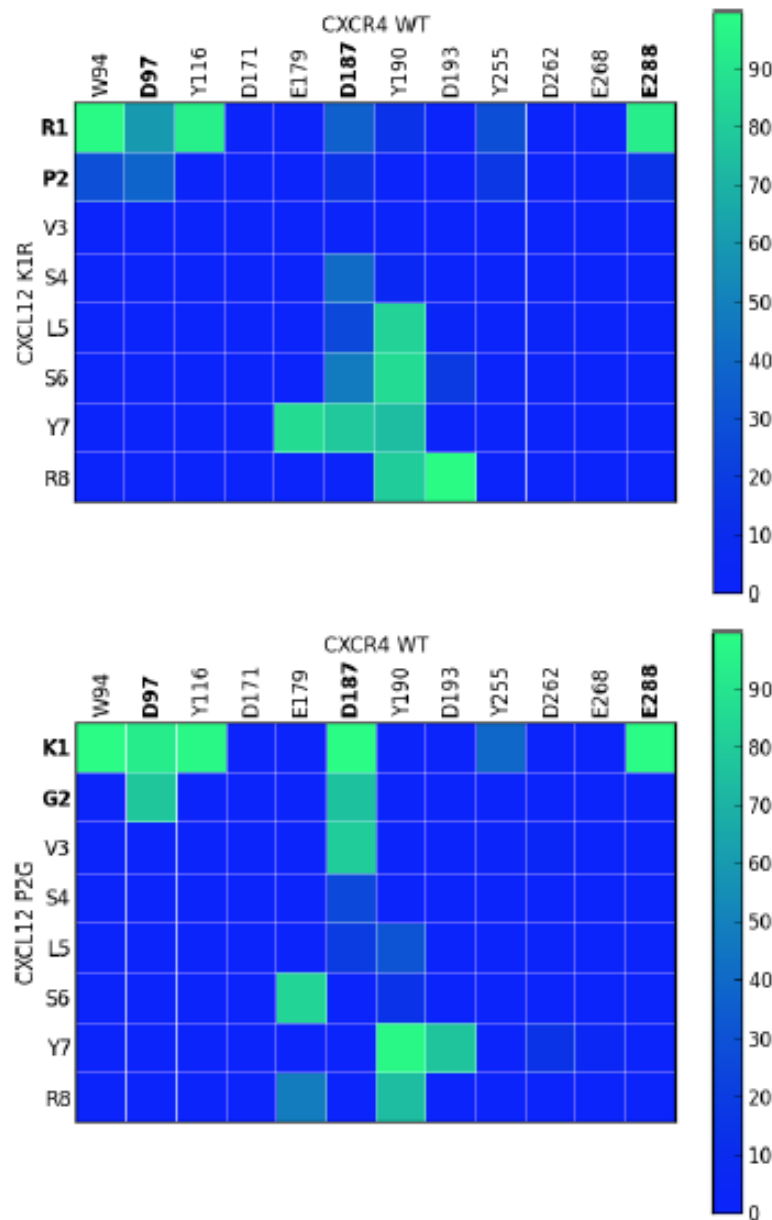


Fig S5. Percentages (right bicolor scale) of the 11-K1R (top) and 11-P2G (bottom) simulation time for which the chemokine N-terminal first eight residues are distant by less than 6 Å to the receptor residues important for activation. Critical residues for CXCR4 activation are emphasized in bold print.

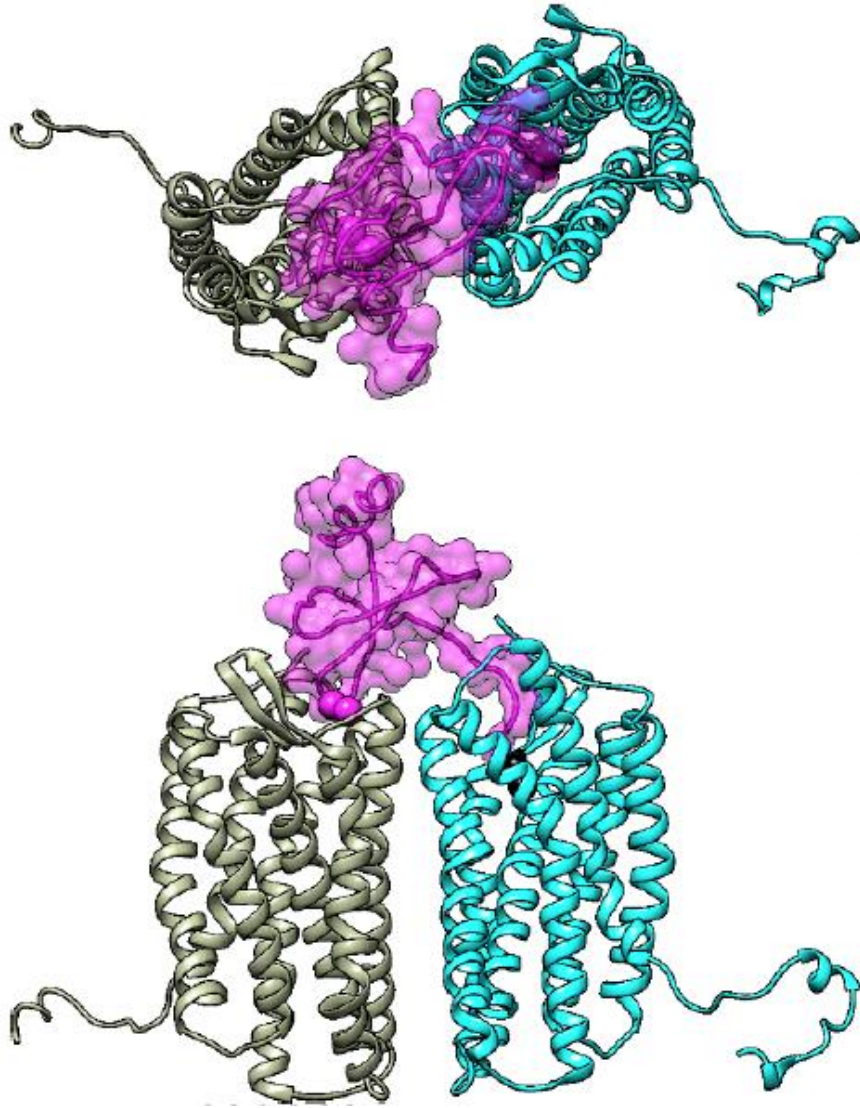


Fig S6. Top and front views of one representative pose of the chemokine CXCL12 (magenta) on the extracellular side of the CXCR4 dimer (cyan and tan).

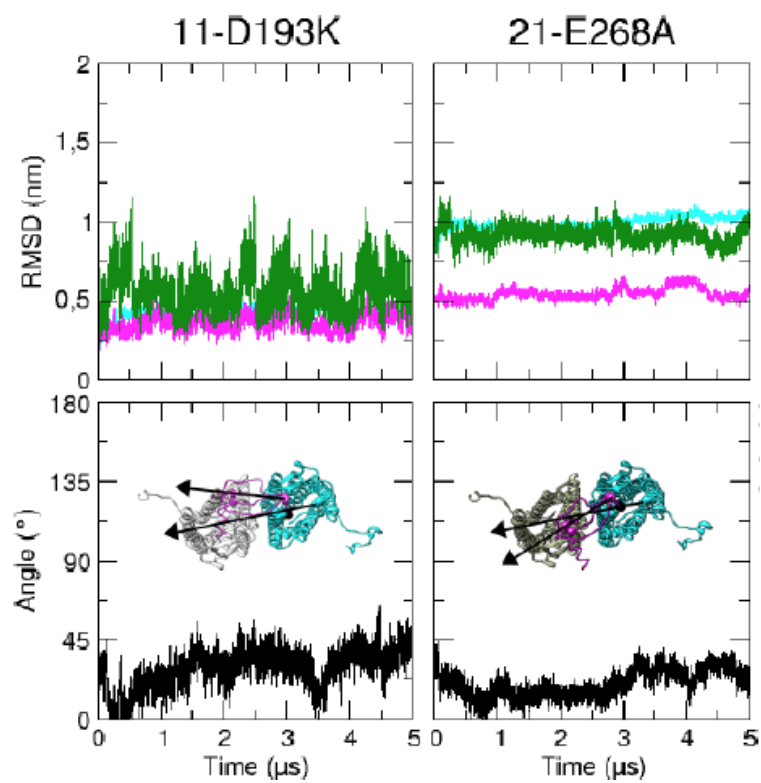


Fig S7. Same as Fig. S4 but for the D193K receptor mutant 1:1 complex (left) and the E268A receptor mutant 2:1 association (right).

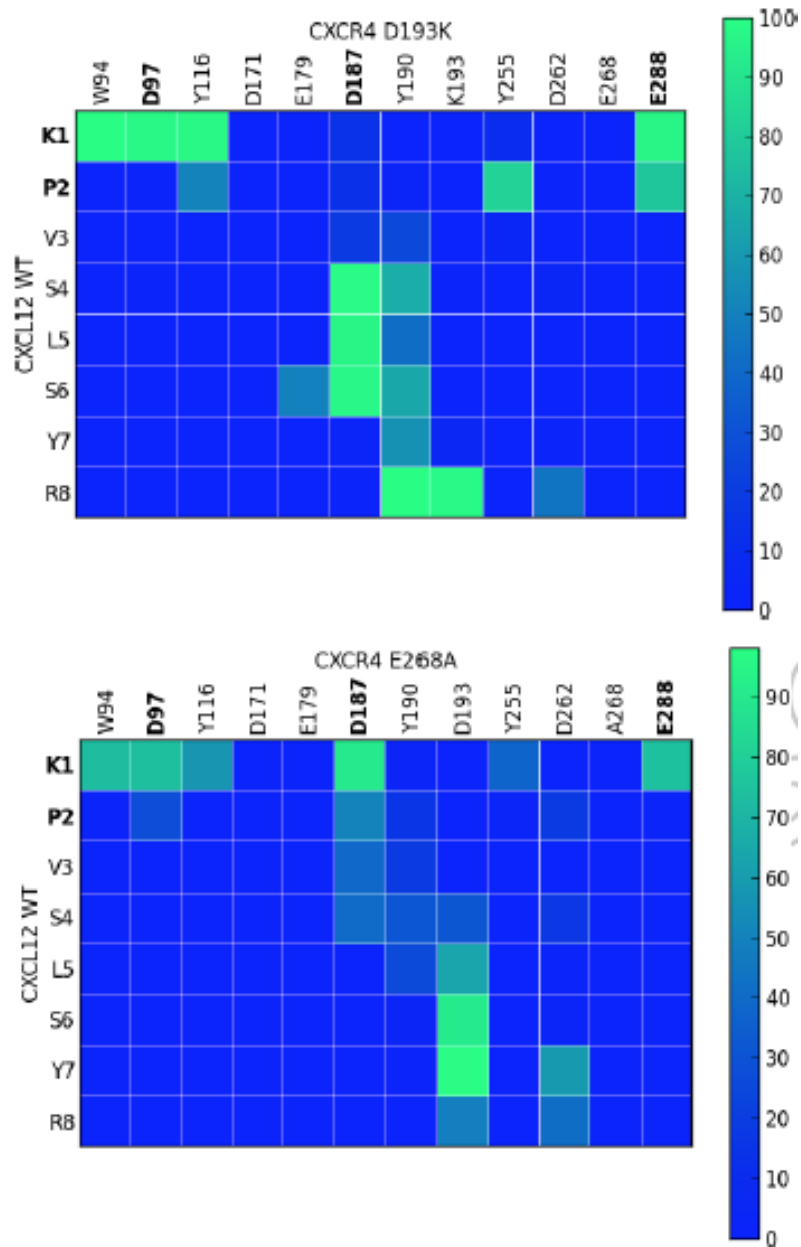


Fig S8. Same as Fig. S5 but for the D193K receptor mutant 1:1 complex (top) and the E268A receptor mutant 2:1 association (bottom).

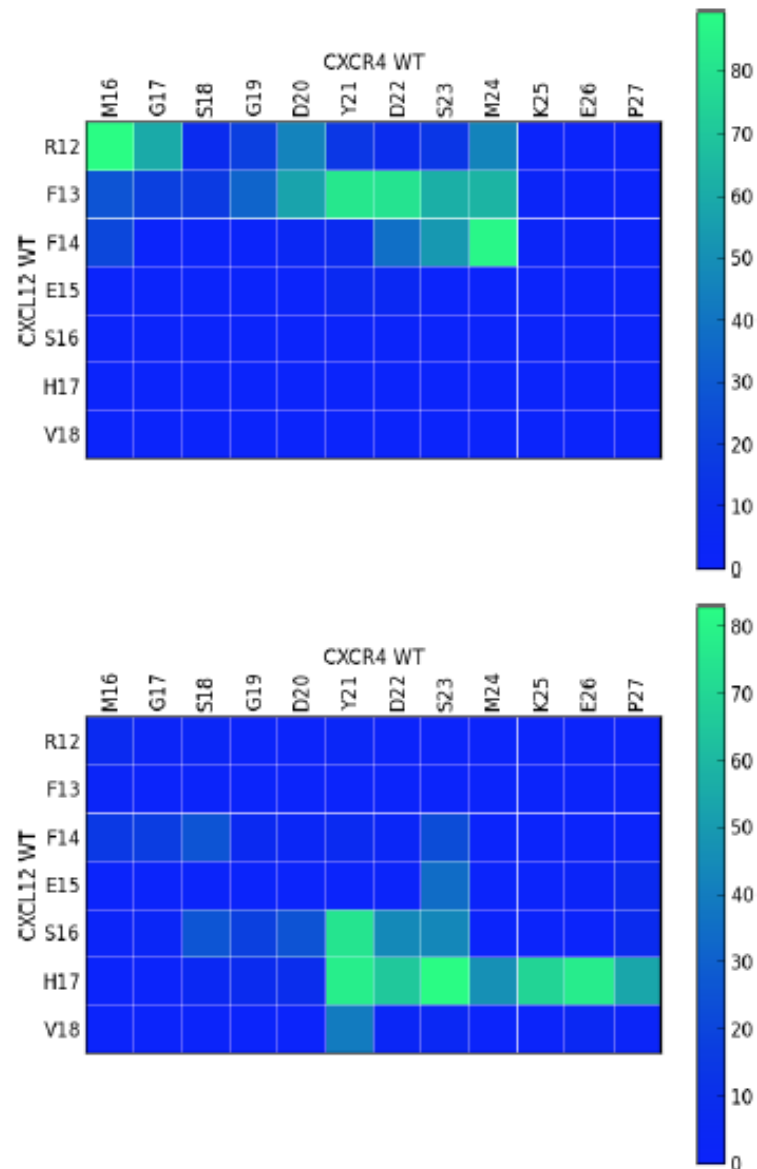


Fig S9. Percentages (right bicolor scale) of the 11-WTC (top) and 21-WT (bottom) simulation time for which the chemokine recognition site residues are distant by less than 6 Å to the receptor N-terminal important residues for binding.

References

Bachelierie, F., Ben-Baruch, A., Burkhardt, A. M., Combadiere, C., Farber, J. M., Graham, G. J., Horuk, R., Sparre-Ulrich, A. H., Locati, M., Luster, A. D., Mantovani, A., Matsushima, K., Murphy, P. M., Nibbs, R., Nomiya, H., Power, C. A., Proudfoot, A. E. I., Rosenkilde, M. M., Rot, A., Sozzani, S., Thelen, M., Yoshie, O., and Zlotnik, A. (2013). International union of pharmacology. LXXXIX. update on the extended family of chemokine receptors and introducing a new nomenclature for atypical chemokine receptors. *Pharmacological Reviews*, 66(1), 1-79.

Balabanian, K., Brodin, E., Biajoux, V., Bouchet-Delbos, L., Lainey, E., Fenneteau, O., Bonnet, D., Fiette, L., Emilie, D., and Bachelierie, F. (2012). Proper desensitization of CXCR4 is required for lymphocyte development and peripheral compartmentalization in mice. *Blood*, 119(24), 5722-5730.

Basdevant, N., Borgis, D., and Ha-Duong, T. (2007). A coarse-grained protein-protein potential derived from an all-atom force field. *Journal of Physical Chemistry B*, 111(31), 9390-9399.

Basdevant, N., Borgis, D., and Ha-Duong, T. (2013). Modeling protein-protein recognition in solution using the coarse-grained force field SCORPION. *Journal of Chemical Theory and Computation*, 9(1), 803-813.

Bleul, C. C., Farzan, M., Choe, H., Parolin, C., Clark-Lewis, I., Sodroski, J., and Springer, T. A. (1996). The lymphocyte chemoattractant SDF-1 is a ligand for LESTR/fusin and blocks HIV-1 entry. *Nature*, 382(6594), 829-833.

Brelot, A., Heveker, N., Montes, M., and Alizon, M. (2000). Identification of residues of CXCR4 critical for human immunodeficiency virus coreceptor and chemokine receptor activities. *Journal of Biological Chemistry*, 275(31), 23736-23744.

Busillo, J. M. and Benovic, J. L. (2007). Regulation of CXCR4 signaling. *Biochimica et Biophysica Acta (BBA) - Biomembranes*, 1768(4), 952-963.

Crump, M. P., Gong, J.-H., Loetscher, P., Rajarathnam, K., Amara, A., Arenzana-Seisdedos, F., Virelizier, J.-L., Baggiolini, M., Sykes, B. D., and Clark-Lewis, I. (1997). Solution structure and basis for functional activity of stromal cell-derived factor-1; dissociation of CXCR4 activation from binding and inhibition of HIV-1. *EMBO journal*, 16(23), 6996-7007.

De Jong, D. H., Singh, G., Bennett, W. F. D., Arnarez, C., Wassenaar, T. A., Schfer, L. V., Periolo, X., Tieleman, D. P., and Marrink, S. J. (2013). Improved parameters for the martini coarse-grained protein force field. *Journal of Chemical Theory and Computation*, 9(1), 687-697.

Doranz, B. J., Orsini, M. J., Turner, J. D., Hofiman, T. L., Berson, J. F., Hoxie, J. A., Peiper, S. C., Brass, L. F., and Doms, R. W. (1999). Identification of CXCR4 domains that support coreceptor and chemokine receptor functions. *Journal of virology*, 73(4), 2752-2761.

Drury, L. J., Ziarek, J. J., Gravel, S., Veldkamp, C. T., Takekoshi, T., Hwang, S. T., Heveker, N., Volkman, B. F., and Dwinell, M. B. (2011). Monomeric and dimeric CXCL12 inhibit metastasis through distinct CXCR4 interactions and signaling pathways. *Proceedings of the National Academy of Sciences*, 108(43), 17655-17660.

Feng, Y., Broder, C. C., Kennedy, P. E., and Berger, E. A. (1996). HIV-1 entry co-factor: Functional cDNA cloning of a seven-transmembrane, G protein-coupled receptor. *Science*, 272(5263), 872-877.

Ferre, S., Casad, V., Devi, L. A., Filizola, M., Jockers, R., Lohse, M. J., Milligan, G., Pin, J.-P., and Guitart, X. (2014). G-protein-coupled receptor oligomerization revisited: Functional and pharmacological perspectives. *Pharmacological Reviews*, 66(2), 413-434.

Freitas, C., Desnoyer, A., Meuris, F., Bachelier, F., Balabanian, K., and Machelon, V. (2014). The relevance of the chemokine receptor ACKR3/CXCR7 on CXCL12-mediated effects in cancers with a focus on virus-related cancers. *Cytokine & Growth Factor Reviews*, 25(3), 307-316.

Hamatake, M., Aoki, T., Futahashi, Y., Urano, E., Yamamoto, N., and Komano, J. (2009).

Ligand-independent higher-order multimerization of CXCR4, a G-protein-coupled chemokine receptor involved in targeted metastasis. *Cancer Science*, 100(1), 95-102.

Hernandez, P. A., Gorlin, R. J., Lukens, J. N., Taniuchi, S., Bohinjec, J., Francois, F., Klotman, M. E., and Diaz, G. A. (2003). Mutations in the chemokine receptor gene CXCR4 are associated with WHIM syndrome, a combined immunodeficiency disease. *Nat Genet*, 34(1), 70-74.

Hess, B., Kutzner, C., van der Spoel, D., and Lindahl, E. (2008). GROMACS 4: Algorithms for highly efficient, load-balanced, and scalable molecular simulation. *Journal of Chemical Theory and Computation*, 4(3), 435-447.

Heveker, N., Montes, M., Germeroth, L., Amara, A., Trautmann, A., Alizon, M., and Schneider-Mergener, J. (1998). Dissociation of the signalling and antiviral properties of SDF-1-derived small peptides. *Current Biology*, 8(7), 369-376.

Huang, Y. and Liu, Z. (2009). Kinetic Advantage of Intrinsically Disordered Proteins in Coupled Folding Binding Process: A Critical Assessment of the Fly-Casting Mechanism. *Journal of Molecular Biology*, 393(5), 1143-1159.

Kofuku, Y., Yoshiura, C., Ueda, T., Terasawa, H., Hirai, T., Tominaga, S., Hirose, M., Maeda, Y., Takahashi, H., Terashima, Y., Matsushima, K., and Shimada, I. (2009). Structural basis of the interaction between chemokine stromal cell-derived factor-1/CXCL12 and its g-protein-coupled receptor CXCR4. *Journal of Biological Chemistry*, 284(50), 35240-35250.

Kryczek, I., Wei, S., Keller, E., Liu, R., and Zou, W. (2006). Stroma-derived factor (SDF-1/CXCL12) and human tumor pathogenesis. *AJP: Cell Physiology*, 292(3), C987-C995.

Kufareva, I., Stephens, B. S., Holden, L. G., Qin, L., Zhao, C., Kawamura, T., Abagyan, R., and Handel, T. M. (2014). Stoichiometry and geometry of the CXC chemokine receptor 4 complex with CXC ligand 12: Molecular modeling and experimental validation. *Proceedings of the National Academy of Sciences*, page 201417037.

Lagane, B., Chow, K. Y. C., Balabanian, K., Levoye, A., Harriague, J., Planchenault, T., Baleux, F., Gunera-Saad, N., Arenzana-Seisdedos, F., and Bachelier, F. (2008). CXCR4 dimerization and -arrestin-mediated signaling account for the enhanced chemotaxis to CXCL12 in WHIM syndrome. *Blood*, 112(1), 34-44.

Ma, Q., Jones, D., Borghesani, P. R., Segal, R. A., Nagasawa, T., Kishimoto, T., Bronson, R. T., and Springer, T. A. (1998). Impaired b-lymphopoiesis, myelopoiesis, and derailed cerebellar neuron migration in CXCR4-and SDF-1-deficient mice. *Proceedings of the National Academy of Sciences*, 95(16), 9448-9453.

Marrink, S. J. and Tieleman, D. P. (2013). Perspective on the Martini model. *Chemical Society Reviews*, 42(16), 6801.

Marrink, S. J., Risselada, H. J., Yefimov, S., Tieleman, D. P., and de Vries, A. H. (2007). The MARTINI force field: Coarse grained model for biomolecular simulations. *Journal of Physical Chemistry B*, 111(27), 7812-7824.

Monticelli, L., Kandasamy, S. K., Periole, X., Larson, R. G., Tieleman, D. P., and Marrink, S.-J. (2008). The MARTINI coarse-grained force field: Extension to proteins. *Journal of Chemical Theory and Computation*, 4(5), 819-834.

Murphy, J. W., Cho, Y., Sachpatzidis, A., Fan, C., Hodsdon, M. E., and Lolis, E. (2007). Structural and functional basis of CXCL12 (stromal cell-derived factor-1) binding to heparin. *Journal of Biological Chemistry*, 282(13), 10018-10027.

Nagasawa, T., Hirota, S., Tachibana, K., Takakura, N., Nishikawa, S.-i., Kitamura, Y., Yoshida, N., Kikutani, H., and Kishimoto, T. (1996). Defects of b-cell lymphopoiesis and bone-marrow myelopoiesis in mice lacking the CXC chemokine PBSF/SDF-1. *Nature*, 382(6592), 635-638.

Oberlin, E., Amara, A., Bachelier, F., Bessia, C., Virelizier, J.-L., Arenzana-Seisdedos, F., Schwartz, O., Heard, J.-M., Clark-Lewis, I., Legler, D. F., Loetscher, M., Baggiolini, M., and

Moser, B. (1996). The CXC chemokine SDF-1 is the ligand for LESTR/fusin and prevents infection by t-cell-line-adapted HIV-1. *Nature*, 382(6594), 833-835.

Peled, A., Wald, O., and Burger, J. (2012). Development of novel CXCR4-based therapeutics. *Expert Opinion on Investigational Drugs*, 21(3), 341-353.

Periole, X., Cavalli, M., Marrink, S.-J., and Ceruso, M. A. (2009). Combining an elastic network with a coarse-grained molecular force field: Structure, dynamics, and intermolecular recognition. *Journal of Chemical Theory and Computation*, 5(9), 2531-2543.

Puchert, M. and Engele, J. (2014). The peculiarities of the SDF-1/CXCL12 system: in some cells, CXCR4 and CXCR7 sing solos, in others, they sing duets. *Cell and Tissue Research*, 355(2), 239-253.

Qin, L., Kufareva, I., Holden, L. G., Wang, C., Zheng, Y., Zhao, C., Fenalti, G., Wu, H., Han, G. W., Cherezov, V., Abagyan, R., Stevens, R. C., and Handel, T. M. (2015). Crystal structure of the chemokine receptor CXCR4 in complex with a viral chemokine. *Science*.

Roumen, L., Scholten, D., de Kruijf, P., de Esch, I., Leurs, R., and de Graaf, C. (2012). C(x)CR in silico: Computer-aided prediction of chemokine receptor/ligand interactions. *Drug Discovery Today: Technologies*, 9(4), e281-e291.

Saladin, A., Fiorucci, S., Poulain, P., Prvost, C., and Zacharias, M. (2009). PTools: an opensource molecular docking library. *BMC Structural Biology*, 9(1), 27. Sun, X., Cheng, G., Hao, M., Zheng, J., Zhou, X., Zhang, J., Taichman, R. S., Pienta, K. J., and Wang, J. (2010). CXCL12 / CXCR4 / CXCR7 chemokine axis and cancer progression. *Cancer and Metastasis Reviews*, 29(4), 709-722.

Tamamis, P. and Floudas, C. A. (2014). Elucidating a key component of cancer metastasis: CXCL12 (SDF-1) binding to CXCR4. *Journal of Chemical Information and Modeling*, 54(4), 1174-1188.

Tian, S., Choi, W.-T., Liu, D., Pesavento, J., Wang, Y., An, J., Sodroski, J. G., and Huang, Z.

(2005). Distinct functional sites for human immunodeficiency virus type 1 and stromal cell-derived factor 1 on CXCR4 transmembrane helical domains. *Journal of Virology*, 79(20), 12667-12673.

Uversky, V. N. and Dunker, A. K. (2010). Understanding protein non-folding. *Biochimica et Biophysica Acta - Proteins and Proteomics*, 1804(6), 1231-1264.

Veldkamp, C. T., Peterson, F. C., Pelzek, A. J., and Volkman, B. F. (2005). The monomer-dimer equilibrium of stromal cell-derived factor-1 (CXCL 12) is altered by pH, phosphate, sulfate, and heparin. *Protein Science*, 14(4), 1071-1081.

Veldkamp, C. T., Seibert, C., Peterson, F. C., Sakmar, T. P., and Volkman, B. F. (2006). Recognition of a CXCR4 Sulfotyrosine by the Chemokine Stromal Cell-derived Factor-1 (SDF-1/CXCL12). *Journal of Molecular Biology*, 359(5), 1400-1409.

Veldkamp, C. T., Seibert, C., Peterson, F. C., De la Cruz, N. B., Haugner III, J. C., Basnet, H., Sakmar, T. P., and Volkman, B. F. (2008). Structural basis of CXCR4 sulfotyrosine recognition by the chemokine SDF-1/CXCL12. *Science signaling*, 1(37), ra4.

Wu, B., Chien, E. Y., Mol, C. D., Fenalti, G., Liu, W., Katritch, V., Abagyan, R., Brooun, A., Wells, P., and Bi, F. C. (2010). Structures of the CXCR4 chemokine GPCR with small-molecule and cyclic peptide antagonists. *Science*, 330(6007), 1066-1071.

Xu, L., Li, Y., Sun, H., Li, D., and Hou, T. (2013). Structural basis of the interactions between CXCR4 and CXCL12/SDF-1 revealed by theoretical approaches. *Molecular BioSystems*, 9(8), 2107.

Yesylevskyy, S. O., Schfer, L. V., Sengupta, D., and Marrink, S. J. (2010). Polarizable Water Model for the Coarse-Grained MARTINI Force Field. *PLoS Computational Biology*, 6(6), e1000810.

Zhou, N. (2001). Structural and functional characterization of human CXCR4 as a chemokine receptor and HIV-1 co-receptor by mutagenesis and molecular modeling studies. *Journal of Biological Chemistry*, 276(46), 42826-42833.

Paper n°2

**Conformationally selective Nanobodies for regulation of
CXCR4 functions**

Full title:

Conformationally selective Nanobodies for regulation of CXCR4 functions

Short title:

Nanobodies as tools

Pasquale Cutolo¹, Agnieszka Jaracz-Ros¹, Joyce Heuinck², Thomas Bourquard³,
Elodie Dupuis⁴, Thomas Roux⁴, Eric Trinquet⁴, Guillaume Bernadat⁵, Thierry
Durroux², Françoise Bachelerie^{1*}

¹ UMR996 - Inflammation, Chemokines and Immunopathology -, Inserm, Univ Paris-Sud,
Université Paris-Saclay, 92296, Clamart, France.

² CNRS UMR 5203, INSERM U1191, Institut de Génomique Fonctionnelle, Université
Montpellier 1 & 2, Montpellier, France

³ BIOS group, INRA, UMR85, Unité Physiologie de la Reproduction et des Comportements,
F-37380 Nouzilly, France; CNRS, UMR7247, F-37380 Nouzilly, France; Université François
Rabelais, 37041 Tours, France; IFCE, Nouzilly, F-37380 France

⁴ Cisbio Bioassays, BP84175, Codolet, France

⁵ BioCIS - UMR 8076, Université Paris-Sud, CNRS, Université Paris-Saclay, Châtenay-
Malabry, France

* Address correspondence to: francoise.bachelerie@u-psud.fr

Abstract

The pair formed by the CXCL12 chemokine and its G-protein-coupled receptor (GPCR) CXCR4 is highly conserved among vertebrates being essential for development, and critical for numerous homeostatic functions such as cell survival and proliferation, adhesion and chemotaxis. This axis is hijacked by various pathogens and deregulated in pathological conditions generating a large body of work devoted to this pair as a therapeutic target. Small molecules and human single-domain antibodies-like scaffold interacting within the CXCL12 binding pocket act as potent inhibitors including VHH-based immunoglobulin single-variable domain or nanobodies from the Camelid family. Here, we set out to study the functional interaction of three nanobodies with CXCR4 to investigate their roles as novel tools for studying the biology of the CXCL12/CXCR4 signaling pathways. We found that two of them inhibited to varying extents CXCL12-induced G-protein activation (cyclic AMP accumulation), β -arrestin-dependent activation (extracellular signal regulated kinase ERK1/2 activation), receptor internalization (diffusion-enhanced resonance energy transfer or DERET) and chemotaxis of both human and murine primary lymphocytes. Binding assays indicate that these functional effects were due to steric blockade of the chemokine for one, but most likely for the other to stabilization of specific receptor conformations, which do not support effector coupling. Whereas the third nanobody, also binds to extracellular loop of CXCR4, it behaves as a biased ligand inhibiting CXCL12-induced CXCR4 internalization but acting as a positive modulator of CXCL12/CXCR4-induced chemotaxis of human lymphocytes, likely as a consequence of stabilization of specific active CXCR4 conformations in complex with G- α -i proteins.

Introduction

CXCR4 is a member of the chemokine subfamily of GPCRs with a unique chemokine ligand, CXCL12 (SDF-1) ^{1,2}. CXCR4 and CXCL12 are expressed by a vast array of cell types in many tissues and are both essential for embryonic development where disruptions of either gene is embryo lethal in mice, promoting defects in cardiac, hematopoietic, and cerebellar development, evidencing a broad spectrum of activities ^{3,4}. In adult life, the CXCR4–CXCL12 axis is endowed with a wide spectrum of physiological functions such as cell migration in the context of immune surveillance and inflammatory responses as well as cell survival and growth, and tissue repair and neovascularization ⁵. Therefore, this axis is involved in numerous pathological settings notably in immune and infectious diseases and in various cancers progression and dissemination ^{6,7}, including virus-related ones ⁸. Like for most GPCRs, such a diversity of biological activities is accounted by ligand-mediated stabilization of receptor conformations that activate or inhibit downstream signaling pathways including G-protein and arrestin-dependent ones triggered by CXCR4–CXCL12 interaction ⁹. Moreover, CXCR4 shares with most GPCRs the capacity to form oligomers ^{10,11}, including with the atypical chemokine receptor ACKR3 (CXCR7), which also binds to CXCL12 ¹² and modulates CXCR4–CXCL12 signaling ^{13–15}. Such higher order GPCR-associated protein complexes might contribute to the stabilization of further distinct receptor conformations differentially recognized and modulated by ligands. In the case of CXCR4, CXCL12 and other orthosteric ligands including small-molecules antagonists, mutant chemokines and antibody-derived molecules were primarily described ^{16–18}. Allosteric ligands, which bind sites distinct from the orthosteric binding pocket, can be useful in binding to specific receptor conformations and were recently described for single-domain Camelid heavy-chain-only antibody (nanobody) ^{19,20} shown to act as strong antagonists of CXCR4–CXCL12 mediated signaling ²¹. Compared to normal antibodies, nanobodies (NBs) are smaller (12–15 kDa), able to bind to cryptic antigenic and were described as crystallization chaperones for GPCRs ^{22,23} and inhibitory molecules directed against chemokine subfamily of GPCRs ^{21,24,25}. In addition, NBs are modular and can be linked to molecules or tags commonly added to proteins or fused between forming multivalent molecules with potentially different mode of action than the monovalent form ²¹. Herein, we characterized three NBs directed against CXCR4 and explored their ability to allosterically target and stabilize distinct CXCR4 conformations. Our studies uncovered that two of the NBs are blocking CXCR4–CXCL12 mediated G-protein and

arrestin activation in a selective fashion but with differing abilities. While the third though inhibiting CXCR4 internalization appears to act as a biased agonist for the Extracellular Signal-regulated Kinase (ERK) signaling thus enhancing CXCL12-induced chemotaxis suggesting that the scaffold function of β -arrestin in signaling can be dissociated from its recruitment to activated receptor for desensitization. Collectively our data are supporting the utility of NBs as novel tools to study GPCR biology.

Results

We selected three NBs upon phage display selections of libraries derived from Llamas immunized with CXCR4-expressing cells. Homogeneous time-resolved Forster resonance energy transfer (HTR-FRET) experiments based on the detection of the NBs with an antibody directed against the Histidine Tag fused to the N-terminus of the NBs confirmed that all NBs bind to CXCR4 (data not shown). Further characterization of these NBs in binding experiments with the Tag-lite assay was performed to examine the potential capacity of the NBs to compete with CXCL12 binding to CXCR4 and then to determine their affinities for CXCR4 (Fig. 1). Cells expressing a chimeric CXCR4 receptor fused on its N-terminus to the HaloTag were incubated for 2 hours in the presence of tracer, CXCL12-red, and increasing concentrations of NBs. Known orthosteric selective CXCR4 inhibitors (i.e. IT1t 10) inhibit CXCL12 binding (Fig. 1). One of NBs (NB1) potently displaced CXCL12-red binding, thus consistent with a simple competitive behavior of this ligand with an inhibition constant of 48nM. A second one (NB2) slightly inhibited CXCL12 binding though the last one (NB3) did not indicate, at least in this setting, a competitive mode of action (Fig. 1). It is noteworthy that further studies performed in the presence of a reduced amount of tracer, CXCL12-red (3nM), allowed to confirmed some inhibitory behavior of NB2 (data not shown).

As a result of these observations, further studies were performed to assess the mechanisms of action of these NBs. The CXCR4 receptor couples to Gi protein, thereby inhibiting adenylate cyclase and decreasing intracellular cAMP. Therefore, we tested the ability of the NBs to modulate cAMP levels downstream endogenous CXCR4 using an HTRF-FRET based assay. Treatment of HEK293T cells, endogenously expressing CXCR4 (Fig. S1), with CXCL12 caused a robust dose-dependent decrease in cAMP (Fig. S2A), which was antagonized by the addition of AMD3100 (Fig. S2B), a selective CXCR4 antagonist²⁶ and by NB1 but also by NB2, though being a weak competitor, in a dose-dependent manner (Fig. 2A). In contrast, adding NB3 didn't modify cAMP levels indicating that this NB doesn't affect CXCL12/CXCR4-dependent Gi activation. Of note, NB3 didn't modify by its own cAMP production (Fig. S2C).

We next turned to Bioluminescence resonance energy transfer (BRET) assay to examine in living cells whether NB1 and NB2 could alter G-alpha-i1 conformational changes proposed to be set in motion during the G-protein activation process in response to CXCL12¹³. We used the G-alpha-i1-Rluc fusion protein previously described,²⁷. We performed real-time kinetics

after CXCL12 addition in presence or not of NBs (375nM) pre-incubated 30 minutes at room temperature before adding CXCL12. CXCL12 promoted a rapid BRET increase in the first seconds of stimulation, which was stable for ~2 minutes before its decline over time reaching basal levels at ~5 minutes post-stimulation (Fig. 2B). This BRET kinetic profile is reflecting a rapid activation of CXCR4-YFP/G-alpha-i1-Rluc complexes, which is then likely followed by desensitization of the complexes as previously proposed²⁸. Adding NB1 neither modified the shape nor the intensity of the BRET kinetic profile. Though NB2 did not alter the increase of the BRET signal it almost stabilized it over the 10 minutes of observation (Fig. 2B) and up to 30 minutes (data not shown). Interestingly, adding NB3 did not modify the shape of the kinetic but significantly increased its intensity (Fig. 2B). Taken together, these data indicate that NB1 and NB2 significantly inhibit G-alpha-i protein activation although to varying levels and by different mechanisms likely implicating a competitive mode for NB1 and the stabilization of inactive CXCR4-YFP/G-alpha-i1-Rluc complexes for NB2. By contrast, NB3, which doesn't not alter CXCL12-induced Gi proteins activation, rather seems to modulate CXCR4-YFP/G-alpha-i1-Rluc complexes conformational rearrangements. Thus, we investigated whether such NB3-associated conformational rearrangements can be abolished by inactivation of G-alpha-i proteins by pertussis toxin (Ptx). The increased BRET signal from CXCR4-YFP/G-alpha-i1-Rluc complexes observed upon stimulation with CXCL12 (2 minutes) was abolished upon Ptx treatment (Fig. 2C). Interestingly, though NB3 doesn't activate G-alpha-i (Fig. S2C), it displayed with the capacity to induce conformational rearrangements within preassembled CXCR4-YFP/G-alpha-i1-Rluc complexes that were decreased by a Ptx pre-treatment (Fig. 2C). Collectively, these observations suggest that NB1 and NB2 can stabilize inactive CXCR4 conformations whereas NB3 stabilize active CXCR4 conformations. They also further confirm that CXCR4 is basally associated with G-alpha-i 13 as other GPCRs²⁹ and that agonist-induced conformational reorganization of CXCR4-G-alpha-i1 protein complexes are linked to G-protein activation.

Next, NBs were tested for their potential to modulate β -arrestin-dependent signaling, which is activated downstream CXCL12/CXCR4, targeting desensitized CXCR4 to clathrin-coated pits for endocytosis but also linking CXCR4 to the stimulation of additional signaling pathways, including extracellular signal-regulated kinase (ERK) MAPKs, which contribute to CXCL12-induced chemotaxis³⁰⁻³². β -arrestin recruitment to CXCR4 was measured in HEK293T cells transiently expressing Rluc- β -arrestin2 and CXCR4-YFP using BRET assays. As expected, adding CXCL12 (100nM) nicely promoted an increase in BRET signals over

time (Fig. 3A) that was markedly inhibited by the addition of NB2, slightly by that of NB1 (Fig. 3A, upper and middle panels) but not by NB3 (Fig. 3A, bottom panel). When tested in the same assay, none of the NBs did significantly affect CXCL12-induced β -arrestin recruitment to activated CXCR7 (Fig. S3). Given these patterns, we analyzed the propensity of the NBs to potentially interfere with CXCL12-induced CXCR4 internalization, which relies on the recruitment to and association of β -arrestin with the CXCR4 C-tail targeting the desensitized receptor to clathrin-coated pits³³. We used an assay allowing following and quantifying ligand-induced and constitutive-induced GPCR internalization in living cells. In this assay GPCR internalization results in a quantifiable reduction of diffusion-enhanced resonance energy transfer (DERET) due to the disappearance of cell surface labelled-GPCR³⁴. We found that when added in CHO cells expressing chimeric receptors bearing HaloTag-CXCR4 (HaloTag-CXCR4), NB2 had strong effects on the CXCL12-induced internalization of CXCR4 whereas NB1 only a partial effect (Fig. 3B). Surprisingly, NB3, which didn't affect β -arrestin recruitment to the activated CXCR4 receptor (Fig. 3), was found to partly inhibit CXCL12-induced internalization of CXCR4 to the same extent that NB1.

We thus investigated whether NBs elicited differential effects when tested for their capacity to modulate β -arrestin signaling such as the ERK1/2 MAPK pathway³⁵, which is rapidly and transiently induced downstream CXCL12/CXCR4³². Using a HTRF-FRET based assay, we observed the typical transient ERK1/2 phosphorylation kinetic upon CXCL12 treatment showing an early response (2 and 5 minutes) and a late response (20 minutes) that declined over time (Fig. 4 and Fig. S4A). Early and late responses are reported to be primarily dependent upon coupling to G-proteins and to involve β -arrestin, respectively,³². We found that both NB2 (Fig. 4A) and NB1 (Fig. S4B) have significant yet variable inhibitory effects over time, significantly inhibiting the early response but more slightly the late response in support of their marked inhibitory effects on G-protein activation (Fig. 2). In contrast, NB3 dramatically increased CXCL12-induced early and late responses but also promoted by its own a signal of the same magnitude that the one reached upon CXCL12 stimulation (Fig. 4B). This suggests that the agonist effect of this NB on receptor signaling may therefore implicate the stabilization of specific CXCR4/G- α -i1 active complexes, or receptor conformations more prone to CXCL12-induced β -arrestin recruitment or a combination of both. Given these effects we set up to assess the ability of the NBs to modulate CXCL12-induced CXCR4-dependent chemotaxis that depends on the release of G-proteins subunits from activated G- α -i proteins together with β -arrestin2-dependent signaling^{9,13,31,32,36}. Primary human CD4

and CD8 blood-derived lymphocytes, which expressed CXCR4 (Fig. S5A), were found to migrate in response to CXCL12 in a dose-dependent manner in a characteristic bell-shaped chemotactic curve (Fig. 5A). We found that the addition of NB3 increased T cells migration at low CXCL12 concentrations (ie, 10nM) but had no effect at higher concentrations of the chemokine (ie, 50nM) (Fig. 5B) thus shifting the chemotactic curve to the left. This higher efficiency of CXCL12 toward CXCR4-expressing cells in presence of NB3 is consistent with our earlier findings regarding ERK1/2 activation (Fig. 4B) and G-alpha-i CXCL12-induced activation (Fig.2). Nevertheless, though NB3 activated by its own ERK1/2 activation with a similar magnitude to that of CXCL12 it was not promoting T lymphocytes chemotaxis (Fig. 5B). In contrast, NB1 and NB2 inhibited in a dose-dependent manner CXCL12-induced human T cells chemotaxis (Fig. S6), along with their capacities to block G-alpha-i activation and β -arrestin recruitment (Fig. 2 and Fig. 3). Importantly, we observed that the three NBs were effective at modulating CXCL12-induced murine T cells chemotaxis (Fig. S7) according to their differential activities on human T lymphocytes (inhibitors for NB1 and NB2 and enhancer for NB3), and in support of the structural and functional conservation of the CXCL12-CXCR4 axis from mice to humans⁶.

To define the binding sites of the three NBs to CXCR4 extracellular domains we first predicted the most likely three-dimensional structures of the NBs by homology modeling, then we applied molecular dynamic simulation for NBs and CXCR4 to cluster all the possible conformations and finally, we used the Frodock peptide-peptide software³⁷ to perform the cross docking of all conformations of NBs with the extracellular domain of CXCR4 and finally model the best NBs/CXCR4 complexes. The NB1 complementarity-determining region (CDR) was found to interact with the CXCR4 pocket defined by side chains from helices I, II, III, and VII, (Fig. 6) known as the chemokine recognition site 2 (CRS2) occupied by the CXCL12 N-terminus for activation^{10,38}. The NB2 and NB3 CDRs interact both with the extracellular loop 2 (ECL2) of CXCR4, known to be targeted by most GPCRs allosteric modulators^{39,40}, but with different quaternary conformations. Though NB3 CDR establishes interactions throughout the CXCR4 ECL2, NB2 displays an external docking (Fig. 6). These results can be conciliated with earlier findings regarding the activities of the NBs: the competitive antagonism of the orthosteric inhibitor NB1 is consistent with its suggested docking on the CRS2; NB2 and NB3 suggested docking is in keeping with an allosteric behavior of the NBs which is associated with a full antagonism for NB2 and a biased ligand behavior for NB3.

Discussion

In this work, we analyzed three closely related single-domain Camelid heavy-chain antibodies (nanobodies, NBs) for their capacity in modulating CXCR4 signaling and functions. Our studies uncovered that the NBs display differing abilities to associate with CXCR4 and to modulate CXCL12-induced CXCR4 signaling, which translate into differential antagonist and agonist effects on CXCR4 internalization and dependent cell migration thus emphasizing their utility as novel tools to study CXCR4 biology.

Targeting the activity of the CXCR4 receptor has tremendous potential in research and for therapeutic given the important roles of the signaling pathways mobilized by CXCL12-CXCR4 engagement in regulating a vast array of physiological and pathological processes. This diversity, however, complicates drug development and raises concerns for side effects of long-term use of antagonists. For the only approved CXCR4 antagonist in clinic, AMD3100, for mobilization of hematopoietic stem cells^{41,42}, its use in chronic diseases (ie. HIV infection, WHIM syndrome) is hampered by the possible occurrence of adverse effects^{43,44,45}. Recently solved crystal structures of CXCR4 provided support for the two-sites model of CXCL12 binding to CXCR4 that separates the binding and signaling functions of CXCL12⁴⁶. These works identified that small CXCR4 ligand molecules (ie. It1t) act as orthosteric competitors of the CXCL12 N-terminus induced-signaling by binding to the so-called chemokine recognition site 2 (CRS2) within the receptor TM pocket^{10,38}. Similarly, AMD3100 acts by displacing the CXCL12 N-terminus from the receptor TM without affecting the chemokine core domain, which interacts with the receptor N-terminus (CRS1)⁴⁷. There is increasing interest in developing allosteric modulators, which have topographically distinct binding to the conserved orthosteric site, are capable of acting independently or cooperatively with the endogenous ligand to stabilize or potentially induce conformational changes in receptors that are capable of modulating one GPCR signaling pathway over another⁴⁸. Such molecules have been identified for CXCR4⁴⁹⁻⁵¹.

Our observations suggest that NB1 and NB2 inhibit G-alpha-i protein activation and β -arrestin recruitment likely by different mechanisms. Though NB1 displays a competitive behavior for CXCL12 in binding experiments, NB2 did not compete with CXCL12 opening the possibility that it binds to other regions of the receptor thus acting as an allosteric antagonist. In support of this possibility, experiments aimed at modeling the NBs/CXCR4 complexes indicated that NB1'CDR could interact within the CRS2 of the receptor whereas

NB2'CDR most favorably would interact with the extracellular loop 2 (ECL2) of CXCR4. Therefore, given the reported ability of GPCRs to reside in an array of conformations^{49,52,53}, NB2 could stabilize specific receptor conformations that are not conducive to effector coupling and would result in inhibition of CXCR4 signaling. Such possibility is supported by our findings that NB2' ability to inhibit β -arrestin recruitment and CXCL12-induced CXCR4 internalization is associated with interference in the CXCL12-induced activation kinetic of the CXCR4/G- α -i complexes leading to the stabilization of conformational states that could fail in permitting desensitization.

The fact that the non-competitive NB3 didn't interfere with CXCL12-induced β -arrestin recruitment but nonetheless, inhibited CXCL12-induced CXCR4 internalization with the same magnitude than NB2 can be accounted for by its agonist effect on ERK1/2 activation that may therefore implicate the stabilization of specific CXCR4/G- α -i active complexes conformations. This behavior is reminiscent with the discovery that β -arrestin signaling can occur independently of G-protein activation leading to the concept that specific GPCR signaling pathway can be pharmacologically isolated, referred to as functional selectivity or biased agonism or antagonism⁵⁴. Supporting this phenomenon for CXCR4⁵³, some peptidic molecules which are lipid-modified peptides can act as a biased agonist on CXCR4 selectively inducing β -arrestin signaling⁵⁵ and most recently, fully human single-domain antibody-like scaffold termed (or i-body) were found to display selective antagonist activity for CXCR4 signaling pathways⁵⁶. Here, NB3 can inhibit CXCL12-induced CXCR4 internalization while enhancing the activity of CXCL12 in promoting T lymphocytes chemotaxis suggesting that the observed bias can be related to selective interactions between β -arrestin and CXCR4. Indeed, NB3 activity further supports the findings that the requirement for β -arrestin in CXCR4-dependent chemotaxis^{31,36} is not related to the role of β -arrestin in receptor internalization but rather to β -arrestin-dependent signaling pathways, which have been associated to the activation of ERK1/2 pathway, the recruitment of molecules involved in cytoskeleton reorganization and the binding of β -arrestin to the receptor ICL3^{32,57}. Here, conformational changes within CXCR4/G- α -i protein complexes that occurred in the presence of NB3 may underlie the stabilization of active conformations of the complex consistent with the fact that CXCR4-dependent chemotaxis also requires G-proteins activation^{13,32}. Though further work, including with mutant receptors for expression and/or activation, will be required to delineate the molecular mechanisms governing this bias, NB3 represents

an original tool for dissecting the relative importance of specific signaling pathways downstream CXCR4 and deepen our understanding of CXCR4 physiopathology.

NBs targeting the ECL2 of CXCR4 were reported as potent antagonists of CXCR4-dependent signaling pathways and function and display potential therapeutic application in CXCR4-related diseases ²¹. Along with the capacity of all three NBs to modulate positively or negatively CXCL12/CXCR4-promoted chemotaxis of primary murine T lymphocytes, these NBs provide novel tools to analyze the contribution of CXCR4-dependent pathways to physiological processes but also represent potential therapeutic tools in murine models of human diseases caused by CXCR4 dysfunction (eg. the WHIM syndrome ⁵⁸).

Experimental Procedures

Cell culture and transfection

HEK293T and CHO cells were grown in culture medium (Dulbecco modified Eagle medium (DMEM) supplemented with 10 % (v/v) fetal bovine serum (FBS), 1% peni-streptomycin) (all reagents are from Invitrogen SARL, Cergy Pontoise, France). Human peripheral blood lymphocytes (PBMCs) were isolated from heparin-treated blood samples of healthy blood donors, cultured, and activated in RPMI medium supplemented with human serum AB. Cells stably expressing the SNAP-tag-fused CXCR4 receptor (ST-CXCR4 cells) were provided by Cisbio Bioassay and were grown in culture medium supplemented with 0,6 µg/ml geneticin. Transient expression was achieved using the calcium phosphate precipitation method for HEK293 cells as described⁵⁹. The JetPEI transfection reagent (Plyplus, Illkirch, France) was used for CHO cells according to the manufacturer's protocol. Briefly, transfections were performed in black 96-well plates. Prior to cell plating, wells were pre-coated with 50 µl of poly-L-ornithine for 30 min at 37°C. Then, cells were added at a density of 100,000 cells/well and incubated at 37 °C under 5% CO₂ for 24 hours.

Reagents and plasmids constructs

Recombinant CXCL12 was from R&D Systems (Lilles, France). The CXCR4 and CXCR7 receptors tagged at the C-tail with Yellow Fluorescent Protein (CXCR4-YFP; CXCR7-YFP) were obtained by inserting in-frame the human CXCR4 or CXCR7 cDNA into the pcDNA3/CMV-Rluc vector as described¹³. Plasmids encoding GapLhai-1-Rluc (Renilla luciferase) and β-arrestin-2-Rluc were previously described¹³. Pertussis toxin (Ptx) were from Sigma-Aldrich (St Louis, MO). The HALO-CXCR4 encoding plasmid was designed with the HaloTag enzyme inserted at the extracellular N-terminus extremity of the receptor (Cisbio Bioassays, Codolet, France). The endogenous signal peptide was removed to avoid cleavage of HaloTag and was replaced by a generic signal peptide (T8) inserted upstream of HaloTag sequence.

Flow cytometric analyses

Cell-surface expression of receptors in human and murine cells was determined as described^{58,59}. For human cells, staining was performed using the phycoerythrin-conjugated anti-human CXCR4 monoclonal antibodies (mAbs) 12G5, allophycocyanin (clone HIT3a)-, phycoerythrin (clone RPA-T8)- and, Fluorescein isothiocyanate (clone RPA-T4)-conjugated anti-human CD3, CD8 and CD4 mAbs (BD Biosciences, San Jose, CA, USA). For murine cells, the antibodies were Pacific blue (clone 145-2C11, hamster IgG1)-, amy-cyan (clone RM4-5, rat IgG2a) and allophycocyanin (clone 53-6.7, rat IgG2a)-conjugated anti-murine CD3, CD4 and CD8 mAbs (R&D Systems, Lille, France). Analysis was carried out on a BD Biosciences FACS Fortessa.

Chemotaxis assays

Chemotaxis of human T lymphocytes were carried out as previously described⁵⁹. Briefly, experiments were conducted using Transwell® chambers with 5-µm pore size polycarbonate filter (Coring Inc.) at 37°C for 2 hours and migrating cells were stained with CD3, CD4 and CD8 antibodies (BD Science, San Jose, CA). Chemotaxis of murine splenic lymphocytes was carried out as previously described⁵⁸. Briefly, 1×10^6 cells were suspended in 150 µL RPMI medium supplemented with 20 mM HEPES (N-2-hydroxyethylpiperazine-N'-2-ethanesulfonic acid) and 0.5% bovine serum albumin (BSA) and placed into the upper chamber of a 6.5-mm diameter, 5-µm pore polycarbonate Transwell® culture insert. The same media, containing or not a CXCL12, was placed in the lower chamber and chemotaxis proceeded for 2 hours at 37°C in humidified air with 5% CO₂. CXCL12 was used at the indicated concentrations and AMD3100 (10µM) was added in both chambers. Analyses were carried out on a BD Biosciences FACS Fortessa. The fraction of cells migrating across the polycarbonate membrane was calculated as follows: [(number of cells migrating to the lower chamber in response to chemokine) - (number of cells migrating spontaneously)] / number of cells added to the upper chamber at the start of the assay} × 100. Results are expressed as a percentage of input cells that migrated to the lower chamber.

Binding and competition assays

CHO cells were plated in black-walled, dark-bottom, 96-well plates (Greiner CELLSTAR plate; Sigma-Aldrich, St. Louis, MO, USA) at 30 000 cells per well in culture medium and transfected 24 hours later with HaloTag-CXCR4 as described above. Cells were labeled as described⁶⁰. Briefly, the day after the transfection, cells were rinsed once with Tag-lite medium (Cisbio Bioassays, Codolet, France) and incubated in the presence of Tag-lite medium containing 100nM Halo-Lumi4-Tb for at 1 hour at 37°C. Cells were then washed four times and incubated in the presence of an increasing concentration range of fluorescent CXCL12 (CXCL12-red)⁶¹ (Cisbio Bioassays, Codolet, France) at room temperature for 2 hours before analysis. Specific signal was obtained by subtracting the nonspecific signal from the total binding signal. For competition assays, a fixed concentration of CXCL12-red (5 to 10nM) was mixed to increasing concentration of competitors at 4°C to prevent receptor internalization. Fluorescent signal was measured at 620nm (fluorescence of the donor) and at 665nm (FRET signal) over 1 hour on a Pherastar (BMG LABTECH, Champigny s/Marne, France). Results were expressed as the 665/620 ratio. Specific variation of the 665/620 ratio was plotted as a function of competitor concentration. All binding data were analyzed with Prism 6 (GraphPad Software, Inc., San Diego, CA) using the one site-specific binding equation. All results are expressed as the mean \pm SEM of at least three independent experiments performed in triplicate. K_{is} were calculated from IC50 values with the Cheng Prusoff equation⁶². The affinity of CXCL12-red is equal to 48nM⁶¹.

cAMP accumulation and ERK1/2 by HTRF-FRET assays

Measurement of intracellular cAMP accumulation in HEK293T cells (endogenously expressing CXCR4) was performed using the cAMP Dynamics 2 competitive immunoassay kit (Cisbio Bioassays, Codolet, France). The cAMP assay uses a cryptate-conjugated anti-cAMP monoclonal antibody and d2-labeled cAMP. HEK293T cells were detached and seeded into white 96-well microplates with 1×10^4 cells/well in 20 μ l DMEM without serum. Prior to lysis, cells were treated or not with CXCL12 at a concentration of 10nM (to stimulate G-alpha-i coupling to endogenous CXCR4) or with NBs as indicated in 10 μ l/well of DMEM and incubated 30 minutes at 37°C. Antagonists (AMD3100 or NBs) were pre-incubated 30

minutes at room temperature before stimulation with CXCL12. Then, cells were incubated for 45 min with forskolin at final concentration of 5 μ M at 37°C and then lysed by addition of 40 μ l/well of the supplied conjugate-lysis buffer containing d2-labeled cAMP and Europium cryptate-labeled anti-cAMP antibody, both reconstituted according to the manufacturer's instructions. Plates were incubated for 1 hour in the dark at room temperature and time-resolved fluorescence signals were measured at 620 and 665 nm, respectively, 50 ms after excitation at 320 nm using a Mithras LB 940 plate reader (Berthold Biotechnologies, Bad Wildbad, Germany).

Measurement of Phospho-ERK was performed in HEK293T cells using the Advance Phospho-ERK1/2 immunoassay kit (Cisbio Bioassays, Codolet, France), which uses a cryptate-labelled anti-ERK monoclonal antibody and a d2-labeled anti-phospho-ERK monoclonal antibody. Cells were cultured overnight in a 96-well black plate half volume (5x10⁴ cells/well) using 50 μ l of medium/well without serum. Then medium was discarded and 20 μ l of free-serum medium, containing or not AMD3100 or NBs at the different concentrations as indicated, was added to the cells. After 45 minutes of incubation, cells were stimulated with 50nM of CXCL12 for 2, 5 and 20 minutes. After stimulation, cells were put on ice and supplemented lysis buffer was added (32 μ l/well) for 20 min at room temperature with shaking. Then anti-ERK1/2-Europium/Terbium Cryptate and anti-Phospho-ERK1/2-d2 antibody solutions were added (4 μ l of each). The plate was then incubated for at least 4 hours at room temperature before reading the fluorescence emission at 620 and 665 nm using a Mithras LB 940 plate reader (Berthold Biotechnologies, Bad Wildbad, Germany).

Bioluminescence resonance energy transfer (BRET) assay, luminescence, and fluorescence measurements

HEK293T cells were transiently transfected with the indicated constructs. Forty-eight hours after transfection, cells were washed in PBS, detached in PBS-EDTA and resuspended in PBS. Cells were then distributed in a white 96-well plate (Optiplate, PerkinElmer) and incubated with CXCL12 (100nM) and NBs at the indicated concentrations for the indicated times (2, 5 and 10 minutes) at 37°C before adding coelenterazine h (5 μ M) (Interchim, Montluçon, France) as reported previously¹³. BRET values were immediately collected and at 5 and 10 minutes using the Mithras LB-940 reader (Berthold Biotechnologies, Bad Wildbad, Germany), which allows the sequential integration of luminescence signals detected with 2 filters settings

(Rluc filter, 485nm and YFP filter, 530nm). Data were collected using the MicroWin2000 software and BRET signals were expressed in milliBRET units (mBU), 1 mBU corresponding to the BRET ratio multiplied by 1000 as previously described¹³. NetBRET is calculated subtracting the signal of basal BRET in untreated cells.

DERET internalization assays

Internalization assays for CXCR4 were performed in 96-well culture cell plates using CHO cells transiently transfected with HaloTag-CXCR4 as previously described³⁴. Briefly, upon SNAP Lumi4-Tb labeling, internalization experiments were performed by incubating cells with Tag-lite labeling medium, either alone or containing CXCL12 (100nM) without or with NBs (at 6 different concentrations ranging from 10^{-5} - 10^{-11} M) pre-incubated at 16°C for 30 minutes, in the presence of fluorescein. Typically, in plates containing SNAP-Lumi4- Tb-labeled cells, 10 μ l of medium containing CXCL12 (100nM) was added, immediately followed by the addition of 80 μ l of 25 μ M fluorescein. DERET was recorded every 15 minutes for 2 hours in a Tecan Infinite® F500 (Switzerland).

NBs/CXCR4 docking

The prediction of NBs structures was made by the way of CASP (Critical Assessment of protein Structure Prediction) experiments as previously reported⁶³ allowing the selection of five structures for each NBs according to the best energetic scores. Then, dynamic molecular simulation of each 15 predicted structures were performed in order to cluster the conformations of the complementarity-determining regions (CDRs) ending to the definition of six clusters that were used for NBs/CXCR4 docking experiments. Molecular dynamics simulation of the crystal structure of CXCR4 (3ODU)¹⁰, in complex with POPC (1-palmitoyl-2-oleoyl-sn-glycero-3-phosphocholine) in a hydrated context, permitted to identify twenty clusters. In order to define the binding sites of the three NBs, we applied the Frodock method³⁷ following the procedure described in⁶⁴. Briefly, this procedure is following three steps; i) generation of pre-calculated grid maps: Three grid potentials were computed from CXCR4 coordinates (van der Waals, electrostatic and desolvation), whereas only one was needed from NBs coordinates (desolvation). Atomic properties were taken from CHARMM 19 force field; ii) docking was then performed with a single tool called FRODOCK

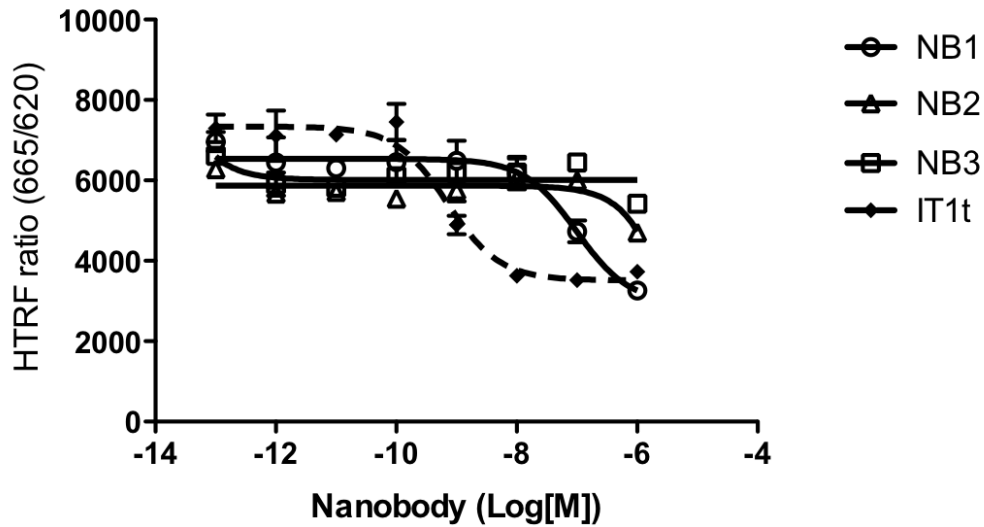
(Chaconlab.org). The rotational and translational sampling resolutions were fixed to 5.6° (6×10^4 rotations) and 2 \AA , respectively. These values were chosen in order to have a good balance between efficiency and accuracy. Since the translational search can eventually explore 105 points, we only considered the best four docking predictions for each translation point in order to avoid a large redundant set of solutions and, iii) clustering was made for each docking run using an explicit comprehensive algorithm⁶⁵. Briefly, once the solution set was ranked according to their docking correlation, we formed clusters with all ligand-docking predictions within 5 \AA RMSD distance from the first ranked solution (i.e. the lowest energy). The final three models were chosen among the first 100 best structures according to the docking score.

Statistical analysis

Results were analyzed by PRISM (GraphPad Software). Data are expressed as mean plus or minus SEM. Student t test was applied for statistical analysis

Immunization and Selection of NBs

Immunization and production was done as previously described²¹. Briefly, Llamas were immunized with cell (10^7) transfected with a vector encoding for CXCR4. After immunization, a nanobody phage library was generated by RT-PCR from blood-derived leukocytes RNA where the phage particles express individual NBs. Phage display selections were performed by using peptide screening (Cisbio Bioassays, Codolet, France) and then production of monoclonal NBs was induced.



	NB1	NB3	NB2	IT1t
Ki	4.897e-008	0.0	~ 0.001841	3.562e-010

Fig. 1. HTRF-based competition assays. To evaluate the affinity of NBs for CXCR4, competition assays were performed with the Tag-lite assay on HaloTag-CXCR4 receptors. CHO cells expressing HaloTag-CXCR4 were incubated in the presence of CXCL12-red tracer (10nM) and increasing concentrations of NBs or the orthosteric CXCR4 antagonist IT1t. FRET signal were measured after overnight incubation at 4°C. Fluorescence ratios (665nm/620nm) were plotted as a function of competitor concentrations. All binding data were analyzed using the one site-specific binding equation. K_i values were calculated from IC_{50} values with the Cheng Prusoff equation and indicated that NB1 competed with CXCL12 but not NB2 and NB3. Results are from one experiment representative of three performed in triplicate. Error bars represent s.e.m.; $n = 3$.

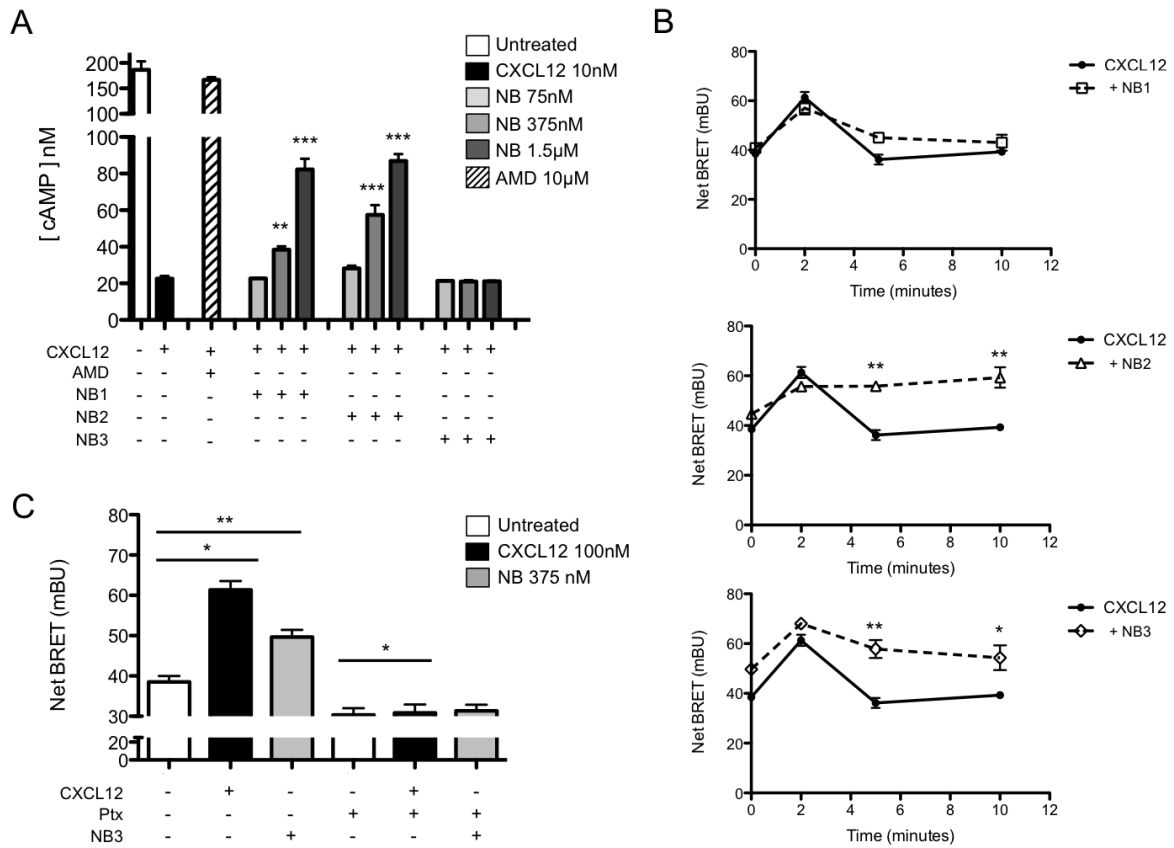


Fig. 2. Effect of NBs on CXCL12/CXCR4-induced G-alpha-i pathway. (A) HTRF-based cAMP assay on HEK293T cells left untreated or treated with CXCL12 (10nM) in the presence or not of the NBs at the indicated concentrations for 30 min. (B) Time course analysis of BRET signals in HEK293T cells transiently transfected with G-alpha-i1-Rluc and CXCR4-YFP upon stimulation with CXCL12 (100nM). NBs (375nM) were pre-incubated 30 minutes at room temperature before adding CXCL12. Signal were immediately collected and at 5 and 10 minutes. (C) BRET signals in HEK293T cells transiently transfected with G-alpha-i1-Rluc and CXCR4-YFP were determined in the absence (untreated) or presence of 100nM CXCL12, NBs at the indicated concentrations and, when indicated, following overnight pretreatment with Pertussis toxin (Ptx 100ng/ml). Signals were recorded 2 minutes after CXCL12 addition. Data represent 3 independent experiments. Data points are mean \pm S.E.M. of triplicate values from a single experiment, and are representative of three individual experiments. T-student analysis for statistics: * $p < 0.05$, ** $p < 0.01$, *** $p < 0.001$.

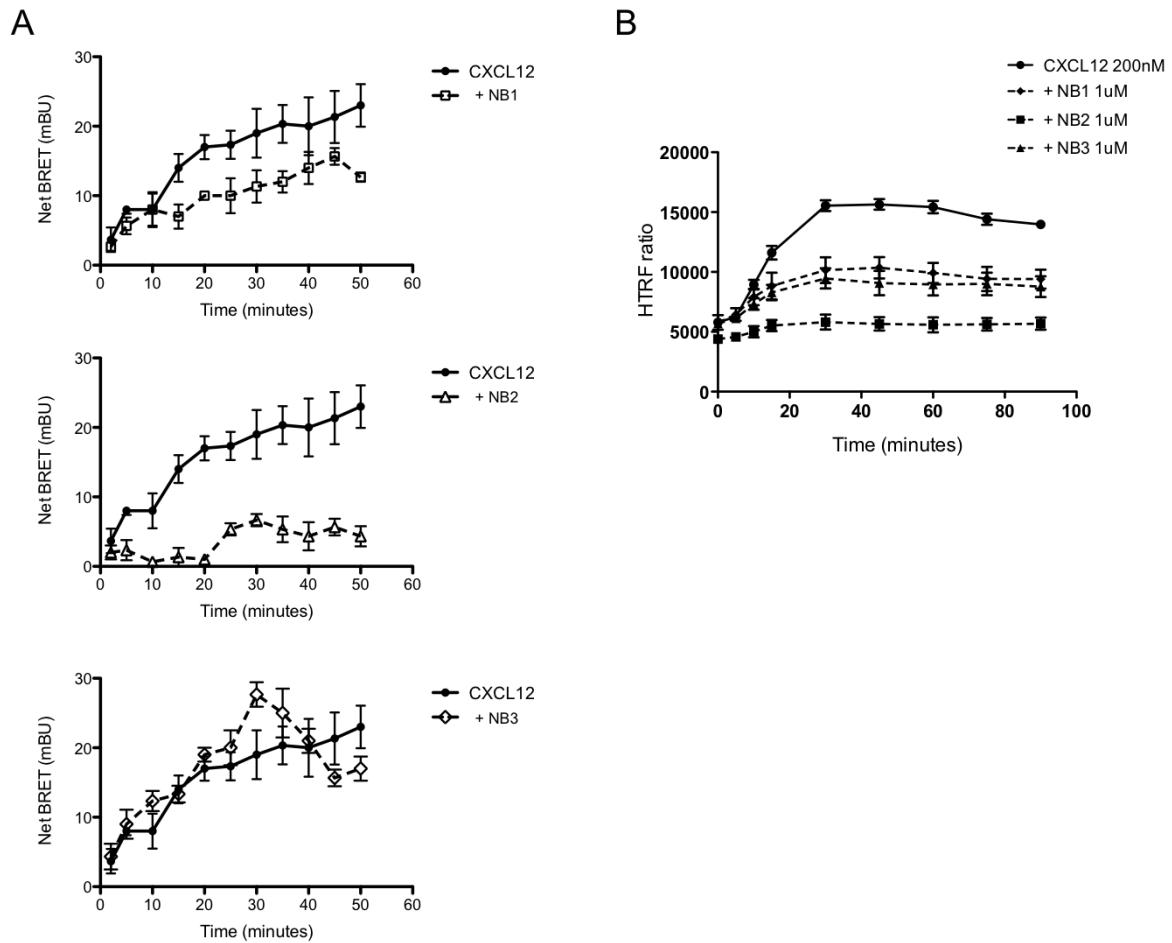


Fig. 3. NBs modulate β -arrestin recruitment to the activated CXCR4 and internalization of the receptor. (A) BRET measure of β -arrestin2 recruitment on CXCR4 in HEK293T cells transiently transfected with β -arrestin-2-Rluc and CXCR4-YFP after 30 minutes of incubation with NBs at the concentration of 375nM, followed by CXCL12 stimulation at 100nM. Data points are mean \pm S.E.M. of triplicate values from a single experiment, and are representative of three independent experiments. (B) DERET assay for the detection of CXCL12-induced internalization of CXCR4. Kinetic analysis of CXCR4 internalization in CHO cells transiently expressing HALO-CXCR4 and labeled with SNAP-Lumi4®-Tb. Internalization was monitored in the presence or absence of 100nM CXCL12 and NBs (1 μ M). Results (mean \pm SEM) were from three independent experiments performed in duplicate.

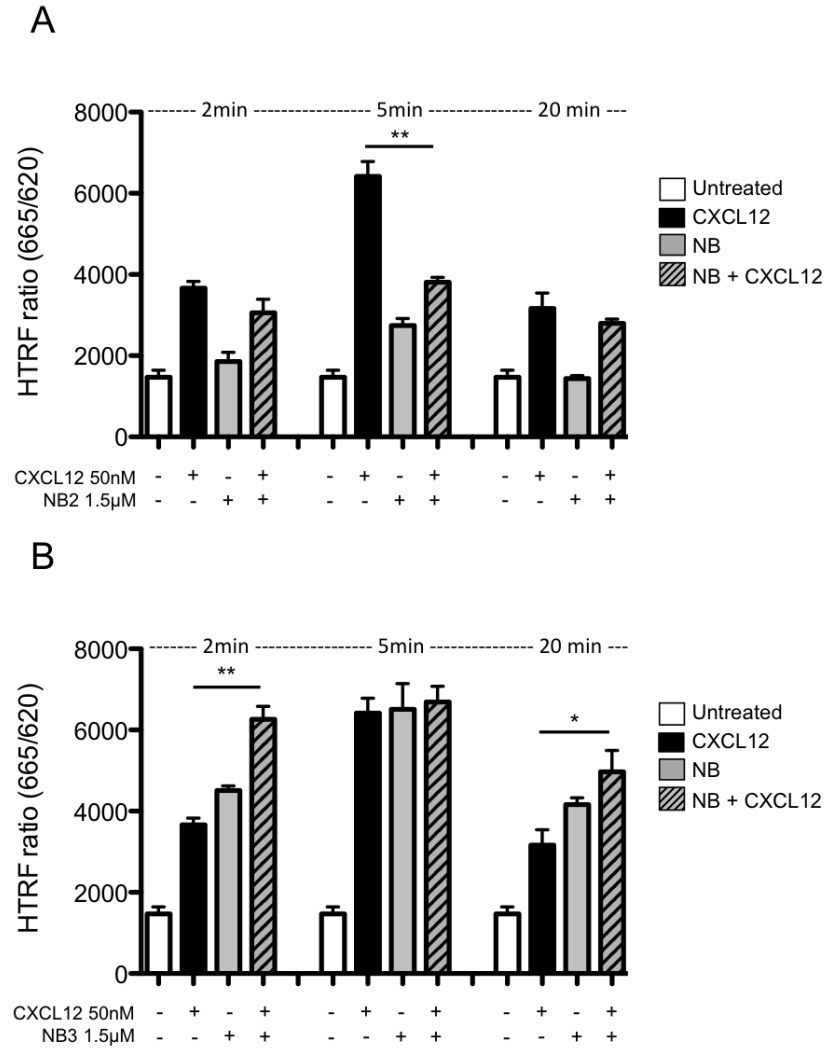
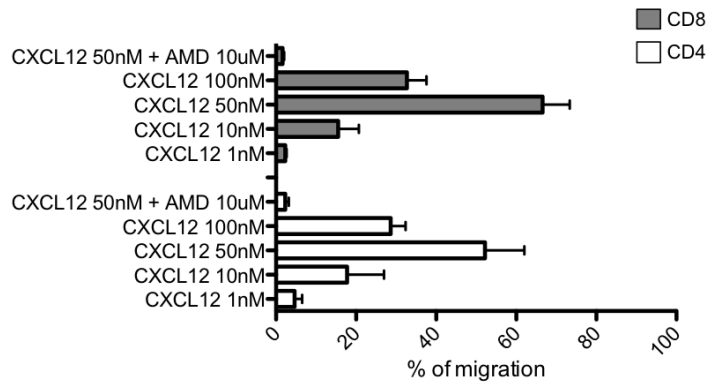


Fig. 4. NBs interfere with ERK/MAPK activation downstream CXCR4. Effect of NB2 (A) and NB3 (B) on CXCR4-dependent ERK phosphorylation using a HTRF-based assay in HEK293T cells expressing endogenous levels of CXCR4. Cells were either pre-incubated with NBs at 1.5µM during 30 minutes on ice before being stimulated with CXCL12 (50nM) or directly stimulated with CXCL12 (50nM) or NBs (1.5µM) for 2, 5 and 20 minutes at 37°C before harvesting. Data points are mean ± S.E.M. of triplicate values from a single experiment, and they are representative of two separate experiments. T-student analysis for statistics: * $p < 0.05$, ** $p < 0.01$.

A



B

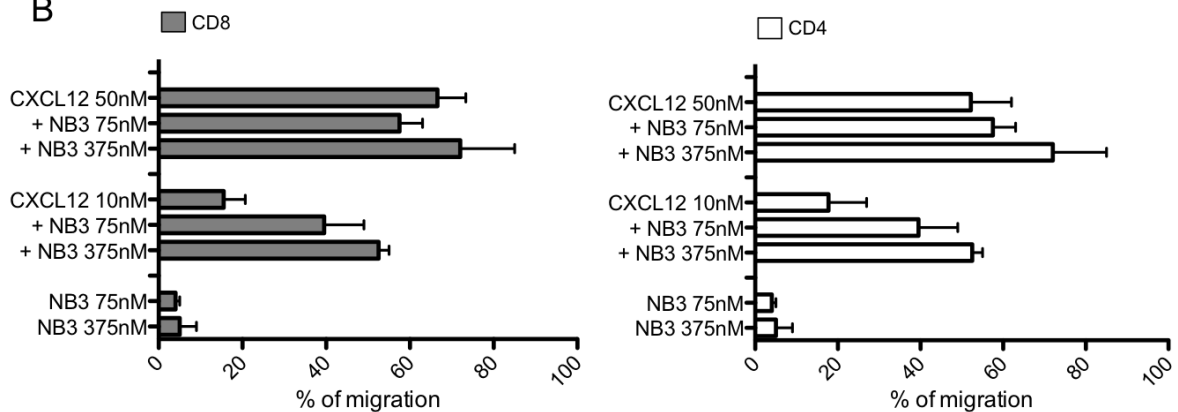


Fig. 5. NB3 positively regulates CXCL12-promoted chemotaxis of T lymphocytes. (A) Chemotaxis assay in transwell chamber of PBMC of independent healthy individuals ($n = 3$) in response to the indicated concentration of CXCL12. Transmigrated cells recovered in the lower chamber were stained with mAbs specific for CD3, CD4 and CD8 antigens and counted by flow cytometry. (B) Migration with NB3 or with CXCL12 at the indicated concentrations in presence or not of NB3 added in both chambers. Results (mean \pm SEM) are from 3 independent experiments and expressed as the percentage of input total (gated CD3+ CD4+ or CD3+ CD8+) T cells that migrated to the lower chamber. * $P < .05$, ** $P < .005$ and *** $P < .0005$.

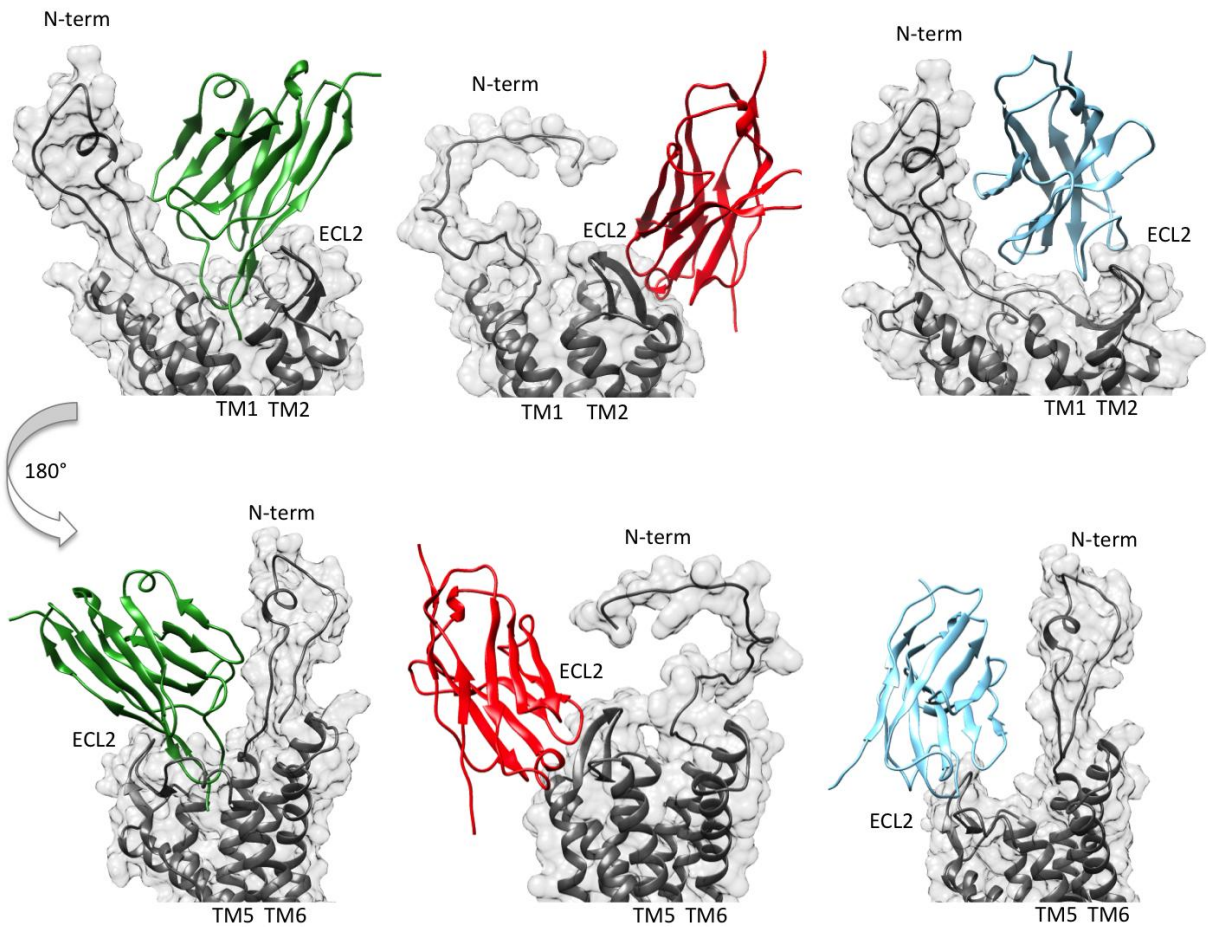


Fig. 6. Predicted binding of NBs on the extracellular region of CXCR4 by Peptide-peptide docking experiments. Overview of the interaction between the NBs' CDR and the receptor extracellular domains from the three selected NBs/CXCR4 complexes. NBs form favorable contacts with the ECL2 (NB2 in red and NB3 in cyan) or the activation domain (NB1 in green) of CXCR4 (in gray) as shown in the two 180°-rotated orientations.

SUPPLEMENTAL MATERIAL FOR

Conformationally selective Nanobodies for regulation of CXCR4 functions

Pasquale Cutolo¹, Agnieszka Jaracz-Ros¹, Joyce Heuinck², Thomas Bourquard³,
Elodie Dupuis⁴, Thomas Roux⁴, Eric Trinquet⁴, Guillaume Bernadat⁵, Thierry
Durroux², Françoise Bachelerie^{1*}

¹ UMR996 - Inflammation, Chemokines and Immunopathology -, Inserm, Univ Paris-Sud,
Université Paris-Saclay, 92296, Clamart, France.

² CNRS UMR 5203, INSERM U1191, Institut de Génomique Fonctionnelle, Université
Montpellier 1 & 2, Montpellier, France

³ BIOS group, INRA, UMR85, Unité Physiologie de la Reproduction et des Comportements,
F-37380 Nouzilly, France; CNRS, UMR7247, F-37380 Nouzilly, France; Université François
Rabelais, 37041 Tours, France; IFCE, Nouzilly, F-37380 France

⁴ Cisbio Bioassays, BP84175, Codolet, France

⁵ BioCIS - UMR 8076, Université Paris-Sud, CNRS, Université Paris-Saclay, Châtenay-
Malabry, France

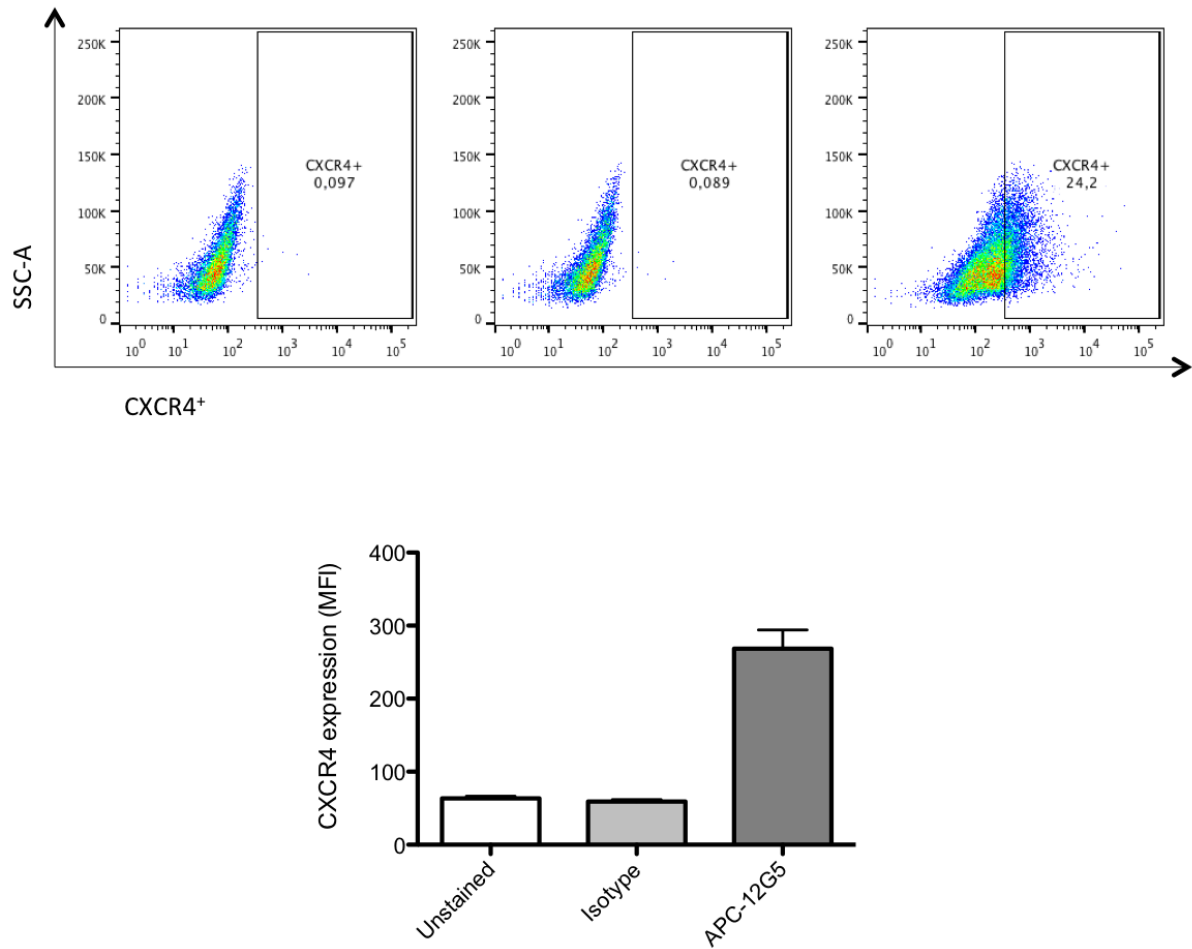


Fig. S1. Surface expression of endogenous CXCR4 in HEK293T cells. Cells, shown in a forward scatter/side scatter dot plot were analyzed for their CXCR4 expression using the 12G5 mAb. The lower panel shows typical cell-surface expression levels of CXCR4 as assessed by flow cytometric analysis using the 12G5 mAb (grey bar) compare with isotype control mAb (light grey bar).

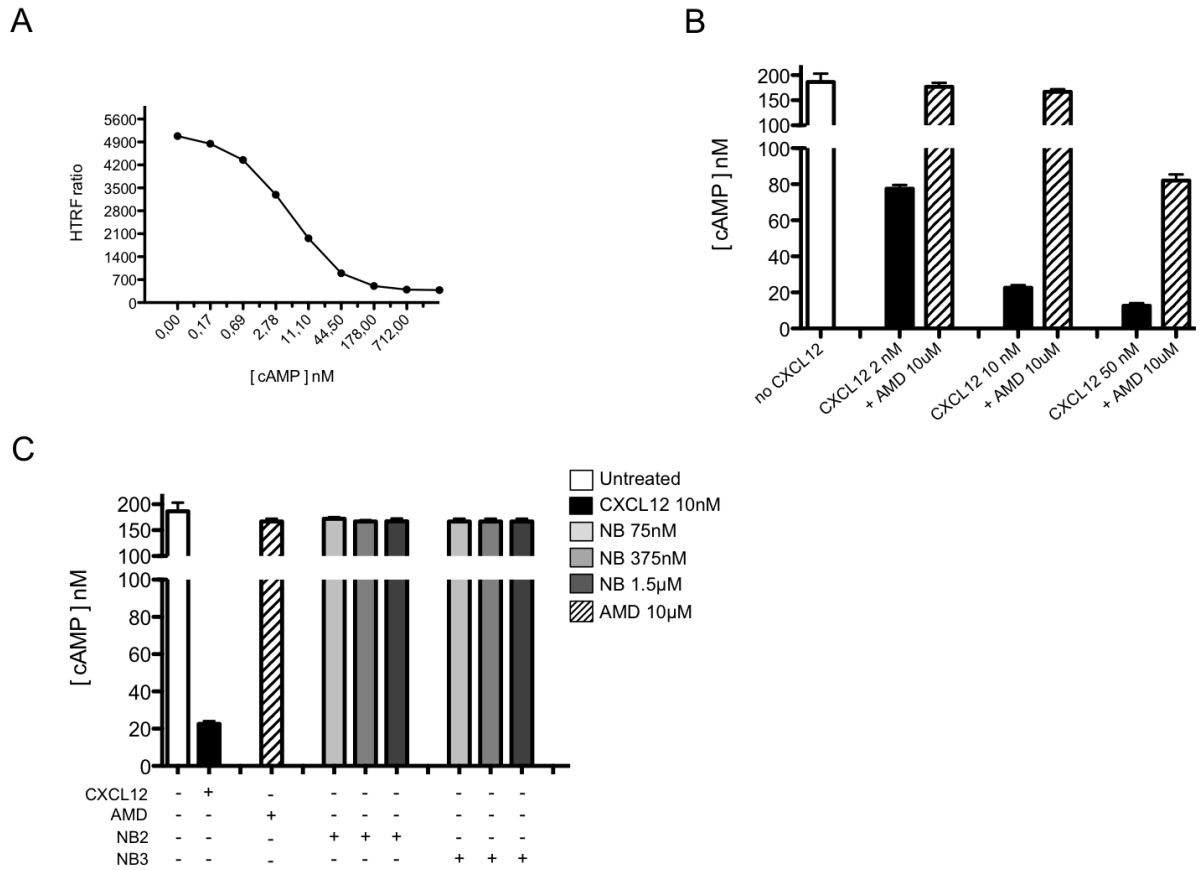


Fig. S2. Measurement of cAMP production using an HTRF-based assay. (A) dynamic range of the standard curve plotting HTRF ratio versus cAMP concentrations. (B) CXCL12 dose-dependent inhibition of cAMP production in endogenous CXCR4 expressed by HEK293T cells. Adding the CXCR4 antagonist AMD3100, inhibited CXCL12-induced responses. (C) NB2 and NB3 at the indicated concentrations did not modulate cAMP production as compared to untreated HEK293T cells and similarly to AMD3100-treated cells. (B, C) Results (mean \pm SEM) are from 3 independent experiments.

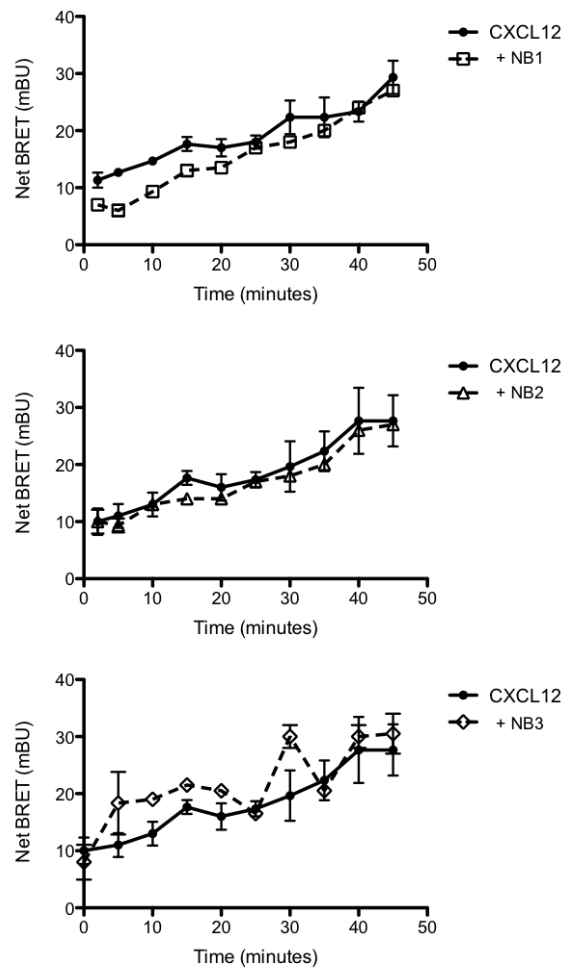


Fig S3. NBs doesn't modify β -arrestin recruitment to the CXCL12-activated CXCR7. BRET measure of β -arrestin-2 recruitment on CXCR7 in HEK293T cells transiently transfected with β -arrestin-2-Rluc and CXCR7-YFP after 30 minutes of incubation with NBs at the concentration of 375nM, followed by CXCL12 stimulation at 100nM. Data points are mean \pm S.E.M. of triplicate values from a single experiment, and they are representative of three separate experiments.

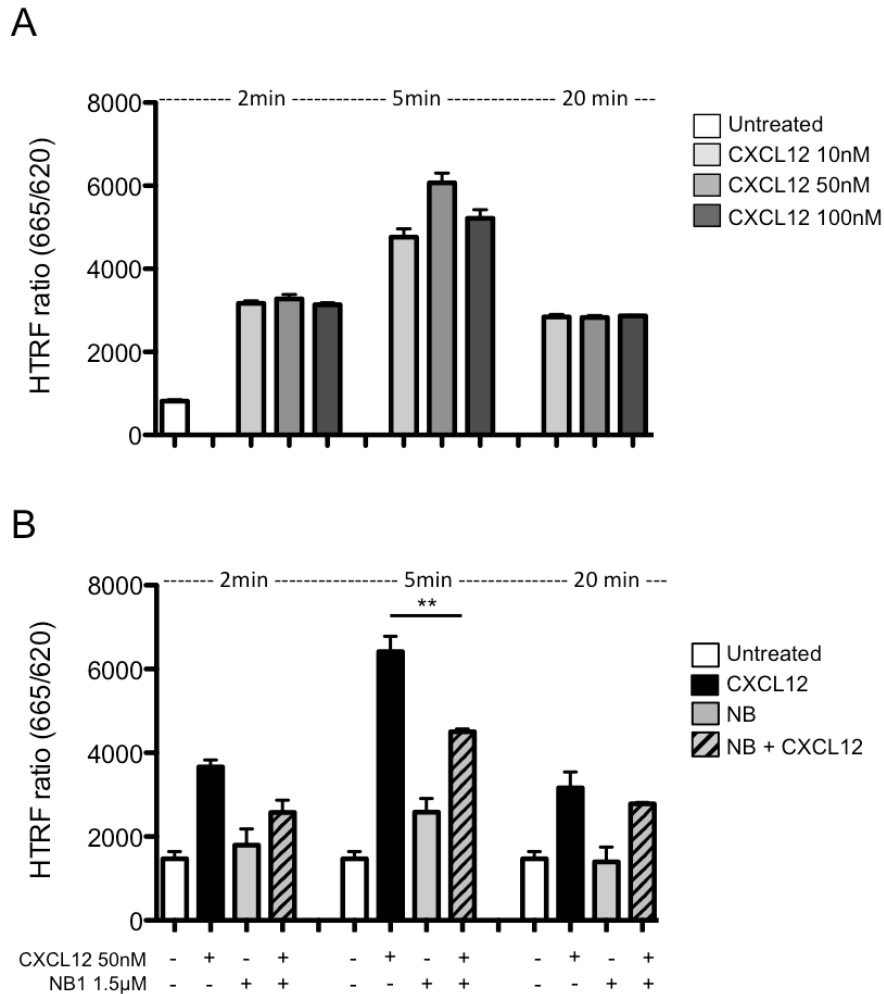


Fig S4. Measurement of ERK activation using an HTRF-based assay. (A) CXCL12 doses-dependent effect on ERK activation (phosphorylation on Thr202/Tyr204) quantitatively detected by a HTRF assay in HEK293T cells expressing endogenous levels of CXCR4. (B) Effect of NB1 on CXCL12-induced CXCR4-dependent ERK phosphorylation using. Cells were either pre-incubated with NB1 at 1.5 μ M during 30 minutes on ice before being stimulated with CXCL12 (50nM) or directly stimulated with CXCL12 (50nM) or NB1 (1.5 μ M) for 2, 5 and 20 minutes at 37°C before harvesting. Data points are mean \pm S.E.M. of triplicate values from a single experiment, and they are representative of two separate experiments. T-student analysis for statistics: * $p < 0.05$, ** $p < 0.01$.

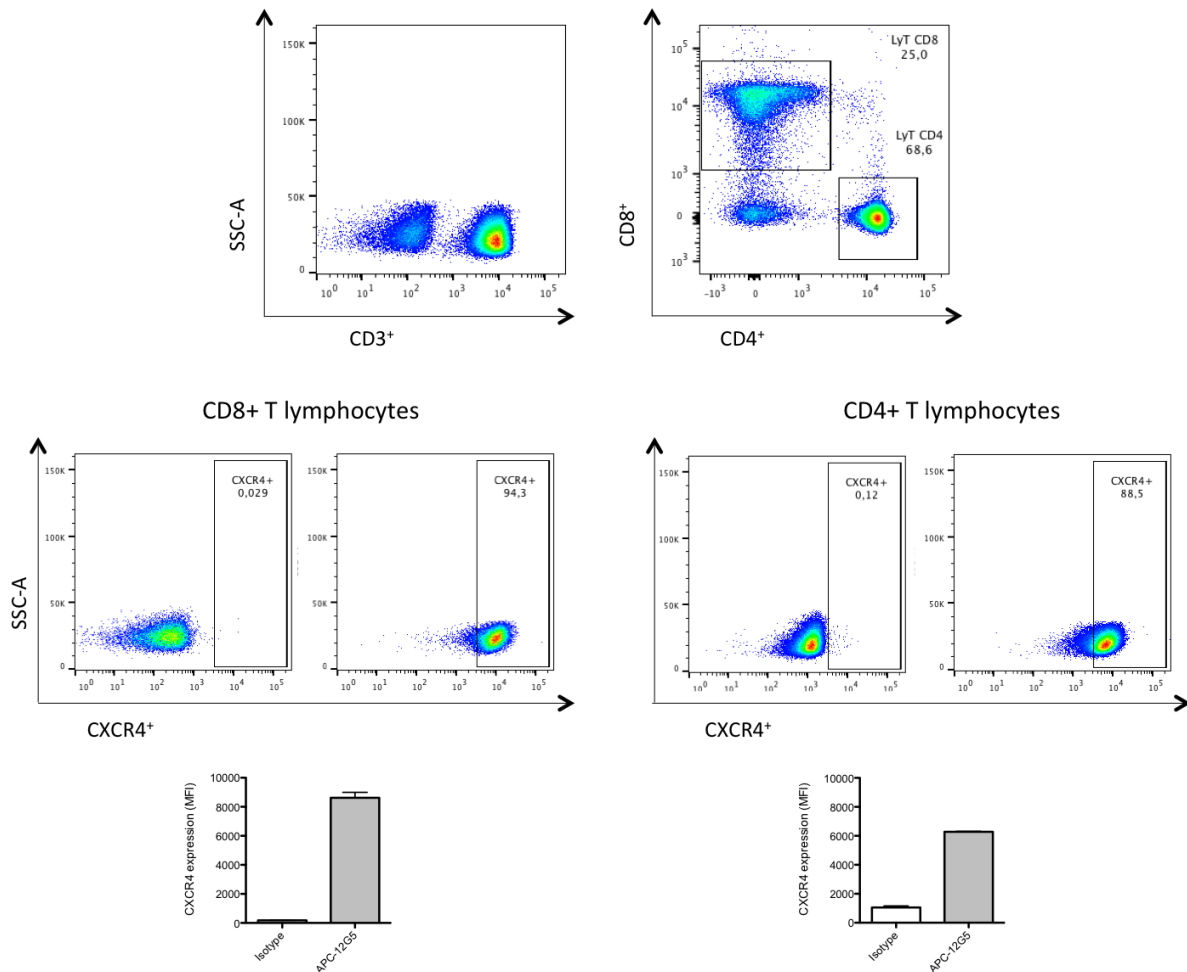


Fig S5. Cell surface expression of endogenous CXCR4 in human T lymphocytes. Gating strategy to select CD4 and CD8 T lymphocytes from CD3 T lymphocytes from healthy individuals PBMCs as identified in a forward scatter/side scatter dot plot by flow cytometric analysis. Middle panels show typical cell-surface expression levels of endogenous CXCR4 in human PBMCs-derived CD8 (left panel) and CD4 T (right panel) lymphocytes as assessed by flow cytometric analysis using the 12G5 mAb (grey bar) compared with isotype control mAb (white bar). Lower panel shows relative MFI (mean fluorescence intensity) for the two populations of lymphocytes.

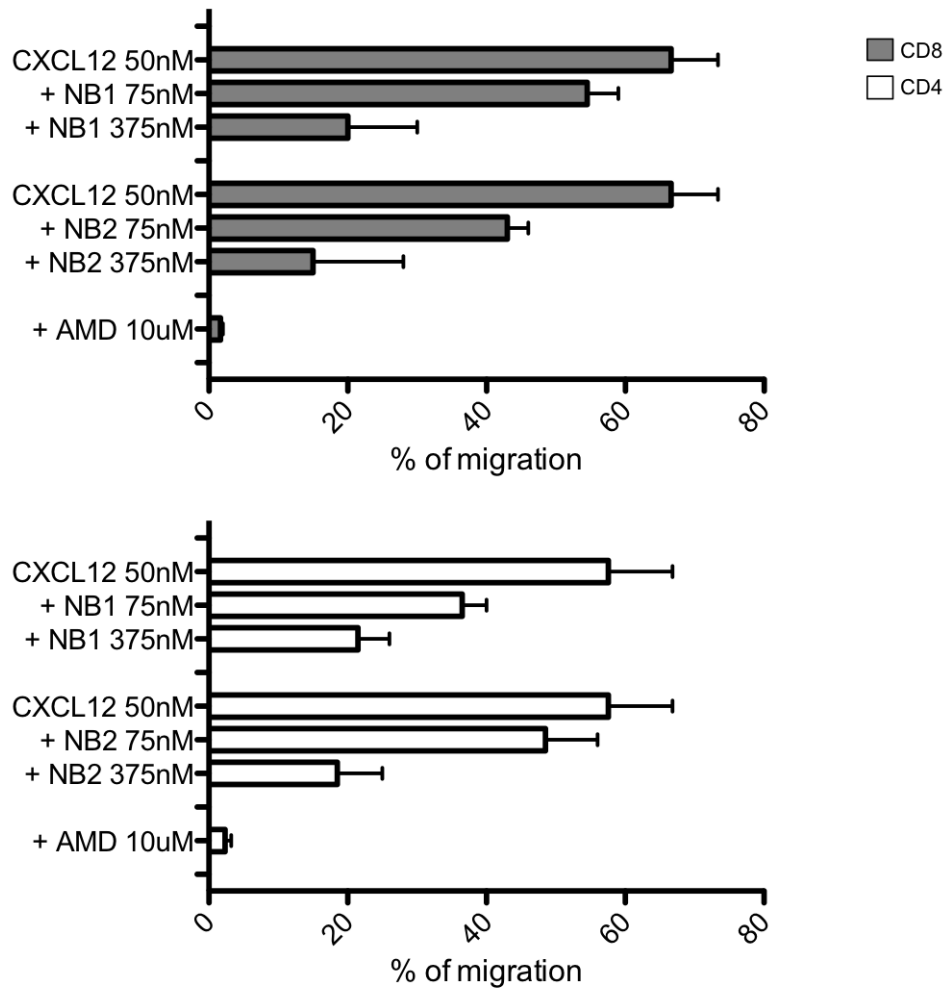


Fig S6. NB1 and NB2 inhibit CXCL12/CXCR4-promoted chemotaxis of human T lymphocytes. Chemotaxis assay in Transwell® chamber of PBMC in response to CXCL12 (50nM) in presence or not of NB1 or NB2 added in both chambers at the indicated concentrations. Results (mean \pm SEM) are from 3 independent experiments and expressed as the percentage of input total (gated CD3⁺ CD4⁺ or CD3⁺ CD8⁺) T cells that migrated to the lower chamber.

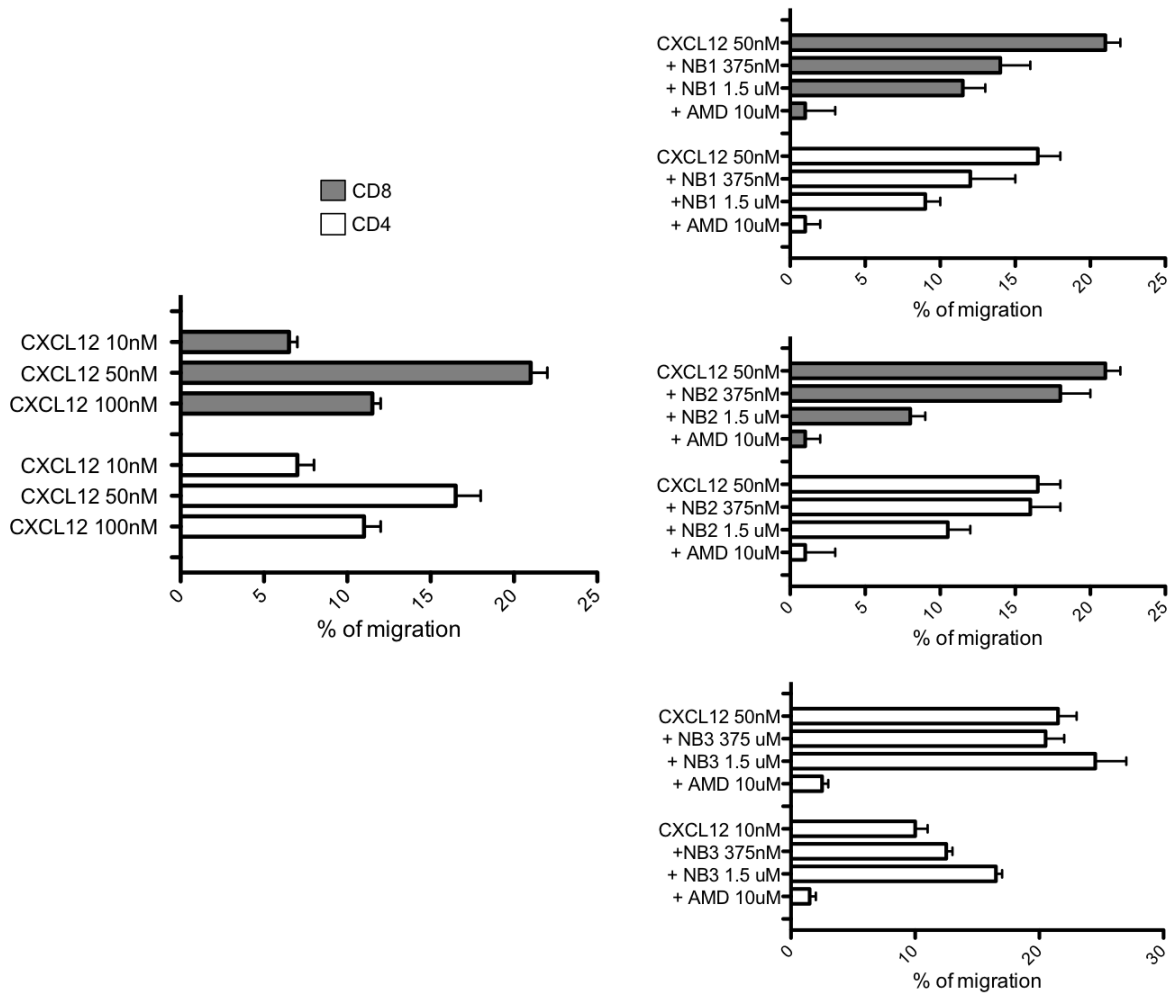


Fig. S7. CXCL12/CXCR4-promoted chemotaxis of murine T lymphocytes is inhibited by NB1 and NB2 but not by NB3. Chemotaxis assay in Transwell® chamber of mouse splenic cells tested for their ability to migrate in response to the indicated concentration of CXCL12 (upper panel). Inhibition of cell migration by AMD3100, NB1 and NB2 added in both chambers is shown. Results (mean \pm SEM) are from 3 independent experiments and expressed as the percentage of input total (gated CD3⁺ CD4⁺ or CD3⁺ CD8⁺) T cells that migrated to the lower chamber.

References

- 1 Bleul, C. C. et al. The lymphocyte chemoattractant SDF-1 is a ligand for LESTR/fusin and blocks HIV-1 entry. *Nature* 382, 829-833 (1996).
- 2 Oberlin, E. et al. The CXC chemokine SDF-1 is the ligand for LESTR/fusin and prevents infection by T-cell-line-adapted HIV-1. *Nature* 382, 833-835 (1996).
- 3 Ma, Q. et al. Impaired B-lymphopoiesis, myelopoiesis, and derailed cerebellar neuron migration in CXCR4- and SDF-1-deficient mice. *Proc Natl Acad Sci U S A* 95, 9448-9453 (1998).
- 4 Nagasawa, T. et al. Defects of B-cell lymphopoiesis and bone-marrow myelopoiesis in mice lacking the CXC chemokine PBSF/SDF-1. *Nature* 382, 635-638 (1996).
- 5 Puchert, M. & Engele, J. The peculiarities of the SDF-1/CXCL12 system: in some cells, CXCR4 and CXCR7 sing solos, in others, they sing duets. *Cell Tissue Res* 355, 239-253, doi:10.1007/s00441-013-1747-y (2014).
- 6 Bachelierie, F. et al. International Union of Basic and Clinical Pharmacology. [corrected]. LXXXIX. Update on the extended family of chemokine receptors and introducing a new nomenclature for atypical chemokine receptors. *Pharmacological reviews* 66, 1-79, doi:10.1124/pr.113.007724 (2014).
- 7 Sun, X. et al. CXCL12 / CXCR4 / CXCR7 chemokine axis and cancer progression. *Cancer Metastasis Rev* 29, 709-722, doi:10.1007/s10555-010-9256-x (2010).
- 8 Freitas, C. et al. The relevance of the chemokine receptor ACKR3/CXCR7 on CXCL12-mediated effects in cancers with a focus on virus-related cancers. *Cytokine Growth Factor Rev* 25, 307-316, doi:10.1016/j.cytogfr.2014.04.006 (2014).
- 9 Busillo, J. M. & Benovic, J. L. Regulation of CXCR4 signaling. *Biochim Biophys Acta* 1768, 952-963 (2007).

- 10 Wu, B. et al. Structures of the CXCR4 chemokine GPCR with small-molecule and cyclic peptide antagonists. *Science* 330, 1066-1071, doi:10.1126/science.1194396 science.1194396 [pii] (2010).

- 11 Ferre, S. et al. G-protein-coupled receptor oligomerization revisited: functional and pharmacological perspectives. *Pharmacol Rev* 66, 413-434, doi:10.1124/pr.113.008052 (2014).

- 12 Balabanian, K. et al. The chemokine SDF-1/CXCL12 binds to and signals through the orphan receptor RDC1 in T lymphocytes. *J Biol Chem* 280, 35760-35766 (2005).

- 13 Levoye, A., Balabanian, K., Baleux, F., Bachelerie, F. & Lagane, B. CXCR7 heterodimerizes with CXCR4 and regulates CXCL12-mediated G-protein signaling. *Blood* 113, 6085-6093, doi:blood-2008-12-196618 [pii] 10.1182/blood-2008-12-196618 (2009).

- 14 Naumann, U. et al. CXCR7 functions as a scavenger for CXCL12 and CXCL11. *PLoS One* 5, e9175, doi:10.1371/journal.pone.0009175.

- 15 Berahovich, R. D. et al. Endothelial expression of CXCR7 and the regulation of systemic CXCL12 levels. *Immunology* 141, 111-122, doi:10.1111/imm.12176 (2014).

- 16 Pawig, L., Klasen, C., Weber, C., Bernhagen, J. & Noels, H. Diversity and Inter-Connections in the CXCR4 Chemokine Receptor/Ligand Family: Molecular Perspectives. *Frontiers in immunology* 6, 429, doi:10.3389/fimmu.2015.00429 (2015).

- 17 Vela, M., Aris, M., Llorente, M., Garcia-Sanz, J. A. & Kremer, L. Chemokine receptor-specific antibodies in cancer immunotherapy: achievements and challenges. *Frontiers in immunology* 6, 12, doi:10.3389/fimmu.2015.00012 (2015).

- 18 Hanes, M. S. et al. Dual targeting of the chemokine receptors CXCR4 and ACKR3 with novel engineered chemokines. *J Biol Chem* 290, 22385-22397, doi:10.1074/jbc.M115.675108 (2015).

- 19 Hamers-Casterman, C. et al. Naturally occurring antibodies devoid of light chains. *Nature* 363, 446-448, doi:10.1038/363446a0 (1993).
- 20 Muyldermans, S. Nanobodies: natural single-domain antibodies. *Annu Rev Biochem* 82, 775-797, doi:10.1146/annurev-biochem-063011-092449 (2013).
- 21 Jahnichen, S. et al. CXCR4 nanobodies (VHH-based single variable domains) potently inhibit chemotaxis and HIV-1 replication and mobilize stem cells. *Proc Natl Acad Sci U S A* 107, 20565-20570, doi:10.1073/pnas.1012865107 (2010).
- 22 Steyaert, J. & Kobilka, B. K. Nanobody stabilization of G-protein-coupled receptor conformational states. *Current opinion in structural biology* 21, 567-572, doi:10.1016/j.sbi.2011.06.011 (2011).
- 23 Pardon, E. et al. A general protocol for the generation of Nanobodies for structural biology. *Nature protocols* 9, 674-693, doi:10.1038/nprot.2014.039 (2014).
- 24 Maussang, D. et al. Llama-derived single variable domains (nanobodies) directed against chemokine receptor CXCR7 reduce head and neck cancer cell growth in vivo. *J Biol Chem* 288, 29562-29572, doi:10.1074/jbc.M113.498436 (2013).
- 25 Bradley, M. E. et al. Potent and efficacious inhibition of CXCR2 signaling by biparatopic nanobodies combining two distinct modes of action. *Mol Pharmacol* 87, 251-262, doi:10.1124/mol.114.094821 (2015).
- 26 De Clercq, E. The bicyclam AMD3100 story. *Nat Rev Drug Discov* 2, 581-587 (2003).
- 27 Ayoub, M. A. et al. Real-time analysis of agonist-induced activation of protease-activated receptor 1/G-alpha-i1 protein complex measured by bioluminescence resonance energy transfer in living cells. *Mol Pharmacol* 71, 1329-1340, doi:10.1124/mol.106.030304 (2007).

- 28 Ayoub, M. A. & Pin, J. P. Interaction of Protease-Activated Receptor 2 with G-proteins and beta-Arrestin 1 Studied by Bioluminescence Resonance Energy Transfer. *Front Endocrinol (Lausanne)* 4, 196, doi:10.3389/fendo.2013.00196 (2013).
- 29 Ayoub, M. A. Resonance Energy Transfer-Based Approaches to Study GPCRs. *Methods Cell Biol* 132, 255-292, doi:10.1016/bs.mcb.2015.10.008 (2016).
- 30 Cheng, Z. J. et al. beta-arrestin differentially regulates the chemokine receptor CXCR4-mediated signaling and receptor internalization, and this implicates multiple interaction sites between beta-arrestin and CXCR4. *J Biol Chem* 275, 2479-2485 (2000).
- 31 Fong, A. M. et al. Defective lymphocyte chemotaxis in beta-arrestin2- and GRK6-deficient mice. *Proc Natl Acad Sci U S A* 99, 7478-7483 (2002).
- 32 Lagane, B. et al. CXCR4 dimerization and beta-arrestin-mediated signaling account for the enhanced chemotaxis to CXCL12 in WHIM syndrome. *Blood* 112, 34-44, doi:blood-2007-07-102103 [pii] 10.1182/blood-2007-07-102103 (2008).
- 33 Orsini, M. J., Parent, J. L., Mundell, S. J., Benovic, J. L. & Marchese, A. Trafficking of the HIV coreceptor CXCR4. Role of arrestins and identification of residues in the C-terminus tail that mediate receptor internalization. *J Biol Chem* 274, 31076-31086 (1999).
- 34 Levoye, A. et al. A Broad G-protein-Coupled Receptor Internalization Assay that Combines SNAP-Tag Labeling, Diffusion-Enhanced Resonance Energy Transfer, and a Highly Emissive Terbium Cryptate. *Front Endocrinol (Lausanne)* 6, 167, doi:10.3389/fendo.2015.00167 (2015).
- 35 Dewire, S. M., Ahn, S., Lefkowitz, R. J. & Shenoy, S. K. beta-Arrestins and Cell Signaling. *Annu Rev Physiol* 69, 483-510 (2007).
- 36 Sun, Y., Cheng, Z., Ma, L. & Pei, G. Beta-arrestin2 is critically involved in CXCR4-mediated chemotaxis, and this is mediated by its enhancement of p38 MAPK activation. *J Biol Chem* 277, 49212-49219, doi:10.1074/jbc.M207294200

M207294200 [pii] (2002).

37 Ritchie, D. W. & Kemp, G. J. Protein docking using spherical polar Fourier correlations. *Proteins* 39, 178-194 (2000).

38 Qin, L. et al. Structural biology. Crystal structure of the chemokine receptor CXCR4 in complex with a viral chemokine. *Science* 347, 1117-1122, doi:10.1126/science.1261064 (2015).

39 Allegretti, M., Cesta, M. C. & Locati, M. Allosteric Modulation of Chemoattractant Receptors. *Frontiers in immunology* 7, 170, doi:10.3389/fimmu.2016.00170 (2016).

40 Muller, C. E., Schiedel, A. C. & Baqi, Y. Allosteric modulators of rhodopsin-like G-protein-coupled receptors: opportunities in drug development. *Pharmacol Ther* 135, 292-315, doi:10.1016/j.pharmthera.2012.06.002 (2012).

41 Devine, S. M. et al. Rapid mobilization of functional donor hematopoietic cells without G-CSF using AMD3100, an antagonist of the CXCR4/SDF-1 interaction. *Blood* 112, 990-998, doi:10.1182/blood-2007-12-130179 (2008).

42 DiPersio, J. F., Uy, G. L., Yasothan, U. & Kirkpatrick, P. Plerixafor. *Nat Rev Drug Discov* 8, 105-106, doi:10.1038/nrd2819 (2009).

43 Hendrix, C. W. et al. Safety, pharmacokinetics, and antiviral activity of AMD3100, a selective CXCR4 receptor inhibitor, in HIV-1 infection. *J Acquir Immune Defic Syndr* 37, 1253-1262 (2004).

44 McDermott, D. H. et al. A phase 1 clinical trial of long-term, low-dose treatment of WHIM syndrome with the CXCR4 antagonist plerixafor. *Blood* 123, 2308-2316, doi:10.1182/blood-2013-09-527226 (2014).

45 Zirafi, O. et al. Discovery and characterization of an endogenous CXCR4 antagonist. *Cell reports* 11, 737-747, doi:10.1016/j.celrep.2015.03.061 (2015).

- 46 Crump, M. P. et al. Solution structure and basis for functional activity of stromal cell-derived factor-1; dissociation of CXCR4 activation from binding and inhibition of HIV-1. *Embo J* 16, 6996-7007 (1997).
- 47 Kofuku, Y. et al. Structural basis of the interaction between chemokine stromal cell-derived factor-1/CXCL12 and its G-protein-coupled receptor CXCR4. *J Biol Chem* 284, 35240-35250, doi:M109.024851 [pii] 10.1074/jbc.M109.024851 (2009).
- 48 Wang, C. I. & Lewis, R. J. Emerging opportunities for allosteric modulation of G-protein coupled receptors. *Biochem Pharmacol* 85, 153-162, doi:10.1016/j.bcp.2012.09.001 (2013).
- 49 Sachpatzidis, A. et al. Identification of allosteric peptide agonists of CXCR4. *J Biol Chem* 278, 896-907, doi:10.1074/jbc.M204667200 (2003).
- 50 Ehrlich, A., Ray, P., Luker, K. E., Lolis, E. J. & Luker, G. D. Allosteric peptide regulators of chemokine receptors CXCR4 and CXCR7. *Biochem Pharmacol* 86, 1263-1271, doi:10.1016/j.bcp.2013.08.019 (2013).
- 51 Scholten, D. J. et al. Pharmacological modulation of chemokine receptor function. *Br J Pharmacol* 165, 1617-1643, doi:10.1111/j.1476-5381.2011.01551.x (2012).
- 52 Ghanouni, P. et al. Functionally different agonists induce distinct conformations in the G-protein coupling domain of the beta 2 adrenergic receptor. *J Biol Chem* 276, 24433-24436, doi:10.1074/jbc.C100162200 (2001).
- 53 Steen, A., Larsen, O., Thiele, S. & Rosenkilde, M. M. Biased and G-protein-independent signaling of chemokine receptors. *Frontiers in immunology* 5, 277, doi:10.3389/fimmu.2014.00277 (2014).
- 54 Reiter, E., Ahn, S., Shukla, A. K. & Lefkowitz, R. J. Molecular mechanism of beta-arrestin-biased agonism at seven-transmembrane receptors. *Annu Rev Pharmacol Toxicol* 52, 179-197, doi:10.1146/annurev.pharmtox.010909.105800 (2012).

- 55 Quoyer, J. et al. Pepducin targeting the C-X-C chemokine receptor type 4 acts as a biased agonist favoring activation of the inhibitory G-protein. *Proc Natl Acad Sci U S A* 110, E5088-5097, doi:10.1073/pnas.1312515110 (2013).
- 56 Griffiths, K. et al. i-bodies, Human Single Domain Antibodies That Antagonize Chemokine Receptor CXCR4. *J Biol Chem* 291, 12641-12657, doi:10.1074/jbc.M116.721050 (2016).
- 57 Gomez-Mouton, C. et al. Filamin A interaction with the CXCR4 third intracellular loop regulates endocytosis and signaling of WT and WHIM-like receptors. *Blood* 125, 1116-1125, doi:10.1182/blood-2014-09-601807 (2015).
- 58 Balabanian, K. et al. Proper desensitization of CXCR4 is required for lymphocyte development and peripheral compartmentalization in mice. *Blood* 119, 5722-5730, doi:blood-2012-01-403378 [pii] 10.1182/blood-2012-01-403378 (2012).
- 59 Balabanian, K. et al. WHIM syndromes with different genetic anomalies are accounted for by impaired CXCR4 desensitization to CXCL12. *Blood* 105, 2449-2457 (2005).
- 60 Hounsou, C. et al. Time-resolved FRET binding assay to investigate hetero-oligomer binding properties: proof of concept with dopamine D1/D3 heterodimer. *ACS Chem Biol* 10, 466-474, doi:10.1021/cb5007568 (2015).
- 61 Zwier, J. M. et al. A fluorescent ligand-binding alternative using Tag-lite(R) technology. *J Biomol Screen* 15, 1248-1259, doi:10.1177/1087057110384611 (2010).
- 62 Cheng, Y. & Prusoff, W. H. Relationship between the inhibition constant (K_1) and the concentration of inhibitor which causes 50 per cent inhibition (I_{50}) of an enzymatic reaction. *Biochem Pharmacol* 22, 3099-3108 (1973).
- 63 Fleishman, S. J. et al. Community-wide assessment of protein-interface modeling suggests improvements to design methodology. *J Mol Biol* 414, 289-302, doi:10.1016/j.jmb.2011.09.031 (2011).

64 Garzon, J. I., Kovacs, J., Abagyan, R. & Chacon, P. ADP_EM: fast exhaustive multi-resolution docking for high-throughput coverage. *Bioinformatics* 23, 427-433, doi:10.1093/bioinformatics/btl625 (2007).

65 Kozakov, D., Clodfelter, K. H., Vajda, S. & Camacho, C. J. Optimal clustering for detecting near-native conformations in protein docking. *Biophys J* 89, 867-875, doi:10.1529/biophysj.104.058768 (2005).

Paper n°3

Differential activities of CXCL12 analogs
at the CXCR4 and CXCR7/ACKR3 receptors:
Study of interaction determinants

Abstract

The involvement of CXCR4 and CXCR7/ACKR3 chemokine receptors in cancer pathogenesis, metastatic development, inflammatory and cardiovascular diseases or viral infection (eg. HIV) has fuelled new research into the development of small inhibitory molecules of these receptors. It has been suggested that CXCR4 inhibitors TC14012 and AMD3100 known to inhibit HIV infection, for example, turn out to be potential allosteric agonists of CXCR7/ACKR3 able to modulate the arrestin-dependent pathway mediated by this receptor. In a similar manner, synthetic orthosteric ligand of CXCR7/ACKR3, such as CCX771, able to reduce tumour growth and endothelial transmigration, turn out to be also a potent activator of arrestin recruitment onto the receptor. These findings and the scarce knowledge of CXCR7/ACKR3 structure and interactions with its chemokine ligand CXCL12 prompted us to compare CXCL12 analogs for their binding and signalling properties with regard to CXCR7/ACKR3 and CXCR4. These analogs, which derived from single substitution or gradual deletion of the first five CXCL12 N-terminal residues were reported to behave as CXCR4 antagonists. Here, using HTRF-based binding and competition assays, we determined the affinities of these derivatives for CXCR7/ACKR3 and found that the four N-terminal residues of CXCL12 are more critical for the binding of CXCL12 to CXCR7/ACKR3 than to CXCR4. We found that substitution and or deletion of the first two CXCL12 residues (i.e. CXCL12 K1R and P2G mutants) did not affect the binding of the chemokine neither to CXCR4 nor to CXCR7/ACKR3. Unexpectedly however, these mutants maintain the wild type chemokine ability to induce arrestin recruitment and activation acting thus as potent agonists of CXCR7/ACKR3 internalization. These results indicate that the two first amino acid residues of CXCL12 (Lys1-Pro2), critically involved in CXCR4 activation, are not required for that of CXCR7/ACKR3, suggesting differing structural determinants requirements for both receptors. To better investigate them, we first generated the three-dimensional structure of CXCR7/ACKR3 using homology-modeling experiments and then investigated the possible interaction domains between CXCL12 and CXCR7/ACKR3 by peptide-peptide docking. Given that CXCL12 N-terminus mutants still display agonist activity on CXCR7/ACKR3, we mutated in the receptor the two residues equivalent as those reported to be important for CXCR4 binding with the ligands T140 and AMD3100 (i.e. D179 and D275 for ACKR3 and D171 and D262 for CXCR4). We found that substituting the

aspartic acid residues on position 179 and 275 with two alanines resulted in the loss for CXCR7/ACKR3 to activate the MAPK pathway upon CXCL12 stimulation. However, this mutation was found to confer CXCR7/ACKR3 with the capability to activate G-proteins (i.e. cAMP inhibition) indicating that the chemokine was still binding to the receptor. Comparing the primary structure of CXCR4 and CXCR7/ACKR3, we substituted the DRYLSITYF motif in the ICL2 by the DRYLAIVHA motif of CXCR4 known as being crucial GPCRs/G proteins interaction, together with that of the two Aspartate (97 and 187) and Glutamate (288) residues involved in CXCR4-dependent G-protein activation (Brelot 2000). This mutant behaved as a “CXCR4 like” receptor, with acquired ability to activate G-proteins while maintaining CXCR7/ACKR3 capacity to activate the MAPK pathway. Herein we present these findings together with modeling results of peptide-peptide docking prediction for the interaction structure between CXCL12 and CXCR7/ACKR3.

Differential activities of CXCL12 analogs
at the CXCR4 and CXCR7/ACKR3 receptors:
Study of interaction determinants

Pasquale Cutolo¹, Guillaume Bernadat², Agnieszka Jaracz-Ros¹, Françoise
Baleux³, Françoise Bachelier^{1‡*} and Angélique Levoye^{4‡*}

¹ UMR996 - Inflammation, Chemokines and Immunopathology -, Inserm, Univ Paris-Sud,
Université Paris-Saclay, 92296, Clamart, France

² BioCIS - UMR 8076, Université Paris-Sud, CNRS, Université Paris-Saclay, Châtenay-
Malabry, France

³ Unité de Chimie des Biomolécules, Département de Biologie Structurale et Chimie, Institut
Pasteur, Paris, France.

⁴ INSERM UMR 1148, Laboratory of Translational Vascular Science, Université Paris 13
Sorbonne Paris Cité, Paris, France.

‡ These authors contributed equally to this work.

* Address correspondence to : Dr. Françoise Bachelier, Inflammation, Chemokines and
Immunopathology -, Inserm, Univ Paris-Sud, Université Paris-Saclay, 32 rue des Carnets,
92140 Clamart, France, Tel : +331 41 28 80 05, Fax: +331 46 32 79 93. Email:
francoise.bachelier@u-psud.fr or Dr. Angélique Levoye, INSERM UMR 698, Bio-ingénierie
cardiovasculaire pour l'imagerie et la thérapeutique, Université Paris 13 Sorbonne Paris Cité,
46, rue Henri Huchard, 75018 Paris, France Tel : +33140258611, Fax: +33140258602. Email:
angelique.levoye@inserm.fr

Results

CXCL12 N-terminal is differently involved in the chemokine engagement to CXCR7 and CXCR4.

In order to study the determinants critical for the interaction between the N-terminal residues of CXCL12 and its receptor CXCR7/ACKR3, we used four different analogs of CXCL12 (Fig 1A), two N-terminal deletions (4-67 and 5-67) and two N-terminal mutations (K1R and P2G). N-terminal truncated forms of CXCL12, deleted of the first three to four residues, were described in physiological contexts as result of leukocyte elastase and matrix metalloproteinase (MMP)-2 cleavage (Val₃-Ser₄ and Ser₄-Leu₅ bonds, respectively) and they fail to activate CXCR4 receptor (Valenzuela-Fernandez et al. 2002, Sadir et al. 2004 and Vergote et al. 2006). Mutations on first two N-terminal residues of CXCL12 (Lys₁ and Pro₂) were also described to bind CXCR4 and unable to activate downstream signaling pathways (Crump et al. 1997). We investigated the capability of these CXCL12 analogs to bind CXCR7/ACKR3 as compared to CXCR4, using a HTRF competition assay (Fig 1B). This assay is using the red-CXCL12 as an acceptor of the energy transferred from excited Snap-tag CXCR4 or CXCR7/ACKR3 receptors stably expressed in HEK293T cells. Snap-tag receptors were shown to display normal expression (Fig S1) and function (data not shown). Cells were incubated in presence of red-CXCL12 and increasing concentrations of unlabeled CXCL12 or analogs. We found, accordingly to an abundant literature, that the binding affinities of CXCL12 and competitive antagonists (AMD3100 and T134) for CXCR4 were in the same range. N-terminus CXCL12 mutants showed altered potential to displace the red-CXCL12 (Fig 1C), as previously shown (Crump et al. 1997). We also confirmed the higher affinity of CXCL12 for CXCR7/ACKR3 (Burns et al. 2006, Struyf et al. 2009), the binding of CXCL11 to CXCR7/ACKR3 and the inability of CXCR7/ACKR3 to bind AMD3100 and T134 (Fig 1D). Although the substitution of the two first residues resulted in a decrease affinity of the chemokine to the same extend for both receptors, deletion of the first four and five N-terminal residues more dramatically jeopardize the binding of the chemokine to CXCR7/ACKR3 than to CXCR4 (Fig 1D and Tab 1). Saturation experiments allowed us to determine the dissociation constant K_d of CXCL12 for CXCR4 and CXCR7/ACKR3 (Fig S2) and the half maximal inhibitory concentration (IC₅₀) and inhibitory constant (K_i) (Tab 1).

It was shown that the binding of N-terminus deleted CXCL12 forms to CXCR4 might be dissociate from the activation potency of the ligand given the two steps model suggested for CXCL12/CXCR4 interaction (Crump et al. 1997, Wu et al., 2010). In light of these results we investigated the potential of these mutants to activate CXCR7/ACKR3-downstream pathways. We then performed internalization assays based on HTRF technology (Levoye et al. 2015), which allowed to compare CXCL12-induced internalization of both receptors in the same HEK293T cells used for the binding assays (ie. expressing snap-tag receptors). Both deleted and mutated CXCL12 analogs were not able to induce CXCR4 internalization acting similarly to the two CXCR4 antagonist ligands AMD3100 and T134 (Fig 2A). In contrast, mutations of the first two N-terminal residues did not modify, or slightly, CXCL12 propensity to induce CXCR7/ACKR3 internalization despite their reduced binding affinity for the receptor. Deleting the first four and five N-terminal residues dramatically affects the capacity of CXCL12 to induce CXCR7/ACKR3 internalization (Fig 2B) in accordance with their dramatically altered binding capacities (Fig 1D).

Since the CXCL12-induced internalization of CXCR4 and CXCR7/ACKR3 was shown as a β -arrestin-2 dependent mechanism (Naumann et al., 2010), we decided to investigate whether mutations on the first two CXCL12 N-terminal residues can promote β -arrestin 2 -activation (followed by intramolecular conformational changes) and -recruitment on CXCR7/ACKR3. This was accessed using BRET assays performed in HEK293T cells transiently transfected with CXCR4 or CXCR7/ACKR3 receptors and β -arrestin-expressing vectors (Fig 3A and 3B). We also performed dose responses in order to compare the half maximal effective concentrations (EC₅₀) for CXCL12 and derivatives able to promote the interaction of β -arrestin 2 with CXCR4 or with CXCR7/ACKR3 (Fig S3 and Table 2). Results indicated that β -arrestin 2 recruitment on CXCR4 receptor was promoted only by wild type CXCL12 (Fig 3A and S3A). In contrast, the two N-terminal mutants of CXCL12 (K1R and P2G), remained able to promote the β -arrestin 2 recruitment to the CXCR7/ACKR3 receptor to the same extend than the wild type CXCL12 chemokine (Fig 3B). Along this line, intramolecular BRET experiences aimed at investigating β -arrestin 2 activation through β -arrestin 2 conformational changes (Fig 3C and 3D) indicated that the two CXCL12 N-terminal mutants were able to promote responses on CXCR7/ACKR3 in contrast to CXCL12 truncated forms (4-67 and 5-67). These results lead us to hypothesize that the third and fourth CXCL12 N-terminal residues (Ser₃ and Val₄) were important determinants for the chemokine binding to and activation of CXCR7/ACKR3.

CXCR7/ACKR3 homology modeling.

In order to investigate this hypothesis we decided to perform firstly the homology modeling of CXCR7/ACKR3 three-dimensional structure and secondly protein-protein docking experiments to model the CXCL12-CXCR7/ACKR3 interaction. Since the crystal structure is not available for the CXCR7/ACKR3 receptor, we performed homology modeling experiments starting from the primary sequence of the receptor (UniProt accession number P25106). We used the HH-Pred online platform (<https://toolkit.tuebingen.mpg.de/hhpred>) to find known crystal and NMR structures of human GPCRs predicted as the most representative for modeling CXCR7/ACKR3 structure and choose the CXCR4 (P61073, isoform 1), CCR5 (P51681) and CXCR1 (P25024) sequences as templates, corresponding to the crystal structures of CXCR4 and CCR5 (3ODU and 4MBS, respectively), and the NMR structure of CXCR1 (2LNL). We performed a multiple alignment (PSI-Blast on MSA-Probs) between the primary sequence of CXCR7/ACKR3 and those of CXCR4, CCR5 and CXCR1 (Fig S4). It is important to note that, in a pairwise alignment, templates share less than a third of their primary sequence with CXCR7/ACKR3 (identity of 28% for CXCR4, 25% for CCR5 and 29% for CXCR1), nevertheless the probability to share the same conformation of secondary and tertiary structures is 100% for all templates.

Therefore, we used the result of MSA-Probs global alignment as query for Modeller software to perform the homology modeling of CXCR7/ACKR3 structure (comparition with CXCR4 structure in Fig S6). After minimization, we put the modeled CXCR7/ACKR3 structure in a lipidic double layer (POPC) membrane in hydrated context with charges in order to relax the structure in an all-atoms molecular dynamics simulation.

RMSD index was calculated on C-alpha between the CXCR7/ACKR3 model and templates structures, before (3ODU: 0,839 Å, 4MBS: 0,871 Å, 2LNL: 1,201 Å) and after molecular dynamic simulation (3ODU: 1.348 Å, 4MBS: 1.270 Å, 2LNL: 1.276 Å). Time evolution of the RMSD of CXCR7/ACKR3 model during the molecular dynamics simulation was analyzed to verify the stability of the structure (Fig S7).

Comparative analysis between CXCR4 and CXCR7/ACKR3.

It is unanimously accepted that CXCR7/ACKR3 is not able to activate G-proteins upon agonists stimulation (CXCL11 and CXCL12) most likely as a consequence of a polymorphism in the DRYLAIV motif on the ICL2 domain, which is conserved in most GPCRs, and found to be DRYLSIT in the CXCR7/ACKR3 sequence. Focusing on the MSA-Probs alignment (Fig S4), we found that two more residues (one Histidine and one Alanine) were conserved among the three selected templates, but not in CXCR7/ACKR3, precisely the DRAILAIVHA became DRAYLSITYF in the CXCR7/ACKR3 sequence. Mutagenesis together with structural studies identified residues potentially involved in G proteins activation downstream CXCR4 (Aspartic acid 97 and 187 and Glutamic acid 288), which were not conserved in the CXCR7/ACKR3 sequence. Then we decided to generate a first mutant of CXCR7/ACKR3 in which we modified the DRYLAIVHA motif and the three residues not conserved according to CXCR4 sequence (called LAIDDE). Finally, two more CXCR4 residues (Aspartic acid 171 and 262), reported to be important for the binding of T140 and AMD3100 ligands and activation of the receptor, were found to be conserved in the CXCR7/ACKR3 sequence. Thus we substituted these residues in CXCR7/ACKR3 by alanine (D179A-D275A and D275A CXCR7/ACKR3 mutants) in order to investigate whether this might modify the binding and activation properties of CXCL12 with regard to CXCR7/ACKR3. Such substitutions in CXCR7/ACKR3 were also analyzed by our peptide-peptide docking experiments to have a model of the interaction between CXCR7/ACKR3 and CXCL12 (Fig 4). After a 1 μ sec of molecular dynamics simulation with our CXCR7/ACKR3 model, we were able to cluster the eight different conformations of the receptor significantly reported in the MD trajectory. We used these conformations to perform a cross docking with the twenty CXCL12 conformations available from the RMN structure (PDB: 2K01). To select the best model of the interaction we used two different scripts: one to perform the cross docking between CXCL12 and the receptor extracellular domain and one to rank all docking results by score and according to the CXCL12 N-terminal orientation on the receptor.

These scripts allowed us to select the best docking conformation (Fig 4) and we focused on the possible interactions between the CXCL12 N-terminus and the CXCR7/ACKR3 residues we decided to modify for mutagenesis studies. Interestingly both aspartic acid residues were in proximity of the CXCL12 N-terminal residues: aspartic acid 179 with the Lys1 of CXCL12 and aspartic acid 275 with the Val4 of CXCL12 (Fig 4A). In contrast, the CXCR7/ACKR3

residues Serine 103, Arginine 197 and Glutamine 301, corresponding in the CXCR4 sequence to the key residues for G proteins activation (Aspartic acid 97 and 187 and Glutamic acid 288), didn't show any interaction with the CXCL12 N-terminus (Fig 4B).

D179A-D275A and LAIDDE mutations conferred CXCR7/ACKR3 with the capacity to activate G-proteins.

We thus investigated the potency of CXCR7/ACKR3 mutants upon CXCL12 stimulation, to activate β -arrestin-dependent signaling such as the ERK1/2 MAPK pathway as does wild type CXCR7/ACKR3 and eventually to modulate cAMP levels. We used HTRF-FRET based assays in HEK293T cells transiently transfected with wild type CXCR4 or CXCR7/ACKR3 receptor or the CXCR7/ACKR3 mutants (expression level in Fig S5). Treatment of HEK293T cells, expressing wild type CXCR4 (Fig. 5A), with CXCL12 caused G proteins activation (ie. robust inhibition of cAMP), which was antagonized by the addition of the selective CXCR4 antagonist AMD3100. In cells transfected with CXCR7/ACKR3, the observed G proteins activation resulted from the activation of the endogenously expressed CXCR4. This was confirmed by the blockade of this effect upon addition of AMD3100 together with the inefficiency of adding the CXCR7/ACKR3 selective antibody clone 9C4, which competes for the binding of CXCL12 to CXCR7/ACKR3 (Balabanian et al., 2005). In contrast for two of the CXCR7/ACKR3 mutants (Fig 5B; LAIDDE and D179A-D275A mutants), CXCL12 apparently promoted G proteins activation independently of CXCR4 since AMD3100 antagonist effect was less effective and no antagonist effect of the 9C4 antibody was observed. The activation pattern downstream the third CXCR7/ACKR3 mutant (D275A) was similar to that of the wild type receptor.

To confirm these results and to unambiguously avoid activation of the endogenous CXCR4, we take advantage of our findings that CXCL12 analogs (such as the P2G CXCL12 mutant) devoid of activity with regard to CXCR4 can still activate CXCR7/ACKR3 (Fig 2 and Fig 3). We found that neither the P2G nor the 5-67 CXCL12 analog, chosen as a negative control for CXCR7/ACKR3 activation, were able to activate G proteins downstream CXCR4 whether expressed exogenously or endogenously (Fig 6A). In this context, the CXCR7/ACKR3 mutants LAIDDE and D179A-D275A remained able to activate G proteins after P2G stimulation similarly to the CXCL12-promoted activation. Moreover, this activation was

completely blocked by the 9C4 antibody (Fig 6B) confirming that it results from the interaction between CXCL12 and CXCR7/ACKR3.

D179A-D275A is an activating mutation for G proteins while inactive for the ERK1/2 MAPK pathway

We performed HTRF-FRET assay for analyzing the ERK1/2 MAPK pathway. After G protein activation that occurs during the first minutes after agonist stimulation, the typical ERK1/2 phosphorylation upon CXCL12 treatment is detectable at 2 minutes after stimulation (Lagane et al. 2008), with an activation kinetics that reaches the maximum signal at 5 minutes and completely disappears after 20 minutes.

We observed the CXCR4 and CXCR7/ACKR3 responses at 5 minutes after CXCL12 stimulation, that are antagonized by AMD3100 and 9C4, respectively (Fig 7A).

LAIIDDE and D275A CXCR7/ACKR3 mutants responded to CXCL12 similarly to the wild type receptor while the double mutant D179A-D275A displayed a pattern related to CXCR4 response (Fig 7B). We proceeded with P2G stimulations, which allowed us to confirm on the one hand MAPK activation (Fig 8A), inhibited by the 9C4 antibody, downstream LAIDDE and D275A mutants (Fig 8B). On the other hand, the D179A-D275A mutant did not show any activation upon P2G stimulation, indicating that this mutation is responsible for the loss of resulting receptor to activate the MAPK pathway.

Conclusion and Perspectives

Our results confirmed the importance of the N-terminus of CXCL12 for the interaction and activation of its receptors and gave new knowledge on residues implicated in the interaction between CXCL12 and CXCR7/ACKR3, showing not only the potential determinants for the interaction but also the capability of receptor residues to bias the consequent activation pathways. In our case, the modification of residues D179 and D275 of CXCR7/ACKR3, modeled as in interaction with CXCL12 N-terminus, is capable to completely reverse the signaling downstream CXCR7/ACKR3 when mutated to alanine. Therefore, the possibility to activate G protein can be consequence of trans-membrane helixes reorganization due to a different conformation of the CXCL12-CXCR7/ACKR3 complex. Moreover, DRYLAIV

motif seems to be not essential for the in G protein activation, explaining the incapability of previous DRYLAIV mutations on CXCR7/ACKR3 to activate the G protein pathway.

To confirm our results we need to study our models of interaction through molecular dynamics simulations and improve our results on the G protein and Arrestin activation. Firstly, molecular dynamics simulations will be performed using the native complex between CXCL12 and CXCR7/ACKR3, then it will be compared to complexes between K1R and P2G CXCL12 analogs and native CXCR7/ACKR3 and complexes between native CXCL12 and CXCR7 mutants LAIDDE and D179A-D275A. Secondly, BRET experiments between D179A-D275A mutant and G alpha-i subunit or β arrestin may allow us to show differences in conformation and recruitment. On the other hand, we need more results in CXCL12 binding on D275A mutant to confirm its involvement in the interaction with the CXCL12 N-terminal Val⁴.

Together these results will permit to understand the structural determinants for the CXCL12-CXCR7/ACKR3 interaction and to compare the different mechanisms of the interaction between CXCL12 and its two receptors.

Experimental Procedures

Reagents

CXCL12, CXCL12 4-67, CXCL12 5-67, CXCL12 K1R, CXCL12 P2G and T134 were provided by Dr. F. Baleux. CXCL11 and AMD3100 were obtained from Almac sciences (Elvingston, RU) and the NIH AIDS Research & Reference Reagent Program. CXCL12 labeled with a red fluorescent probe was developed by Cisbio Bioassays (Codolet, France). The Tag-lite labeling medium was from Cisbio Bioassays. The 96-well plates and 384-well small volume plates were purchased from Greiner Bio-One (Monroe, NC, USA). The Lumi4-Tb derivative of O6-benzylguanine was synthesized by Cisbio Bioassays and is commercialized as SNAP-Lumi4-Tb (Codolet, France). Poly-L-ornithine (MW of 30,000–70,000 Da) and forskolin were from Sigma-Aldrich (Saint Louis, MO, USA).

Plasmid constructions

The Rluc- β -arrestin2 and Rluc8- β -arrestin2-YPet plasmids previously reported (Scott 2002, Kamal 2009) were a gift from M.G. Scott (Institut Cochin, Paris, France) and C. Couturier (INSERM U761, Université de Lille 2, Lille, France), respectively. The ACKR3 and CXCR4 receptors tagged at the C-terminus with YFP (ACKR3-YFP and CXCR4-YFP) have been previously described (Levoye et al., 2009). The pCDNA3.1-ACKR3WT and derived-mutants, pCDNA3.1-ACKR3 LAIDDE (LAIDDE), pCDNA3.1-ACKR3 D179A + D275A (D179A-D275A) and pCDNA3.1-ACKR3 D275A (D275A), were produced by Eurofins (Eurofins Scientific, Luxemburg).

Cell culture and transfection

HEK293T cells were grown in culture medium (DMEM supplemented with 10 % (v/v) FBS, 4.5 g/l glucose, 100U/ml penicillin, 0.1mg/ml streptomycin, 1mM glutamine, 20mM Hepes) (all reagents are from Invitrogen SARL, Cergy Pontoise, France). HEK293T cells stably expressing the SNAP-tag-fused CXCR4 or ACKR3 receptors (ST-CXCR4 or ST-ACKR3

cells) were provided by Cisbio Bioassay and were grown in culture medium supplemented with 0.6µg/ml geneticin. Transient expressions were achieved using the transfection reagent FuGene 6 (Roche, Basel, Switzerland) or Lipofectamine 2000 (Invitrogen, CA, USA) according to the manufacturer's protocol.

Flow cytometric analyses

Cell-surface expression of CXCR4, ACKR3 or ACKR3 mutants receptors in HEK293T cells stably expressing WT receptors (ST-CXCR4 or ST-ACKR3 cells) or 48 hours following transient transfection with ACKR3-expressing vectors. Staining was performed using the anti-human CXCR4 mAb 12G5 (BD Biosciences, San Jose, CA, USA) or ACKR3 mAb 9C4, which prevents CXCL12 binding to ACKR3 (Balabanian et al. 2005, Infantino et al. 2006) (a gift from M. Thelen, Institute for Research in Biomedicine, Bellinzona, Switzerland). Analysis was carried out on a BD Biosciences FACS Fortessa.

HTRF-based Binding assay

The protocol has been adapted from Zwier et al. Briefly, Lumi4-Tb-labelled-frozen ST-CXCR4 or ST-ACKR3 cells were thawed quickly at 37 °C, suspended in the Tag-lite labeling medium and dispatched into a black 384-well plate at a density of 10.000 cells per well. Cells were incubated with the indicated increasing concentrations of red-CXCL12. For each concentration, nonspecific binding was determined using excess of the CXCR4 antagonist AMD3100 (1µM) or unlabeled CXCL12 (500nM). Competition experiments were performed by incubating ST-CXCR4- or ST-ACKR3-cells with a fixed concentration of red-CXCL12 (12.5nM or 6.25nM, respectively according to the respective Kd) in presence of increasing concentrations of the indicated ligands for 1 hour at room temperature. Signal was detected using fluorescence microplate reader Rubystar (BMG Labtech, Offenburg, Germany) equipped with a HTRF optic module allowing a donor (terbium) excitation at 337 nm and a signal collection both at 620 nm and 665 nm, wavelengths corresponding to the total donor emission and to the FRET signal, respectively. The signal was collected using the following time-resolved settings: delay 50 µs and integration time 400 µs. HTRF ratios correspond to the ratio between acceptor (665 nm) and donor signal (620 nm) and multiplied by 10.000. Kd values of the fluorescent chemokine were determined from saturation curves of the specific

binding using GraphPad Prism software (GraphPad Software, Inc., San Diego, CA). The K_i values for ligands were calculated from binding competition experiments according to the Cheng and Prusoff equation: $K_i = IC_{50} \times (K_d/K_d + [L])$, where IC_{50} is the concentration of ligands leading to half-maximal inhibition of specific binding, K_d is the affinity of fluorescent chemokine for the receptor studied, and $[L]$ is the concentration of the red-CXCL12 present in the assay.

DERET internalization assays

Internalization assays for CXCR4 and ACKR3 were performed in 96-well culture cell plates using ST-CXCR4 or ST-ACKR3 cells as previously described (Levoye, 2015). Briefly, upon SNAP Lumi4-Tb labeling, internalization experiments were performed by incubating cells with Tag-lite labeling medium, either alone or containing ligands (CXCL12, CXCL11, CXCL12-derivatives and small molecules AMD3100 and T134) in the presence of fluorescein. Typically, in plates containing SNAP-Lumi4- Tb-labeled cells, 10 μ l of medium containing ligands (100nM) was added, immediately followed by the addition of 80 μ l of 25 μ M fluorescein. Plates were incubated for 1 hour at 4°C and signals were detected using fluorescence microplate reader (Envision, Perkin Elmer) thermostated at 37°C. HTRF ratios were obtained by dividing the acceptor signal (520 nm) by the donor signal (620 nm) and multiplying this value by 10 000.

BRET experiments

HEK293T cells were transiently transfected with the indicated constructs. Forty-eight hours after transfection, cells were washed in PBS, detached in PBS-EDTA and resuspended in PBS. Cells were then distributed in a white 96-well plate (Optiplate, PerkinElmer, MA, USA) and incubated with 1 μ M ligands before adding coelenterazine h (Interchim, Montluçon, France). For dose-response experiments, cells were incubated with ligands at the indicated concentrations for 10 or 20 minutes at 37°C before adding coelenterazine h (5 μ M), as previously reported (Levoye et al. 2009). BRET values were collected using the MicroWin2000 software on Mithras LB940 reader (Berthold Biotechnologies, Bad Wildbad, Germany). BRET signals were expressed in milliBRET units (mBU) of BRET ratio, 1 mBU corresponding to the BRET ratio multiplied by 1000 as previously described, (Levoye et al.

2009). NetBRET is calculated subtracting the signal of basal BRET in untreated cells. The curves were fitted with a nonlinear regression and sigmoid dose-response model with variable slope using Prism GraphPad software (GraphPad Software, Inc., San Diego, CA).

cAMP accumulation and ERK1/2 by HTRF-FRET assays

Measurement of intracellular cAMP accumulation in HEK293T cells transiently transfected with CXCR4 WT, ACKR3 WT and ACKR3 mutants was performed using the cAMP Dynamics 2 competitive immunoassay kit (Cisbio Bioassays, Codolet, France). The cAMP assay uses a cryptate-conjugated anti-cAMP monoclonal antibody and d2-labeled cAMP. HEK293T cells were detached and seeded into white 96-well microplates with 1×10^4 cells/well in 20 μ l DMEM without serum. Prior to lysis, cells were treated or not with CXCL12 at a concentration of 10nM (to stimulate G-alpha-i coupling to endogenous CXCR4) in 10 μ l/well of DMEM and incubated 30 minutes at 37°C. Antagonists (AMD3100 or mAb 9C4) were pre-incubated 30 minutes at room temperature before stimulation with CXCL12. Then, cells were incubated for 45 minutes with forskolin at final concentration of 5 μ M at 37°C and then lysed by addition of 40 μ l/well of the supplied conjugate-lysis buffer containing d2-labeled cAMP and Europium cryptate-labeled anti-cAMP antibody, both reconstituted according to the manufacturer's instructions. Plates were incubated for 1 hour in the dark at room temperature and time-resolved fluorescence signals were measured at 620 and 665 nm, respectively, 50 ms after excitation at 320 nm using a Mithras LB 940 plate reader (Berthold Biotechnologies, Bad Wildbad, Germany). Results are expressed as HTRF ratio between 665 nm measure and 620 measure (665/620).

Measurement of Phospho-ERK was performed in HEK293T cells transiently transfected with CXCR4 WT, ACKR3 WT and ACKR3 mutants using the Advance Phospho-ERK1/2 immunoassay kit (Cisbio Bioassays, Codolet, France), which uses a cryptate-labelled anti-ERK monoclonal antibody and a d2-labeled anti-phospho-ERK monoclonal antibody. Cells were cultured overnight in a 96-well black plate half volume (5×10^4 cells/well) using 50 μ l of medium/well without serum. Then medium was discarded and 20 μ l of free-serum medium, containing or not AMD3100 or mAb 9C4, was added to the cells. After 45 minutes of incubation, cells were stimulated with 50nM of CXCL12 for 2, 5 and 20 minutes. After stimulation, cells were put on ice and supplemented lysis buffer was added (32 μ l/well) for 20 minutes at room temperature with shaking. Then anti-ERK1/2-Europium/Terbium Cryptate

and anti-Phospho-ERK1/2-d2 antibody solutions were added (4µl of each). The plate was then incubated for at least 4 hours at room temperature before reading the fluorescence emission at 620 and 665 nm using a Mithras LB 940 plate reader (Berthold Biotechnologies, Bad Wildbad, Germany).

Homology modeling on HHpred toolkit

Prediction of ACKR3 structure was performed starting from the amino acid sequence UniProt P25106, selecting the closest related UniProt amino acid sequence using the PSI-BLAST alignment algorithm and aligning the selected templates (CXCR4 P61073, CCR5 P51681 and CXCR1 P25024) using MSAProb algorithm. Results from MSAProb were forwarded in HHpred software with HHblits options (hidden Markov model predictions (Soding et al. 2005), and models were created using Modeller software matching the three-dimensional PDB-structures of CXCR4 (3ODU), CCR5 (4MBS) and CXCR1 (2LNL).

CXCL12/ACKR3 docking

Model structure of ACKR3 generated using Homology modeling was analyzed after dynamic molecular simulation (1µsec) in complex with POPC (1-palmitoyl-2-oleoyl-sn-glycero-3-phosphocholine) in a hydrated context with charges. AMBER99SB-ILDN was used as force field in GROMACS software for MD simulation, then the trajectory was analyzed to permit the clustering of the 8 most representative conformations (RMSD parameter 0.30). We used the NMR structure of CXCL12 (2K05, containing 20 conformations) to model the chemokine interaction with the 8 different conformations of ACKR3. We made a cross docking for all 20 conformations of CXCL12 with the 8 conformations of ACKR3 using Frodock software (Ritchie, 2000) following the procedure described in Garzon, 2007. Briefly, this procedure is following three steps: i) generation of pre-calculated grid maps, three grid potentials were computed from each ACKR3 coordinates (van der Waals, electrostatic and desolvation), whereas 20 were needed from CXCL12 coordinates (desolvation). Atomic properties were taken from CHARMM 19 force field; ii) docking was then performed with a single tool called FRODOCK (Chaconlab.org). The rotational and translational sampling resolutions were fixed to 5.6 Å (6×10⁴ rotations) and 2 Å, respectively. These values were chosen in order to have a good balance between efficiency and accuracy. Since the translational search can eventually

explore all the receptor surface, we only considered the extracellular part of the receptor and taken the best 10 docking predictions for each translation point in order to avoid a large redundant set of solutions and, iii) clustering was made for each docking run using an explicit comprehensive algorithm (Kozakov, 2005). Briefly, once the solution set was ranked according to their docking correlation, we formed clusters with all ligand-docking predictions within 5 Å RMSD distance from the first ranked solution (i.e. the lowest energy). The final models were chosen among the first 100 best structures according to the docking score, chemokine orientation and distance between CXCL12 N-terminus and the intra helix domains of ACKR3.

Statistical analysis

Results were analyzed by PRISM (GraphPad Software Inc., San Diego, CA). Data are expressed as mean \pm SEM. Student t-test was applied for statistical analysis.

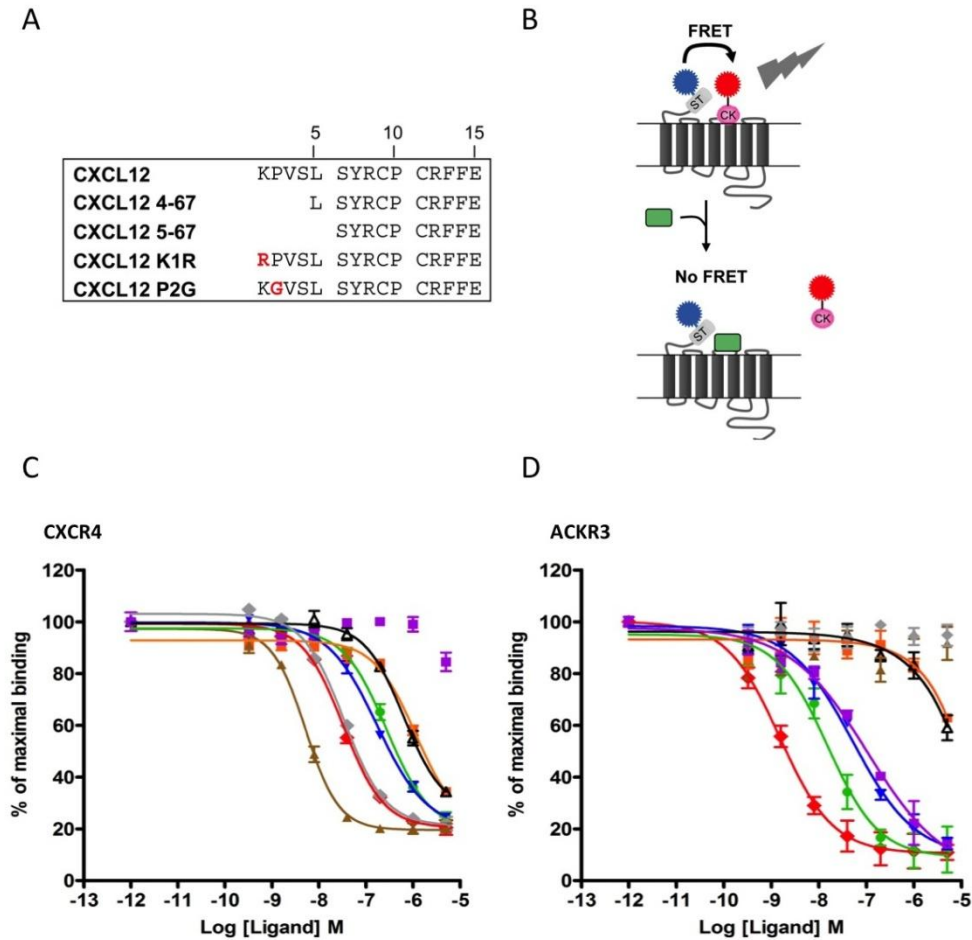


Fig 1. CXCL12 N-terminal mutated analogs differentially bind to CXCR4 and ACKR3.

(A) 15 first N-terminal residues of CXCL12 and mutated analogs sequences. Analogs encompass either deleted residues or substituted residues (in red). (B) Principle of the HTRF-based competition experiments indicating the tagged receptor (blue dot), the red-CXCL12 (red dot) and the potential competitors (in green). (C-D) HTRF-based competition experiments performed in CXCR4-expressing HEK293T cells (C) and ACKR3-expressing HEK293T cells (D) incubated in presence of red-CXCL12 and the increasing indicated concentrations of CXCL12 (red), CXCL12-K1R (green), CXCL12-P2G (blue), CXCL12 4-67 (orange), CXCL12 5-67 (black), AMD3100 (gray), T134 (ochre) or CXCL11 (purple) for 2 hours at room temperature. Values are expressed as percent of the maximal binding obtained without competitor. IC₅₀ and K_i values are presented in Table 1. Values are mean ± SEM of four experiments, each performed in triplicate.

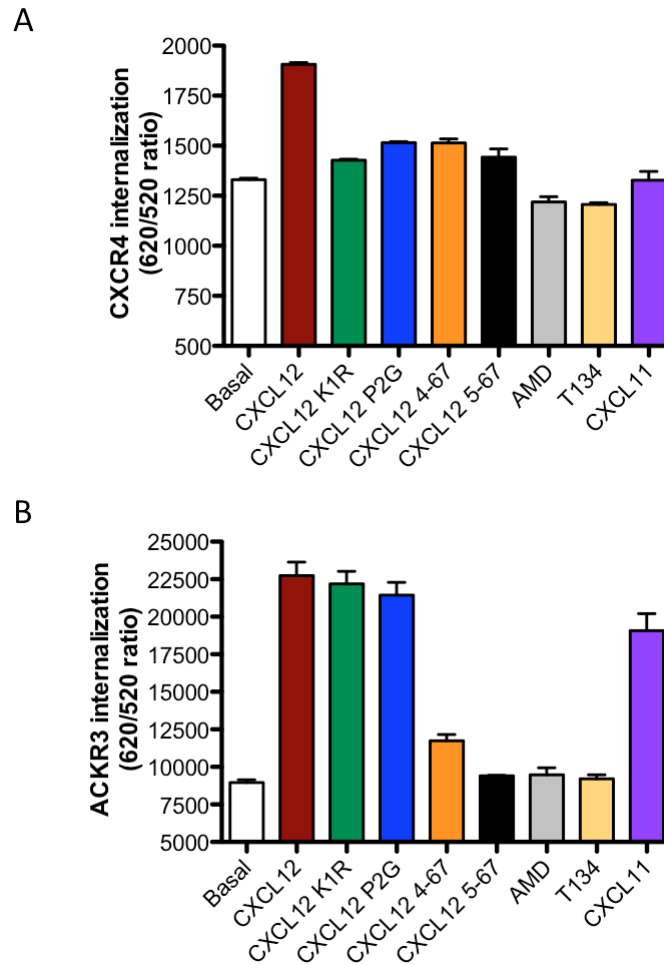


Fig 2. Requirement of CXCL12 two first residues for inducing CXCR4 but not ACKR3 internalization. (A) HEK293T cells stably expressing ST-CXCR4 (A) or ST-ACKR3 (B) were labeled with SNAP-Lumi4Tb fluorescent substrate and incubated in the presence of a large excess of acceptor with medium or saturating concentrations of the indicated ligands (1 μ M). Receptor internalization was then evaluated by the DERET assay. Results are expressed as 620/520 ratio and represent the mean \pm SEM of two independent experiments performed in duplicates.

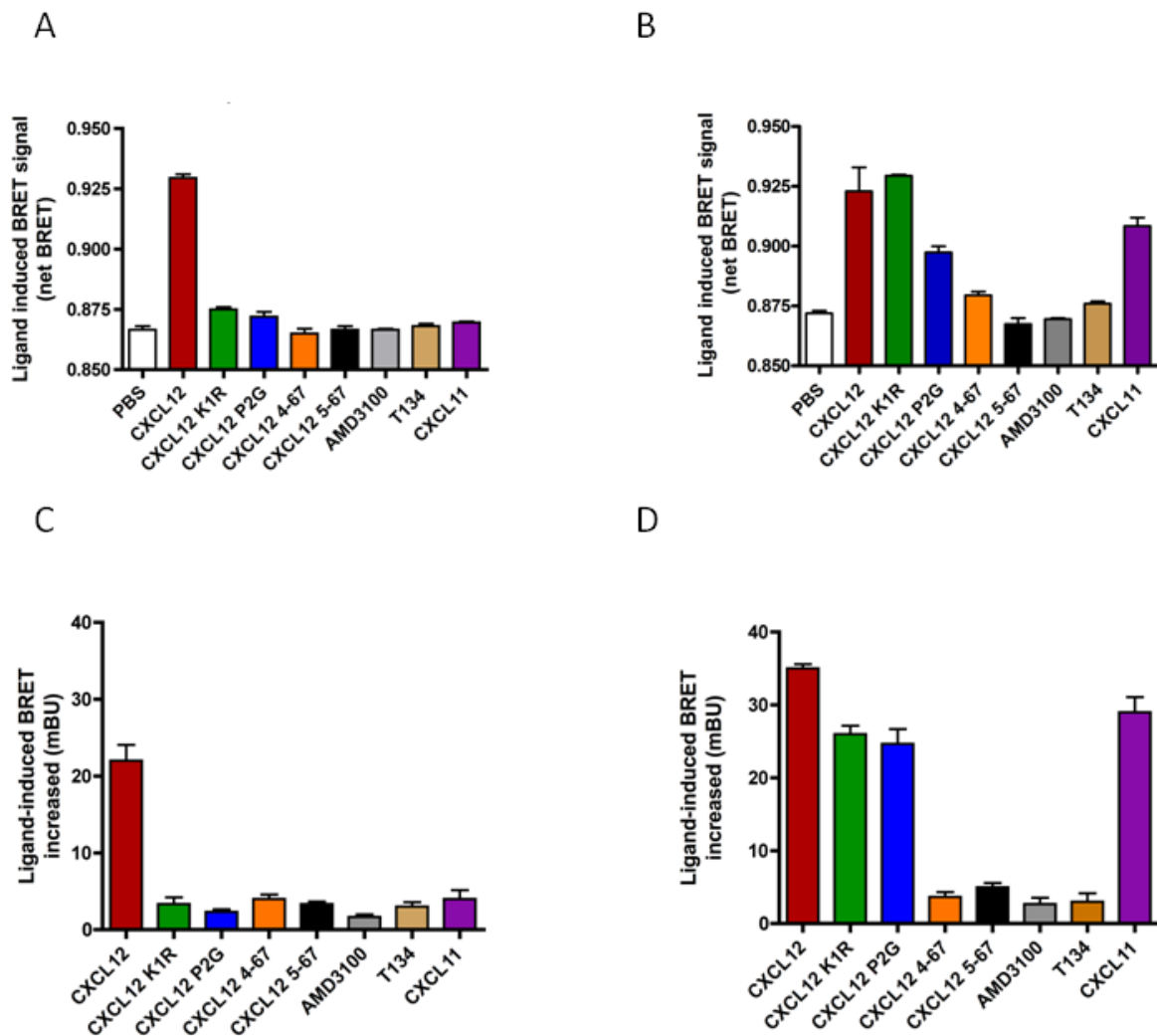


Fig 3. CXCL12 analogs differentially induce β -arrestin2 recruitment to receptors and β -arrestin2 intramolecular conformational changes. (A-B) BRET signal between Rluc- β -arrestin2 and CXCR4-YFP (A) or ACKR3-YFP (B) was measured 48 hours post-transfection in HEK293T cells stimulated or not by the indicated ligands (1 μ M). (C-D) Ligand-promoted conformational change of β -arrestin2 monitored by intramolecular BRET. HEK293T cells were transfected with Rluc8- β -arrestin2-Ypet and either CXCR4 (C) or ACKR3 (D). Cells were stimulated by the indicated ligands (1 μ M). Data represent the mean \pm SEM of three independent experiments performed in duplicates.

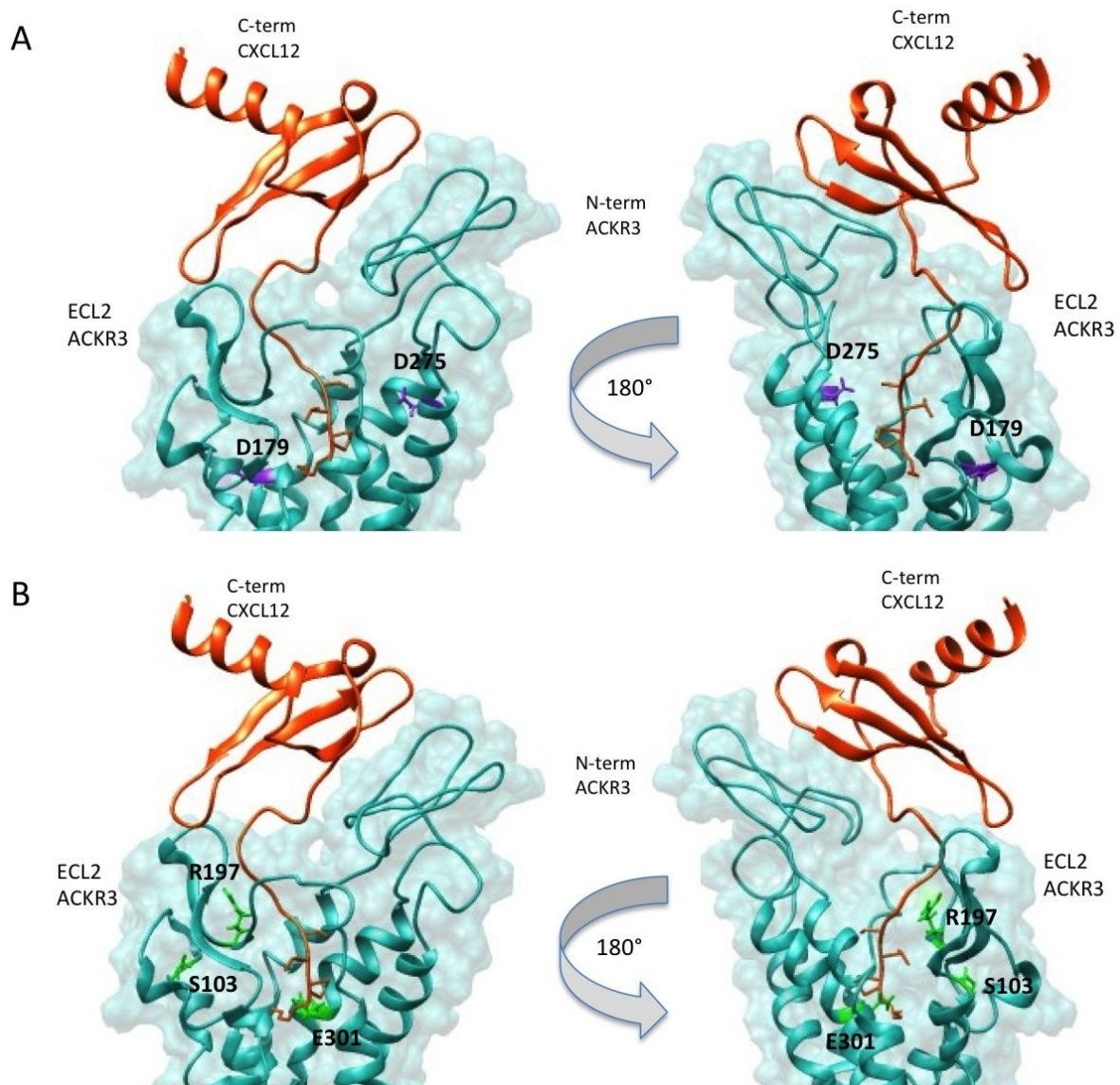


Fig 4. Predicted interactions between CXCL12 and ACKR3 by Peptide-peptide docking experiments. A model of the interactions between CXCL12 (orange ribbon) and ACKR3 (cyan ribbon) showing the likelihood positions of CXCL12 N-terminus residues toward ACKR3 residues (A) conserved in CXCR4 and considered as critical for interaction with CXCL12 (ACKR3 D179 vs CXCR4 D171; ACKR3 D275 vs CXCR4 D262) and (B) considered as critical for CXCR4-induced Gi protein activation but not conserved (identity and charges) in ACKR3 (ACKR3 S103 vs CXCR4 D97; ACKR3 R197 vs CXCR4 D187; ACKR3 Q301 vs CXCR4 E288). CXCL12/ACKR3 interactions are shown in the two 180°-rotated orientations. Three different mutants were generated modifying the two conserved residues (D179A and D275A) or all residues critical for G-protein activation (LAIDDE).

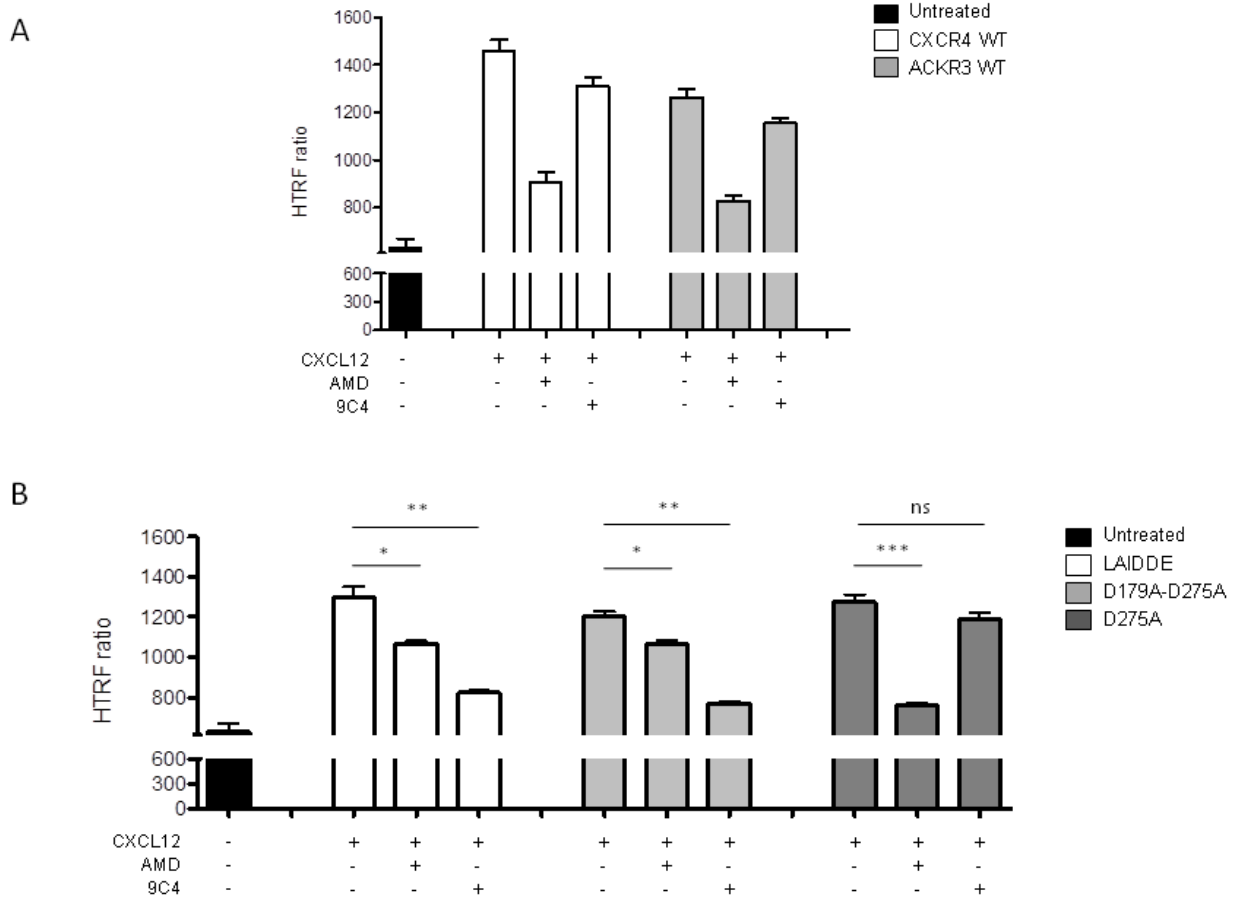


Fig 5. Inhibition of cAMP production indicates G-protein activation downstream ACKR3 mutants. HTRF-based cAMP assay in HEK293T cells transiently transfected with CXCR4, WT ACKR3 (A) or the indicated ACKR3 mutants (LAIDDE, D179A-D275A and D275A) (B) and left untreated or treated with CXCL12 (10nM), AMD (10 μ M) in presence or not of the anti-human ACKR3 9C4 mAb for 30 minutes. Results are expressed as 665/620 ratio. Data points are mean \pm S.E.M. of duplicate values from a single experiment, and are representative of three individual experiments. T-student analysis for statistics: * $p < 0.05$, ** $p < 0.01$, *** $p < 0.001$. ns (non significant).

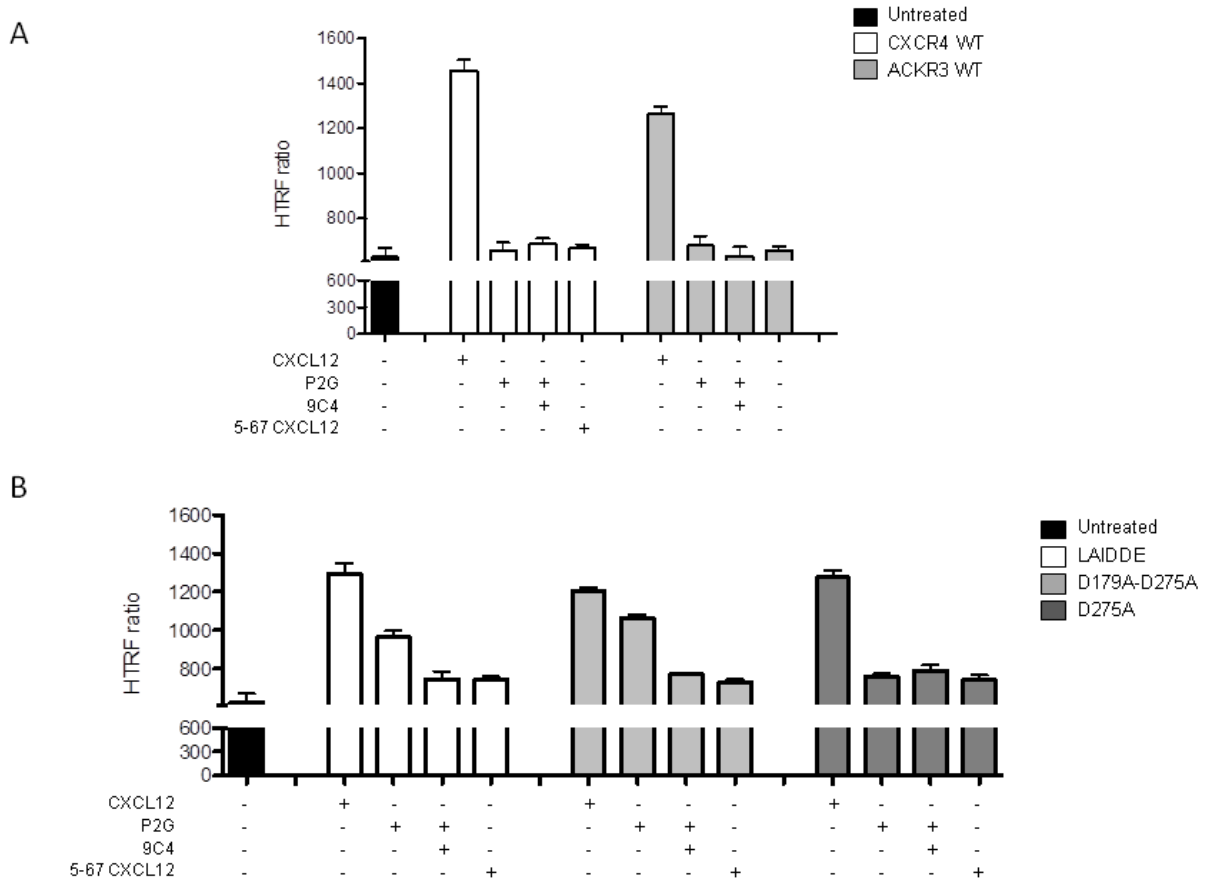


Fig 6. ACKR3 LAIDDE and D179A-D275A mutants activate G-proteins. HTRF-based cAMP assay in HEK293T cells transiently transfected with CXCR4, WT ACKR3 (A) or the indicated ACKR3 mutants (LAIDDE, D179A-D275A and D275A) (B) and left untreated or treated with CXCL12 (10nM), CXCL12-P2G mutant (50nM) and CXCL12 5-67 truncation (100nM), in presence or not of the anti-human ACKR3 9C4 mAb for 30 minutes. Results are expressed as 665/620 ratio. Data points are mean \pm S.E.M. of duplicate values from a single experiment.

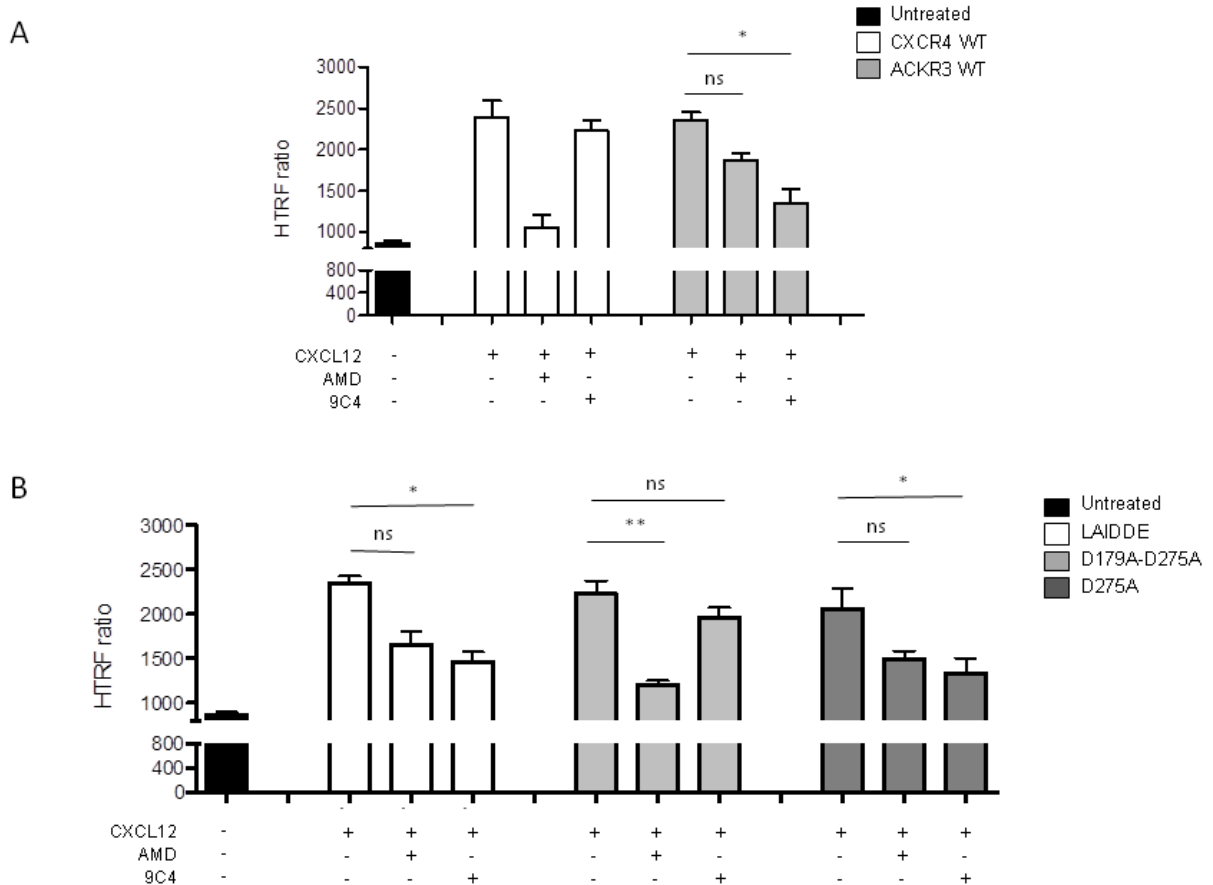


Fig 7. D179A-D275A double mutation abolishes the capacity of ACKR3 to activate the ERK1/2 pathway upon CXCL12 stimulation. HTRF-based assay in HEK293T cells transiently transfected with CXCR4, WT ACKR3 (A) or the indicated ACKR3 (LAIDDE, D179A-D275A and D275A) mutants (B) and left untreated or treated 5 minutes with CXCL12 (50nM), in presence or not of AMD (10 μ M) or the anti-human ACKR3 9C4 mAb for 30 minutes. Results are expressed as 665/620 ratio. Data points are mean \pm S.E.M. of duplicate values from a single experiment, and are representative of three individual experiments. T-student analysis for statistics: * $p < 0.05$, ** $p < 0.01$, ns (non significant).

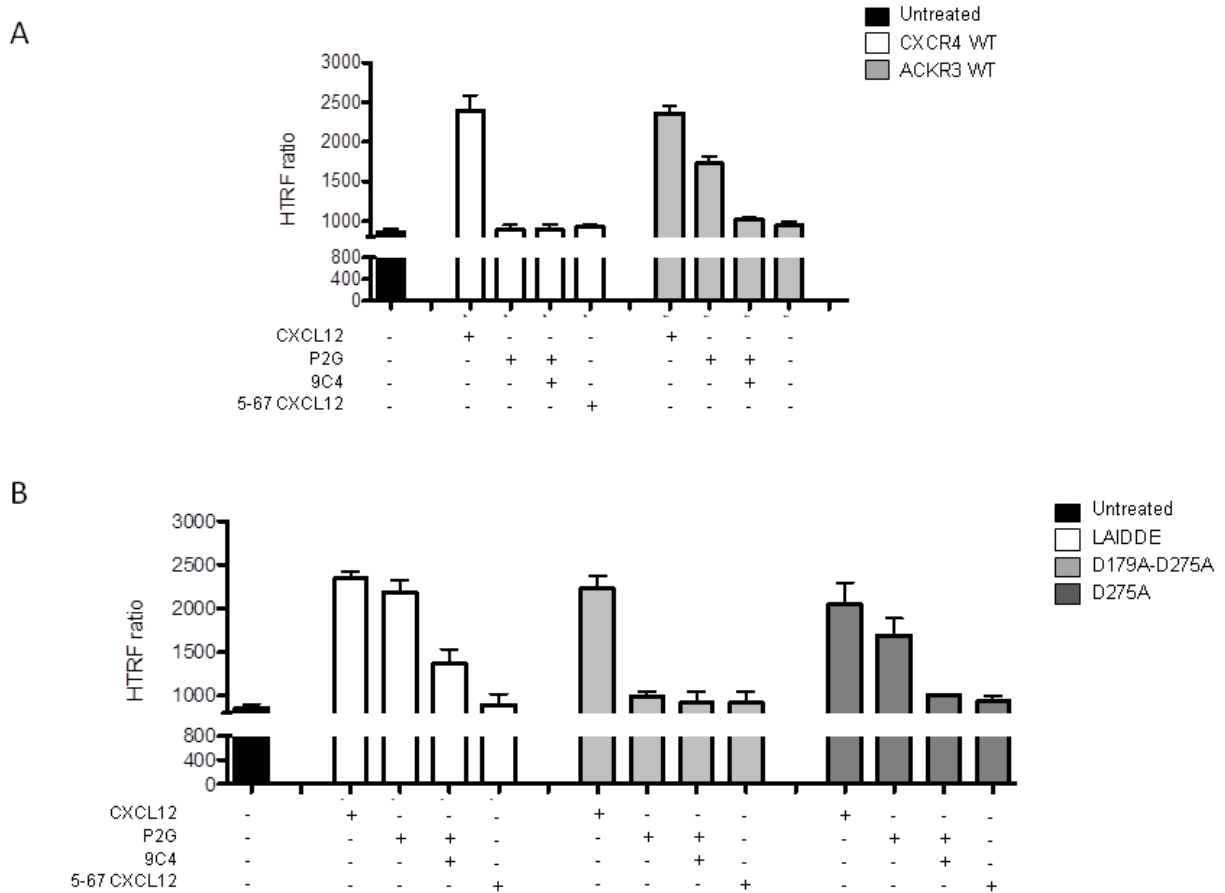


Fig 8. CXCL12 mutant P2G confirms that the ACKR3 mutant LAIDDE activates the ERK1/2 pathway while the D179A-D275A double mutation abolishes it. HTRF-based assay in HEK293T cells transiently transfected with CXCR4, WT ACKR3 (A) or the indicated ACKR3 (LAIDDE, D179A-D275A and D275A) mutants (B) and left untreated or treated with CXCL12 (50nM), CXCL12-P2G (100nM) and CXCL12 5-67 (200nM) in presence or not of the anti-human ACKR3 9C4 mAb for 30 minutes. Results are expressed as 665/620 ratio. Data points are mean \pm S.E.M. of duplicate values from a single experiment.

Ligands	IC ₅₀ (nM)		K _i (nM)	
	CXCR4	ACKR3	CXCR4	ACKR3
CXCL12	36.8 ± 3.8	1.1 ± 0.4	24.5 ± 2.5	0.3 ± 0.1
CXCL12 K1R	211.6 ± 62.4	12.2 ± 2.9	140.6 ± 41.5	1.32 ± 0.3
CXCL12 P2G	147.5 ± 27.5	49.3 ± 2.3	98.1 ± 18.3	5.34 ± 0.2
CXCL12 4-67	947.0 ± 53.0	> 10000	594.3 ± 0.0	> 10000
CXCL12 5-67	544.0 ± 104.0	> 10000	361.6 ± 69.1	> 10000
CXCL11	nd	112.2 ± 7.5	nd	12.1 ± 0.8
AMD	61.5 ± 27.5	nd	40.9 ± 18.3	nd
T134	5.3 ± 0.1	nd	3.5 ± 0.1	nd

Table 1. Binding affinities (IC₅₀ and K_i values) from HTRF assays in cells expressing ST-CXCR4 and ST-ACKR3 receptors. Data are means ± SEM of three independent experiments each performed in triplicates. nd: not determined.

Ligands	EC ₅₀ (nM)	
	Rluc-βarr 2 + ACKR3-YFP	Rluc-βarr 2 + CXCR4-YFP
CXCL12	22.6 ± 0.2	59.5 ± 0.1
CXCL12 K1R	23.9 ± 0.2	nd
CXCL12 P2G	66.5 ± 0.9	nd
CXCL12 4-67	nd	nd
CXCL12 5-67	nd	nd
CXCL11	47.6 ± 1.0	nd
AMD	nd	nd
T134	nd	nd

Table 2. Efficient concentrations (EC50) values of the indicated ligands for promoting the interaction between β-arrestin2 and receptors. Data from dose-response curves shown in Fig.S3 are presented as mean ± SEM EC50 values (nM) were calculated as described under Experimental procedures. nd: not determined.

SUPPLEMENTAL MATERIAL FOR

Differential activities of CXCL12 analogs at the CXCR4 and CXCR7/ACKR3 receptors: Study of interaction determinants

Pasquale Cutolo¹, Guillaume Bernadat², Agnieszka Jaracz-Ros¹, Françoise
Baleux³, Françoise Bachelier^{1‡*} and Angélique Levoye^{4‡*}

¹ UMR996 - Inflammation, Chemokines and Immunopathology -, Inserm, Univ Paris-Sud,
Université Paris-Saclay, 92296, Clamart, France

² BioCIS - UMR 8076, Université Paris-Sud, CNRS, Université Paris-Saclay, Châtenay-
Malabry, France

³ Unité de Chimie des Biomolécules, Département de Biologie Structurale et Chimie, Institut
Pasteur, Paris, France.

⁴ INSERM UMR 1148, Laboratory of Translational Vascular Science, Université Paris 13
Sorbonne Paris Cité, Paris, France.

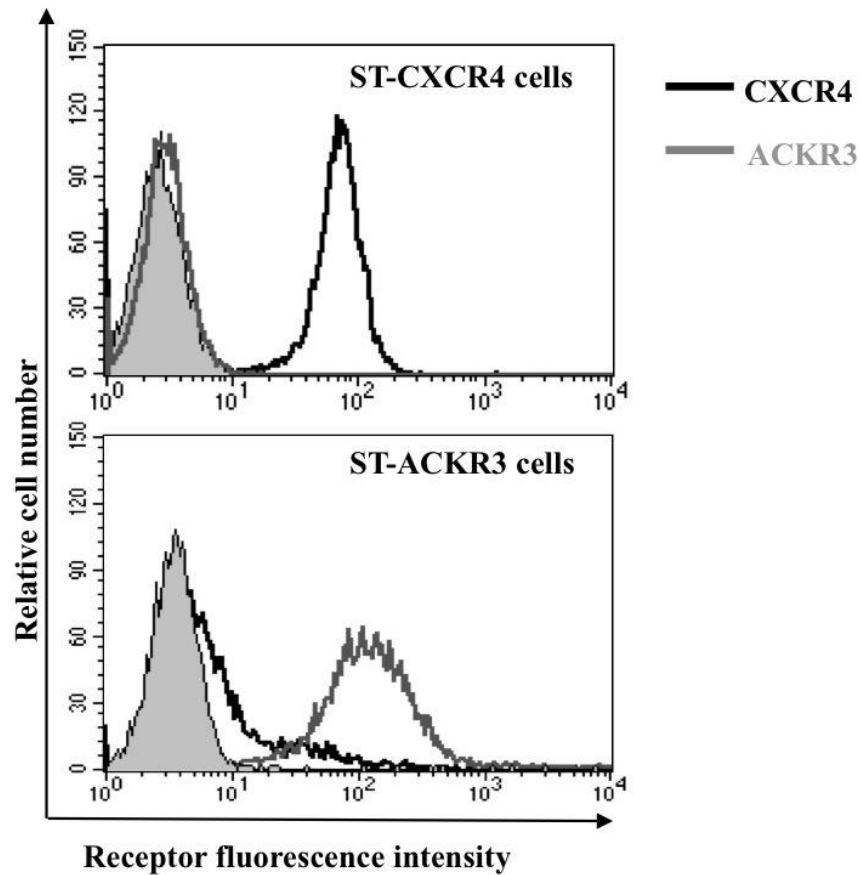


Fig S1. Expression of CXCR4 and ACKR3 in HEK293T cells stably expressing ST-CXCR4 or ST-ACKR3. Cell surface expression levels of CXCR4 and ACKR3 receptors in ST-CXCR4 (upper panel) and ST-ACKR3 (lower panel) expressing cells were determined by flow cytometry using mAb directed against CXCR4 and ACKR3. Open histograms show receptors specific staining and filled histograms show isotype control. Receptors expression is presented as mean fluorescence intensity (MFI). Results are representative of three independent experiments.

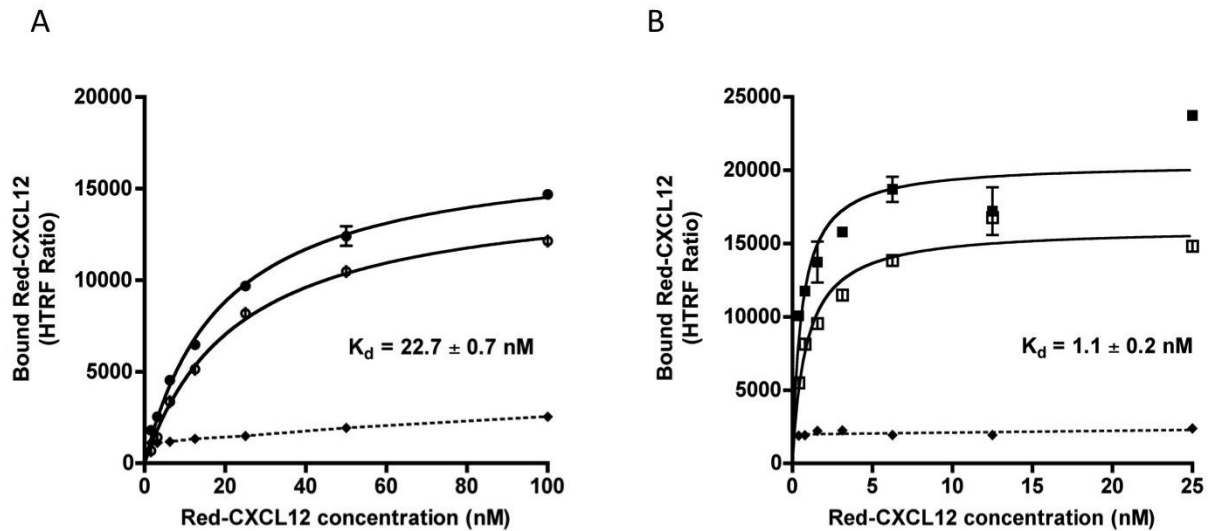


Fig S2. HTRF-based saturation binding experiments on CXCR4- and ACKR3-expressing cells. Labelled HEK293T cells stably expressing (A) SNAP-Tag CXCR4 (ST-CXCR4) or (B) SNAP-Tag ACKR3 (ST-ACKR3) were incubated with increasing concentrations of red-CXCL12 for 1 hour at room temperature. Nonspecific binding (dotted line) was measured by adding AMD (A) or unlabelled-CXCL12 (B) in each well and was subtracted from total binding (closed symbols) to obtain specific binding (open symbols). K_d values (mean \pm SEM) for red-CXCL12 were determined from data analysis using a nonlinear regression equation applied to a single binding site model. Values are mean \pm SEM of four experiments, each performed in triplicate.

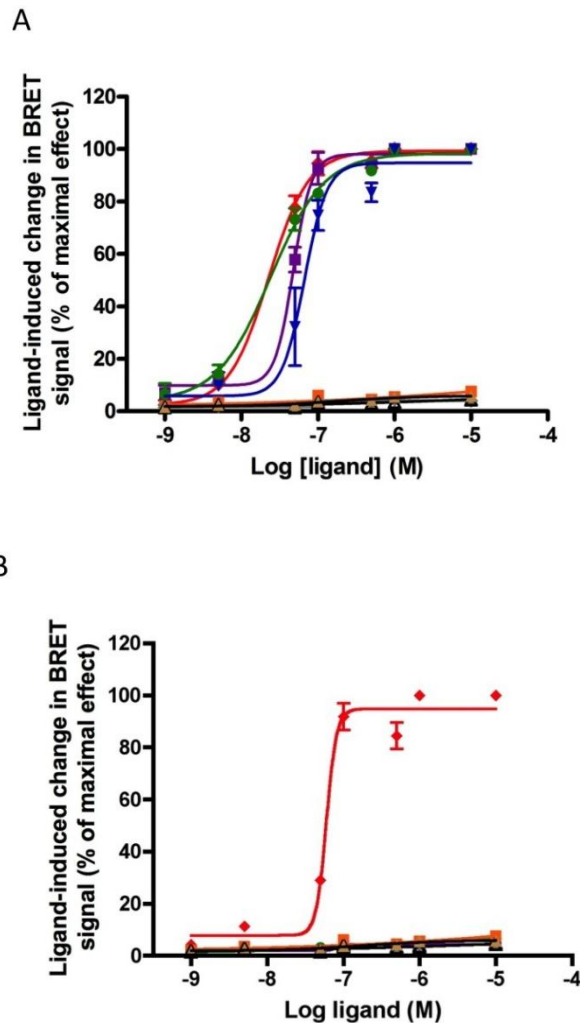


Fig S3. Dose-response curves for ligands-induced interactions between β -arrestin2 and receptors. HEK293T cells transiently expressing Rluc- β -arrestin2 and ACKR3-YFP (A) or CXCR4-YFP (B) were stimulated with increasing indicated concentrations of CXCL12 (red), CXCL12-K1R (green), CXCL12-P2G (blue), CXCL12 4-67 (orange), CXCL12 5-67 (black), AMD3100 (gray), T134 (ochre) or CXCL11 (purple). Results are expressed as percentage of maximal ligand-induced BRET signal. EC₅₀ values were determined by nonlinear regression using a sigmoidal dose response model with variable slope (GraphPad Software Inc.). Data represent the mean \pm SEM of two to three independent experiments each performed in duplicate.

```

ACKR3 MD----LHLFDYSE-----PGNFSDISWPCNSSDCIVVDTVMCPNMPNKSULLYTLFSFIY
CXCR4 MEGISIIYTSNDNYTEE--MGSGDYDSMKEPCFREE-----NANFNKIFLPTIY
CCR5 MDYQVSSPIYDIN-----Y-YTSEPCQKIN-----VKQIAARLLPPLY
CXCR1 MSNITDPQMWFDDLNFTGMPPAEDYSPCMLE-----TETLNKYVVIIAY

ACKR3 IFIFVIGMIANSVVVWVNIQAKTGYDTHCYILNLAIADLWVVLTIIPVWVVS1L2VQHNQWP
CXCR4 SIIFLTGIVGNGLVILVMGYQKKLRSMTDKYRLHLSVADLLFVITLFPFAVD1AV--ANWY
CCR5 SLVFIFGFVGNMLVILILINCKRLKSMTDIYLLNLAISDLFFLLTVPFAHYAA--AQWD
CXCR1 ALVFLLSLLGNSLVMLVILYSRVGRSVTDVYLLNLALADLLFALTLP1IWAASKV--NGWI

ACKR3 MGELTCKVTHLIFSINLFGSIFFLT3CMSV4DRYLSITYF5TNTPSSRKKM6VRRVVCILVWLL
CXCR4 FGNFLCKAVHVIYTVNLYSSVILAFISL3DRYLAIVHATNSQRPRKLLA5EKV6VYVGVWIP
CCR5 FGNTMCQLLTGLYFIGFFSGIFFIILLT3DRYLAVVH5AVFALKARTVTFGVVTSVITWV
CXCR1 FGTF3LCKVVSLLKEVNFYSGILLACIS4DRYLAIVHATRTLTQKRHLV-KFVCLGCWGL

ACKR3 AFCVSL7FD8TYYLKTVTSASN9NETYCR10SFYPEHSIKEWLIGMELVSVVLGFAVPFSIIAVF
CXCR4 ALLLTIP7DFIFA-NVSEAD-DRYI9CDRFYPND---LWVVVFQFHIMVGLILPGIVILSC
CCR5 AVFASLPGIIFT-RSQKEG-LHYT10CSSHFPYSQYQFWKNFQTLKIVILGLVPLLLVMVIC
CXCR1 SMNLSLPFFLFR-QAYHPN9SSPVCYEVLGND-TAKWRMVLRLPHTFGFIVPLFVMLFC

ACKR3 YFLARAIASASSDQ-EKHSSRKIIFS11YVVVFLVCWLPYHVAVL12DI13FSILHYIPFTCRLE
CXCR4 YCIIISKLSHSGH-QKRKALKTTVILILAFFACWLPYYIGIS12DSFILLEI13IKQGCEFE
CCR5 YSGILKTL11RCRNEKRRHRAVRLIFTIMIVYFLWAPYNIVLLNTFQE12EFFGL-NNCSSS
CXCR1 YGFTLRTL11FKAHMG-QKHRAMR12VIFAVVLIFLLCWL13PYNLVLLADTL14MRTQVIQESCERR

ACKR3 HALFTALHVT15Q16CLSLVHCCVNPVLYSFINRNYRYELMKAFIFKYS17AKTGLTKLI-----
CXCR4 NTVHKWISIT15EALAFFHCCLNPILYAFLGAKFKTSAQHALTS-VSRGSSL-KIL-----
CCR5 NRLDQAMQVTE15TLGMTHCCINPIYAFVGEKFRNYLLVFFQK-H---IAK-RFCKCCSIF
CXCR1 NNIGRALDATEILGLHLSCLNPIYAFIGQ17FRHGFLKILAM-H-GLVSK-EFL-----

ACKR3 ---DASRVSE--TEYSA----LEQSTK
CXCR4 ---SKGKRGG-HSSVSTESESSSFHSS
CCR5 QQEAPERASSVYTRSTG--EQEISVGL
CXCR1 ---ARHRVTS-YTSSSV----NVSSNL

```

Fig S4. Multiple sequences alignment from MSAPROBS algorithm. Alignment of human ACKR3 sequence (P25106) with the selected templates (CXCR4 P61073, CCR5 P51681 and CXCR1 P25024). Blue regions indicate TM3 and TM4 and yellow region indicates ICL2 domain. Red rectangles surround critical residues for CXCR4-dependent G-protein activation and not conserved in ACKR3 sequence (CXCR4 D97, ACKR3 S103; CXCR4 D187, ACKR3 R197; CXCR4 E288, ACKR3 Q301). Green rectangles surround critical D (aspartic acid) residues for CXCR4 interaction with CXCL12 and conserved within ACKR3 sequence (CXCR4 D171, ACKR3 D179; CXCR4 D262, ACKR3 D275).

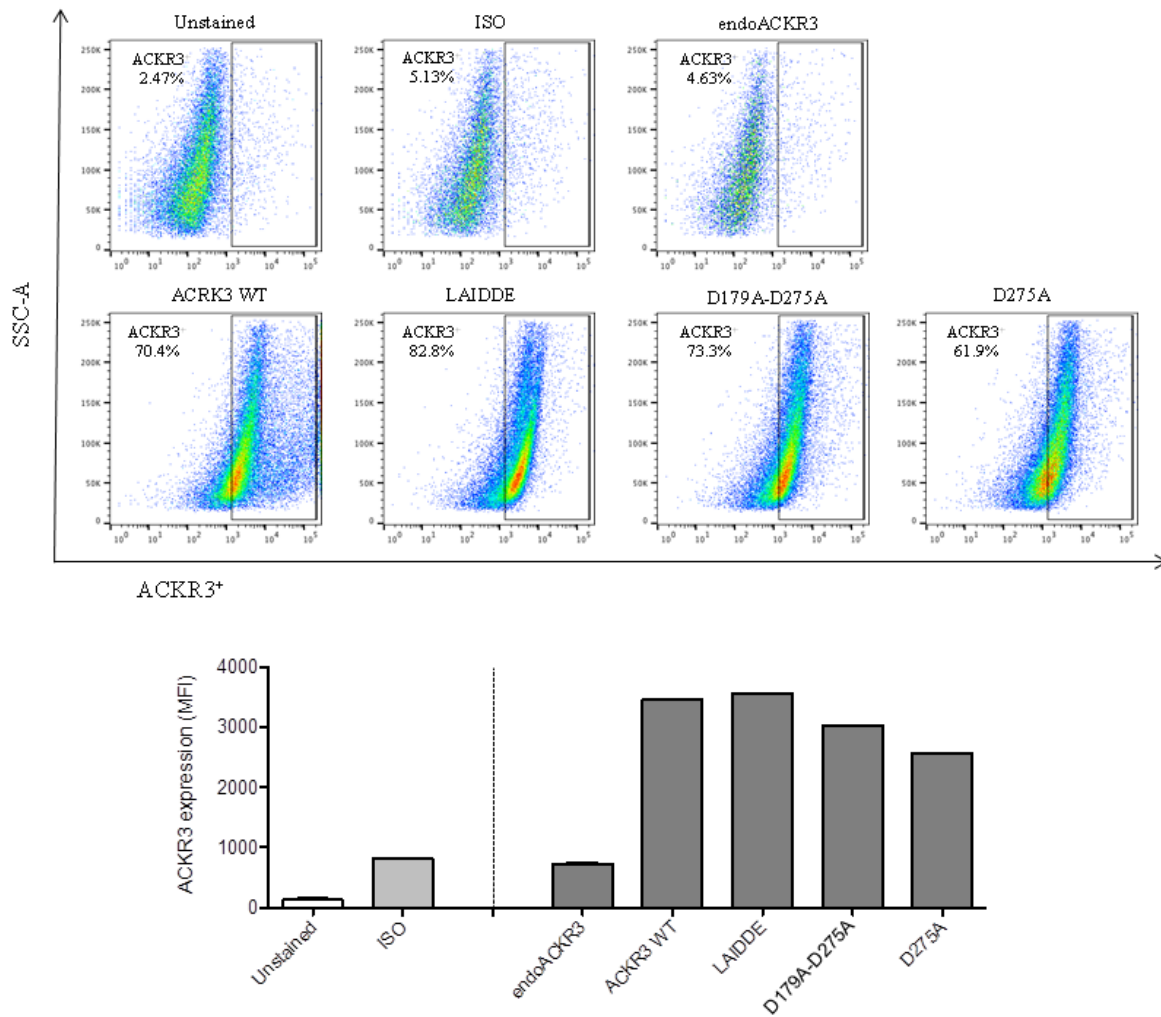


Fig S5. Cell surface expression of WT ACKR3 and the indicated ACKR3 mutant receptors in HEK293T cells. Cell surface expression levels of ACKR3 in non-transfected HEK293T cells (i.e. endogene ACKR3 expression (endoACKR3), upper dot plots) and in HEK293T cells transfected with ACKR3-WT and the indicated ACKR3 mutants (LAIDDE, D179A-D275A and D275A) (lower dot plots). Cells were analyzed by flow cytometry using the 9C4 mAb directed against ACKR3. Negative controls were cells unstained or stained with the control isotype (ISO). Percent of positive cells delineated by the gate (right rectangle) are indicated in the right corner of the dot plots. Receptors expression presented as mean fluorescence intensity (MFI) is shown in lower histogrammes. A representative experiment is shown.

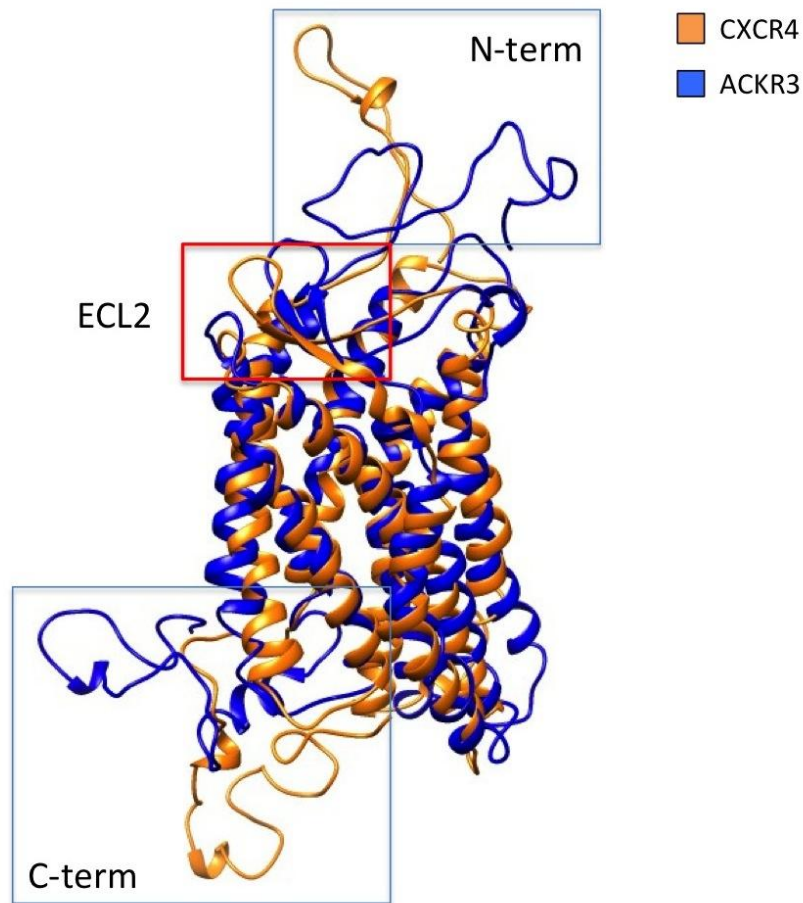


Fig S6. Fitting CXCR4 X ray-derived structure and ACKR3 structure derived from molecular dynamic simulations. Matching the secondary structures between CXCR4 (orange ribbon) and ACKR3 (blue ribbon) revealed that the overall structure of the ACKR3 receptor is conserved including the helical TM domains with the exception of the three indicated domains; the N- and C-terminus (N-term and C-term, blue rectangles) and the ECL2 (orange rectangle). CXCL12/ACKR3 interactions are shown in the two 180°-rotated orientations.

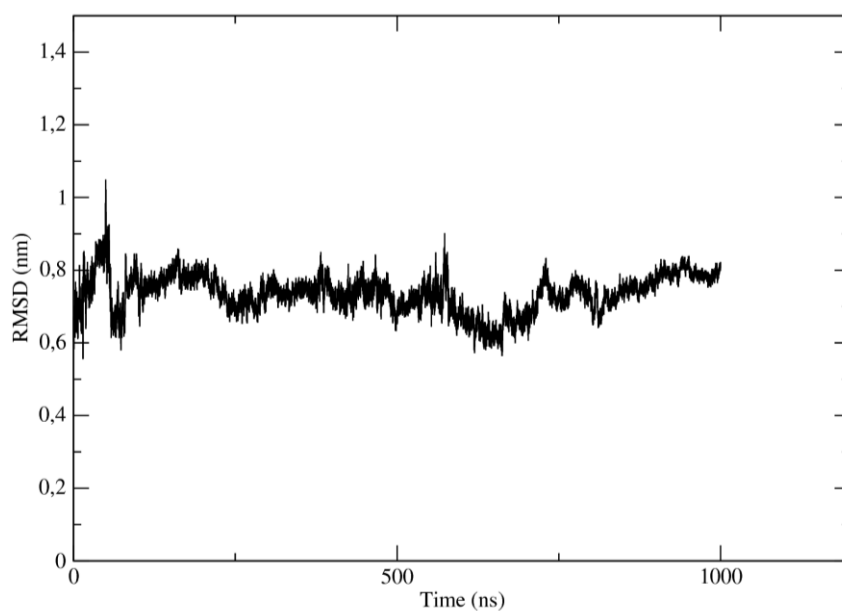


Fig S7. RMSD during time derived from molecular dynamic simulation. RMSD index was calculated on C-alpha after lsq fit to C-alpha during 1 μ s of molecular dynamics simulation on CXCR7/ACKR3 structure modeled by homology.

References

Balabanian, K., B. Lagane, S. Infantino, K. Y. Chow, J. Harriague, B. Moepps, F. Arenzana-Seisdedos, M. Thelen and F. Bachelierie (2005). "The chemokine SDF-1/CXCL12 binds to and signals through the orphan receptor RDC1 in T lymphocytes." *J Biol Chem* 280(42): 35760-35766.

Burns, J. M., B. C. Summers, Y. Wang, A. Melikian, R. Berahovich, Z. Miao, M. E. Penfold, M. J. Sunshine, D. R. Littman, C. J. Kuo, K. Wei, B. E. McMaster, K. Wright, M. C. Howard and T. J. Schall (2006). "A novel chemokine receptor for SDF-1 and I-TAC involved in cell survival, cell adhesion, and tumor development." *J Exp Med* 203(9): 2201-2213.

Crump, M. P., J. H. Gong, P. Loetscher, K. Rajarathnam, A. Amara, F. Arenzana-Seisdedos, J. L. Virelizier, M. Baggiolini, B. D. Sykes and I. Clark-Lewis (1997). "Solution structure and basis for functional activity of stromal cell-derived factor-1; dissociation of CXCR4 activation from binding and inhibition of HIV-1." *EMBO J* 16(23): 6996-7007.

Garzon, J. I., Kovacs, J., Abagyan, R. & Chacon, P. ADP_EM: fast exhaustive multi-resolution docking for high-throughput coverage. *Bioinformatics* 23, 427-433, doi:10.1093/bioinformatics/btl625 (2007).

Infantino, S., B. Moepps and M. Thelen (2006). "Expression and regulation of the orphan receptor RDC1 and its putative ligand in human dendritic and B cells." *J Immunol* 176(4): 2197-2207.

Kozakov, D., Clodfelter, K. H., Vajda, S. & Camacho, C. J. Optimal clustering for detecting near-native conformations in protein docking. *Biophys J* 89, 867-875, doi:10.1529/biophysj.104.058768 (2005).

Lagane, B., K. Y. Chow, K. Balabanian, A. Levoe, J. Harriague, T. Planchenault, F. Baleux, N. Gunera-Saad, F. Arenzana-Seisdedos and F. Bachelierie (2008). "CXCR4 dimerization and beta-arrestin-mediated signaling account for the enhanced chemotaxis to CXCL12 in WHIM syndrome." *Blood* 112(1): 34-44.

Levoye, A., K. Balabanian, F. Baleux, F. Bachelierie and B. Lagane (2009). "CXCR7 heterodimerizes with CXCR4 and regulates CXCL12-mediated G protein signaling." *Blood* 113(24): 6085-6093.

Levoye, A. et al. A Broad G-protein-Coupled Receptor Internalization Assay that Combines SNAP-Tag Labeling, Diffusion-Enhanced Resonance Energy Transfer, and a Highly Emissive Terbium Cryptate. *Front Endocrinol (Lausanne)* 6, 167, doi:10.3389/fendo.2015.00167 (2015).

Naumann, U., E. Cameroni, M. Pruenster, H. Mahabaleshwar, E. Raz, H. G. Zerwes, A. Rot and M. Thelen (2010). "CXCR7 functions as a scavenger for CXCL12 and CXCL11." *PLoS One* 5(2): e9175.

Ritchie, D. W. & Kemp, G. J. Protein docking using spherical polar Fourier correlations. *Proteins* 39, 178-194 (2000).

Sadir R, Imberty A, Baleux F, Lortat-Jacob H. "Heparan sulfate/heparin oligosaccharides protect stromal cell-derived factor-1 (SDF-1)/CXCL12 against proteolysis induced by CD26/dipeptidyl peptidase IV". *J Biol Chem.* 2004 Oct 15;279(42):43854-60.Scott 2002

Struyf, S., S. Noppen, T. Loos, A. Mortier, M. Gouwy, H. Verbeke, D. Huskens, S. Luangsay, M. Parmentier, K. Geboes, D. Schols, J. Van Damme and P. Proost (2009). "Citruination of CXCL12 differentially reduces CXCR4 and CXCR7 binding with loss of inflammatory and anti-HIV-1 activity via CXCR4." *J Immunol* 182(1): 666-674.

Valenzuela-Fernández A, Planchenault T, Baleux F, Staropoli I, Le-Barillec K, Leduc D, Delaunay T, Lazarini F, Virelizier JL, Chignard M, Pidarid D, Arenzana-Seisdedos F. Leukocyte elastase negatively regulates Stromal cell-derived factor-1 (SDF-1)/CXCR4 binding and functions by amino-terminal processing of SDF-1 and CXCR4. *J Biol Chem.* 2002 May 3;277(18):15677-89.Vergote 2006

Wu, B., E. Y. Chien, C. D. Mol, G. Fenalti, W. Liu, V. Katritch, R. Abagyan, A. Brooun, P. Wells, F. C. Bi, D. J. Hamel, P. Kuhn, T. M. Handel, V. Cherezov and R. C. Stevens (2010). "Structures of the CXCR4 chemokine GPCR with small-molecule and cyclic peptide antagonists." *Science* 330(6007): 1066-1071.

Discussion and perspectives

❖ *I - Mechanism of the interaction and stoichiometry of CXCL12 with CXCR4 and CXCR7/ACKR3 receptors*

❖ *II – Nanobodies application on GPCRs*

Discussion and perspectives

I - Mechanism of the interaction and stoichiometry of CXCL12 with CXCR4 and CXCR7/ACKR3 receptors

I.1 Modeling the three-dimensional structure of receptors

Experimental structures exist only for a limited number of GPCRs, however the insights provided by these structures go beyond the specific receptors to which they refer. In fact, they significantly contribute to shedding light onto the topology of a much wider array of receptors by serving as templates for the construction of homology models (Costanzi 2012). Homology modeling lays its foundations on the observation that the three-dimensional structure of proteins has been evolutionarily conserved to a very high degree. Thus, orthologous and paralogous proteins that derive from a common ancestors share highly similar structures. For GPCRs, the sharing of a common three-dimensional topology was first proposed in the 1980s by Robert Lefkowitz and coworkers, through observations based on the comparison of the amino acid sequences of rhodopsin and the b2 adrenergic receptors. This intuition was strikingly confirmed by the recent disclosure of the X-ray structure of several members of the superfamily and the structural comparisons that said structures allowed (Jacobson and Costanzi 2012). As a number of controlled assessments have demonstrated, the accuracy of the models is strongly dependent on the closeness of template and target receptor, in terms of sequence similarity. Thus, it is natural to expect that, in the next several years, the scope and the accuracy of GPCR modeling will increase in tandem with the anticipated continued advances in X-ray crystallography.

In our recent article published, we outlined procedures and technical aspects behind the construction of coarse-grained models. Specifically, the article illustrates the principles at the basis of the stoichiometry of the CXCL12/CXCR4 interaction as well as the extracellular and intra-helix involved domains. Among them, the second ECL deserves a particular attention, since it is involved in ligand recognition for most receptors, and residues impaired in the G-protein activation as showed in previous mutagenesis studies.

Our results fit with the hypothesis of the dimer existence for CXCR4 and support the two-step model for the binding/activation mechanism. The possibility that one protomer of CXCR4

engages the binding with the CK core domain, to allow the activation of the nearby CXCR4 protomer, may explain the negative dominance of a gain of function mutant form of CXCR4, known to be responsible of the rare immunodeficient WHIM syndrome, but also the potential of CXCR7/ACKR3 to influence the CXCR4 signaling pathway into heterodimers.

A recent paper discuss the asymmetry of oligomers (Maurice, Kamal et al. 2011) and how this oligomeric receptor organization can account for the diversity and biased behavior of GPCRs. It will be interesting to explore residues in the dimerization domain, showed in the CXCR4 crystal structure in 2010, and study their conformational changes generated after interaction with CXCL12 using MD in a long simulation.

In our project it was important to first establish a structural model for CXCR7/ACKR3, to investigate its interaction with CXCL12 and compare it with that of CXCL12/CXCR4.

GPCRs structures share the helical bundles conformations, but other domains are characterized by a much higher degree of sequence variability, in terms of amino acid composition and length. Consequently, while homology modeling is generally suited for the construction of the helical bundle, this is not always the case for the remainder part of the receptor: unless the target receptor is particularly close to the template. De novo modeling, that is, first-principles modeling based exclusively on molecular mechanics considerations, is typically more suited for the modeling of domains other than the helical bundle (Goldfeld, Zhu et al. 2011).

Using the online software HHpred, we found three structures as templates for the homology modeling of CXCR7/ACKR3. We made our choice with regard to the highest percentage of the prediction of shared secondary structure (we took only those with 100% of probability) selecting only those that are human GPCRs.

Interestingly and as can be expected, we found CXCR4 and CCR5 crystal structures and CXCR1 NMR structure as being best templates. We then analyzed the CXCR7/ACKR3 structure generated with homology modeling during a 1 μ s MD simulation to find conformational clusters that might be representative of receptor states and we use these for CXCL12 docking. Now, the next step will be to reproduce the study we did for CXCR4 and analyze results from the MD simulation of CXCR7/ACKR3-CXCL12 interaction model to complete the comparative analysis.

1.2 Modeling the binding of ligands to GPCRs

Experimentally solved as well as modeled GPCR structures can be utilized as the basis to infer the three-dimensional details of receptor–ligand complexes through a variety of molecular docking techniques. This possibility is very appealing, since hundreds of natural and synthetic ligands, endowed with different signaling properties, are known for many receptors. Thus, molecular modeling provides a framework to expand the knowledge derived from X-ray crystallography. In particular, various modeling techniques have been applied to generate experimentally testable hypotheses on the mode of binding of diverse ligands as well as the conformational nature associated with different signaling states of a receptor. Specifically, while single crystal structures of GPCRs provide a static representation of a given receptor–ligand in a given signaling state, the comparison of multiple structures and models obtained with different ligands and under different conditions provides a means to speculate on the nature and the magnitudes of the conformational changes that trigger signaling (Rasmussen, Choi et al. 2011). Moreover, molecular dynamics simulations applied to crystal structures provide the basis to shed light onto the dynamic nature of these complex systems. For instance, as a result of the recent implementation of rapid and accurate theoretical algorithms and the construction of dedicated hardware, novel hypotheses have been formulated on the process of ligand binding and receptor activation (Dror, Arlow et al. 2009, Dror, Arlow et al. 2011).

As suggested by the abovementioned controlled assessments on the structural accuracy of GPCR models, the determination of the correct binding mode of CXCL12 into CXCR7 is by far the most difficult aspect of GPCR modeling (Costanzi 2012). Moreover, when the docking exercise is based on homology models, the accuracy of the determination of the ligand binding mode decreases substantially as the distance between target and template receptors increases (Beuming and Sherman 2012). The use of the most advanced computational tools for the production of a number of possible docking solutions is fundamental for the construction of meaningful models. Importantly, some of these tools take into account the flexibility of both ligands and binding sites to generate hypotheses on the predominant conformations of receptor–ligand complexes. However, a thorough support from experimental mutagenesis data is, without any doubt, the most crucial element for the selection of the most probable binding mode (Costanzi 2012). The compatibility between

models and mutagenesis data is typically assessed with a thorough analysis of the interactions that the ligand establishes with the mutated residues. However, the fact that a residue significantly contributes to ligand binding does not necessarily imply a direct interaction with the ligand, as indirect effects due to the induction of conformational changes to the receptor are also possible. To avoid these pitfalls, we have to apply more complex approaches based on the complementary alteration of receptors and ligands regarding the MD trajectory (Jacobson, Gao et al. 2007). If the contribution of experimental data is always important, it becomes paramount when dealing with homology models rather than crystal structures. Our study on the mutant we generated provides a first idea on the importance of a conserved aspartic acid (D179). This residue when mutated in Ala conferred the mutant CXCR7/ACKR3 with a completely inversed signalization pathway upon stimulation with CXCL12 (G-protein activation and loss in MAPK cascade). Our hypothesis is that residues charged on the ECLs might establish interaction with the N-terminus of the CK to avoid the inception in the intra-helix pocket. We cannot focus on the model just after docking, because we need to study the MD simulation to understand how the residue may interact with CXCL12 N-terminus. BRET and HTRF studies with tagged CXCR7/ACKR3 mutants will also permit to characterize more details on the altered G-protein and MAP-kinase signaling pathways. We showed that the subtle local changes that occur within the binding pocket of the CXCR4 receptor in the course of its transitions from the inactive to the activated states can be successfully modeled. Our approach based on induced-fit docking methods that consider the flexibility of both the ligand and the receptor applied in tandem with statistical linear discriminant analysis can be reproduced on CXCR7/ACKR3-CXCL12 model.

Beyond virtual screenings, modeled structures can also be directly applied to the design of novel ligands endowed with enhanced binding affinities for specific domains. In addition to the advances in GPCR crystallography and modeling, these drug design efforts are also supported by recent theoretical developments that enabled a detailed estimation of the physicochemical aspects underlying ligand binding, including the thermodynamic consequences of the displacement of specific water molecules.

1.3 Conclusions

The recent boom of GPCR crystallography is profoundly revolutionizing the pharmaceutical research concerned with these highly druggable targets. Importantly, besides providing direct drug discovery platforms, crystal structures provide also templates for the construction of homology models.

Currently, crystal structures are available only for receptors belonging to class A, which is the largest family of GPCRs, thus making the modeling of the members of the other families still very challenging. The disclosure of the structure of receptors outside class A will substantially increase our structural understanding of this variegated superfamily and, consequently, expand the horizon of homology modeling. The determination of the binding mode of GPCR modulators, through docking experiments that target crystal structures or homology models, is a very challenging aspect of GPCR modeling.

Importantly, a skilled use of state-of-the-art modeling tools in tandem with the application of constraints derived from experimental site-directed mutagenesis data are crucial aspects for the success of these modeling exercises and for the determination of accurate receptor–ligand complexes applicable to drug discovery. As crystal structures and accurate models of GPCRs in complex with their modulators are proving to be effective tools for rational structure-based drug discovery campaigns, we expect to see a growing number of GPCR modulators discovered through computer-aided techniques in the coming year, with substantial beneficial consequences for the pharmaceutical sector and human health.

Based on observations as to the role of CXCR7/ACKR3 in progression and metastasis of several tumor types, therapies to block the receptor have been developed. Some small molecular inhibitors, siRNA, and blocking antibodies are already employed in experimental models *in vitro* and *in vivo* (Hartmann, Grabovsky et al. 2008). Yet the ability of CXCL12 to activate CXCR7 as well as CXCR4, raises some doubts as to whether the “selective blockage” of CXCR4 by T140 or AMD3100 without simultaneous blocking of CXCR7 will be effective. In fact, blockage of CXCR4 only partially inhibited responsiveness of tumor cells to CXCL12 gradients in several animal models.

The development of a number of potent inhibitors of the CXCL12-CXCR4-CXCR7/ACKR3 axis, which have low toxicity, has opened the possibilities that investigations aimed at disrupting this axis will have therapeutic benefit. While most studies are still in their infancy, there is great hope that agents that modulate the CXCL12/CXCR4 or CXCL12/CXCR7/ACKR3 axis will be useful in clinics. Importantly, the use of CXCR4/CXCL12 inhibitors in the treatment of cancer has produced some encouraging preclinical data. However, to be truly effective, a greater understanding of the role of CXCL12 and CXCR4 or CXCR7/ACKR3 in tumorigenesis and their other functions is required, as well as a greater knowledge of molecular determinant for this axis.

II – Nanobodies

II.1 Characterization of NB against CXCR4

We described three NBs for their different modulation of CXCR4 signaling and functions. Our studies showed differential antagonist and agonist effects of these nanobodies on CXCR4 G-protein and β -arrestin signaling cascades thus qualifying them as novel tools to study CXCR4 biology.

We identified the NB1 as being a competitive CXCR4 antagonists, like other NBs already described in literature, binding to the same “binding” site as CXCL12 (the activating intra helix one), as shown in docking analysis of receptor:NB interaction models. The competitive blocking of CXCR4 by this VHH-based immunoglobulin single variable domains, to our knowledge, has not been described for conventional antibodies like 12G5, possibly as a result of allosteric and/or receptor state-dependent binding of conventional surface-binding antibodies to CXCR4 (Baribaud, Edwards et al. 2001). The small-molecule CXCR4 ligand AMD3100 also fully inhibiting CXCL12 binding, interacts to well characterized sites within this cavernous binding pocket of CXCR4 within the TM helices and the ECL2 (Wong et al 2008).

Protein-protein docking showed that the identified nanobodies in this study bind to the activation domain (NB1) or to distinct but not overlapping sites in CXCR4 ECL2 (NB2 and NB3). In contrast to the nanobodies targeting CXCR4 reported so far that are highly selective for the human receptor, we found that the three clones nanobodies cross reacted with the murine form, a property which makes them important biological tool, indicating the conservation of important ECL residues between the human and murine CXCR4 receptors.

II.2 NBs applications

Studying the three NBs clones against CXCR4 identified three different mechanisms of modulating CXCL12/CXCR4 signaling pathways providing these new tools with differential potential applications for future uses.

We can consider NB1 like most of other nanobodies reported so far against most GPCRs. This behavior as a competitive antagonist, like other therapeutic molecules used against GPCRs, can be used as a new testing neutral antagonist targeting this pathway.

Since NB2 affects CXCR4 conformation, blocking the receptor in a structural complex that lost the capability to activate pathways downstream the interaction with CXCL12, this effect fits with the structural nanobodies characteristics.

We can prospect for this tool the application in the CXCR4 crystalisation, for example, because not only we have a stable conformation with the receptor, but the receptor can still interact with the CK in its inactive state.

NB3 is the most unusual nanobody because of its biased pharmacological activity in MAP-kinase pathway and even more for its capability to synergize with the CK to improve migration. If we suppose that the active state of CXCR4 is improved upon interaction with NB3 and with CXCL12, we can still imagine a structural application (as the opposite of NB2), in this case the crystal derived might elucidate the active state conformation and, moreover, with or without the CK we might separate a conformation biased on β -arrestin2 activation.

The other peculiar characteristic of these three NBs is the possibility to interact with the murine receptor. NBs antagonists for CXCR4 known in literature and interacting with the ECL2 are no more active on the murine receptor, so their applications are limited.

In microscope and imaging approaches the NBs we described that recognize the murine receptor can find applications as optical tools. We already generated tagged forms of allosteric NBs with HTRF-compatible marker molecules (ie. Tb-cryptate and D2 acceptor) and our short-term perspectives are to study the CXCR4 live-internalization and the oligomerization in native conditions. This application can be imagined also on murine tissues.

II.3 Conclusions

In view of their high affinity and selectivity, GPCR-targeting NBs may serve as excellent tools as diagnostics and, potentially, as therapeutics. With advances in microscope and imaging technologies, GPCR-targeting NBs may be ideal to monitor GPCR expression at high resolution and in vivo, respectively. As diagnostics and as modulators of GPCR function, GPCR-targeting NBs will serve as important tools to validate the role of GPCRs in pathology. They combine the advantages of both small molecules (e.g., cavity binding, low production costs) and mAb(e.g., high affinity and specificity). Through engineering methods, NBs can be

formatted to increase their potencies, target multiple GPCRs (distinct or homo/heterodimers), or tailor their half-life, broadening their applicability as therapeutics for both acute and chronic treatments. Hence, the emergence of this novel class of antibodies as high-quality research tools, diagnostics, and therapeutics is likely to herald exciting advancements in GPCR research.

References

References

Abskharon, R. N., G. Giachin, A. Wohlkönig, S. H. Soror, E. Pardon, G. Legname and J. Steyaert (2014). "Probing the N-terminal beta-sheet conversion in the crystal structure of the human prion protein bound to a nanobody." *J Am Chem Soc* 136(3): 937-944.

Acharya, P., T. S. Luongo, I. S. Georgiev, J. Matz, S. D. Schmidt, M. K. Louder, P. Kessler, Y. Yang, K. McKee, S. O'Dell, L. Chen, D. Baty, P. Chames, L. Martin, J. R. Mascola and P. D. Kwong (2013). "Heavy chain-only IgG2b llama antibody effects near-pan HIV-1 neutralization by recognizing a CD4-induced epitope that includes elements of coreceptor- and CD4-binding sites." *J Virol* 87(18): 10173-10181.

Aggarwal, S. R. (2012). "What's fueling the biotech engine-2011 to 2012." *Nat Biotechnol* 30(12): 1191-1197.

Albizu, L., M. Cottet, M. Kralikova, S. Stoev, R. Seyer, I. Brabet, T. Roux, H. Bazin, E. Bourrier, L. Lamarque, C. Breton, M. L. Rives, A. Newman, J. Javitch, E. Trinquet, M. Manning, J. P. Pin, B. Mouillac and T. Durroux (2010). "Time-resolved FRET between GPCR ligands reveals oligomers in native tissues." *Nat Chem Biol* 6(8): 587-594.

Ali, S., G. O'Boyle, P. Mellor and J. A. Kirby (2007). "An apparent paradox: chemokine receptor agonists can be used for anti-inflammatory therapy." *Mol Immunol* 44(7): 1477-1482.

Ali, S., H. Robertson, J. H. Wain, J. D. Isaacs, G. Malik and J. A. Kirby (2005). "A non-glycosaminoglycan-binding variant of CC chemokine ligand 7 (monocyte chemoattractant protein-3) antagonizes chemokine-mediated inflammation." *J Immunol* 175(2): 1257-1266.

Allen, S. J., S. E. Crown and T. M. Handel (2007). "Chemokine: receptor structure, interactions, and antagonism." *Annu Rev Immunol* 25: 787-820.

Angers, S., A. Salahpour, E. Joly, S. Hilairret, D. Chelsky, M. Dennis and M. Bouvier (2000). "Detection of beta 2-adrenergic receptor dimerization in living cells using bioluminescence resonance energy transfer (BRET)." *Proc Natl Acad Sci U S A* 97(7): 3684-3689.

- Arbabi Ghahroudi, M., A. Desmyter, L. Wyns, R. Hamers and S. Muyldermans (1997). "Selection and identification of single domain antibody fragments from camel heavy-chain antibodies." *FEBS Lett* 414(3): 521-526.
- Arnatt, C. K. and Y. Zhang (2013). "G Protein-Coupled Estrogen Receptor (GPER) Agonist Dual Binding Mode Analyses toward Understanding of its Activation Mechanism: A Comparative Homology Modeling Approach." *Mol Inform* 32(7): 647-658.
- Bachelierie, F., A. Ben-Baruch, A. M. Burkhardt, C. Combadiere, J. M. Farber, G. J. Graham, R. Horuk, A. H. Sparre-Ulrich, M. Locati, A. D. Luster, A. Mantovani, K. Matsushima, P. M. Murphy, R. Nibbs, H. Nomiyama, C. A. Power, A. E. Proudfoot, M. M. Rosenkilde, A. Rot, S. Sozzani, M. Thelen, O. Yoshie and A. Zlotnik (2014). "International Union of Basic and Clinical Pharmacology. [corrected]. LXXXIX. Update on the extended family of chemokine receptors and introducing a new nomenclature for atypical chemokine receptors." *Pharmacol Rev* 66(1): 1-79.
- Bai, M. (2004). "Dimerization of G-protein-coupled receptors: roles in signal transduction." *Cell Signal* 16(2): 175-186.
- Balabanian, K., B. Lagane, S. Infantino, K. Y. Chow, J. Harriague, B. Moepps, F. Arenzana-Seisdedos, M. Thelen and F. Bachelierie (2005). "The chemokine SDF-1/CXCL12 binds to and signals through the orphan receptor RDC1 in T lymphocytes." *J Biol Chem* 280(42): 35760-35766.
- Balabanian, K., B. Lagane, J. L. Pablos, L. Laurent, T. Planchenault, O. Verola, C. Lebbe, D. Kerob, A. Dupuy, O. Hermine, J. F. Nicolas, V. Latger-Cannard, D. Bensoussan, P. Bordigoni, F. Baleux, F. Le Deist, J. L. Virelizier, F. Arenzana-Seisdedos and F. Bachelierie (2005). "WHIM syndromes with different genetic anomalies are accounted for by impaired CXCR4 desensitization to CXCL12." *Blood* 105(6): 2449-2457.
- Baribaud, F., T. G. Edwards, M. Sharron, A. BreLOT, N. Heveker, K. Price, F. Mortari, M. Alizon, M. Tsang and R. W. Doms (2001). "Antigenically distinct conformations of CXCR4." *J Virol* 75(19): 8957-8967.

Barington, L., P. C. Rummel, M. Luckmann, H. Pihl, O. Larsen, V. Daugvilaite, A. H. Johnsen, T. M. Frimurer, S. Karlshoj and M. M. Rosenkilde (2016). "Role of Conserved Disulfide Bridges and Aromatic Residues in Extracellular Loop 2 of Chemokine Receptor CCR8 for Chemokine and Small Molecule Binding." *J Biol Chem*.

Beall, C. J., S. Mahajan, D. E. Kuhn and P. E. Kolattukudy (1996). "Site-directed mutagenesis of monocyte chemoattractant protein-1 identifies two regions of the polypeptide essential for biological activity." *Biochem J* 313 (Pt 2): 633-640.

Beuming, T. and W. Sherman (2012). "Current assessment of docking into GPCR crystal structures and homology models: successes, challenges, and guidelines." *J Chem Inf Model* 52(12): 3263-3277.

Blanchet, X., M. Langer, C. Weber, R. R. Koenen and P. von Hundelshausen (2012). "Touch of chemokines." *Front Immunol* 3: 175.

Blanchetot, C., D. Verzijl, A. Mujic-Delic, L. Bosch, L. Rem, R. Leurs, C. T. Verrips, M. Saunders, H. de Haard and M. J. Smit (2013). "Neutralizing nanobodies targeting diverse chemokines effectively inhibit chemokine function." *J Biol Chem* 288(35): 25173-25182.

Blanpain, C., B. J. Doranz, A. Bondue, C. Govaerts, A. De Leener, G. Vassart, R. W. Doms, A. Proudfoot and M. Parmentier (2003). "The core domain of chemokines binds CCR5 extracellular domains while their amino terminus interacts with the transmembrane helix bundle." *J Biol Chem* 278(7): 5179-5187.

Blaszczyk, J., E. V. Coillie, P. Proost, J. V. Damme, G. Opendakker, G. D. Bujacz, J. M. Wang and X. Ji (2000). "Complete crystal structure of monocyte chemotactic protein-2, a CC chemokine that interacts with multiple receptors." *Biochemistry* 39(46): 14075-14081.

Boldajipour, B., H. Mahabaleshwar, E. Kardash, M. Reichman-Fried, H. Blaser, S. Minina, D. Wilson, Q. Xu and E. Raz (2008). "Control of chemokine-guided cell migration by ligand sequestration." *Cell* 132(3): 463-473.

- Bonecchi, R., E. Galliera, E. M. Borroni, M. M. Corsi, M. Locati and A. Mantovani (2009). "Chemokines and chemokine receptors: an overview." *Front Biosci (Landmark Ed)* 14: 540-551.
- Bouchard, H., C. Viskov and C. Garcia-Echeverria (2014). "Antibody-drug conjugates-a new wave of cancer drugs." *Bioorg Med Chem Lett* 24(23): 5357-5363.
- Brelot, A., N. Heveker, M. Montes and M. Alizon (2000). "Identification of residues of CXCR4 critical for human immunodeficiency virus coreceptor and chemokine receptor activities." *J Biol Chem* 275(31): 23736-23744.
- Brown, Z., M. E. Gerritsen, W. W. Carley, R. M. Strieter, S. L. Kunkel and J. Westwick (1994). "Chemokine gene expression and secretion by cytokine-activated human microvascular endothelial cells. Differential regulation of monocyte chemoattractant protein-1 and interleukin-8 in response to interferon-gamma." *Am J Pathol* 145(4): 913-921.
- Burns, J. M., B. C. Summers, Y. Wang, A. Melikian, R. Berahovich, Z. Miao, M. E. Penfold, M. J. Sunshine, D. R. Littman, C. J. Kuo, K. Wei, B. E. McMaster, K. Wright, M. C. Howard and T. J. Schall (2006). "A novel chemokine receptor for SDF-1 and I-TAC involved in cell survival, cell adhesion, and tumor development." *J Exp Med* 203(9): 2201-2213.
- Busillo, J. M. and J. L. Benovic (2007). "Regulation of CXCR4 signaling." *Biochim Biophys Acta* 1768(4): 952-963.
- Calebiro, D., V. O. Nikolaev and M. J. Lohse (2010). "Imaging of persistent cAMP signaling by internalized G protein-coupled receptors." *J Mol Endocrinol* 45(1): 1-8.
- Cardin, A. D. and H. J. Weintraub (1989). "Molecular modeling of protein-glycosaminoglycan interactions." *Arteriosclerosis* 9(1): 21-32.
- Casi, G. and D. Neri (2012). "Antibody-drug conjugates: basic concepts, examples and future perspectives." *J Control Release* 161(2): 422-428.

- Chabot, D. J., P. F. Zhang, G. V. Quinnan and C. C. Broder (1999). "Mutagenesis of CXCR4 identifies important domains for human immunodeficiency virus type 1 X4 isolate envelope-mediated membrane fusion and virus entry and reveals cryptic coreceptor activity for R5 isolates." *J Virol* 73(8): 6598-6609.
- Chow, K. Y., E. Brotin, Y. Ben Khalifa, L. Carthagen, S. Teissier, A. Danckaert, J. L. Galzi, F. Arenzana-Seisdedos, F. Thierry and F. Bachelier (2010). "A pivotal role for CXCL12 signaling in HPV-mediated transformation of keratinocytes: clues to understanding HPV-pathogenesis in WHIM syndrome." *Cell Host Microbe* 8(6): 523-533.
- Cinamon, G., V. Shinder and R. Alon (2001). "Shear forces promote lymphocyte migration across vascular endothelium bearing apical chemokines." *Nat Immunol* 2(6): 515-522.
- Clackson, T. and J. A. Wells (1995). "A hot spot of binding energy in a hormone-receptor interface." *Science* 267(5196): 383-386.
- Clark-Lewis, I., K. S. Kim, K. Rajarathnam, J. H. Gong, B. Dewald, B. Moser, M. Baggiolini and B. D. Sykes (1995). "Structure-activity relationships of chemokines." *J Leukoc Biol* 57(5): 703-711.
- Clark-Lewis, I., C. Schumacher, M. Baggiolini and B. Moser (1991). "Structure-activity relationships of interleukin-8 determined using chemically synthesized analogs. Critical role of NH₂-terminal residues and evidence for uncoupling of neutrophil chemotaxis, exocytosis, and receptor binding activities." *J Biol Chem* 266(34): 23128-23134.
- Clore, G. M., E. Appella, M. Yamada, K. Matsushima and A. M. Gronenborn (1990). "Three-dimensional structure of interleukin 8 in solution." *Biochemistry* 29(7): 1689-1696.
- Comerford, I. and R. J. Nibbs (2005). "Post-translational control of chemokines: a role for decoy receptors?" *Immunol Lett* 96(2): 163-174.

- Conrath, K. E., U. Wernery, S. Muyldermans and V. K. Nguyen (2003). "Emergence and evolution of functional heavy-chain antibodies in Camelidae." *Dev Comp Immunol* 27(2): 87-103.
- Costanzi, S. (2012). "Homology modeling of class a G protein-coupled receptors." *Methods Mol Biol* 857: 259-279.
- Cottet, M., L. Albizu, S. Perkowska, F. Jean-Alphonse, R. Rahmeh, H. Orcel, C. Mejean, S. Granier, C. Mendre, B. Mouillac and T. Durroux (2010). "Past, present and future of vasopressin and oxytocin receptor oligomers, prototypical GPCR models to study dimerization processes." *Curr Opin Pharmacol* 10(1): 59-66.
- Cottet, M., O. Faklaris, D. Maurel, P. Scholler, E. Doumazane, E. Trinquet, J. P. Pin and T. Durroux (2012). "BRET and Time-resolved FRET strategy to study GPCR oligomerization: from cell lines toward native tissues." *Front Endocrinol (Lausanne)* 3: 92.
- Couturier, C. and B. Deprez (2012). "Setting Up a Bioluminescence Resonance Energy Transfer High throughput Screening Assay to Search for Protein/Protein Interaction Inhibitors in Mammalian Cells." *Front Endocrinol (Lausanne)* 3: 100.
- Crump, M. P., J. H. Gong, P. Loetscher, K. Rajarathnam, A. Amara, F. Arenzana-Seisdedos, J. L. Virelizier, M. Baggiolini, B. D. Sykes and I. Clark-Lewis (1997). "Solution structure and basis for functional activity of stromal cell-derived factor-1; dissociation of CXCR4 activation from binding and inhibition of HIV-1." *EMBO J* 16(23): 6996-7007.
- Crump, M. P., K. Rajarathnam, K. S. Kim, I. Clark-Lewis and B. D. Sykes (1998). "Solution structure of eotaxin, a chemokine that selectively recruits eosinophils in allergic inflammation." *J Biol Chem* 273(35): 22471-22479.
- Dambly-Chaudiere, C., N. Cubedo and A. Ghysen (2007). "Control of cell migration in the development of the posterior lateral line: antagonistic interactions between the chemokine receptors CXCR4 and CXCR7/RDC1." *BMC Dev Biol* 7: 23.

- De Buck, S., V. Viridi, T. De Meyer, K. De Wilde, R. Piron, J. Nolf, E. Van Lerberge, A. De Paepe and A. Depicker (2012). "Production of camel-like antibodies in plants." *Methods Mol Biol* 911: 305-324.
- de Haas, A. H., H. R. van Weering, E. K. de Jong, H. W. Boddeke and K. P. Biber (2007). "Neuronal chemokines: versatile messengers in central nervous system cell interaction." *Mol Neurobiol* 36(2): 137-151.
- Decailot, F. M., M. A. Kazmi, Y. Lin, S. Ray-Saha, T. P. Sakmar and P. Sachdev (2011). "CXCR7/CXCR4 heterodimer constitutively recruits beta-arrestin to enhance cell migration." *J Biol Chem* 286(37): 32188-32197.
- Desmyter, A., C. Farenc, J. Mahony, S. Spinelli, C. Bebeacua, S. Blangy, D. Veessler, D. van Sinderen and C. Cambillau (2013). "Viral infection modulation and neutralization by camelid nanobodies." *Proc Natl Acad Sci U S A* 110(15): E1371-1379.
- Desmyter, A., T. R. Transue, M. A. Ghahroudi, M. H. Thi, F. Poortmans, R. Hamers, S. Muyldermans and L. Wyns (1996). "Crystal structure of a camel single-domain VH antibody fragment in complex with lysozyme." *Nat Struct Biol* 3(9): 803-811.
- Deuel, T. F., P. S. Keim, M. Farmer and R. L. Heinrikson (1977). "Amino acid sequence of human platelet factor 4." *Proc Natl Acad Sci U S A* 74(6): 2256-2258.
- Dias, J. M., C. Losberger, M. Deruaz, C. A. Power, A. E. Proudfoot and J. P. Shaw (2009). "Structural basis of chemokine sequestration by a tick chemokine binding protein: the crystal structure of the complex between Evasin-1 and CCL3." *PLoS One* 4(12): e8514.
- Doranz, B. J., L. G. Fillion, F. Diaz-Mitoma, D. S. Sitar, J. Sahai, F. Baribaud, M. J. Orsini, J. L. Benovic, W. Cameron and R. W. Doms (2001). "Safe use of the CXCR4 inhibitor ALX40-4C in humans." *AIDS Res Hum Retroviruses* 17(6): 475-486.

Doranz, B. J., M. J. Orsini, J. D. Turner, T. L. Hoffman, J. F. Berson, J. A. Hoxie, S. C. Peiper, L. F. Brass and R. W. Doms (1999). "Identification of CXCR4 domains that support coreceptor and chemokine receptor functions." *J Virol* 73(4): 2752-2761.

Drake, M. T., J. D. Violin, E. J. Whalen, J. W. Wisler, S. K. Shenoy and R. J. Lefkowitz (2008). "beta-arrestin-biased agonism at the beta2-adrenergic receptor." *J Biol Chem* 283(9): 5669-5676.

Dror, R. O., D. H. Arlow, D. W. Borhani, M. O. Jensen, S. Piana and D. E. Shaw (2009). "Identification of two distinct inactive conformations of the beta2-adrenergic receptor reconciles structural and biochemical observations." *Proc Natl Acad Sci U S A* 106(12): 4689-4694.

Dror, R. O., D. H. Arlow, P. Maragakis, T. J. Mildorf, A. C. Pan, H. Xu, D. W. Borhani and D. E. Shaw (2011). "Activation mechanism of the beta2-adrenergic receptor." *Proc Natl Acad Sci U S A* 108(46): 18684-18689.

Dubel, S. (2007). "Recombinant therapeutic antibodies." *Appl Microbiol Biotechnol* 74(4): 723-729.

Dumoulin, M., K. Conrath, A. Van Meirhaeghe, F. Meersman, K. Heremans, L. G. Frenken, S. Muyldermans, L. Wyns and A. Matagne (2002). "Single-domain antibody fragments with high conformational stability." *Protein Sci* 11(3): 500-515.

Eigenbrot, C., H. B. Lowman, L. Chee and D. R. Artis (1997). "Structural change and receptor binding in a chemokine mutant with a rearranged disulfide: X-ray structure of E38C/C50AIL-8 at 2 Å resolution." *Proteins* 27(4): 556-566.

El-Hage, N., S. M. Dever, E. M. Podhaizer, C. K. Arnatt, Y. Zhang and K. F. Hauser (2013). "A novel bivalent HIV-1 entry inhibitor reveals fundamental differences in CCR5-mu-opioid receptor interactions between human astroglia and microglia." *AIDS* 27(14): 2181-2190.

Faklaris, O., M. Cottet, A. Falco, B. Villier, M. Laget, J. M. Zwier, E. Trinquet, B. Mouillac, J. P. Pin and T. Durroux (2015). "Multicolor time-resolved Forster resonance energy transfer microscopy reveals the impact of GPCR oligomerization on internalization processes." *FASEB J* 29(6): 2235-2246.

Fanelli, F. and P. G. De Benedetti (2011). "Update 1 of: computational modeling approaches to structure-function analysis of G protein-coupled receptors." *Chem Rev* 111(12): PR438-535.

Farzan, M., G. J. Babcock, N. Vasilieva, P. L. Wright, E. Kiprilov, T. Mirzabekov and H. Choe (2002). "The role of post-translational modifications of the CXCR4 amino terminus in stromal-derived factor 1 alpha association and HIV-1 entry." *J Biol Chem* 277(33): 29484-29489.

Farzan, M., T. Mirzabekov, P. Kolchinsky, R. Wyatt, M. Cayabyab, N. P. Gerard, C. Gerard, J. Sodroski and H. Choe (1999). "Tyrosine sulfation of the amino terminus of CCR5 facilitates HIV-1 entry." *Cell* 96(5): 667-676.

Fernandez, E. J. and E. Lolis (2002). "Structure, function, and inhibition of chemokines." *Annu Rev Pharmacol Toxicol* 42: 469-499.

Ferre, S., V. Casado, L. A. Devi, M. Filizola, R. Jockers, M. J. Lohse, G. Milligan, J. P. Pin and X. Guitart (2014). "G protein-coupled receptor oligomerization revisited: functional and pharmacological perspectives." *Pharmacol Rev* 66(2): 413-434.

Fotiadis, D., Y. Liang, S. Filipek, D. A. Saperstein, A. Engel and K. Palczewski (2003). "Atomic-force microscopy: Rhodopsin dimers in native disc membranes." *Nature* 421(6919): 127-128.

Fra, A. M., M. Locati, K. Otero, M. Sironi, P. Signorelli, M. L. Massardi, M. Gobbi, A. Vecchi, S. Sozzani and A. Mantovani (2003). "Cutting edge: scavenging of inflammatory CC chemokines by the promiscuous putatively silent chemokine receptor D6." *J Immunol* 170(5): 2279-2282.

Fredriksson, R., M. C. Lagerstrom, L. G. Lundin and H. B. Schioth (2003). "The G-protein-coupled receptors in the human genome form five main families. Phylogenetic analysis, paralogon groups, and fingerprints." *Mol Pharmacol* 63(6): 1256-1272.

Frenken, L. G., R. H. van der Linden, P. W. Hermans, J. W. Bos, R. C. Ruuls, B. de Geus and C. T. Verrips (2000). "Isolation of antigen specific llama VHH antibody fragments and their high level secretion by *Saccharomyces cerevisiae*." *J Biotechnol* 78(1): 11-21.

George, S. R., T. Fan, Z. Xie, R. Tse, V. Tam, G. Varghese and B. F. O'Dowd (2000). "Oligomerization of mu- and delta-opioid receptors. Generation of novel functional properties." *J Biol Chem* 275(34): 26128-26135.

George, S. R., B. F. O'Dowd and S. P. Lee (2002). "G-protein-coupled receptor oligomerization and its potential for drug discovery." *Nat Rev Drug Discov* 1(10): 808-820.

Gerlach, L. O., R. T. Skerlj, G. J. Bridger and T. W. Schwartz (2001). "Molecular interactions of cyclam and bicyclam non-peptide antagonists with the CXCR4 chemokine receptor." *J Biol Chem* 276(17): 14153-14160.

Gerrits, H., D. S. van Ingen Schenau, N. E. Bakker, A. J. van Disseldorp, A. Strik, L. S. Hermens, T. B. Koenen, M. A. Krajnc-Franken and J. A. Gossen (2008). "Early postnatal lethality and cardiovascular defects in CXCR7-deficient mice." *Genesis* 46(5): 235-245.

Goldfeld, D. A., K. Zhu, T. Beuming and R. A. Friesner (2011). "Successful prediction of the intra- and extracellular loops of four G-protein-coupled receptors." *Proc Natl Acad Sci U S A* 108(20): 8275-8280.

Gorinski, N., N. Kowalsman, U. Renner, A. Wirth, M. T. Reinartz, R. Seifert, A. Zeug, E. Ponimaskin and M. Y. Niv (2012). "Computational and experimental analysis of the transmembrane domain 4/5 dimerization interface of the serotonin 5-HT(1A) receptor." *Mol Pharmacol* 82(3): 448-463.

Gosling, J., D. J. Dairaghi, Y. Wang, M. Hanley, D. Talbot, Z. Miao and T. J. Schall (2000). "Cutting edge: identification of a novel chemokine receptor that binds dendritic cell- and T cell-active chemokines including ELC, SLC, and TECK." *J Immunol* 164(6): 2851-2856.

Gouldson, P. R., C. Higgs, R. E. Smith, M. K. Dean, G. V. Gkoutos and C. A. Reynolds (2000). "Dimerization and domain swapping in G-protein-coupled receptors: a computational study." *Neuropsychopharmacology* 23(4 Suppl): S60-77.

Govaert, J., M. Pellis, N. Deschacht, C. Vincke, K. Conrath, S. Muyldermans and D. Saerens (2012). "Dual beneficial effect of interloop disulfide bond for single domain antibody fragments." *J Biol Chem* 287(3): 1970-1979.

Greenberg, A. S., D. Avila, M. Hughes, A. Hughes, E. C. McKinney and M. F. Flajnik (1995). "A new antigen receptor gene family that undergoes rearrangement and extensive somatic diversification in sharks." *Nature* 374(6518): 168-173.

Habib, I., D. Smolarek, C. Hattab, M. Grodecka, G. Hassanzadeh-Ghassabeh, S. Muyldermans, S. Sagan, C. Gutierrez, S. Laperche, C. Le-Van-Kim, Y. C. Aronovicz, K. Wasniowska, S. Gangnard and O. Bertrand (2013). "V(H)H (nanobody) directed against human glycoporphin A: a tool for autologous red cell agglutination assays." *Anal Biochem* 438(1): 82-89.

Hamel, D. J., I. Sielaff, A. E. Proudfoot and T. M. Handel (2009). "Chapter 4. Interactions of chemokines with glycosaminoglycans." *Methods Enzymol* 461: 71-102.

Hamers-Casterman, C., T. Atarhouch, S. Muyldermans, G. Robinson, C. Hamers, E. B. Songa, N. Bendahman and R. Hamers (1993). "Naturally occurring antibodies devoid of light chains." *Nature* 363(6428): 446-448.

Harris, H. (1953). "Chemotaxis of granulocytes." *J Pathol Bacteriol* 66(1): 135-146.

Harris, H. (1953). "Chemotaxis of monocytes." *Br J Exp Pathol* 34(3): 276-279.

Harris, L. J., E. Skaletsky and A. McPherson (1998). "Crystallographic structure of an intact IgG1 monoclonal antibody." *J Mol Biol* 275(5): 861-872.

Hartmann, T. N., V. Grabovsky, R. Pasvolsky, Z. Shulman, E. C. Buss, A. Spiegel, A. Nagler, T. Lapidot, M. Thelen and R. Alon (2008). "A crosstalk between intracellular CXCR7 and CXCR4 involved in rapid CXCL12-triggered integrin activation but not in chemokine-triggered motility of human T lymphocytes and CD34+ cells." *J Leukoc Biol* 84(4): 1130-1140.

Hassaine, G., C. Deluz, L. Grasso, R. Wyss, M. B. Tol, R. Hovius, A. Graff, H. Stahlberg, T. Tomizaki, A. Desmyter, C. Moreau, X. D. Li, F. Poitevin, H. Vogel and H. Nury (2014). "X-ray structure of the mouse serotonin 5-HT₃ receptor." *Nature* 512(7514): 276-281.

Hebert, T. E., S. Moffett, J. P. Morello, T. P. Loisel, D. G. Bichet, C. Barret and M. Bouvier (1996). "A peptide derived from a beta2-adrenergic receptor transmembrane domain inhibits both receptor dimerization and activation." *J Biol Chem* 271(27): 16384-16392.

Heesen, M., M. A. Berman, A. Charest, D. Housman, C. Gerard and M. E. Dorf (1998). "Cloning and chromosomal mapping of an orphan chemokine receptor: mouse RDC1." *Immunogenetics* 47(5): 364-370.

Hemmerich, S., C. Paavola, A. Bloom, S. Bhakta, R. Freedman, D. Grunberger, J. Krstenansky, S. Lee, D. McCarley, M. Mulkins, B. Wong, J. Pease, L. Mizoue, T. Mirzadegan, I. Polsky, K. Thompson, T. M. Handel and K. Jarnagin (1999). "Identification of residues in the monocyte chemotactic protein-1 that contact the MCP-1 receptor, CCR2." *Biochemistry* 38(40): 13013-13025.

Heveker, N., M. Montes, L. Germeroth, A. Amara, A. Trautmann, M. Alizon and J. Schneider-Mergener (1998). "Dissociation of the signalling and antiviral properties of SDF-1-derived small peptides." *Curr Biol* 8(7): 369-376.

Hoogewerf, A. J., G. S. Kuschert, A. E. Proudfoot, F. Borlat, I. Clark-Lewis, C. A. Power and T. N. Wells (1997). "Glycosaminoglycans mediate cell surface oligomerization of chemokines." *Biochemistry* 36(44): 13570-13578.

Hounsou, C., J. F. Margathe, N. Oueslati, A. Belhocine, E. Dupuis, C. Thomas, A. Mann, B. Ilien, D. Rognan, E. Trinquet, M. Hibert, J. P. Pin, D. Bonnet and T. Durroux (2015). "Time-resolved FRET binding assay to investigate hetero-oligomer binding properties: proof of concept with dopamine D1/D3 heterodimer." *ACS Chem Biol* 10(2): 466-474.

Huang, L., L. O. Gainkam, V. Caveliers, C. Vanhove, M. Keyaerts, P. De Baetselier, A. Bossuyt, H. Revets and T. Lahoutte (2008). "SPECT imaging with ^{99m}Tc-labeled EGFR-specific nanobody for in vivo monitoring of EGFR expression." *Mol Imaging Biol* 10(3): 167-175.

Huehls, A. M., T. A. Coupet and C. L. Sentman (2015). "Bispecific T-cell engagers for cancer immunotherapy." *Immunol Cell Biol* 93(3): 290-296.

Humpert, M. L., M. Tzouros, S. Thelen, A. Bignon, A. Levoye, F. Arenzana-Seisdedos, K. Balabanian, F. Bachelerie, H. Langen and M. Thelen (2012). "Complementary methods provide evidence for the expression of CXCR7 on human B cells." *Proteomics* 12(12): 1938-1948.

Infantino, S., B. Moepps and M. Thelen (2006). "Expression and regulation of the orphan receptor RDC1 and its putative ligand in human dendritic and B cells." *J Immunol* 176(4): 2197-2207.

Irannejad, R., J. C. Tomshine, J. R. Tomshine, M. Chevalier, J. P. Mahoney, J. Steyaert, S. G. Rasmussen, R. K. Sunahara, H. El-Samad, B. Huang and M. von Zastrow (2013). "Conformational biosensors reveal GPCR signalling from endosomes." *Nature* 495(7442): 534-538.

Jaakola, V. P., M. T. Griffith, M. A. Hanson, V. Cherezov, E. Y. Chien, J. R. Lane, A. P. Ijzerman and R. C. Stevens (2008). "The 2.6 angstrom crystal structure of a human A2A adenosine receptor bound to an antagonist." *Science* 322(5905): 1211-1217.

Jacobson, K. A. and S. Costanzi (2012). "New insights for drug design from the X-ray crystallographic structures of G-protein-coupled receptors." *Mol Pharmacol* 82(3): 361-371.

Jacobson, K. A., Z. G. Gao and B. T. Liang (2007). "Neoreceptors: reengineering GPCRs to recognize tailored ligands." *Trends Pharmacol Sci* 28(3): 111-116.

Jahnichen, S., C. Blanchetot, D. Maussang, M. Gonzalez-Pajuelo, K. Y. Chow, L. Bosch, S. De Vrieze, B. Serruys, H. Ulrichs, W. Vandeveldel, M. Saunders, H. J. De Haard, D. Schols, R. Leurs, P. Vanlandschoot, T. Verrips and M. J. Smit (2010). "CXCR4 nanobodies (VHH-based single variable domains) potently inhibit chemotaxis and HIV-1 replication and mobilize stem cells." *Proc Natl Acad Sci U S A* 107(47): 20565-20570.

Kajumo, F., D. A. Thompson, Y. Guo and T. Dragic (2000). "Entry of R5X4 and X4 human immunodeficiency virus type 1 strains is mediated by negatively charged and tyrosine residues in the amino-terminal domain and the second extracellular loop of CXCR4." *Virology* 271(2): 240-247.

Kalatskaya, I., Y. A. Berchiche, S. Gravel, B. J. Limberg, J. S. Rosenbaum and N. Heveker (2009). "AMD3100 is a CXCR7 ligand with allosteric agonist properties." *Mol Pharmacol* 75(5): 1240-1247.

Keizer, D. W., M. P. Crump, T. W. Lee, C. M. Slupsky, I. Clark-Lewis and B. D. Sykes (2000). "Human CC chemokine I-309, structural consequences of the additional disulfide bond." *Biochemistry* 39(20): 6053-6059.

Klein, T. J. and M. Mlodzik (2004). "A conserved signaling cassette regulates hair patterning from *Drosophila* to man." *Proc Natl Acad Sci U S A* 101(25): 9173-9174.

Kobilka, B. K. (2007). "G protein coupled receptor structure and activation." *Biochim Biophys Acta* 1768(4): 794-807.

Koenen, R. R., P. von Hundelshausen, I. V. Nesmelova, A. Zerneck, E. A. Liehn, A. Sarabi, B. K. Kramp, A. M. Piccinini, S. R. Paludan, M. A. Kowalska, A. J. Kungl, T. M. Hackeng, K. H. Mayo and C. Weber (2009). "Disrupting functional interactions between platelet chemokines inhibits atherosclerosis in hyperlipidemic mice." *Nat Med* 15(1): 97-103.

Kofuku, Y., C. Yoshiura, T. Ueda, H. Terasawa, T. Hirai, S. Tominaga, M. Hirose, Y. Maeda, H. Takahashi, Y. Terashima, K. Matsushima and I. Shimada (2009). "Structural basis of the interaction between chemokine stromal cell-derived factor-1/CXCL12 and its G-protein-coupled receptor CXCR4." *J Biol Chem* 284(50): 35240-35250.

Kolmar, H. (2011). "Natural and engineered cystine knot miniproteins for diagnostic and therapeutic applications." *Curr Pharm Des* 17(38): 4329-4336.

Kruse, A. C., A. M. Ring, A. Manglik, J. Hu, K. Hu, K. Eitel, H. Hubner, E. Pardon, C. Valant, P. M. Sexton, A. Christopoulos, C. C. Felder, P. Gmeiner, J. Steyaert, W. I. Weis, K. C. Garcia, J. Wess and B. K. Kobilka (2013). "Activation and allosteric modulation of a muscarinic acetylcholine receptor." *Nature* 504(7478): 101-106.

Kufareva, I., B. S. Stephens, L. G. Holden, L. Qin, C. Zhao, T. Kawamura, R. Abagyan and T. M. Handel (2014). "Stoichiometry and geometry of the CXC chemokine receptor 4 complex with CXC ligand 12: molecular modeling and experimental validation." *Proc Natl Acad Sci U S A* 111(50): E5363-5372.

Kumar, R., V. Tripathi, M. Ahmad, N. Nath, R. A. Mir, S. S. Chauhan and K. Luthra (2012). "CXCR7 mediated G α independent activation of ERK and Akt promotes cell survival and chemotaxis in T cells." *Cell Immunol* 272(2): 230-241.

Kunkel, S. L. (1999). "Promiscuous chemokine receptors and their redundant ligands play an enigmatic role during HIV-1 infection." *Am J Respir Cell Mol Biol* 20(5): 859-860.

Kuo, J. H., Y. P. Chen, J. S. Liu, A. Dubrac, C. Quemener, H. Prats, A. Bikfalvi, W. G. Wu and S. C. Sue (2013). "Alternative C-terminal helix orientation alters chemokine function: structure of the anti-angiogenic chemokine, CXCL4L1." *J Biol Chem* 288(19): 13522-13533.

Kuschert, G. S., F. Coulin, C. A. Power, A. E. Proudfoot, R. E. Hubbard, A. J. Hoogewerf and T. N. Wells (1999). "Glycosaminoglycans interact selectively with chemokines and modulate receptor binding and cellular responses." *Biochemistry* 38(39): 12959-12968.

Lagane, B., K. Y. Chow, K. Balabanian, A. Levoye, J. Harriague, T. Planchenault, F. Baleux, N. Gunera-Saad, F. Arenzana-Seisdedos and F. Bachelierie (2008). "CXCR4 dimerization and beta-arrestin-mediated signaling account for the enhanced chemotaxis to CXCL12 in WHIM syndrome." *Blood* 112(1): 34-44.

Lagane, B., J. Garcia-Perez and E. Kellenberger (2013). "Modeling the allosteric modulation of CCR5 function by Maraviroc." *Drug Discov Today Technol* 10(2): e297-305.

Laguri, C., F. Arenzana-Seisdedos and H. Lortat-Jacob (2008). "Relationships between glycosaminoglycan and receptor binding sites in chemokines-the CXCL12 example." *Carbohydr Res* 343(12): 2018-2023.

Lau, E. K., C. D. Paavola, Z. Johnson, J. P. Gaudry, E. Geretti, F. Borlat, A. J. Kungl, A. E. Proudfoot and T. M. Handel (2004). "Identification of the glycosaminoglycan binding site of the CC chemokine, MCP-1: implications for structure and function in vivo." *J Biol Chem* 279(21): 22294-22305.

Laurence, J. S., C. Blanpain, J. W. Burgner, M. Parmentier and P. J. LiWang (2000). "CC chemokine MIP-1 beta can function as a monomer and depends on Phe13 for receptor binding." *Biochemistry* 39(12): 3401-3409.

Lee, B. J., U. H. Koszinowski, S. R. Sarawar and H. Adler (2003). "A gammaherpesvirus G protein-coupled receptor homologue is required for increased viral replication in response to chemokines and efficient reactivation from latency." *J Immunol* 170(1): 243-251.

- Levoye, A., K. Balabanian, F. Baleux, F. Bachelierie and B. Lagane (2009). "CXCR7 heterodimerizes with CXCR4 and regulates CXCL12-mediated G protein signaling." *Blood* 113(24): 6085-6093.
- Libert, F., M. Parmentier, A. Lefort, C. Dinsart, J. Van Sande, C. Maenhaut, M. J. Simons, J. E. Dumont and G. Vassart (1989). "Selective amplification and cloning of four new members of the G protein-coupled receptor family." *Science* 244(4904): 569-572.
- Lodi, P. J., D. S. Garrett, J. Kuszewski, M. L. Tsang, J. A. Weatherbee, W. J. Leonard, A. M. Gronenborn and G. M. Clore (1994). "High-resolution solution structure of the beta chemokine hMIP-1 beta by multidimensional NMR." *Science* 263(5154): 1762-1767.
- Loetscher, P., J. H. Gong, B. Dewald, M. Baggiolini and I. Clark-Lewis (1998). "N-terminal peptides of stromal cell-derived factor-1 with CXC chemokine receptor 4 agonist and antagonist activities." *J Biol Chem* 273(35): 22279-22283.
- Lortat-Jacob, H., A. Grosdidier and A. Imberty (2002). "Structural diversity of heparan sulfate binding domains in chemokines." *Proc Natl Acad Sci U S A* 99(3): 1229-1234.
- Lowman, H. B., P. H. Slagle, L. E. DeForge, C. M. Wirth, B. L. Gillece-Castro, J. H. Bourell and W. J. Fairbrother (1996). "Exchanging interleukin-8 and melanoma growth-stimulating activity receptor binding specificities." *J Biol Chem* 271(24): 14344-14352.
- Lu, Z., J. F. Berson, Y. Chen, J. D. Turner, T. Zhang, M. Sharron, M. H. Jenks, Z. Wang, J. Kim, J. Rucker, J. A. Hoxie, S. C. Peiper and R. W. Doms (1997). "Evolution of HIV-1 coreceptor usage through interactions with distinct CCR5 and CXCR4 domains." *Proc Natl Acad Sci U S A* 94(12): 6426-6431.
- Lubkowski, J., G. Bujacz, L. Boque, P. J. Domaille, T. M. Handel and A. Wlodawer (1997). "The structure of MCP-1 in two crystal forms provides a rare example of variable quaternary interactions." *Nat Struct Biol* 4(1): 64-69.

Luker, K., M. Gupta and G. Luker (2009). "Bioluminescent CXCL12 fusion protein for cellular studies of CXCR4 and CXCR7." *Biotechniques* 47(1): 625-632.

Luker, K. E., M. Gupta and G. D. Luker (2009). "Imaging chemokine receptor dimerization with firefly luciferase complementation." *FASEB J* 23(3): 823-834.

Luker, K. E., M. Gupta, J. M. Steele, B. R. Foerster and G. D. Luker (2009). "Imaging ligand-dependent activation of CXCR7." *Neoplasia* 11(10): 1022-1035.

Luker, K. E., J. M. Steele, L. A. Mihalko, P. Ray and G. D. Luker (2010). "Constitutive and chemokine-dependent internalization and recycling of CXCR7 in breast cancer cells to degrade chemokine ligands." *Oncogene* 29(32): 4599-4610.

Lulf, S., J. Matz, M. C. Rouyez, A. Jarviluoma, K. Saksela, S. Benichou and M. Geyer (2014). "Structural basis for the inhibition of HIV-1 Nef by a high-affinity binding single-domain antibody." *Retrovirology* 11: 24.

Luo, J., Z. Luo, N. Zhou, J. W. Hall and Z. Huang (1999). "Attachment of C-terminus of SDF-1 enhances the biological activity of its N-terminal peptide." *Biochem Biophys Res Commun* 264(1): 42-47.

Ma, X., K. Norsworthy, N. Kundu, W. H. Rodgers, P. A. Gimotty, O. Goloubeva, M. Lipsky, Y. Li, D. Holt and A. Fulton (2009). "CXCR3 expression is associated with poor survival in breast cancer and promotes metastasis in a murine model." *Mol Cancer Ther* 8(3): 490-498.

Maho, A., A. Carter, A. Bensimon, G. Vassart and M. Parmentier (1999). "Physical mapping of the CC-chemokine gene cluster on the human 17q11. 2 region." *Genomics* 59(2): 213-223.

Manglik, A., A. C. Kruse, T. S. Kobilka, F. S. Thian, J. M. Mathiesen, R. K. Sunahara, L. Pardo, W. I. Weis, B. K. Kobilka and S. Granier (2012). "Crystal structure of the micro-opioid receptor bound to a morphinan antagonist." *Nature* 485(7398): 321-326.

Mantovani, A., M. Locati, A. Vecchi, S. Sozzani and P. Allavena (2001). "Decoy receptors: a strategy to regulate inflammatory cytokines and chemokines." *Trends Immunol* 22(6): 328-336.

Marquardt, A., S. Muyldermans and M. Przybylski (2006). "A synthetic camel anti-lysozyme peptide antibody (peptibody) with flexible loop structure identified by high-resolution affinity mass spectrometry." *Chemistry* 12(7): 1915-1923.

Maurice, P., M. Kamal and R. Jockers (2011). "Asymmetry of GPCR oligomers supports their functional relevance." *Trends Pharmacol Sci* 32(9): 514-520.

Maussang, D., A. Mujic-Delic, F. J. Descamps, C. Stortelers, P. Vanlandschoot, M. Stigter-van Walsum, H. F. Vischer, M. van Roy, M. Vosjan, M. Gonzalez-Pajuelo, G. A. van Dongen, P. Merchiers, P. van Rompaey and M. J. Smit (2013). "Llama-derived single variable domains (nanobodies) directed against chemokine receptor CXCR7 reduce head and neck cancer cell growth in vivo." *J Biol Chem* 288(41): 29562-29572.

Mc, C. M. (1946). "Chemotaxis in leukocytes." *Physiol Rev* 26(3): 319-336.

Mellado, M., A. J. Vila-Coro, C. Martinez and J. M. Rodriguez-Frade (2001). "Receptor dimerization: a key step in chemokine signaling." *Cell Mol Biol (Noisy-le-grand)* 47(4): 575-582.

Miao, Z., K. E. Luker, B. C. Summers, R. Berahovich, M. S. Bhojani, A. Rehemtulla, C. G. Kleer, J. J. Essner, A. Nasevicius, G. D. Luker, M. C. Howard and T. J. Schall (2007). "CXCR7 (RDC1) promotes breast and lung tumor growth in vivo and is expressed on tumor-associated vasculature." *Proc Natl Acad Sci U S A* 104(40): 15735-15740.

Middleton, J., S. Neil, J. Wintle, I. Clark-Lewis, H. Moore, C. Lam, M. Auer, E. Hub and A. Rot (1997). "Transcytosis and surface presentation of IL-8 by venular endothelial cells." *Cell* 91(3): 385-395.

- Millard, C. J., J. P. Ludeman, M. Canals, J. L. Bridgford, M. G. Hinds, D. J. Clayton, A. Christopoulos, R. J. Payne and M. J. Stone (2014). "Structural basis of receptor sulfotyrosine recognition by a CC chemokine: the N-terminal region of CCR3 bound to CCL11/eotaxin-1." *Structure* 22(11): 1571-1581.
- Moelants, E. A., A. Mortier, J. Van Damme and P. Proost (2013). "In vivo regulation of chemokine activity by post-translational modification." *Immunol Cell Biol* 91(6): 402-407.
- Monteclaro, F. S. and I. F. Charo (1997). "The amino-terminal domain of CCR2 is both necessary and sufficient for high affinity binding of monocyte chemoattractant protein 1. Receptor activation by a pseudo-tethered ligand." *J Biol Chem* 272(37): 23186-23190.
- Mordenti, J., R. A. Cuthbertson, N. Ferrara, K. Thomsen, L. Berleau, V. Licko, P. C. Allen, C. R. Valverde, Y. G. Meng, D. T. Fei, K. M. Fourre and A. M. Ryan (1999). "Comparisons of the intraocular tissue distribution, pharmacokinetics, and safety of 125I-labeled full-length and Fab antibodies in rhesus monkeys following intravitreal administration." *Toxicol Pathol* 27(5): 536-544.
- Moser, B., B. Dewald, L. Barella, C. Schumacher, M. Baggiolini and I. Clark-Lewis (1993). "Interleukin-8 antagonists generated by N-terminal modification." *J Biol Chem* 268(10): 7125-7128.
- Movahedi, K., S. Schoonooghe, D. Laoui, I. Houbracken, W. Waelput, K. Breckpot, L. Bouwens, T. Lahoutte, P. De Baetselier, G. Raes, N. Devoogdt and J. A. Van Ginderachter (2012). "Nanobody-based targeting of the macrophage mannose receptor for effective in vivo imaging of tumor-associated macrophages." *Cancer Res* 72(16): 4165-4177.
- Murphy, J. W., H. Yuan, Y. Kong, Y. Xiong and E. J. Lolis (2010). "Heterologous quaternary structure of CXCL12 and its relationship to the CC chemokine family." *Proteins* 78(5): 1331-1337.
- Muyldermans, S. (2001). "Single domain camel antibodies: current status." *J Biotechnol* 74(4): 277-302.

Nagasawa, T., H. Kikutani and T. Kishimoto (1994). "Molecular cloning and structure of a pre-B-cell growth-stimulating factor." *Proc Natl Acad Sci U S A* 91(6): 2305-2309.

Nasser, M. W., S. K. Raghuwanshi, D. J. Grant, V. R. Jala, K. Rajarathnam and R. M. Richardson (2009). "Differential activation and regulation of CXCR1 and CXCR2 by CXCL8 monomer and dimer." *J Immunol* 183(5): 3425-3432.

Naumann, U., E. Cameroni, M. Pruenster, H. Mahabaleshwar, E. Raz, H. G. Zerwes, A. Rot and M. Thelen (2010). "CXCR7 functions as a scavenger for CXCL12 and CXCL11." *PLoS One* 5(2): e9175.

Nguyen, V. K., R. Hamers, L. Wyns and S. Muyldermans (2000). "Camel heavy-chain antibodies: diverse germline V(H)H and specific mechanisms enlarge the antigen-binding repertoire." *EMBO J* 19(5): 921-930.

Nijmeijer, S., R. Leurs, M. J. Smit and H. F. Vischer (2010). "The Epstein-Barr virus-encoded G protein-coupled receptor BILF1 hetero-oligomerizes with human CXCR4, scavenges Galphai proteins, and constitutively impairs CXCR4 functioning." *J Biol Chem* 285(38): 29632-29641.

Nomiyama, H., S. Fukuda, M. Iio, S. Tanase, R. Miura and O. Yoshie (1999). "Organization of the chemokine gene cluster on human chromosome 17q11.2 containing the genes for CC chemokine MPIF-1, HCC-2, HCC-1, LEC, and RANTES." *J Interferon Cytokine Res* 19(3): 227-234.

Nomiyama, H., A. Mera, O. Ohneda, R. Miura, T. Suda and O. Yoshie (2001). "Organization of the chemokine genes in the human and mouse major clusters of CC and CXC chemokines: diversification between the two species." *Genes Immun* 2(2): 110-113.

Nomiyama, H., N. Osada and O. Yoshie (2010). "The evolution of mammalian chemokine genes." *Cytokine Growth Factor Rev* 21(4): 253-262.

O'Donovan, N., M. Galvin and J. G. Morgan (1999). "Physical mapping of the CXC chemokine locus on human chromosome 4." *Cytogenet Cell Genet* 84(1-2): 39-42.

Overington, J. P., B. Al-Lazikani and A. L. Hopkins (2006). "How many drug targets are there?" *Nat Rev Drug Discov* 5(12): 993-996.

Paavola, C. D., S. Hemmerich, D. Grunberger, I. Polsky, A. Bloom, R. Freedman, M. Mulkins, S. Bhakta, D. McCarley, L. Wiesent, B. Wong, K. Jarnagin and T. M. Handel (1998). "Monomeric monocyte chemoattractant protein-1 (MCP-1) binds and activates the MCP-1 receptor CCR2B." *J Biol Chem* 273(50): 33157-33165.

Pakianathan, D. R., E. G. Kuta, D. R. Artis, N. J. Skelton and C. A. Hebert (1997). "Distinct but overlapping epitopes for the interaction of a CC-chemokine with CCR1, CCR3 and CCR5." *Biochemistry* 36(32): 9642-9648.

Paoletti, S., V. Petkovic, S. Sebastiani, M. G. Danelon, M. Ugucioni and B. O. Gerber (2005). "A rich chemokine environment strongly enhances leukocyte migration and activities." *Blood* 105(9): 3405-3412.

Pasche, N. and D. Neri (2012). "Immunocytokines: a novel class of potent armed antibodies." *Drug Discov Today* 17(11-12): 583-590.

Patel, D. D. and B. F. Haynes (2001). "Leukocyte homing to synovium." *Curr Dir Autoimmun* 3: 133-167.

Pathare, G. R., I. Nagy, P. Sledz, D. J. Anderson, H. J. Zhou, E. Pardon, J. Steyaert, F. Forster, A. Bracher and W. Baumeister (2014). "Crystal structure of the proteasomal deubiquitylation module Rpn8-Rpn11." *Proc Natl Acad Sci U S A* 111(8): 2984-2989.

Pease, J. E., J. Wang, P. D. Ponath and P. M. Murphy (1998). "The N-terminal extracellular segments of the chemokine receptors CCR1 and CCR3 are determinants for MIP-1alpha and eotaxin binding, respectively, but a second domain is essential for efficient receptor activation." *J Biol Chem* 273(32): 19972-19976.

Pfleger, K. D. and K. A. Eidne (2005). "Monitoring the formation of dynamic G-protein-coupled receptor-protein complexes in living cells." *Biochem J* 385(Pt 3): 625-637.

Poznansky, M. C., I. T. Olszak, R. Foxall, R. H. Evans, A. D. Luster and D. T. Scadden (2000). "Active movement of T cells away from a chemokine." *Nat Med* 6(5): 543-548.

Proudfoot, A. E., T. M. Handel, Z. Johnson, E. K. Lau, P. LiWang, I. Clark-Lewis, F. Borlat, T. N. Wells and M. H. Kosco-Vilbois (2003). "Glycosaminoglycan binding and oligomerization are essential for the in vivo activity of certain chemokines." *Proc Natl Acad Sci U S A* 100(4): 1885-1890.

Proudfoot, A. E., C. A. Power, A. J. Hoogewerf, M. O. Montjovent, F. Borlat, R. E. Offord and T. N. Wells (1996). "Extension of recombinant human RANTES by the retention of the initiating methionine produces a potent antagonist." *J Biol Chem* 271(5): 2599-2603.

Qin, L., I. Kufareva, L. G. Holden, C. Wang, Y. Zheng, C. Zhao, G. Fenalti, H. Wu, G. W. Han, V. Cherezov, R. Abagyan, R. C. Stevens and T. M. Handel (2015). "Structural biology. Crystal structure of the chemokine receptor CXCR4 in complex with a viral chemokine." *Science* 347(6226): 1117-1122.

Rahbarizadeh, F., M. J. Rasaee, M. Forouzandeh and A. A. Allameh (2006). "Over expression of anti-MUC1 single-domain antibody fragments in the yeast *Pichia pastoris*." *Mol Immunol* 43(5): 426-435.

Rajagopal, S., J. Kim, S. Ahn, S. Craig, C. M. Lam, N. P. Gerard, C. Gerard and R. J. Lefkowitz (2010). "Beta-arrestin- but not G protein-mediated signaling by the "decoy" receptor CXCR7." *Proc Natl Acad Sci U S A* 107(2): 628-632.

Rajarathnam, K., M. P. Crump, I. Clark-Lewis and B. D. Sykes (1999). "Spectroscopic characterization of chemokines: relevance for quality control and standardization." *Dev Biol Stand* 97: 49-57.

Rasmussen, S. G., H. J. Choi, J. J. Fung, E. Pardon, P. Casarosa, P. S. Chae, B. T. Devree, D. M. Rosenbaum, F. S. Thian, T. S. Kobilka, A. Schnapp, I. Konetzki, R. K. Sunahara, S. H. Gellman, A. Pautsch, J. Steyaert, W. I. Weis and B. K. Kobilka (2011). "Structure of a nanobody-stabilized active state of the beta(2) adrenoceptor." *Nature* 469(7329): 175-180.

Rasmussen, S. G., H. J. Choi, D. M. Rosenbaum, T. S. Kobilka, F. S. Thian, P. C. Edwards, M. Burghammer, V. R. Ratnala, R. Sanishvili, R. F. Fischetti, G. F. Schertler, W. I. Weis and B. K. Kobilka (2007). "Crystal structure of the human beta2 adrenergic G-protein-coupled receptor." *Nature* 450(7168): 383-387.

Ray, P., L. A. Mihalko, N. L. Coggins, P. Moudgil, A. Ehrlich, K. E. Luker and G. D. Luker (2012). "Carboxy-terminus of CXCR7 regulates receptor localization and function." *Int J Biochem Cell Biol* 44(4): 669-678.

Ries, J., C. Kaplan, E. Platonova, H. Eghlidi and H. Ewers (2012). "A simple, versatile method for GFP-based super-resolution microscopy via nanobodies." *Nat Methods* 9(6): 582-584.

Ring, A. M., A. Manglik, A. C. Kruse, M. D. Enos, W. I. Weis, K. C. Garcia and B. K. Kobilka (2013). "Adrenaline-activated structure of beta2-adrenoceptor stabilized by an engineered nanobody." *Nature* 502(7472): 575-579.

Roby, P. and M. Page (1995). "Cell-binding and growth-stimulating activities of the C-terminal part of human MGSA/Gro alpha." *Biochem Biophys Res Commun* 206(2): 792-798.

Rollins, B. J. (1997). "Chemokines." *Blood* 90(3): 909-928.

Rot, A. (1993). "Neutrophil attractant/activation protein-1 (interleukin-8) induces in vitro neutrophil migration by haptotactic mechanism." *Eur J Immunol* 23(1): 303-306.

Rueda, P., A. Richart, A. Recalde, P. Gasse, J. Vilar, C. Guerin, H. Lortat-Jacob, P. Vieira, F. Baleux, F. Chretien, F. Arenzana-Seisdedos and J. S. Silvestre (2012). "Homeostatic and tissue reparation defaults in mice carrying selective genetic invalidation of CXCL12/proteoglycan interactions." *Circulation* 126(15): 1882-1895.

Sadir, R., F. Baleux, A. Grosdidier, A. Imberty and H. Lortat-Jacob (2001). "Characterization of the stromal cell-derived factor-1alpha-heparin complex." *J Biol Chem* 276(11): 8288-8296.

Schmitz, K. R., A. Bagchi, R. C. Roovers, P. M. van Bergen en Henegouwen and K. M. Ferguson (2013). "Structural evaluation of EGFR inhibition mechanisms for nanobodies/VHH domains." *Structure* 21(7): 1214-1224.

Schonemeier, B., S. Schulz, V. Hoellt and R. Stumm (2008). "Enhanced expression of the CXCL12/SDF-1 chemokine receptor CXCR7 after cerebral ischemia in the rat brain." *J Neuroimmunol* 198(1-2): 39-45.

Schraufstatter, I. U., D. S. Barritt, M. Ma, Z. G. Oades and C. G. Cochrane (1993). "Multiple sites on IL-8 responsible for binding to alpha and beta IL-8 receptors." *J Immunol* 151(11): 6418-6428.

Selvin, P. R. (2002). "Principles and biophysical applications of lanthanide-based probes." *Annu Rev Biophys Biomol Struct* 31: 275-302.

Sharp, C. D., M. Huang, J. Glawe, D. R. Patrick, S. Pardue, S. C. Barlow and C. G. Kevil (2008). "Stromal cell-derived factor-1/CXCL12 stimulates chemorepulsion of NOD/LtJ T-cell adhesion to islet microvascular endothelium." *Diabetes* 57(1): 102-112.

Shaw, J. P., Z. Johnson, F. Borlat, C. Zwahlen, A. Kungl, K. Roulin, A. Harrenga, T. N. Wells and A. E. Proudfoot (2004). "The X-ray structure of RANTES: heparin-derived disaccharides allows the rational design of chemokine inhibitors." *Structure* 12(11): 2081-2093.

Shimizu, N., Y. Soda, K. Kanbe, H. Y. Liu, R. Mukai, T. Kitamura and H. Hoshino (2000). "A putative G protein-coupled receptor, RDC1, is a novel coreceptor for human and simian immunodeficiency viruses." *J Virol* 74(2): 619-626.

Sierro, F., C. Biben, L. Martinez-Munoz, M. Mellado, R. M. Ransohoff, M. Li, B. Woehl, H. Leung, J. Groom, M. Batten, R. P. Harvey, A. C. Martinez, C. R. Mackay and F. Mackay (2007). "Disrupted cardiac development but normal hematopoiesis in mice deficient in the second CXCL12/SDF-1 receptor, CXCR7." *Proc Natl Acad Sci U S A* 104(37): 14759-14764.

Skelton, N. J., F. Aspiras, J. Ogez and T. J. Schall (1995). "Proton NMR assignments and solution conformation of RANTES, a chemokine of the C-C type." *Biochemistry* 34(16): 5329-5342.

Skelton, N. J., C. Quan, D. Reilly and H. Lowman (1999). "Structure of a CXC chemokine-receptor fragment in complex with interleukin-8." *Structure* 7(2): 157-168.

Smith, E. B., R. A. Ogert, D. Pechter, A. Villafania, S. J. Abbondanzo, K. Lin, A. Rivera-Gines, C. Rebsch-Mastykarz and F. J. Monsma, Jr. (2014). "HIV cell fusion assay: phenotypic screening tool for the identification of HIV entry inhibitors via CXCR4." *J Biomol Screen* 19(1): 108-118.

Soria, G., Y. Lebel-Haziv, M. Ehrlich, T. Meshel, A. Suez, E. Avezov, P. Rozenberg and A. Ben-Baruch (2012). "Mechanisms regulating the secretion of the promalignancy chemokine CCL5 by breast tumor cells: CCL5's 40s loop and intracellular glycosaminoglycans." *Neoplasia* 14(1): 1-19.

Staus, D. P., L. M. Wingler, R. T. Strachan, S. G. Rasmussen, E. Pardon, S. Ahn, J. Steyaert, B. K. Kobilka and R. J. Lefkowitz (2014). "Regulation of beta2-adrenergic receptor function by conformationally selective single-domain intrabodies." *Mol Pharmacol* 85(3): 472-481.

Stephens, B. and T. M. Handel (2013). "Chemokine receptor oligomerization and allostery." *Prog Mol Biol Transl Sci* 115: 375-420.

Steyaert, J. and B. K. Kobilka (2011). "Nanobody stabilization of G protein-coupled receptor conformational states." *Curr Opin Struct Biol* 21(4): 567-572.

- Sticht, H., S. E. Escher, K. Schweimer, W. G. Forssmann, P. Rosch and K. Adermann (1999). "Solution structure of the human CC chemokine 2: A monomeric representative of the CC chemokine subtype." *Biochemistry* 38(19): 5995-6002.
- Stoler-Barak, L., C. Moussion, E. Shezen, M. Hatzav, M. Sixt and R. Alon (2014). "Blood vessels pattern heparan sulfate gradients between their apical and basolateral aspects." *PLoS One* 9(1): e85699.
- Strieter, R. M., P. J. Polverini, D. A. Arenberg and S. L. Kunkel (1995). "The role of CXC chemokines as regulators of angiogenesis." *Shock* 4(3): 155-160.
- Struyf, S., S. Noppen, T. Loos, A. Mortier, M. Gouwy, H. Verbeke, D. Huskens, S. Luangsay, M. Parmentier, K. Geboes, D. Schols, J. Van Damme and P. Proost (2009). "Citrullination of CXCL12 differentially reduces CXCR4 and CXCR7 binding with loss of inflammatory and anti-HIV-1 activity via CXCR4." *J Immunol* 182(1): 666-674.
- Szymborska, A., A. de Marco, N. Daigle, V. C. Cordes, J. A. Briggs and J. Ellenberg (2013). "Nuclear pore scaffold structure analyzed by super-resolution microscopy and particle averaging." *Science* 341(6146): 655-658.
- Takekoshi, T., J. J. Ziarek, B. F. Volkman and S. T. Hwang (2012). "A locked, dimeric CXCL12 variant effectively inhibits pulmonary metastasis of CXCR4-expressing melanoma cells due to enhanced serum stability." *Mol Cancer Ther* 11(11): 2516-2525.
- Tan, Q., Y. Zhu, J. Li, Z. Chen, G. W. Han, I. Kufareva, T. Li, L. Ma, G. Fenalti, J. Li, W. Zhang, X. Xie, H. Yang, H. Jiang, V. Cherezov, H. Liu, R. C. Stevens, Q. Zhao and B. Wu (2013). "Structure of the CCR5 chemokine receptor-HIV entry inhibitor maraviroc complex." *Science* 341(6152): 1387-1390.
- Tian, S., W. T. Choi, D. Liu, J. Pesavento, Y. Wang, J. An, J. G. Sodroski and Z. Huang (2005). "Distinct functional sites for human immunodeficiency virus type 1 and stromal cell-derived factor 1alpha on CXCR4 transmembrane helical domains." *J Virol* 79(20): 12667-12673.

- Valentin, G., P. Haas and D. Gilmour (2007). "The chemokine SDF1 α coordinates tissue migration through the spatially restricted activation of Cxcr7 and Cxcr4b." *Curr Biol* 17(12): 1026-1031.
- van der Linden, R., B. de Geus, W. Stok, W. Bos, D. van Wassenaar, T. Verrips and L. Frenken (2000). "Induction of immune responses and molecular cloning of the heavy chain antibody repertoire of *Lama glama*." *J Immunol Methods* 240(1-2): 185-195.
- Vaneycken, I., M. D'Huyvetter, S. Hernot, J. De Vos, C. Xavier, N. Devoogdt, V. Caveliers and T. Lahoutte (2011). "Immuno-imaging using nanobodies." *Curr Opin Biotechnol* 22(6): 877-881.
- Veldkamp, C. T., F. C. Peterson, A. J. Pelzek and B. F. Volkman (2005). "The monomer-dimer equilibrium of stromal cell-derived factor-1 (CXCL 12) is altered by pH, phosphate, sulfate, and heparin." *Protein Sci* 14(4): 1071-1081.
- Veldkamp, C. T., C. Seibert, F. C. Peterson, N. B. De la Cruz, J. C. Haugner, 3rd, H. Basnet, T. P. Sakmar and B. F. Volkman (2008). "Structural basis of CXCR4 sulfotyrosine recognition by the chemokine SDF-1/CXCL12." *Sci Signal* 1(37): ra4.
- Vincke, C., R. Loris, D. Saerens, S. Martinez-Rodriguez, S. Muyldermans and K. Conrath (2009). "General strategy to humanize a camelid single-domain antibody and identification of a universal humanized nanobody scaffold." *J Biol Chem* 284(5): 3273-3284.
- Vives, R. R., E. Crublet, J. P. Andrieu, J. Gagnon, P. Rousselle and H. Lortat-Jacob (2004). "A novel strategy for defining critical amino acid residues involved in protein/glycosaminoglycan interactions." *J Biol Chem* 279(52): 54327-54333.
- Vu, K. B., M. A. Ghahroudi, L. Wyns and S. Muyldermans (1997). "Comparison of llama VH sequences from conventional and heavy chain antibodies." *Mol Immunol* 34(16-17): 1121-1131.

- Wagner, U. G., P. J. Kurtin, A. Wahner, M. Brackertz, D. J. Berry, J. J. Goronzy and C. M. Weyand (1998). "The role of CD8⁺ CD40L⁺ T cells in the formation of germinal centers in rheumatoid synovitis." *J Immunol* 161(11): 6390-6397.
- Wang, J., Y. Shiozawa, J. Wang, Y. Wang, Y. Jung, K. J. Pienta, R. Mehra, R. Loberg and R. S. Taichman (2008). "The role of CXCR7/RDC1 as a chemokine receptor for CXCL12/SDF-1 in prostate cancer." *J Biol Chem* 283(7): 4283-4294.
- Wang, L., M. Fuster, P. Sriramarao and J. D. Esko (2005). "Endothelial heparan sulfate deficiency impairs L-selectin- and chemokine-mediated neutrophil trafficking during inflammatory responses." *Nat Immunol* 6(9): 902-910.
- Wang, X., J. S. Sharp, T. M. Handel and J. H. Prestegard (2013). "Chemokine oligomerization in cell signaling and migration." *Prog Mol Biol Transl Sci* 117: 531-578.
- Ward, A. B., P. Szewczyk, V. Grimard, C. W. Lee, L. Martinez, R. Doshi, A. Caya, M. Villaluz, E. Pardon, C. Cregger, D. J. Swartz, P. G. Falson, I. L. Urbatsch, C. Govaerts, J. Steyaert and G. Chang (2013). "Structures of P-glycoprotein reveal its conformational flexibility and an epitope on the nucleotide-binding domain." *Proc Natl Acad Sci U S A* 110(33): 13386-13391.
- Warne, T., M. J. Serrano-Vega, J. G. Baker, R. Moukhametzianov, P. C. Edwards, R. Henderson, A. G. Leslie, C. G. Tate and G. F. Schertler (2008). "Structure of a beta1-adrenergic G-protein-coupled receptor." *Nature* 454(7203): 486-491.
- Weber, M., R. Hauschild, J. Schwarz, C. Moussion, I. de Vries, D. F. Legler, S. A. Luther, T. Bollenbach and M. Sixt (2013). "Interstitial dendritic cell guidance by haptotactic chemokine gradients." *Science* 339(6117): 328-332.

- Westfield, G. H., S. G. Rasmussen, M. Su, S. Dutta, B. T. DeVree, K. Y. Chung, D. Calinski, G. Velez-Ruiz, A. N. Oleskie, E. Pardon, P. S. Chae, T. Liu, S. Li, V. L. Woods, Jr., J. Steyaert, B. K. Kobilka, R. K. Sunahara and G. Skiniotis (2011). "Structural flexibility of the G alpha s alpha-helical domain in the beta2-adrenoceptor Gs complex." *Proc Natl Acad Sci U S A* 108(38): 16086-16091.
- Williams, G., N. Borkakoti, G. A. Bottomley, I. Cowan, A. G. Fallowfield, P. S. Jones, S. J. Kirtland, G. J. Price and L. Price (1996). "Mutagenesis studies of interleukin-8. Identification of a second epitope involved in receptor binding." *J Biol Chem* 271(16): 9579-9586.
- Wu, B., E. Y. Chien, C. D. Mol, G. Fenalti, W. Liu, V. Katritch, R. Abagyan, A. Brooun, P. Wells, F. C. Bi, D. J. Hamel, P. Kuhn, T. M. Handel, V. Cherezov and R. C. Stevens (2010). "Structures of the CXCR4 chemokine GPCR with small-molecule and cyclic peptide antagonists." *Science* 330(6007): 1066-1071.
- Xu, C., H. Zhao, H. Chen and Q. Yao (2015). "CXCR4 in breast cancer: oncogenic role and therapeutic targeting." *Drug Des Devel Ther* 9: 4953-4964.
- Zabel, B. A., Y. Wang, S. Lewen, R. D. Berahovich, M. E. Penfold, P. Zhang, J. Powers, B. C. Summers, Z. Miao, B. Zhao, A. Jalili, A. Janowska-Wieczorek, J. C. Jaen and T. J. Schall (2009). "Elucidation of CXCR7-mediated signaling events and inhibition of CXCR4-mediated tumor cell transendothelial migration by CXCR7 ligands." *J Immunol* 183(5): 3204-3211.
- Zarschler, K., S. Witecy, F. Kapplusch, C. Foerster and H. Stephan (2013). "High-yield production of functional soluble single-domain antibodies in the cytoplasm of *Escherichia coli*." *Microb Cell Fact* 12: 97.
- Zhang, Y. J., B. J. Rutledge and B. J. Rollins (1994). "Structure/activity analysis of human monocyte chemoattractant protein-1 (MCP-1) by mutagenesis. Identification of a mutated protein that inhibits MCP-1-mediated monocyte chemotaxis." *J Biol Chem* 269(22): 15918-15924.

Zhou, N., Z. Luo, J. Luo, D. Liu, J. W. Hall, R. J. Pomerantz and Z. Huang (2001). "Structural and functional characterization of human CXCR4 as a chemokine receptor and HIV-1 co-receptor by mutagenesis and molecular modeling studies." *J Biol Chem* 276(46): 42826-42833.

Zlatopolskiy, A. and J. Laurence (2001). "'Reverse gear' cellular movement mediated by chemokines." *Immunol Cell Biol* 79(4): 340-344.

Annexes

❖ *The CXCL12/CXCR4 Signaling Pathway: a New Susceptibility Factor in Human Papillomavirus Pathogenesis*

❖ *Natural amines inhibit activation of human plasmacytoid dendritic cells through CXCR4 engagement*

❖ *Curriculum Vitae*

Full title:

**The CXCL12/CXCR4 Signaling Pathway: a New Susceptibility
Factor in Human Papillomavirus Pathogenesis**

Short title: The CXCL12/CXCR4 Pathway in HPV Pathogenesis

Floriane Meuris¹, Laetitia Carthagna¹, Agnieszka Jaracz-Ros^{1*}, Françoise Gaudin^{1,2*},
Pasquale Cutolo¹, Claire Deback¹, Yuezhen Xue³, Françoise Thierry³, John Doorbar⁴,
Françoise Bachelier¹

¹ UMR996 - Inflammation, Chemokines and Immunopathology -, Inserm, Univ Paris-Sud,
Université Paris-Saclay, 92296, Clamart, France.

² US31-UMS3679 -Plateforme PHIC, Institut Paris-Saclay d'Innovation Thérapeutique
(IPSIT), Inserm, CNRS, Univ Paris-Sud, Université Paris-Saclay, Clamart, France.

³ Papillomavirus Regulation and Cancer Laboratory, Institute of Medical Biology, Biopolis,
Singapore City, 138648; Singapore.

⁴ Department of Pathology, University of Cambridge, Cambridge, CB2 1QP; United Kingdom.

* These authors contributed equally to this work

Corresponding author: francoise.bachelier@u-psud.fr

Abstract

The productive human papillomavirus (HPV) life cycle is tightly linked to the differentiation and cycling of keratinocytes. Deregulation of these processes and stimulation of cell proliferation by the action of viral oncoproteins and host cell factors underlies HPV-mediated carcinogenesis. Severe HPV infections characterize the wart, hypogammaglobulinemia, infection, and myelokathexis (WHIM) immunodeficiency syndrome, which is caused by a gain-of-function mutant of the CXCR4 receptor for the CXCL12 chemokine (CXCR4¹⁰¹³). We investigated whether CXCR4¹⁰¹³ interferes in the HPV18 life cycle in epithelial organotypic cultures. Expression of CXCR4¹⁰¹³ promoted stabilization of HPV oncoproteins, thus disturbing cell cycle progression and proliferation at the expense of the ordered expression of the viral genes required for virus production. Conversely, blocking CXCR4¹⁰¹³ function restored virus production and limited HPV-induced carcinogenesis. Thus, CXCR4 and its potential activation by genetic alterations in the course of the carcinogenic process can be considered as an important host factor for HPV carcinogenesis.

Natural amines inhibit activation of human plasmacytoid dendritic cells through CXCR4 engagement

Nikaïa Smith^{1,2}, Nicolas Pietrancosta^{1,2}, Sophia Davidson³, Jacques Dutrieux⁴, Lise Chauveau⁵, **Pasquale Cutolo**⁶, Michel Dy⁷, Daniel Scott-Algara⁸, Bénédicte Manoury⁹, Onofrio Zirafi¹⁰, Isabelle McCort-Tranchepain¹, Thierry Durroux¹¹, Françoise Bachelier⁶, Olivier Schwartz⁵, Jan Münch¹⁰, Andreas Wack³, Sébastien Nisole⁴, Jean-Philippe Herbeuval^{1,2}.

¹ CNRS UMR-8601, Université Paris Descartes, CICB, 45 rue des Saints-Pères, 75006 Paris, France.

² Chemistry & Biology, Nucleo(s)tides & Immunology for Therapy, CBNIT

³ Francis Crick Institute, Mill Hill Laboratory, London, NW7 1AA, UK

⁴ INSERM UMR-S 1124, Université Paris Descartes, 45 rue des Saints-Pères, 75006 Paris, France

⁵ Institut Pasteur, Virus & Immunity Unit, 25-28 Rue du Dr Roux, Paris 75015, France

⁶ INSERM UMR996 - Inflammation, Chemokines and Immunopathology, Univ Paris-Sud, Université Paris-Saclay, 92296, Clamart, France

⁷ CNRS UMR-8147, Institut Necker Enfants Malades, 156 Rue de Vaugirard, 75015 Paris, France

⁸ Institut Pasteur, Unité de Régulation des Infections Rétrovirales, 25-28 Rue du Dr Roux, Paris 75015, France

⁹ INSERM U1151, Hôpital Necker, 156 Rue de Vaugirard, 75015 Paris, France

¹⁰ Institute of Molecular Virology, Ulm University Medical Centre, Ulm 89081, Germany

¹¹ CNRS, UMR 5203, Institut de Génomique Fonctionnelle, Montpellier, France and INSERM, U. 1191, Montpellier, France and Université Montpellier, 1,2, Montpellier, France

Address for co-corresponding authors:

- Dr Jean-Philippe Herbeuval, CBNIT, CNRS UMR8601, Université Paris Descartes, Faculté des Saints Pères, 45 rue des Saints-Pères, 75006 France, jean-philippe.herbeuval@parisdescartes.fr, Tel: +33 1 42 86 38 32.
- Dr Nicolas Pietrancosta, CBNIT, CNRS UMR8601, Université Paris Descartes, Faculté des Saints Pères, 45 rue des Saints-Pères, 75006 France, nicolas.pietrancosta@parisdescartes.fr.

Abstract

Plasmacytoid dendritic cells (pDC) are specialized in secretion of type I interferon (IFN I) in response to pathogens. We show here that natural monoamines, polyamines and synthetic amines strongly inhibit pDC activation by RNA viruses. Furthermore, a synthetic analogue of histamine drastically reduces IFN I production in an Influenza A infected mouse model. We further identify CXC chemokine receptor 4 (CXCR4) as the receptor used by amines to inhibit pDC. Using in silico docking experiments, we localize a binding pocket for amino molecules in the extracellular region of CXCR4. Our study establishes a functional link between natural amines and innate immune system and identifies CXCR4 as a potential "on off" switch of pDC activity with promising therapeutic perspectives.

Curriculum Vitae

Pasquale CUTOLO

Docteur en Immunologie et Biothérapies

Date de naissance : 22 septembre 1988

67, boulevard Felix Faure, 92320, Châtillon

Téléphone : +33 (0)781405529

Mail : pasquale.cutolo@u-psud.fr

Linkedin : pasquale-cutolo-47aa9964


Permis de conduire B



Formation

- **2013 – 2016** : Thèse en Immunologie et Biothérapies à l'Ecole Doctorale d'Innovation Thérapeutiques : du fondamental à l'appliqué (Paris-Saclay)
Inserm UMR-S 996 : Inflammation, Chimiokines et Immunopathologie
Projet : *Etude de l'interaction structurelle et fonctionnelle entre la chimiokine CXCL12 et ses récepteurs : CXCR4 et ACKR3/CXCR7.*
(Directeur de thèse : **Dr Françoise Bachelerie**) Financement **Labex**
LERMIT du 01/10/13 au 30/09/16
- **2010 – 2012** : Master 1 et 2 en Biotechnologies Médicales (Università degli Studi di Napoli "Federico II") notation : **110 cum laude/110**
Projet : *Experimental Invalidation of the memory Consolidation Hypothesis*
- **2007 – 2010** : Licence en Biotechnologies pour la santé (Università degli Studi di Napoli "Federico II") notation : 108/110
Projet : *Direct Immunofluorescence against Cryptosporidium in snakes of regional origin*
- **2006 – 2007** : Premier cycle de licence en Sciences Statistiques (Università degli Studi di Napoli "Federico II")
- **2001 – 2006** : BAC de Commerce (I.T.C.G. "Annibale Giordano") notation : 100/100

Expériences

- **Octobre 2013 – Septembre 2016** : **Développement de la nouvelle Start-up Biotech : Beamedex**
Développement de la plateforme Beads4med, création et gestion du site internet, **création de la start-up en Décembre 2014**
Position : **Président**
(Réfèrent : **Prof. Sola Christophe**, Université Pars-Sud : IGEPE)

www.beamedex.com
- **Mars 2015 – Septembre 2015**: **Encadrement étudiante en Master 2**
Supervision et apprentissage pour l'étudiante Erasmus Maria Ester De Biase pour le stage de Master 2.
Projet : **Les récepteurs de la chimiokine CXCL12 : génération de mutants pour comprendre les mécanismes d'internalisation.**
- **Février 2012 - Juillet 2012** : « **Lifelong Learning Programme (LLP) » (Stage Erasmus)**
Echange Erasmus à l'Université Paris-Sud (notation : **18/20**)
Stage dans l'équipe : Amnesic Process: from normal to pathologies. (Group Leader : **Dr. Pascale Gisquet-Verrier**)
CNPS (Centre de Neurosciences de Paris-Sud), Université de Paris-Sud, Orsay, Paris.
- **Juillet 2011 - Septembre 2011** : **Student Mobility for Placement**
Stage dans l'équipe de Stem Cells in Brain Repair. (Group Leader : **Dr. Pascale Durbec**)
IBDML de Marseille (Institut de Biologie du Développement de Marseille Luminy), Université de la Méditerranée, Marseille.
- **Avril 2011 - Janvier 2012** : **Stage Master 1** en : Zebrafish Brain Development as model in Medulloblastoma disease
Equipe de recherche : Cell Biology, Development and Evolution (Group Leader : **Dr. Paolo Sordino**), Zoological Station "Anton Dohrn"; Naples (Italie)
- **Juin 2010 - Octobre 2010** : **Stage Licence 3** dans l'équipe de Pathologie et Santé Animale
Directeur : **Prof. Laura Rinaldi**; Università degli Studi di Napoli "Federico II" (notation : 30 cum laude/30)

- Mars 2010 - Juin 2010 : **Stage** en: Méthodes Histologiques en Modèles Animaux (notation : 30/30)
Département de Morphologie Animale (Directeur : **Prof. Caterina Squillaciotti**), Università degli Studi di Napoli "Federico II".
- Octobre 2011 - Octobre 2012 : **Tutorat universitaire et orientation professionnelle** ; Università degli Studi di Napoli "Federico II".
Orientation pour les nouveaux étudiants, aide à la prise de décisions et la préparation aux examens ; collaboration avec les professeurs et le staff de l'université.
- Mars 2011 – Juin 2011 : **Expérience d'enseignement** ; Università degli Studi di Napoli "Federico II".
 - Fatty acids of the cell wall: Molecular mechanisms involved in the pathogenesis of Mycobacterium tuberculosis
 - ROLE OF LOX-1 in the initiation of ATHEROSCLEROSIS and its development
- Juin 2006 - Juin 2010 : **Team Manager** pour l'entreprise Star Dust Italia Spa. (Management et direction d'un workgroup, Manager ventes, Comptabilité).
Acquisition de compétences techniques, opérationnelles, managériales et interpersonnelles. (Directeur Régionale : **Linda Sodano**)



www.stardustitalia.net

Autres informations

Juillet 2014 : 3^e édition de l'École d'été du LERMIT « La chaîne du Médicament »

Programme dense et interdisciplinaire, avec conférences animées par des acteurs de la recherche académique, clinique et des entreprises pharmaceutiques.

Août 2012 : Bourse **Roche Continents** : échange entre science et arts. (100 étudiants sélectionnés en Europe)

Participation à :

- ✓ ECMC 2015 : **European Chemokine and Cell Migration Conference** - Villars-sur-Ollon (VD), Suisse - Juin 2015 – **Présentation Orale et Poster**
- ✓ GDR 3545 : **Groupe de recherche sur les GPCR** - Montpellier – Octobre 2014 – **Présentation Poster (Premier prix pour les Doctorants)**
- ✓ ITMO (Thematic Multi-organization Institute) "CANCER" Paris - Septembre 2011 - **Institut Pasteur**
- ✓ Cours en Nanobiotechnologies: Applications et Perspectives futures Rome - Avril 2011 - **Fédération Italienne des Biotechnologistes (F.I.Bio.)**

Compétences

Techniques : Immuno-isto-chimie, Immunofluorescence (Microscopie Confocale, Ibridation In situ), Biologie Moléculaire (Cultures bactériennes, Clonage, Electrophorèse, PCR, Western Blot, dosage de protéines), Biologie Cellulaire (Extraction ADN et ARN, qPCR), Cultures Cellulaires (Maintien en culture de Cellules Primaires et Lignées, Transfection, L2 Lab), Cytométrie en flux (LRS Fortessa), Biochimie (Dosage enzymatiques), Pharmacologie (Tests de Liaison, Compétition et Cinétique), Modélisation Moléculaire (Dynamique, peptide-peptide Docking, Homology Modeling, analyse GROMACS), Interaction prot-prot (BRET, HTRF), Etudes Comportementales (manipulation et maintien d'animaux : rat, souris et zebrafish).

Managériale : Management, stratégie du marché, comptabilité, communication, marketing, esprit d'initiative, habilité à déléguer, résoudre problèmes, travailler sous pression, prendre des décisions, identifier les objectifs et avoir des résultats

Interpersonnelles : Motiver un groupe, team building, travailler avec managers et échanger des bonnes relations avec les commerciales, clients et fournisseurs. Habilité à communiquer et créer des bonnes relations professionnelles.

Langues : langue maternelle ITALIEN

- **Anglais**: C1 (Professionnel)

- **Français**: C2 (Bilingue)

Informatiques : ECDL (European Computer Driving Licence) File Management, Word Processing, Spreadsheet (Excel), Database (Access), Presentation (Powerpoint), Computer networks - Internet, Photoshop, Statistics software (R, Var3, pVar, Prism), Molecular biology and protein databases (Primer 3, Pubmed, Blast, Pdb), Cryométrie en flux (FlowJo), Logiciels de modélisation moléculaire (Chimera, VMD, Frodock, GROMACS)

Publications

Publiés :

Interaction of chemokine receptor CXCR4 in monomeric and dimeric state with its endogenous ligand CXCL12: Coarse-grained simulations identify differences.

Cutolo P, Basdevant N, Bernadat G, Bachelerie F, Ha-Duong T.

J Biomol Struct Dyn. 2016 Jan 26:1-56. PMID: 26813575

Integration of New Information with Active Memory Accounts for Retrograde Amnesia: A Challenge to the Consolidation/Reconsolidation Hypothesis?

Gisquet-Verrier P, Lynch JF 3rd, Cutolo P, Toledano D, Ulmen A, Jasnow AM, Riccio DC.

J Neurosci. 2015 Aug 19; 35(33):11623-33. PMID: 26290239

The CXCL12/CXCR4 Signaling Pathway: a New Susceptibility Factor in Human Papillomavirus Pathogenesis

Meuris F, Carthagena L, Jaracz-Ros A, Gaudin F, Cutolo P, Deback C, Xue Y, Thierry F, Doorbar J, Bachelerie F.

PLoS Pathogens

Natural amines inhibit activation of human plasmacytoid dendritic cells through CXCR4 engagement

Smith M, Pietrancosta N, Davidson S, Dutrieux J, Chauveau L, Cutolo P, Dy M, Algara DS, Manoury B, Zirafi O, McCort Tranchepain I, Durroux T,

Bachelerie F, Schwartz O, Münch J, Wack A, Nisole S, Herbeuval JP.

Nature Communications

En redaction :

Conformationally selective Nanobodies for regulation of CXCR4 functions

Cutolo P, Jaracz-Ros A, Heuinck J, Bourquard T, Dupuis E, Roux T, Trinquet E, Bernadat G, Durroux T, Bachelerie F.

Differential activities of CXCL12 analogs at the CXCR4 and ACKR3/ACKR3 receptors: study of interaction determinants

Cutolo P, Bernadat G, Jaracz-Ros A, Baleux F, Bachelerie F and Levoye A.

Centre d'intérêts

- **Sociale** : Décembre 2007 - Décembre 2008 : Service Civil pour l'Union Italienne des Aveugles (UIC); Secrétariat, Enseignant Braille, Guide pour les aveugles.
Septembre 2005 - Septembre 2006 : Membre de la Protection civile de Naples.
- **Musique** : Joueur de piano depuis 2003 -
- **Sport** : Joueur de Volleyball depuis 2004 – Entraîneur depuis 2014 (PAC Volley)

Acknowledgements

Acknowledgements

Firstly, I would like to express my sincere gratitude to my director and advisor Dr. Françoise Bachelerie for the continuous support during my Ph.D study and related research, for her big patience, motivation, and immense knowledge. Her guidance helped me in all the time of research and the writing of this thesis, pushing me to do always the best and motivating me in worst moments.

Besides my advisor, I would like to thank the rest of my thesis committee: Dr. Esther Kellenberger and Dr. Eric Reiter, who have evaluated my manuscript; Dr. Philippe Deterre, who evaluated my project during the “mi-thèse” defense; Dr. Thierry Durroux, who allowed me to learn new approaches in pharmacology with HTRF technics in Montpellier and advised me during my thesis; Prof. Sandrine Onger, who was always interested in my research and exchanged with me interesting scientific conversations.

I thank all of them in advance for their insightful comments and encouragement, but also for the questions that will incite me to widen my research from various perspectives.

My sincere thanks also goes to Dr. Tap Ha-Duong, who provided me an opportunity of collaboration, and who helped me for the first publication in the modeling field.

A special thanks goes to Dr. Guillaume Bernadat, who taught me all I know today in molecular modeling and without his precious support it would not be possible to conduct my research on CXCR7 and NBs modeling. I want to thank him for his availability, helping me all the time and spent long days of work programming and advising me.

I thank all my U996 labmates for the stimulating discussions, for the sleepless nights we were working together before deadlines, and for all the fun we have had in the last years.

Thanks to all leaders in the lab, Dr. Karl Balabanian, Dr. Géraldine Schlecht-Louf, Dr. Marion Espeli, Dr. Viviana Esteban and Anne-Marie Cassard, for their support, availability and help.

A big thanks goes to Dr. Agnieszka Jaracz-Ros, who helped me since the first day of my Ph.D, not only in a working context, pushing me to try new approaches in my research, but also for moral and private support and sharing my hobby for aquariology.

Thanks to Marie-Laure Aknin, Françoise Gaudin and Hélène Gary to helping me using the platforms equipment, but also for our long and fun conversations and personal discussions.

I want also say thank you to members of Cisbio that gave us the three nanobodies and discussed results with us to better understand them.

Switch the langue, pour remercier l'ensemble de mes amis et amies qui m'ont aidé et soutenu au long de ma thèse. Pas de liste car je risque forcément d'oublier quelque nom !

Je tiens aussi à remercier « les filles » du labo pour l'ambiance qu'elles arrivent à créer dans le laboratoire, essayez maintenant de prendre bien soin du pauvre aquarium. Merci ma petite Nagham pour ton soutien à chaque fois que j'avais une baisse de moral, tes nombreuses perles qui m'ont donné le souris et souviens-toi toujours du « silicone ».

Merci Odile pour l'énorme travail que tu fais pour nous tous dans le laboratoire, mais principalement pour l'écoute, les belles paroles que tu as toujours eu pour moi et ton amour inconditionné pour l'Italie !

Un gros merci pour les dernières arrivées Karlijn, Joyce et Carmen qui sont devenues vite un groupe de travail mais surtout un groupe d'amies très important, avec qui j'ai pu partager les meilleurs moments de cette dernière année de thèse. Je n'oublierai jamais vos petits et grands gestes de vraie amitié.

Je veux remercier aussi mon meilleur ami Louis, pour le grand soutien durant les moments difficiles de la thèse. Je te remercie pour ta confiance en moi et d'avoir toujours trouvé le moyen de m'encourager et rassurer, en me donnant la force de croire en moi sans jamais douter.

Un merci très spécial va aussi à Christopher, qui a su me donner du courage pendant le stress de la rédaction. Merci de m'avoir écouté à chaque fois que j'avais des problèmes et pendant les nombreuses nuits blanches de boulot... et merci de faire de moi une personne meilleure !

Infine (ancora un cambio di lingua), non posso che ringraziare la mia famiglia e i miei amici di sempre. Anche in questo caso evito l'elenco perché dimenticherei sicuramente qualcuno.

Un grazie particolare e immenso va a Olimpia, l'anima gemella che crede in me da sempre e mi accompagna in ogni traguardo della mia vita. Grazie per il tifo incondizionato per tuo marito e per essere la mia spalla solida, sempre !

Grazie a Maria Ester, che ha subito la mia "direzione" per sette mesi in laboratorio e ha contribuito al progetto in modo professionale senza mollare nei momenti di pressione, ma anche per la persona "amabile" che si è dimostrata.

Dulcis in fundo... grazie a mio fratello per l'orgoglio che mostra sempre nei miei confronti e GRAZIE a mia madre, una grande donna in formato tascabile, per l'aiuto di una vita intera e la capacità di seguirmi ed aiutarmi anche a km di distanza.

Grazie anche a te papà, che ispiri sempre questo "ragazzino" a diventare un uomo come te... che tu possa essere ancora una volta orgoglioso di me guardandomi da lassù.

Etude de l'interaction structurelle et fonctionnelle entre la chimiokine CXCL12 et ses récepteurs : CXCR4 et ACKR3/CXCR7

Mots clés : GPCRs, protein-protein interaction, Molecular modeling, Nanobodies

Résumé :

L'axe formé par la chimiokine CXCL12 et son récepteur CXCR4 est conservé chez les vertébrés où il joue un rôle important dans l'embryogenèse et la vie adulte, et régule de nombreux processus des réponses immunitaires grâce à ses fonctions dans la migration cellulaire, la survie et la prolifération. En outre, cet axe est impliqué dans les processus pathologiques tels que les cancers (croissance et métastase) et immunodéficiences, ainsi que des dysfonctionnements (par exemple l'expression dérégulée, polymorphismes ou mutations) et il est également détourné par certains agents pathogènes (par exemple le virus de l'immunodéficiences humaine, virus du papillome humain).

Un grand groupe de travail est consacré à cette paire comme cible thérapeutique, mais seulement un composé (Plérixafor) a atteint l'approbation pour une utilisation clinique, faisant du potentiel de cet axe une cible des médicaments encore inexploré.

Bien que cet axe est l'objet d'un grand intérêt, des questions demeurent quant aux déterminants structurels impliqués dans l'interaction CXCL12/CXCR4.

Cependant, la structure récemment résolue par diffraction de CXCR4 a donné quelque indice au sujet de ces questions, et en particulier, de la possible stoechiométrie entre CXCL12 et CXCR4. Plusieurs éléments de preuve appuient le concept que CXCR4 forme des homo- et hétéro- oligomères (qui peuvent contribuer à la diversité des fonctions du récepteur), telles que la structure de diffraction, le gain de fonction d'un récepteur CXCR4 mutant responsable du syndrome WHIM et la modulation allostérique des fonctions de CXCR4 par CXCR7 (ACKR3), le second récepteur de CXCL12.

La possibilité de former des oligomères ouvre des nombreuses questions en matière de CXCL12 et ses interactions avec CXCR4 et CXCR7/ACKR3. La stoechiométrie de cette interaction reste une question ouverte, comme le récepteur est capable de former des oligomères avec le même récepteur ou autre récepteurs, en particulier CXCR7/ACKR3. Ce récepteur, connu comme scavenger, n'a pas de structure résolue et son mécanisme d'interaction avec CXCL12 reste inconnu. Afin d'étudier les interactions CXCL12/CXCR4/CXCR7, nous avons appliqué plusieurs techniques de modélisation moléculaire tels que le peptid-peptide docking et les simulations de dynamique moléculaire.

Objets du projet ont été : la résolution des possibles formes stoechiométriques de l'interaction CXCR4/CXCL12 (modélisation moléculaire, docking et dynamique); la modélisation de la structure du récepteur CXCR7/ACKR3 et son interaction avec CXCL12 (homology modeling et docking), avec caractérisation des domaines et des résidus clef de l'activation des pathways de signalisation en aval du récepteur (mutants CXCR7/ACKR3); l'étude et la caractérisation de nouveaux outils innovants pour la détection de l'oligomérisation de ces récepteurs en conditions endogènes. (Nanobodies, HTRF)

Les résultats du premier objectif ont été publiés en janvier 2016 : PMID 26813575.

La modélisation de CXCR7/ACKR3 nous a permis de générer plusieurs mutants du récepteur pour tester nos hypothèses sur l'activation.

Les nanobodies caractérisés pour CXCR4 seront utilisé dans une deuxième étude pour l'identification des formes oligomériques du récepteur sur tissus et cellules.

Laboratoire de rattachement

Inserm UMR-S996 Inflammation, chimiokines et immunopathology

32 rue des Carnets, 92140 Clamart